UNCLASSIFIED

AD NUMBER
AD048311
CLASSIFICATION CHANGES
TO: unclassified
FROM: confidential
LIMITATION CHANGES
TO: Approved for public release, distribution unlimited
FROM: Distribution authorized to U.S. Gov't. agencies and their contractors; Administrative/Operational Use; May 1954. Other requests shall be referred to Ballistic Research Laboratories, Aberdeen Proving Ground, MD.
AUTHORITY
BRL ltr, 28 Nov 1980; BRL ltr, 16 May 1988

THIS PAGE IS UNCLASSIFIED

UNCLASSIFIED

AD 048311

CLASSIFICATION CHANGED
TO: UNCLASSIFIED
FROM CONFIDENTIAL
AUTHORITY: BRL D/A
ltr, 28 Nov 80

UNCLASSIFIED

Armed Services Technical Information Agency

Because of our limited supply, you are requested to return this copy WHEN IT HAS SERVED YOUR PURPOSE so that it may be made available to other requesters. Your cooperation will be appreciated.

AD 483 11

NOTICE: WHEN GOVERNMENT OR OTHER DRAWINGS, SPECIFICATIONS OR OTHER DATA ARE USED FOR ANY PURPOSE OTHER THAN IN CONNECTION WITH A DEFINITELY RELATED GOVERNMENT PROCUREMENT OPERATION, THE U. S. GOVERNMENT THEREBY INCURS NO RESPONSIBILITY, NOR ANY OBLIGATION WHATSOEVER; AND THE FACT THAT THE GOVERNMENT MAY HAVE FORMULATED, FURNISHED, OR IN ANY WAY SUPPLIED THE SAID DRAWINGS, SPECIFICATIONS, OR OTHER DATA IS NOT TO BE REGARDED BY IMPLICATION OR OTHERWISE AS IN ANY MANNER LICENSING THE HOLDER OR ANY OTHER PERSON OR CORPORATION, OR CONVEYING ANY RIGHTS OR PERMISSION TO MANUFACTURE, USE OR SELL ANY PATENTED INVENTION THAT MAY IN ANY WAY BE RELATED THERETO.

Reproduced by

DOCUMENT SERVICE CENTER

KNOTT BUILDING, DAYTON, 2, OHIO

Best Available Copy

NOTICE: THIS DOCUMENT CONTAINS INFORMATION AFFECTING THE NATIONAL DEFENSE OF THE UNITED STATES WITHIN THE MEANING OF THE ESPIONAGE LAWS, TITLE 18, U.S.C., SECTIONS 793 and 794. THE TRANSMISSION OR THE REVELATION OF ITS CONTENTS IN ANY MANNER TO AN UNAUTHORIZED PERSON IS PROHIBITED BY LAW.

CONFIDENTIAL

0654

AD No. 48311
ASTIA FILE COPY

CRITICAL REVIEW OF SHAPED CHARGE INFORMATION

REPORT No. 905

Contributing Authors:

W. T. August . . . . . Naval Ordnance Laboratory
Garrett Birkhoff . . . . . Harvard University
R. J. Eichelberger . . . . . Carnegie Institute of Technology
R. V. Heine-Geldern . . . . . Carnegie Institute of Technology
F. I. Hill . . . . . Ballistic Research Laboratories
William Piper . . . . . National Bureau of Standards
Emerson M. Pugh . . . . . Carnegie Institute of Technology
J. Rabinow . . . . . National Bureau of Standards
John E. Shaw . . . . . Ballistic Research Laboratories
A. D. Solem . . . . . Naval Ordnance Laboratory
L. H. Thomas . . . . . Watson Scientific Computing Laboratory
Hugh Winn . . . . . Firestone Tire and Rubber Company
Louis Zernow . . . . . Ballistic Research Laboratories

Editor in Chief . . . . Louis Zernow, BRL
Associate Editor . . John L. Squier, BRL

Department of the Army Project No. 503-04-009
Ordnance Research and Development Project No. TB3-0134

MAY 1954

BALLISTIC RESEARCH LABORATORIES
ABERDEEN PROVING GROUND, MD.

DEC 1 1954

CONFIDENTIAL 54AA 72756

DISCLAIMER NOTICE

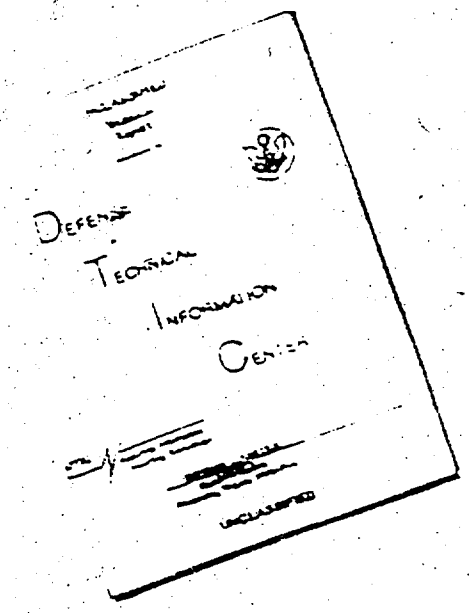

THIS DOCUMENT IS BEST QUALITY AVAILABLE. THE COPY FURNISHED TO DTIC CONTAINED A SIGNIFICANT NUMBER OF PAGES WHICH DO NOT REPRODUCE LEGIBLY.

REPRODUCED FROM
BEST AVAILABLE COPY

PAGES _____

ARE

MISSING

IN

ORIGINAL

DOCUMENT

CONFIDENTIAL

BALLISTIC RESEARCH LABORATORIES

REPORT NO. 905

May 1954

CRITICAL REVIEW OF SHAPED CHARGE INFORMATION

Contributing Authors:

W. T. August . . . . . Naval Ordnance Laboratory
Garrett Birkhoff . . . . . Harvard University
R. J. Eichelberger . . . . . Carnegie Institute of Technology
R. v. Heine-Geldern . . . . . Carnegie Institute of Technology
F. I. Hill . . . . . Ballistic Research Laboratories
William Piper . . . . . National Bureau of Standards
Emerson M. Pugh . . . . . Carnegie Institute of Technology
J. Rabinow . . . . . National Bureau of Standards
John F. Shaw . . . . . Ballistic Research Laboratories
A. D. Solan . . . . . Naval Ordnance Laboratory
L. H. Thomas . . . . . Watson Scientific Computing Laboratory
Hugh Winn . . . . . Firestone Tire and Rubber Company
Louis Zernow . . . . . Ballistic Research Laboratories

Editor in Chief . . . . . Louis Zernow, BRL
Associate Editor . . . . . John L. Squier, BRL

Department of the Army Project No. 503-04-009
Ordnance Research and Development Project No. TB3-0134

ABERDEEN PROVING GROUND, MARYLAND

AMA 7275

FOREWORD

From time to time in every active scientific field of endeavor it is profitable to make a searching and critical re-examination of its foundations. Such a critical review can serve many useful purposes. There is little doubt that the field of shaped charge can profit greatly from such a re-examination.

We can enumerate the useful purposes which a critical review of the shaped charge field can hope to accomplish at this time.

(1) It can extract from the welter of raw experimental data the reliable design bases which are needed by the designer.

(2) It can indicate the areas in which reliable design bases are lacking, or the soundness of the available information is open to question, or marred by inconsistencies. By so doing it can stimulate research people to investigate those areas which are in need of additional effort. The benefit to the designer is apparent.

(3) Since the contributors are selected widely from among those active in research and development, it can provide an authoritative and reasonably complete picture of the present position, over a large portion of the entire field, for the research worker who is occupied with less general aspects, and finds it difficult to keep up with the entire rapidly advancing frontier. Who among us can fail to profit in this respect?

Perhaps one of the most useful contributions which a critical review can make, is to point out the "facts of life" to those people who have the impression that most answers to most questions are available somewhere and that it's simply a matter of listing and indexing systematically everything that has ever been done in the field. It is perhaps instructive to point out that over the years, tremendous amounts of money and man hours of effort have been invested in "horseless carriages" and automotive development, and yet today it's not difficult to pose practical design questions which cannot be answered except by carrying out an additional set of experiments. Even then there can be no guarantee of a conclusive and unique answer. The investment in research and development of shaped charges, although large, has been much more modest both in money and man hours of effort than that in the automotive field. Comparatively, it is likely that we are still in the "horseless carriage" stage. It is therefore quite unreasonable for the designer to expect to find all the rules laid out in handbook form. The field is advancing too rapidly and the rules of the game are changing too quickly. We hope that the critical review can at least spell out the rules which apply today and which are likely to continue in effect because they are firmly based. It can also provide appropriate warnings in the less firmly established areas, and provide a preview of things to come.

Even with this modified objective, it will become apparent that during the time required to prepare this volume, rapid progress is being made in areas already covered in the review as well as in new areas of interest that have opened up since. Among the areas falling into these categories are those of wave shaping, lethality measurement, instrumentation, metallurgy and the applications of solid state physics to the problems of jet behavior. It should be apparent that this state of affairs is unavoidable in a field as active as this. The only hope of keeping up, lies in a planned, short and long term coordination program. Coordination and exchange of information such as is provided by the Ordnance Corps Shaped Charge Research and Development Steering and Coordinating Committee serves as a quarterly basis for short term coordination. In this connection the Shaped Charge Journal sponsored by the Committee and published on a trial basis by the Ballistic Research Laboratories will serve to disseminate the new information. For the long term problem, the biennial Symposia have been found very valuable. The transactions of the Symposia will always be very significant sources of information. It is apparent, however, that they do not serve the same functions as a Critical Review. Current thinking is therefore in terms of a continuing issuance of new volumes of the critical review whose frequency would be determined by the rate of progress in various areas. It can definitely be said that the experience which has been acquired during the preparation of this first volume will help ease the burden of the organization of any later volumes, and will also help assure a much more prompt publication of the manuscripts. Many of the areas which are treated superficially in this volume can be expected to undergo critical scrutiny in any later issues of the Critical Review.

Expressions of appreciation are due to all of the contributors to this first volume of the Critical Review. They are all very busy people who, with practically no cajolery took the time from their regular tasks not only to prepare their own chapters but also to proof-read and criticise all the other chapters, and to modify and remodify their own chapters in accordance with the criticism of the other contributors and outside critics. Although this procedure delayed the completion of the final draft of the Critical Review, it is expected that the resultant improvements will compensate for the delay.

Among the agencies whose criticism was found to be valuable, we would like to mention the Naval Ordnance Laboratory, Picatinny Arsenal, and the Office Chief of Ordnance, ORDTA. Mr. Mark V. Massey and Dr. E. A. Littleton of that office, were particularly helpful in suggesting material to be added and in providing some of the pertinent information.

We are grateful to Dr. Emerson M. Pugh of the Carnegie Institute of Technology, not only for making many valuable suggestions and criticisms but for the introductory chapter and historical survey based on his intimate and personal participation in the development of both the earliest as well as the very recent theoretical foundations. These include shaped

charge jet penetration theory as well as non-steady state collapse theory. The confirmation of his very early inferences regarding jet break-up characteristics by the flash radiographs taken at BRL and Kerr cell photography at C.I.T. are tributes to his keen perception.

The continuing contributions of the fine group at the Carnegie Institute of Technology are evident not only from the frequent references to their work by other authors, but also from the fact that C.I.T. has provided the authors for three of the ten chapters.

We are indebted also to Professor Garrett Birkhoff who was the first one in this country to work out the classical hydrodynamic theory of wedge collapse and jet formation. His contributions to the recent progress in the shaped charge field are especially noticeable in the area of the theory of the effects of rotation. Professor Birkhoff's continued interest and advice have been invaluable in the preparation of this volume.

We would also like to express our appreciation to Dr. L. H. Thomas of the Watson Scientific Computing Laboratories who collaborated in the preparation of Chapter II on the theory. Computing machines will undoubtedly be essential for efficiency in the calculations required for the extensions of the theory of jet formation and penetration. Dr. Thomas has been instrumental in laying out the plan for the series of theoretical calculations of successively increasing generality and physical complexity. These will require the use of computing machines and we are fortunate to have Dr. Thomas's advice and guidance.

Although this first volume of the Critical Review did not readily provide an opportunity for participation by British scientists we have not forgotten that they have a very illustrious roster of contributors to the present state of knowledge. Sir Geoffrey Taylor and Dr. Tuck were of course responsible for the classical hydrodynamic wedge collapse theory in Great Britain. They did this independently and essentially simultaneously with the work of Birkhoff in the US. In addition Professor Mott and Drs. Evans, Hill, Pack and Ubbelohde are among those who have made substantial contributions to this field. It is definitely planned to invite participation by both British and Canadians in the next volume of the Critical Review.

Finally, we would like to acknowledge the contributions made by Mr. Irving Lieberman in preparing the index and Appendices on foreign and American ammunition performance and design data; Mr. Hixmer of the Ordnance Technical Intelligence Section for supplying large amounts of data for Appendices. Messrs. J. M. Regan and J. Simon in the proof reading of the final text and the Weapon Systems Laboratory for the material on tank armor in Appendix IV.

The cooperation of many other people, too numerous to name, in the preparation of the material for publication is also gratefully acknowledged. In particular, however, the work done in this connection by Mr. John L. Squier, the associate editor, warrants special attention. His supervision of the final manuscript preparation and proof reading as well as his attention to the many details of figure preparation and pagination constitute major contributions to the value of this volume.

L. ZERNOW

Editor-In-Chief

TABLE OF CONTENTS

			Page
FOREWORD by Louis Zernow			iii
CHAPTER			
I	INTRODUCTION	Emerson M. Pugh	1
II	STATUS OF THEORY	G. Birkhoff, L. H. Thomas	19
III	LINER PERFORMANCE	John E. Shaw	45
IV	THE UNFUZED WARHEAD	Hugh Winn	103
V	THE EXPLOSIVE COMPONENT OF SHAPED CHARGES	A.D. Solem, W. T. August	119
VI	FUZES FOR SHAPED-CHARGE MISSILES	J. Rabinow, William Piper	139
VII	THE EFFECTS OF ROTATION UPON SHAPED CHARGE JETS	Louis Zernow	177
	APPENDIX TO CHAPTER VII: Derivation of the Expression for ω_0 IN TERMS OF CHARGE PARAMETERS	F. P. Bethel	210
VIII	SPIN COMPENSATION	R. J. Eichelberger	215
IX	DEFEAT OF SHAPED CHARGE WEAPONS	R. v. Heine-Geldern	255
X	TERMINAL BALLISTIC EFFECTIVENESS OF SHAPED CHARGES AGAINST TANKS	F. I. Hill	269
	APPENDIX I. AMERICAN HEAT AMMUNITION		299
	APPENDIX II FOREIGN AMMUNITION (SOVIET)		311
	APPENDIX III FOREIGN AMMUNITION (MISCELLANEOUS)		319
	APPENDIX IV SOVIET ARMOR		325
	INDEX		335

CHAPTER I

INTRODUCTION

Emerson M. Pugh

Carnegie Institute of Technology
Pittsburgh, Pennsylvania

Need for a Critical Review

High explosive charges with lined cavities possess the property of producing deep holes in target materials against which they are exploded. This remarkable property was utilized by practically all of the belligerents in World War II in a number of different weapons and demolition devices: rocket grenades, rifle grenades, hand grenades, recoilless rifle projectiles, standard antitank gun projectiles, engineers demolition charges, cable and beam cutting devices, etc. For security reasons this class of high explosive charges was designated "Shaped Charges" by the British and American Armed Services. In spite of the fact that this designation is misleading it is still the most commonly used term for these charges with lined cavities. Another term, "HEAT round" (High Explosive Anti-Tank), which is equally misleading, also is frequently used to designate rounds that employ the lined cavity charge. "HEAT round" is misleading because it suggests that the jets from these charges "burn their way through the armor plate", when in fact, the process of penetration does not involve any chemical reaction and the temperatures of these jets have practically no effect upon this process.

While a wide variety of weapons and demolition devices were manufactured for use during World War II, they were not as widely used as should have been expected from their known potentialities. The restricted use of these devices was due partly to lack of understanding of their capabilities and partly to the shortcomings of the weapons as manufactured. Lack of reliability was undoubtedly one of the chief reasons for their lack of popularity. Their poor performance when they were used in projectiles shot from rifled guns was another reason.

Modern research and development has been pointing the way to the elimination or reduction of many of these shortcomings and there is every reason to believe that much more progress in this direction is possible. The principles involved in the lined cavity charge certainly offer great potentialities for the improvement of conventional weapons. If the wars in Korea and Indo-China can be taken as typical of what may be expected in the next several years, conventional weapons will be of very great importance. At the 1953 symposium on shaped charges at the Aberdeen Proving Ground, it was pointed out by Col. Del Campo that, even if nuclear weapons are used in an all-out war, conventional weapons

should still play a decisive role, since they may be used to crowd the enemy until he is vulnerable to attack by nuclear weapons.

The importance of achieving maximum effectiveness with the shaped charge devices makes the compilation of a critical review of great importance. This Critical Review is designed to provide up-to-date information concerning what is known and what is not known about these charges. It is also intended to stimulate curiosity and motivate research. It is hoped that the references supplied will be sufficient to make it relatively easy for the research worker to find original papers on any part of the subject that interests him. For this purpose a brief historical review of the development of the subject should be valuable.

Unlined Charges

As early as 1792 it was known that when an explosive was placed in contact with a target plate and exploded, a deeper hole would be made in the target if the explosive contained a cavity in contact with the target. This remarkable fact apparently has been forgotten and rediscovered several times. Although knowledge of the cavity charge effect is very old, the fact that a much greater effect could be produced by lining the cavity with a thin metal liner was not recognized until the 1930's*. This now seems hard to understand since liners were used in the cavities of explosive charges at least as early as 1910. The failure to recognize the importance of the liner for making deep penetrations must have been due to two facts; first, the liners must be well designed and well fabricated and second, the charges with these lined cavities must be detonated at some distance (standoff) from the target to exhibit their remarkable penetrating power. Though charges with lined cavities require standoff, charges with unlined cavities produce the greatest effect when they are detonated in direct contact with the target. A well made liner placed in the cavity of the charge and fired at optimum standoff, can increase the depth of penetration produced in a given target. The discovery of the effectiveness of the liner was purely accidental. After this discovery several years elapsed before a reasonable explanation of the phenomenon was obtained.

---

*The Germans appear to have recognized the importance of the liner as early as 1924 as noted in my brief history and bibliography printed in the back of [illegible] Report No. 837, Nov. 1951 (C). The information on this is sketchy and was not available until after World War II. It apparently had no influence on developments in this country or England. This chapter is based upon my recent studies re-evaluating developments in the U.S.A.

Remarkably well designed weapons and demolition devices were in general use for sometime before an explanation of the effectiveness of the liner was obtained. The early attempts to explain the action of the liner failed because they were attempts to show how a qualitative theory that had been devised for the unlined cavity could be modified to account for the effect produced by introducing a liner. Success came only when it was recognized that the process of penetration by the lined cavity charge is entirely different* from that of the unlined charge. Since the two processes are so different no further mention will be made of the unlined cavity charges except to show how they did lead to the accidental discovery of the effect of the lining. The earliest liners were introduced only to support or to protect the charge or to help form the cavity in the charge. Recognition of the effectiveness of these liners in producing penetrations came much later.

Early Use of Liners

Charles E. Munroe in 1888 stacked dynamite sticks around an empty tin can and blew a hole in a safe door. According to Munroe the tin can served only to hold the dynamite in place. German and United Kingdom patents were issued to the Westfälish-Anhaltische Sprengstoff-Actien-Gesellschaft (WASAG) of Berlin for hollow charges to be used for blasting operations in mines, for torpedoes and explosive shells. The German patent application was dated 14 Dec. 1910. The United Kingdom patent, accepted in 1912, shows a projectile loaded with high explosive having a conical cavity lined with thin steel, brass, or zinc. It is clearly stated, however, that the sole purpose of the liner is to protect and support the explosive while it is being shot out of a gun with high velocity. Paraffined paper liners are suggested to protect the explosive from moisture when it is to be used for mine blasting.

Early manufacturers of detonators had found that the effect of detonating caps is highest, if "the explosive is compressed only softly in its part close to the point of ignition and compressed strongly in its part located at the bottom of the cap." In 1921 M. Andrea Schulze took out French patent No. 532,753 to accomplish this result cheaply by forcing a conically shaped tool up into the bottom of the detonator cap. The tool permanently deformed the light metal casing, which surrounded the explosive, leaving a conical cavity lined with the thin metal of the casing. According to Schulze, however, the sole purpose of the process was to produce a highly compressed explosive right at the bottom of the cap which he claimed would make it a much more efficient detonator.

---

*The approximations required to obtain the theory for lined charges are valid for a fairly wide range of liner thicknesses around the optimum thickness. When liners are made thinner and thinner, the process changes rapidly but smoothly to that of the unlined cavity.

Thus Schulze inadvertently produced an explosive charge with a metal-lined conical cavity. Since the efficiency of detonators was being determined at this time by the depth of the hole they could produce in a lead plate, it is not surprising that these detonators performed well in tests. At almost the same time, Wilhelm Eschbach obtained German patent No. 172,914 (Dec. 1921) for making detonators by a technique that was almost identical with that of Schulze. Eschbach's primary purpose was, like that of Schulze, to compress the explosive in the bottom of the cup. However, Eschbach did recognize that the cavity might provide added effectiveness. He said nothing about the fact that his cavities were lined with thin metal.

The first to recognize the importance of liners in the cavities of these charges seems to have been R. W. Wood (2). A young woman had opened the door of the coal furnace in her home and had been killed by a small copper pellet that severed an artery. As technical expert in the ensuing law case Wood demonstrated that identical copper pellets were formed and projected at very high velocity by detonators having cavities lined with thin sheet copper. The cavities in the detonators used by Wood were so shallow that the liner remained intact; that is, there was no separation into jet and slug as is observed with smaller angle cones. Thus Wood performed the first experiments on the effect that was later called the Misnay-Schardin effect.

During the period 1940-42, a number of patents were applied for on projectiles which used lined-cavity charges. The claims in these patents all show that the inventors erroneously expected the liner to form a single high-speed projectile, like that studied by Wood. The first of these appears to be French patent No. 113,685 (applied for on 27 Nov. 1940), issued to Berthold Mohaupt, Henry Mohaupt and Erich Kauders, which was assigned by them to the Gasab Society of Switzerland. The first American patent, which was issued to J. C. Gray, W. E. Thibodeau, J. H. Church and G. J. Kessenrich, was applied for on 10 March 1941. Henry Mohaupt came to America and was responsible for arousing the interest of the U. S. Army Ordnance Department in the principle. He applied for his U. S. patent No. 2,419,414 on 3 Oct. 1941, and sold it to the U.S. Army.

Once recognized, the principle was incorporated with amazing rapidity into many practical devices. Most of this development work in the United States was done by Army engineers in cooperation with engineers and scientists from private companies. Patents No. 2,427,989 (for the M9 rifle grenade and M10 machine gun grenade) and No. 2,413,666 (for the M66 and M67 howitzer projectiles) were issued to G. W. Blackington and J. J. Calhoun, Budd Company engineers. Dates of application were 19 Aug. 1942 and 21 Nov. 1942 respectively. Patent No. 2,466,752 (for the M6 Bazooka*) was issued to Lieut. E. G. Uhl and Lt. Col. Leslie A. Skinner, of the U. S. Army Ordnance Department. The date of this application was 22 Sept. 1943.

*The M10 shaped charge head was used in the Bazooka.

These patents were each assigned to the United States government without cost. Each of the weapons was in production before or shortly after the date of the corresponding patent application. According to Col. C. H. M. Roberts, the M9A1 rifle grenade was developed before and the M6 Bazooka was developed just after he joined the Office of the Chief of Ordnance in March 1942. The grenades and howitzer projectiles were in quantity production by this date.

The demolition charges, including the M3 with a 9.5 in. diam. steel cone and the M2A3 with a 6.5 in. diam. glass cone, were developed between 1942 and 1943. Dr. C. O. Davis, working for DuPont on an Ordnance contract, provided much of the design information needed for these developments. He and his assistants, starting work in Sept. 1940, provided rules for optimum liner angles, liner thicknesses and charge diameters. They also provided empirical scaling laws that Garret Birkhoff later showed to be theoretically sound. Corning Glass Co. developed the glass cone to take the place of steel cones, since there was then a critical shortage of steel. Work similar to that done at DuPont was also being done by W. M. Evans and A. R. Ubbelhode working for the British Ministry of Supply. They appear to have been the first to recognise that the holes were formed by some kind of jet and that the slug, which could be recovered, played no part in the penetration. They also developed photographic methods for determining the character of the jet and for determining its velocity.

Coordination and Expansion of U. S. Research

J. B. Conant of Harvard inspired the organisation of the Explosives Research Laboratory (ERL) which operated on the grounds of the U. S. Bureau of Mines at Bruceton under an N.D.R.C. contract with the Carnegie Institute of Technology with W. N. Jones as supervisor.

The shaped charge studies at ERL were started in Sept. 1941 under the direct supervision of D. P. MacDougall. G. B. Kistiakowsky, who was stationed at Bruceton as head of Div. 8 of N.D.R.C., also participated actively in the work. These two visited Evans and Ubbelhode in 1941 and brought back many useful ideas for research.

MacDougall's experiments, started in 1941, were beautifully designed to find many of the answers. By shooting into steel target plates through predrilled holes in the first plate he demonstrated that the jet has a much smaller diameter than the hole it produces. He collected steel jets and found they consisted of small steel fragments that obviously had not been melted in the process. With a rotating drum camera he demonstrated the existence of gradients of velocity within the jets.

The Ballistic Research Laboratories were busily engaged on high priority Ordnance problems. Dr. J. C. Clark, who had been doing X-Ray research at Michigan State and had been commissioned as an Army Captain, was brought in to develop the new flash radiography of Slack and Ehrke (3) to aid the study of these problems.

Because of the secrecy restrictions and the lack of an effective system of liaison, the various laboratories worked almost independently until January of 1943. Each laboratory had its own theory which seemed to explain its own experiments. To remedy this lack of coordination, a joint Army, Navy, N.D.R.C. Committee on Shaped Charges was set up. The committee consisted of Col. C. H. M. Roberts, chairman for the Army; Lieut. Commander E. H. Ohl (later replaced by Commander Stephen Brunauer) for the Navy; and Dr. G. B. Kistiakowsky (later replaced by Dr. D.P. MacDougall) for the N.D.R.C. This committee performed three very important functions;

1. They organized a system for distributing reports within the security regulations. This system included exchange of reports with Great Britain.
2. They organized symposia that were attended by representatives from each group.
3. They persuaded the N.D.R.C. to place new contracts for research in areas that were not being covered adequately.

The Gulf Research Laboratory at Harmarville, Pa. was awarded a contract under Dr. Morris Muskat to develop a "follow-through" projectile.

The Carnegie Institute of Technology was awarded a contract to develop methods of defeating shaped charge weapons. Originally the theoretical part of this defense contract was under Drs. Frederick Seitz and Otto Stern while the experimental part was under Dr. Turner L. Smith and the author. Shortly, however, the first three moved to other projects leaving the author and a few graduate students to carry on the work.

The new system for distributing reports was an enormous improvement, but even so, the coverage was necessarily spotty and there were long delays. The N.D.R.C. set up a service library of all classified reports at Princeton. In 1943 this contained mostly British reports but became more complete, especially in American reports, by the end of 1944.

The improved liaison and distribution of reports was certainly responsible for the rapid development of the theories in this country and in England. The fact that the distribution was necessarily slow and spotty, caused much of the work to be done independently in the two countries and makes it very difficult to plot the logical historical development of the theory. In view of these facts, this history will be limited primarily to the development of the theory in this country, but will show how it was influenced by British developments.

Influence of Foreign Developments

Shortly after hostilities ended in Europe, groups of scientists and engineers from England and the United States visited laboratories and factories in France and Germany. They brought back reports showing

that active research on lined cavity charges had been going on in both countries which arrived at conclusions that were qualitatively very much like ours. However, the author has found no evidence that individuals or groups working in these or any other countries have achieved mathematical formulations of the phenomena that were nearly as satisfactory as those achieved by the cooperative efforts of the United States and Great Britain. Since secrecy prevented the scientific work of countries other than Great Britain from influencing our developments, here, it would be meaningless to attempt to connect their work historically with ours.

Emergence of Shaped Charge Theories in 1943

Since complete objectivity in relating historical developments is very difficult, it seems best to abandon the conventional third-person and pursue a more personal approach. I will, therefore proceed to sketch the development of the theory in this country from the point of view of an observer and an active participant in the process.

The NRL group freely discussed their work with the group at the Gulf Research Laboratory and with our group, who were working on the Carnegie Institute of Technology campus. This was a great help to both groups. The field was entirely new to all of the personnel in these groups.

By March 1943 MacDougall (4) had obtained, from momentum considerations, the equation $\rho_j V_j(V_j - U) = \rho U^2$ relating the velocity of penetration of the jet, U, into a target of density, ρ, to the density, ρ_j, and the velocity, V_j, of the jet. From this he predicted that the ratio V_j/U should increase monotonically with ρ. His data*, taken from drum camera records of jets passing through target plates, showed this behavior.

In seeking a principle to guide my search for methods of defense, I noticed that MacDougall had correctly assumed the mass of jet hitting the target per second to be proportional to $\rho_j(V_j - U)$, but in calculating the rate of momentum transfer, had multiplied this by V_j instead of $(V_j - U)$. Correcting this gave the now well known equation $\rho_j(V_j - U)^2 = \rho U^2$. I multiplied the left-hand side of this equation by the factor $A/A_j > 1$ to account for the fact that due to the lack of perfect symmetry in the charges and their liners, as manufactured, the effective area A on which the jet impinged must be greater than the ideal jet cross section A_j. This corrected relation then predicted a straight line plot for

* The original plot of V_j/U versus ρ is found in the NRL monthly interim reports CF-9 (May 15, 1943).

MacDougall's V_j/U data if plotted against $\sqrt{\rho}$. In replotting MacDougall's points in this manner, I found that they fell on a good straight line. To make sure that this was not just accidental I analyzed all that I could find of the relevant* ERL data from which V_j/U could be computed. The resulting averages plotted against $\sqrt{\rho}$ again fell on a good straight line through the predicted intercept unity. Furthermore, it appeared that, if sufficient data were available, the maximum and the minimum values of V_j/U would each fall on different straight lines through the intercept unity. The lines through the maximum values corresponded to the charges with poor symmetry and therefore with large values for A/A_j, while the lines through the minimum and average values corresponded to the minimum and average values of A/A_j respectively. With this fact settled to my satisfaction, I started applying the theoretical predictions to all of the other data which had up to then appeared so mysterious. T. L. Smith and I had fastened steel target plates to a ballistic pendulum and had observed the total momentums of jets whose penetration was also recorded. The fact that there was absolutely no correlation between the depth of penetration and the total momentum of the jet producing it had been disturbing. However, this new velocity equation made it possible to explain the apparent anomaly. On integrating $\int U\,dt$ to find the total penetration, I was amazed to find that all velocities cancelled out and left the total penetration dependent only on jet and target densities, the ratio of areas A_j/A and the jet length. Since depths of penetration did not depend on velocities they should not correlate with jet momentums. The pieces to a big jig-saw puzzle seemed to be fitting together. The fact that penetration depended on jet length, and in fact was proportional to it, now provided a ready explanation for the mysterious fact that penetration increased with standoff, for MacDougall had shown that the jets lengthened as they traveled. His drum camera measurements had shown a gradient in velocity within the jets.

Qualitatively this explanation was fine, but my first attempt to account numerically for the penetration versus standoff curve failed because the observed penetration increased too fast with standoff to be accounted for on the basis of a mere lengthening of a particle jet. To account for the observed rapid rise in penetration, I found it necessary to presume that the average density of the jet remained constant during the early part of its elongation. In other words it

---

* The equation predicted that V_j/U should be linear with $\sqrt{\rho}$, only if $\rho_j A_j/A$ remained constant during perforation of the target plates. For this reason only the data that was taken with target plates near the optimum standoff were considered. This data was scattered through the ERL interim reports (5).

remained continuous and lengthened by ductile drawing of the liner material. Since the jet particles collected by MacDougall's group were fine sharp edged particles, I presumed that break-up of the jet took place after the elongation had proceeded to a point determined by the ductility of the liner. This accounted for the slower rise in penetration beyond a certain standoff, for the rate of increase of penetration with standoff should decrease when the jet is broken into particles. Now I could understand why the penetration produced by copper* and aluminum liners continued to increase up to relatively large standoffs, since these metals are much more ductile than steel. I attributed the drop in penetration beyond the optimum standoff to A/A_j increasing as the square of the standoff. With perfectly symmetrical charges and liners $A/A_j = 1$ and the penetration should not** drop off with standoff. The occasional shot that gave a large penetration at large standoff was presumed to be evidence for this point of view. Further proof was found in the fact that approximately the same average A/A_j and the same variation in A/A_j were obtained from both the P versus S curve and the V_j/U versus $\sqrt{P}$ curve.

These steady and non-steady theories of jet penetration together with the experimental correlations were reported (7) in June 1944. Two weeks later I received a copy of a British paper (8) that treated the penetration by a steady state jet. It contained the same form of velocity equation and the same form of penetration equation as I had obtained. This paper by Hill, Mott and Pack differentiated between fluid and particle type jets, for which they obtained different proportionality constants. These different proportionality constants were supposed to account for the observed differences in penetrations that were obtained with liners of different materials. However, penetrations do not correlate with melting points of liners in the manner required by their theory. The paper did not discuss standoff effects. I realized (9) that if fluid and particle jets should be treated with different proportionality constants as proposed in this Hill, Mott, and Pack paper, my theory should be modified, because the continuous jets with negligible strength should be treated like fluids until they break up into particles. This modification*** which consisted of introducing into my velocity equation a proportionality constant, λ, proved to be unimportant for it did not affect any of the correlations that had been obtained with experimental data. It only affected the

---

* Convincing proof of this is now found in B.R.L. radiographs.(6)

** L. Zernow has recently shown good charges give good penetrations at very long standoff.

*** Recent considerations make it appear that this modification was undesirable, because the model used by R. Hill, N. L. Mott and D. C. Pack to represent the particle jet was unrealistic.

estimate as to how close to the original position of the liner base the jets broke into particles.

It was gratifying that the theory accounted for the well known fact that depths of penetration into armor were almost as great as in mild steel, since the penetration by a given charge should depend only on the target density. However, the fact that penetrations into armor were somewhat less than into mild steel showed that some modification based upon target strength should be introduced into the theory. Some shots into lead cylinders, showing much deeper total penetrations than were predicted by the theory, had clearly demonstrated the need for such a modification.

MacDougall early recognised (4) that penetrations by the front of the jet depended largely upon the target density while total penetrations depended on target strength. He presumed that the additional penetration into soft targets was due to residual momentum* continuing to open the hole after the last fast jet particle had struck. Eichelberger demonstrated (10) that the rear of the jet was responsible for the deep penetrations observed in lead. By placing armor plate (1/2 in. thick) at various depths in a stack of lead plates, he found that a very small total penetration was obtained when the armor was in the proper position to stop the rear of the jet. In my first paper (7) I included a crude empirical attempt, based upon MacDougall's assumption, to take account of the target strength.

The difficulty in accounting for the strength of the target could be avoided by using a standard target material to absorb the rear of the jet after the front of the jet had been absorbed by any target material that was being tested. Thus in searching for target materials useful for defense, I employed standardized mild steel target plates to measure the residual penetration. The use of the residual penetration as a means of testing materials made it possible for me to develop with E. L. Fireman (11), a "residual penetration theory" which should be practically independent of target strength. Actually this "residual penetration theory" and the velocity equation applied to the front of the jet are the only ones that should be called "density laws," since they are the only ones that have succeeded in predicting results with many materials.

*This point of view was retained by the author until Eichelberger pointed out that the low velocity tail-end of the jet was responsible for the added penetrations observed in low strength targets.

Using the residual penetration technique with more than a hundred different materials, Eichelberger showed that practically all of them followed the theory to within the accuracy of his experiments. According to this theory, the thickness of target, t, required to absorb a given length of jet is proportional to $1/\sqrt{\rho}$, while the weight of the protective material is proportional to ρt. Thus the weight required for protection is proportional to $\rho(1/\sqrt{\rho}) = \sqrt{\rho}$ and materials with low density provide protection with the least weight. This is the reason that we very early proposed the use of aluminum armor. Of course, with very low densities the thickness required is very great and the weight of the devices for fastening the material greatly reduce this advantage.

In cooperation with P. R. Smith of the Flintkote Company, a mixture of gravel and pitch mastic called HCR (hollow charge resisting) was developed. It had a low density and provided somewhat better protection than was predicted by the residual penetration theory. Protective panels of HCR were built for tanks and tested, but the war ended before final tests were completed.

In 1945 R. Heine-Geldern showed (12) that glass affords much better protection than the density law predicts. He then showed that this accounted for the stopping power of HCR whose gravel was mostly quartzite. Heine-Geldern has explained the stopping power of glass by the fact that in addition to being very hard so that the jet makes only a small diameter hole, it bounces back and disrupts* the jet that is passing through this small hole. (13)

Jet Formation

Historically, a fair qualitative picture of the process of jet penetration had been obtained by MacDougall (4) before anyone had obtained any reasonable model for the process of jet formation. Both the Hill-Mott-Pack and my penetration relations were developed from the MacDougall model.

---

*L. Zernow and J. Simon of the HRL have verified the secondary interference with and the disruption of the jet, on passing through glass, by means of their very high quality flash radiographs.

I look back on the Shaped Charge Symposium held at 1703 Thirty-Second St., Washington, D. C. on March 29, 1943, where I was first introduced to this subject, as the most interesting symposium I have attended. The list* of individuals who attended that meeting assured that it could not be dull. Seeger presented von Neumann's theory of interacting shock waves as an explanation of the unlined cavity effect. MacDougall presented the ERL theory of jet formation with lined cavities, which was based on von Neumann's theory for unlined cavities. He also presented his model for jet penetration which I have discussed. The early British view of penetration was not presented because no one was there to sponsor it. W. E. Lawson presented the DuPont theory of jet formation.

*The minutes of this meeting list the names of the following persons as being present.

Joint Committee on Shaped Charges:
Lt. Col. C.H.M. Roberts, Chairman, Office of Chief of Army Ordnance.
Lt. S. N. Ohl, Bureau of Naval Ordnance
G. B. Kistiakowsky, National Defense Research Committee

Office, Chief of Ordnance (Army):
Mark F. Massey

Navy Bureau of Ordnance:
R. J. Seeger
W. E. Land

National Defense Research Committee:
D. P. MacDougall
J. G. Kirkwood

Johns Hopkins University:
R. W. Wood

New York University:
R. Courant

Ballistic Research Laboratories, Aberdeen Proving Ground:
O. Veblen
J. H. Fraser
Hans Lewy
Martin Schwarzschild
R. H. Kent

Development and Proof Services, Aberdeen Proving Ground:
C. E. Hawk

E. I. DuPont deNemours and Co:
C. O. Davis
W. E. Lawson
Leslie B. Seely, Jr.
Melvin A. Cook

Picatinny Arsenal:
J. W. Givens

Gulf Research:
Morris Muskat
F. W. Parker

Both of the theories of jet formation were ingenious and appeared to explain many of the experimental results. ERL experiments favored the ERL theory, DuPont experiments favored the DuPont theory. The dicussion became very heated. At one point, a member of the group said to Kistiakowsky, "Then you do not believe in experimental evidence," to which he quickly and emphatically rejoined, "Yes I do, when properly interpreted." The rejoinder was a classic that could not be forgotten.

A few weeks later I was fortunate to be visiting J. C. Clark at B. R. L. when he obtained his first good radiograph (14)* of a collapsing liner. We had just been carrying on a lively discussion of the merits of the two theories and had favored opposite sides of the question. When the negative came out of his dark room still wet, he held it up to the light. We looked long and hard and simultaneously agreed, "They are both wrong."

Birkhoff visited Clark a week or so later and after looking at the radiographs is said to have written down his hydrodynamics theory (15) on the spot. Tuck in England obtained radiographs much like Clark's, which prompted Sir Geoffrey Taylor (16) to formulate a hydrodynamic

---

Footnote continued from preceding page. .

Carnegie Institute of Technology:
Emerson M. Pugh
Frederick Seitz

Explosives Research Laboratory:

M. A. Paul
Eugene H. Eyster
George H. Messerly

At the June 30 meeting, this same group were in attendance and the following names were added to the list of those present.

J. E. Mayer
Capt. J. C. Clark
L. R. Littleton
J. von Neumann
Col. S. B. Smith
M. F. Roy
W. Kehl
E. B. Wilson
Otto Stern

* These radiographs were obtained on a cooperative program between DuPont (Dr. L. B. Seeley) and BRL (Dr. J. C. Clark).

theory almost identical with Birkhoff's. The two reports bear dates less than a month apart.

Taylor's (17) study of the explosion of a long cylindrical bomb resulted in his theorem* which made the predictions of the hydrodynamic theory more realistic.

Without this theorem one might conclude that a collapsing cylinder (a cone with zero apex angle) should produce a jet with infinite velocity. With this theorem the predicted jet velocity from a cylindrical liner is only twice the detonation velocity. Actually the measurement of the velocity of a jet produced by a collapsing cylinder is a sensitive check on the validity of the Taylor theorem. Measurements with large charges at Los Alamos have furnished a striking confirmation (18)** of this theorem.

Non Steady Jet Formation

An example of how much one's evaluation of experimental evidence inevitably is influenced by one's preconceived ideas, is found in the early conclusions reached from the early radiographs of Clark and Seeley. Because most of the scientists examining these radiographs were looking for evidence for the steady-state assumption that must be made to justify the Taylor-Birkhoff theories, the almost universal conclusion was that the collapse angle remained constant throughout the collapse process. It was then necessary to invoke a new phenomenon to account for a secondary jet issuing from the slug long after the collapse process was completed.

It was fortunate that I was deep in my analysis of the non-steady process of penetration long before I had an opportunity to view the complete set of collapse radiographs. Furthermore, my interest in the collapse theory was at first only academic because it seemed to be of little importance in the defense problem. I did not hear the conclusions reached by others before I viewed the radiographs. My immediate conclusion was that the collapse angle increased continuously throughout the collapse process, slowly at first and much more rapidly at the end. It appeared to me that the basal elements of the liner collapsed very slowly and I could see no evidence for a sudden or even rapid change in the process. Thus when hostilities ended in 1945 and Col. Roberts suggested that I continue my fundamental studies by moving most of my group to Bruceton, I welcomed the opportunity. At Bruceton we were able to take over the ERL facilities vacated by MacDougall and his group.

---

* Attempts to obtain a copy of RC 193 have met with no success. My information consists of a brief note relayed from Taylor through Birkhoff for inclusion in Jour. Appl. Phys. 19, No. 6 pp. 563-582 (June 1948), where it is included as Fig. 12, with legend, on p. 570. The theorem appears in simpler form in Jour. Appl. Phys. 23, No. 5 (May 1952), Eq. (1) p. 533-534.

** It is suggested in this article that the failure to observe penetrating jet velocities as high as expected represents a failure of the theory. It does, in fact, represent a failure of the steady-state theory, which was being used. However, the non-steady theory, to be mentioned later, shows that these high velocities should not be observable with the experimental arrangements described in this article.

Since I still had many duties on the campus, Eichelberger took over direct charge of the Bruceton group. The two of us worked in close collaboration on the theory (19) of non-steady jet formation. Norman Rostoker, who joined the group in 1948, smoothed out many of the rough spots and investigated the validity of the assumptions.

Eichelberger (20 was primarily responsible for the development of the techniques used in verifying the theory.

How the techniques of flash radiography have been improved by the Aberdeen group can be seen by the fact that the new radiographs by H. I. Breidenbach (21) and by Zernow et al (22) can leave no doubt that the collapse angle does increase with time and furthermore, that the contour of the collapsing wall is not conical but curved. The mathematical formulation can be expected to be right only for those processes of jet formation in which the loss of energy in the form of heat can be ignored. It is, however, gratifying that when heat energy cannot be ignored the deviations of results from those predicted by mathematics appear to be in the expected direction.

Conclusion

It is hoped that this brief historical account will be found interesting and helpful especially to newcomers in the field. Many topics have been left out or inadequately covered. The available space, however, does not justify their inclusion. In some cases brief historical accounts are included in the chapters, as for example, in Chapter VII on spin compensation.

For two reasons the recent history has been subordinated to the older: first, recent history can be found in easily available modern reports; and second, it is too difficult to evaluate objectively the developments that are very new.

1. Emerson M. Pugh, Bibliography, Transactions of Symposium on Shaped Charges held at Ballistic Research Laboratories Nov. 13-16, 1951. BRL Report No. 837, Appendix I.

2. R. W. Wood, "Optical and Physical Effects of High Explosives," Proc. Roy. Soc. London 157,249 (1936). Wood credits W. E. Lawson of E. I. DuPont de Nemours, Inc. with assisting him with these experiments.

3. C. M. Slack and L. F. Ehrke, Journ. Appl. Phys. 12, 165, 1941.

4. G. B. Kistiakowsky, D. P. MacDougall, and G. H. Messerly, "The Mechanism of Action of Cavity Charges," OSRD 1338, April 1943. Kistiakowsky informed me that the penetration theory in this report was due to MacDougall.

5. Explosives Research Laboratory interim reports from CF-3 (Nov. 15, 1942) to CF-12 (Aug. 15, 1943) and in SC-1 (Sept. 15, 1943) and SC-2 (Oct. 15, 1943).

6. Louis Bernow, M. Kronman, J. Passek and B. Taylor, "Flash Radiographic Study of Jets from Unrotated 105mm Shaped Charges," Transactions of Symposium on Shaped Charges held at Ballistic Research Laboratories Nov. 13-16, 1951, BRL Report No. 837.

7. Emerson M. Pugh, "A Theory of Jet Penetration," OSRD No. 3752, June 5, 1944.

8. R. Hill, N. L. Mott and D. C. Pack, "Penetration by Munroe Jets," A. C. 5756, Feb. 16, 1944.

9. "Symposium on Shaped Charges," OSRD No. 5754, May 9, 1945.

10. R. J. Eichelberger, "Fundamental Principles of Jet Penetration," OSRD No. 4148g, pp. 36-37, Sept. 15, 1944.

11. Monthly Report CIT-6h, OSRD 4629h, NDRC Div. 2 (March 15, 1945).

12. E. M. Pugh, R. J. Eichelberger and R. Heine-Geldorn, OSRD No. 5462c, pp. 25-31, Aug. 15, 1945.

13. CIT-ORD-41, Sect. B (Oct. 1952).

14. L. B. Seeley and J. C. Clark, "High-speed Radiography Studies of Controlled Fragments," BRL Rpt. 368, June 16, 1943.

15. Garret Birkhoff, "Mathematical Jet Theory of Lined Hollow Charges," B.R.L. No. 370, June 18, 1943.

16. G. I. Taylor (later Sir Geoffrey Taylor), "A Formulation of Mr. Tuck's Conception of Munroe Jets," AC 3724, May 27, 1943.

17. G. I. Taylor, "The Explosion of Long Cylindrical Bomb," RC 193, date unknown.

18. W. S. Koski, F. A. Lucy, R. G. Shreffler and F. J. Willig. Jour. Appl. Phys. 23, 1300-5, (Dec. 1952).

19. E. M. Pugh, R. J. Eichelberger and N. Rostoker, Jour. Appl. Phys. 23, No. 5 pp. 532-536 (May 1952)

20. R. J. Eichelberger and E. M. Pugh, Jour. Appl. Phys. 23, pp. 537-542 (May 1952).

21. H. I. Breidenbach, "The Evolution of Jets from Cavity Charges as Shown by Flash Radiographs," BRL Rpt. 808, April 1952.

22. L. Zernow, S. Kronman, F. Rayfield and J. Simon, "Flash Radiography of Collapsing 105mm Shaped Charge Liners," BRL Rpt. 846, Feb. 1953.

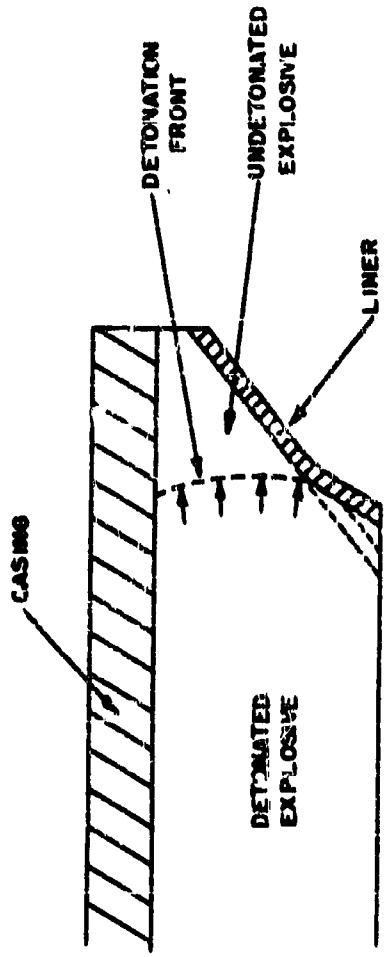
DETONATION FRONT
UNDETONATED EXPLOSIVE
LINER
CASING
DETONATED EXPLOSIVE

FIGURE 1

CHAPTER II

STATUS OF THEORY

Garrett Birkhoff

Harvard University
Cambridge, Massachusetts

L. H. Thomas

Watson Scientific Computing Laboratory
New York, N. Y.

§ 1. Detonation wave

The detonation process is most easily pictured in terms of the passage of a "detonation front" (see Fig. 1) through the explosive, with the velocity V_D in the range (1), (2) 5-9 mm/μsec (km/sec). Behind this detonation front, pressures p_1 of the order of 250,000 atm and temperatures $T_1 = 2500^\circ - 4000^\circ C$ are commonly observed (3). The total chemical energies feeding the detonation are of the order (1), (2) of $E = 1{,}000$ cal/gram. The detonation front is regarded as a shock surface followed by a "reaction zone" in which chemical reaction takes place, and the thickness of which is estimated (4)* to be of the order of 1mm for most solid explosives, corresponding to 0.1 microsecond reaction time.

From V_D, E, and an assumed equation of state, one can estimate p_1, T_1, and the particle velocity behind the detonation front by the conservation of mass, momentum, and energy. The so-called Chapman-Jouguet condition (5) gives a fourth equation, from which V_D itself can be predicted. However, the equations of state of solids under high temperatures and shock pressures are not accurately known (6), and so the preceding method is of limited practical value. See Chapter 7, § 2 for a more detailed discussion.

If one assumes that V_D is a constant for a given explosive, so that the detonation front propagates by Huygens' principle (7) (just as in geometrical optics), one has a rational basis for "shaping" explosive waves by peripheral initiation, or by using composite charges having different detonation velocities in different regions (e.g., having inert cores). Actually, V_D may be affected by the curvature of the detonation front, and composite charges are especially liable to imperfections.

*Some workers (see for instance Techn. Report XIII, Univ. of Utah, May 15, 1953, by Cook, Filler, and Keyes) consider it necessary to take into account a much wider band even for a first approximation.

In lined cavity charges, the primary effect of the explosive is through the collapse velocity V which it transmits to the liner, in the high-pressure zone behind the detonation front. This velocity is transmitted, by a complicated process of multiple shock reflection, (8), (9) in 5-50 μsecs. The net effect of these multiple reflections has been shown by Rostoker and Murray (10) (11) to be nearly the same as if the liner were rigid. The effect of finite charge dimensions and confinement are not easy to determine; Eichelberger* (12), (13), (14) has made rough estimates of these effects using a crude "release wave" concept which involves an empirical parameter K estimated by other experiments. Related estimates of the dependence $V = f(C/M)$ of casing fragment velocity on the charge to mass ratio C/M may be found in the classified literature. (15), (16), (17), (18), (19)

However, even for plane liners, the quantitative accuracy of the predictions is uncertain. The extension of the analysis to conical liners in cylindrical casings presents formidable new difficulties. Especially, the applicability of analogous formulas near the apex, the base flange, and to deeply fluted liners (§ § 4, 11) should be viewed with skepticism, until much more progress has been made.

§ 2. Jet formation: "zero order" theory

In the case of conical liners with cone angle 2α the simplest picture is to assume that the liner collapses with a constant velocity V_o, and in a constant direction. Applying Bernoulli's equation to a moving reference frame, this direction bisects the angle 2θ between the normal to the uncollapsed liner, and the normal to the collapsing liner (see Fig. 2a). If one then neglects internal shear stresses and shocks (increase of entropy), one obtains the steady state hydrodynamical theory of jet formation. According to this theory, the collapsing cone divides into a high speed jet and a slower slug, whose mass-ratio is (in terms of the angle β between the collapsing liner and the axis).

$$(1)\quad m_j/m_s = (1 + \cos\beta)/(1 - \cos\beta) = \cot^2(\beta/2),$$

and whose velocities are respectively

$$(2)\quad V_j = V_o \frac{\cos\alpha/2}{\sin\beta/2}, \qquad V_s = V_o \frac{\sin\alpha/2}{\cos\beta/2}.$$

As the details of this theory have been published**, we shall not repeat them here.

---

* Estimates of $V_o(x)$ may vary by 50% or more, depending on K.

** See (20) for the derivation. The form used here is that given in (21), equations (5a) - (6b), p. 534.

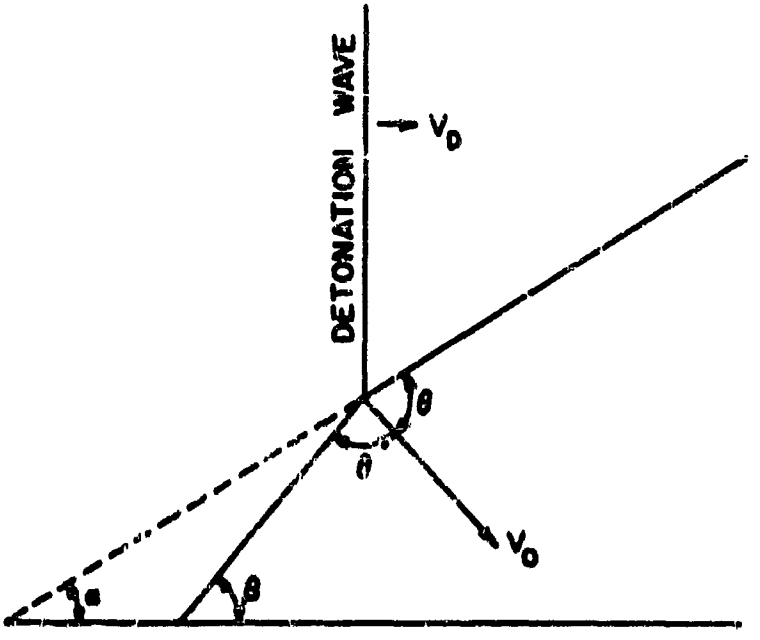

FIGURE 2a

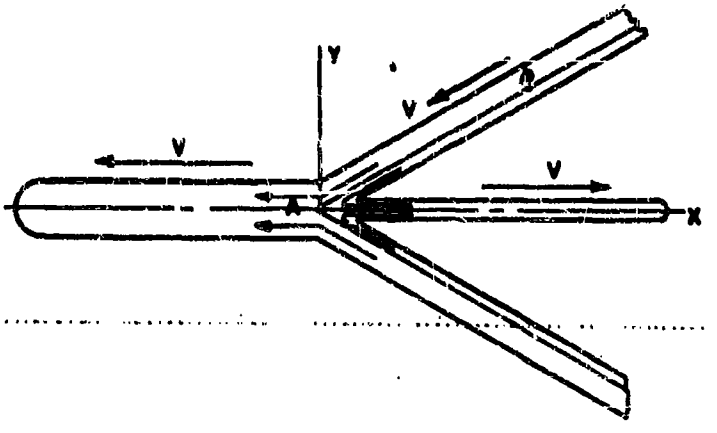

FIGURE 2b

We recall, however, that if an incompressible wedge-shaped liner is considered, the complete velocity field may be found by conformal mapping (22). This has sometimes led to the erroneous impression that incompressibility must be assumed in deriving equations (1) - (2). In fact, the assumptions needed to derive (1) - (2) are the following (cf. § 4).

(i) Steady state flow, in a moving reference frame. Strictly speaking, this requires a plane detonation wave, and a liner whose thickness is inversely proportional to the distance from the cone apex.

(ii) Shear forces are negligible. Since the yield stress of mild steel is only 8,000 atm.

(iii) Isentropic, shock-free flow (cf. § 5).

(iv) Constant pressure on the liner near the stagnation point J, the same inside and outside the liner.

(v) Asymptotically uniform flow in the liner, jet, and slug, away from the stagnation point J.

From the preceding assumptions, it follows that, relative to axes moving with the collapse (stagnation) point J, we have the Bernouilli equation (by (i) - (iii), and hence (by (iv) - (v)) the same relative velocity in the jet, slug, and collapsing liner (see Fig. 2b).

The equations (1) - (2) have been confirmed experimentally near the apex of the cone. Especially is this true of the predictions that the jet length should equal the slug length, and of the initial V_j. However, near the base of the cone, the collapse angle increases rapidly, the observed m_j/m_s is considerably larger (23)* than that predicted by (1), and the jet becomes several times longer than the slug. We shall now attempt to rationalise these facts, following ideas first explicitly formulated by Pugh. (21), (24), (25)** (26)

§ 3. Jet formation: "first order" theory

In H.E.A.T. shell with conical liners (Fig. 1), it is obvious that C/M, the charge/mass ratio in a cross-section, decreases from infinity to a small quantity, as one moves along the liner axis (x-axis) from apex to base. Hence (cf. § 1) the collapse velocity $V_o(x)$ may be expected to decrease correspondingly, in a way which can be roughly predicted. It would be desirable to have accurate direct experimental measurements of $V_o(x)$. However, inferences from X-radiographs are not accurate, and the "pin techniques" (27)*** seems difficult to apply.

* This was found in 1943 at Bruceton.

** See (25), where the theory purports to predict everything from m_j/m and v_j.

***The data were reported by Dean Mallory of the N. O. L.

If one assumes that (vi) there is negligible momentum transfer after the initial phases of the collapse process, one concludes that each liner element from the ring-shaped zone with initial position x moves with constant velocity $V_0(x)$ in a straight line until it reaches the liner axis.* Since the collapse direction bisects the initial angle between the initial normal to the collapsing liner and the normal to the original cone, one can predict from $V_0(x)$ and the initial collapse angle, the shape of the collapsing liner at all times. The predicted collapse profile agrees with observation, at least qualitatively.

As emphasized by Pugh, Eichelberger and Rostoker (30), (22) who originated the preceding "first order" theory, the inferred local collapse angle $\beta(x)$ and local relative velocity $V_1(x)$ on the axis will increase and decrease markedly as we move from apex to base. By (2), the increase in $\beta(x)$ accentuates the jet velocity gradient, so that $V_1(x)$ decreases to a fraction of its initial value.**

With thin cones, the relative change in $\beta(x)$ and $V_1(x)$ per liner thickness is small; hence it seems reasonable to assume that the theory of § 2 is locally applicable to these quantities. At least, this assumption gives a simple basis for calculating, as functions of x, the velocity $V_j(x)$ of jet formation and mass-ratio $m_j(x)/m(x)$.

§ 4. Applicability of theory

The group at Carnegie Tech. has published (32), (33), (34) experimental evidence confirming the idea that the jet mass and velocity gradient can be predicted approximately by the preceding "first order" theory. Briefly outlined, their confirmation proceeds as follows:

"The theory has been worked out in detail for the case where a plane detonation wave travels parallel to the axis of a conical liner. Four independent equations are obtained relating seven different variable functions of the coordinate x, where x defines the original position of a small element in the undisturbed liner. These seven variables are listed below, together with their definitions and the methods of determining them.

Variable	Definition	Method of Determining	Expt.
dm	Mass of original cone element.	Direct weighing of sectioned cones.	A
dm_s	Mass of slug element.	Slug sections from sectioned cones are recovered and weighed.	B
dm_j	Mass of jet element.	Inferred from $dm_j = dm - dm_s$.	

* The stability of this method of calculation has been discussed by Hudson and Gardner (28); see also § 12 below. Actually, plastic forces cause some deflection; see (29).

** Very good data are given in (31) by Breidenbach.

Variable	Definition	Method of Determining	Expt.
V_j	Velocity of jet element.	Measured as a function of M_j with a rotating mirror camera:	C
		combined with the collection and weighing of sections of the jet.	D
V_o	Velocity of collapsing cone element.	Difficult to measure directly, but may be approximated from the release wave theory.	
δ	Angle defining the direction of collapse of the liner element.	Difficult to measure.	
β	Angle between collapsing element and the cone axis.	Flash radiographs provide semi-quantitative values.	

Experiments A, B, C, and D, (35) performed on standard charges with steel liners, provided sets of values which could be used with the four independent equations to determine two independent sets of values for $V_o(x)$ and $\beta(x)$. The agreement between these two independent sets was excellent. Flash radiographs by Clark, (36) Breidenbach (31) and Zernow (37) on similarly shaped charges provide values of $\beta(x)$ that are in good qualitative agreement with the above sets. Experiments A, B, and C, performed on cones of aluminum copper, and steel, with apex angles from 22° to 88° and with liner thicknesses from 0.022 in. to 0.056 in. have provided similar semi-quantitative verifications for this wider range of variables. With this large variety of charges, the values of $V_o(x)$ estimated from "release wave" calculations are in fair agreement with those obtained by substituting the results of experiments A, B, and C into the four equations. Deviations appear to be in the direction expected from consideration of strength effects. "Release wave" calculations also have provided similar verification with charges having explosives shaped very differently from those in the standard charge."

However, the accuracy of the preceding "first order" hydrodynamical theory is obviously limited by the validity of assumptions (ii) - (v) of § 2, and the assumption (vi) of § 3, that the relative change in $\beta(x)$ and $V_1(x)$ per liner thickness is small. We shall now give an *a priori* discussion of the validity of these assumptions.* The magnitudes of the resulting departures from the simplified picture are not known and are very difficult to estimate.

(i) Near the end of collapse, when the liner necks down (see Fig. 3) it is hard to see why the Bernoulli equation should be locally applicable. Also, (v) seems unconvincing, and there is a considerable interchange of

*See (34) for a somewhat different analysis.

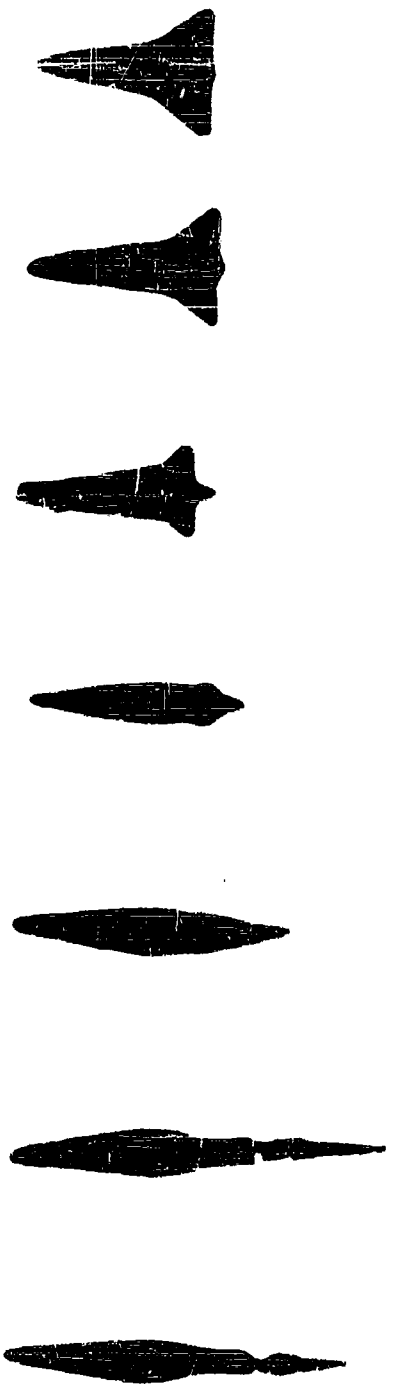

FIGURE 3

momentum between liner elements, contradicting (vi).

(ii) Metallurgical evidence indicates (38), (39) that the shear stresses are enough to heat the core of the liner up to 1500°F, corresponding to the mechanical energy of a velocity of 2500 meters/sec, or to a velocity drop from 8000 to 7600 meters/sec. Also, early Brucaton experiments (40), (41) showed that with reduced explosive energy, the ratio m_j/m_s was appreciably altered. Incidentally, shear strength is increased markedly by hydrostatic pressure (42). These facts indicate that hydrodynamical theories cannot be used much beneath the range of explosive energies involved, especially near the tail of the jet.

(iii) Heating by shock waves. The data of § 5 show that, with jet velocities only 2-3 times those obtained from service rounds, such effects are critical.

(iv) The explosive exerts a considerable pressure 'squeeze' on the slug. It is hard to estimate the magnitude of the pressure, but it would, of course, tend to lengthen the jet. X-radiographs reveal a high-pressure zone in the shape of an inverted cone,* and a change in the shape of the slug after collapse is complete.

- -

EDITORIAL NOTE

Since the preparation of this chapter by the authors, a useful analysis of shaped charge liner collapse has been developed to which attention should be called. Jackson and Clark considered the Problem of Lagrange. The equations of motion of two pistons driven by gas confined between them, were obtained in terms of dimensionless parameters and integrated in closed form. Rostoker (CIT) obtained a similar result for a more restricted case. The Jackson and Clark solution was applied to the element of a shaped charge liner. The shock reflected from the liner was included by using an enhanced sound velocity. The motion of the liner was taken normal to the surface, modified by a small component parallel to the surface due to the continuously varying pressure behind the detonation front.

Having thus obtained the mass, direction and velocity of the liner element, the characteristics of the slug and jet elements were obtained by the usual hydrodynamic methods.

The equations have been coded for use with the ORDVAC and solutions can be readily obtained for any liner whose generator can be represented by a continuous equation, and for point or peripheral initiation. To date several cases have been computed for which experimental values are available for comparison. The agreement was good.

The end result obtained is similar to that obtained by the CIT Release Wave and Generalized Shaped Charge Theories but no direct comparison of numerical results from the two theories has yet been made.

*Evident in BRL photographs, taken by Sultanoff. For the change in the slug, see Breidenbach, BRL 808. (31)

§ 5. Ultra-fast jets

Some light is shed on the limitations of hydrodynamical jet theories by data recently released by Los Alamos (6). Among the relevant facts observed experimentally, the following deserve mention.

As first suggested in 1945 by K. Fuchs and P. Stein, for a sufficiently small angle between two impinging plane surfaces (corresponding to the collapse of a wedge-shaped liner), a jetless impact is possible. The critical angle is the same as for attached shock flow past a wedge, and is about 30° for dural, mild steel, lead, and brass, at impact velocities of around 3 Km/sec. (Fig. 4).

Mathematical analysis shows (43) that no analogous jetless collapse of conical liners is possible. Consequently, the use of converging detonation waves and very small cone angles 2α should yield arbitrarily high jet velocities V_j of about $2V_0 \csc \alpha$, according to the hydrodynamical theories (44)* of §§ 2-3. However, actual jets traveling at these speeds tend to spread laterally as if they were gaseous, and deviations from the hydrodynamical theory become evident for V_j around 50 Km/sec.

§ 6. Jet break-up

Due to the jet velocity gradient already mentioned, the jet may be expected to lengthen continuously, while moving ahead in a straight line.** In the case of well-formed (cf. Ch. III), unrotated (cf. Ch. VII) charges and liners, a straight, steadily lengthening jet is in fact observed. However, real jets always break-up into streams of particles sooner or later (See Fig. 3). The time of break-up has an important effect on penetration (cf. § 8 below).

With steel liners, break-up ordinarily occurs within a few cone diameters of travel (48), while for copper liners, as first predicted (49)*** by Pugh and later confirmed experimentally, considerable ductile drawing occurs, and break-up is much later. There are extensive empirical data on the mass-distribution of jet particles (52)**** while the existence of

---

* For example, if V_0 = 3 Km/sec. and $2\alpha = 10^\circ$, V_j = 80 Km/sec.

** For mathematical details, see (45), (46), or (47).

*** For experimental confirmation, see (50) and (51).

**** See recent jet x-ray pictures taken at the BRL, and CIT data.

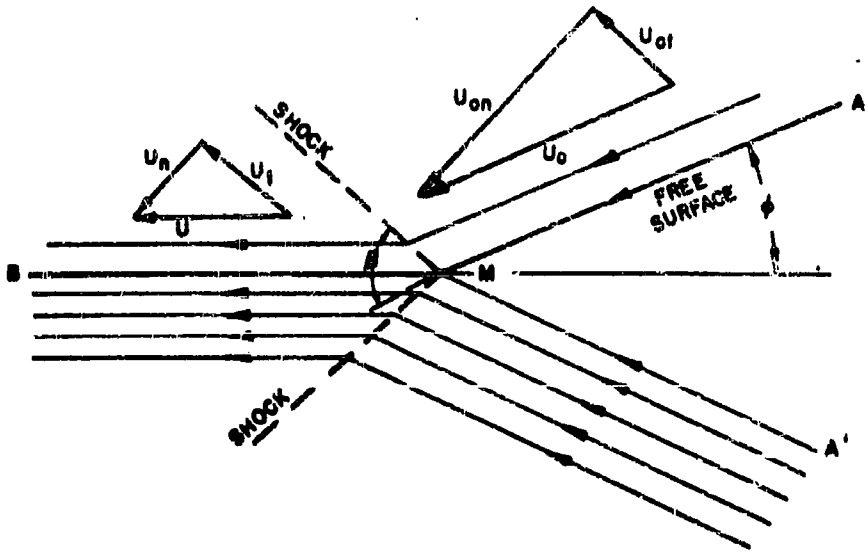

FIGURE 4

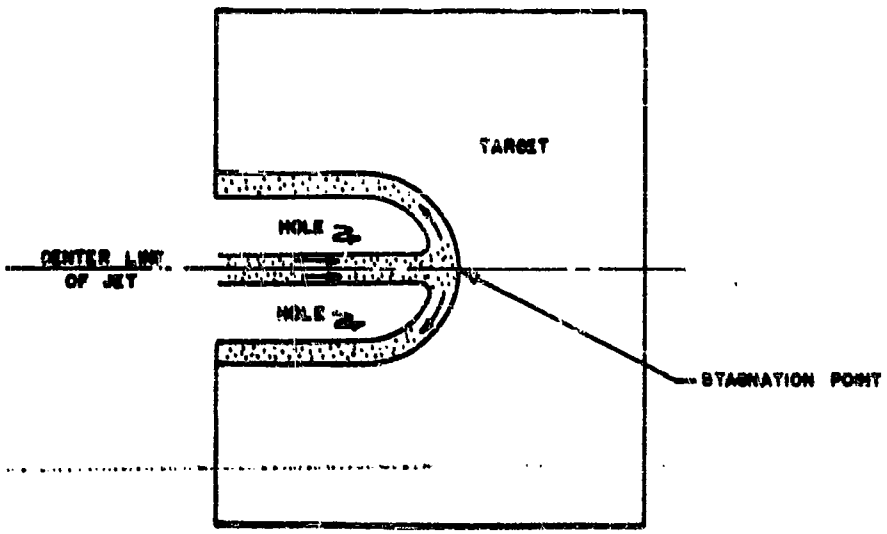

FIGURE 5

adequate theories* of the break-up of steel shell and bomb cases suggests that analogous quasiempirical theories of jet break-up can perhaps be constructed, within the framework of the classical mechanics of continua.

The conditions of fracture under tension are not yet very clearly understood. For a good theory we would need to know, in the first place, how the stress in the material depends not only on the strain but on the rate of strain and on the past history. (54)**

The facts that face-centered cubic crystals tend to be ductile (56) and that cast iron and steel behave so differently under ordinary conditions suggest that a fundamental theory must take account of crystalline and polycrystalline structure of the material. Further, actual fracture may involve an instability of plastic flow or the propagation of a crack (54)** and may, for this reason, also happen differently at high speeds.

§ 7. Similarity

If the diameter is taken as the unit of length, the "Law of Crans" asserts that geometrically similar shaped charge rounds of widely varying diameter d behave approximately similarly (57), (58).***

The best theoretical basis for this fact consists in the principle (30, 30a) that the inertial and explosive stresses involved depend mainly on the (57), (58)*** strain and much less on the time rate of strain. Although this principle is not exact, and is presumably not applicable to the reaction zone, to viscous effects, or to jet break-up, it has sufficient validity to be very useful in analyzing existing data.

Applied to rotating shaped charges, it predicts that the relative deterioration in shaped charge performance due to spin, with similar rounds of different diameter d spinning at ω r.p.s., should be determined by the spin parameter ωd measuring the peripheral velocity rather than by ω itself. This peripheral velocity ωd is clearly V_1/n, where V_1 is the impact velocity, and $1/n$ the twist of rifling (in turns per caliber).

---

* For theories of shell fragmentation, see N. F. Mott, (53).
** For the variation in stress with rate of strain, see (55).
***See also the extensive tests by Schardin, to be reported in Vol. 6 of the Comm. Appl. Math.
****For the argument, see G. Birkhoff (59), where various special cases are treated.

The preceding prediction is in fair agreement with available experimental data.*

Considerations of similitude often help greatly in determining the limits of applicability of theories, which are commonly invariant under large groups of transformations. For instance, with explosives having the same adiabatic constant γ, if the liner and casing are treated as incompressible fluids, then the behavior is geometrically similar with reduced velocity $\propto v/\sqrt{E}$, regardless of the explosive energy E, provided that the detonation velocity is lowered in proportion to $\sqrt{E}$. Hence, reductions in penetration which occur ** with dilute explosives like those due to the strength of the target material are probably correlated with limitations in the applicability of strictly hydrodynamical theories like those of §§ 2-3 and § 8.

§ 8. Penetration: "zero order" theory

A continuous perfectly formed fluid jet of density ρ_j, moving with constant velocity V_j, should penetrate a target of density ρ with a constant velocity U, which can be roughly predicted*** from the continuity of pressure at the "stagnation point" (Fig. 5), where the tip of the jet is boring into the target. In a reference frame moving with velocity U, neglecting target strength and compressibility, Bernoulli's Theorem assumes the simple form

$$(3)\quad \tfrac{1}{2}\rho_j (V_j - U)^2 = \tfrac{1}{2}\rho U^2.$$

Hence, the rate of penetration U satisfies the equation

$$U = (\rho_j/\rho)^{1/2} (V_j - U),$$

where $V_j - U$ is the rate at which the jet is being used up. Solving, we get the Hill-Mott-Pack equation****

$$(4)\quad P = (\rho_j/\rho)^{1/2} L,$$

connecting the total depth of penetration P with the total jet-length L, for uniform, incompressible fluid jets.

---

* See (60), where the contrary conclusion is reached that $P/d = f(\omega)$; Theory suggests $P/d = f(\omega d)$. However, "spitback" fuzes support the view expressed here, as do more recent C.I.T. experiments. See (61).

** Early Bruceton experiments.

*** The method is due to R. Hill, N. F. Mott, and D. C. Pack (62).

**** MacDougall and Pugh obtained this equation independently.

Because of the assumption V_j = const., which corresponds to the model of § 2, this may be called a "zero order" theory. Combining with § 2, we see that $L = (d/2) \csc \beta$ is nearly the cone slant height. Actually, total penetrations several times this depth are obtained at large standoff for reasons explained in § 9. However, equation (3) can be used to infer the useful equations

$$(5) \quad U = V_j/(1 + \sqrt{\rho/\rho_j})$$

$$(5') \quad p_s + \tfrac{1}{2} \rho U^2 = \tfrac{1}{2} \rho_j V_j^2/(1 + 2\sqrt{\rho_j/\rho} + \rho_j/\rho),$$

from which the <u>instantaneous</u> penetration velocity U and stagnation pressure p_s can be approximately inferred.

Thus (63) Ca jets penetrating H_2O at 4 mm/μsec have been observed by Kerr cell photography. Again, a 10 mm/μsec steel jet will penetrate a steel target at $U = V_j/2 = 5$ mm/μsec, according to (5), giving a stagnation pressure $p_s \cong 500{,}000$ atm., roughly. This obviously greatly exceeds the yield strength of steel, justifying the hydrodynamical model.

In two dimensions (e.g., for wedge-shaped cutting charges), even the pressure <u>distribution</u> can be determined mathematically. (64)

§ 9. <u>Penetration: "first order" theory</u>

The considerations of § 3 lead to an important modification of formula (4) due to Pugh and Fireman (65), (66), (46) (67)* which explains the observed variation in penetration with standoff. In this modification, one assumes a <u>gradual</u> variation in the jet velocity and density along its length, so that Bernoulli's Theorem is <u>locally</u> applicable. This gives

$$(4a) \quad P = 1/\sqrt{\rho} \int d\ell / \sqrt{\rho_j(x)}$$

where $\rho_j(x)$ is the "effective" density of the jet when it reaches the target.

Looking only at the first factor in (4a), we see that, <u>for different target materials</u>, $P \propto 1/\sqrt{\rho}$. Thus, weight for weight, low density materials provide the best defense against shaped charges, as long as $V_j(x)$ is so large that the target yield-strength is negligible. For mild steel, with a yield strength of 8000 atm., this corresponds to $V_j >> 450$ meters/sec, which is not verified near the tail end of the jet. This explains qualitatively why penetrations into mild steel are 10% - 15% deeper than into armor: The latter has greater yield strength.

---

* The qualitative idea is in (68).

However, the proportionality $P \propto 1/\sqrt{\rho}$ has been confirmed approximately for many materials, quartz-like materials being the most notable exceptions.* A more detailed discussion will be given in Ch. IX.

Looking directly at (4), or at its refinement (4a), it is clear that the improvement in penetration P with standoff S may be explained qualitatively by the tendency of the jet to lengthen as it progresses, and hence, indirectly, by the velocity gradient along the jet. This factor, rather than any overall increase in velocity, is considered responsible for the improvement in penetration with peripheral initiation. (69), (70)

The quantitative application of (4a) requires a successful prediction of ρ_j. This is variable, because of jet break-up, rotation, and other factors. It is convenient to distinguish several cases, in trying to describe the dependence of penetration P on standoff S.

I. In the case of well-formed Cu jets, it is believed that ductile drawing makes ρ_j constant, out to a large standoff. Hence $P = P_o(1 + a S)$. Other fluid jets are less effective: this may be due to lower density, wavering, or other factors (71).

II. In the case of perfectly aligned particle jets, ρ_j decreases in inverse proportion to de, so that a formula of the type $P = P_o\sqrt{1 + a S}$ is inferred.

III. In the case of unaligned jets, whether due to imperfections or rotation, ρ_j decreases also in proportion to S^2 due to "spreading," so that a formula of the type $P = \frac{P_o\sqrt{1 + aS}}{S}$ is inferred.

Curves of the preceding type can be roughly fitted to observed data; the large experimental scatter prevents more exact conclusions from being drawn. Ideally, especially in Case I, it might be possible to infer an optimum $V_o(x)$ from theoretical considerations. But a large amount of empirical work at Bruceton, during World War II, failed to improve substantially on conical liners.

Remark 1. Although the preceding "first order" hydrodynamical theory of penetration has been applied above only to homogeneous targets, simple extensions give a quite adequate explanation of penetration into non-homogeneous, spaced or laminated targets. These extensions involve a concept of "residual penetration," which we have not space enough to explain here.**

* For a discussion of this, see Chap. IX, § 5. Another exception is provided by abnormally deep penetrations into lead; still another, by the fact that penetrations into mild steel are 10% - 15% deeper than those into lead. These facts may be correlated with differences in yield point, or with the concept of "afterflow" (cf. (68), and (66) p.87).

** See (72) for details.

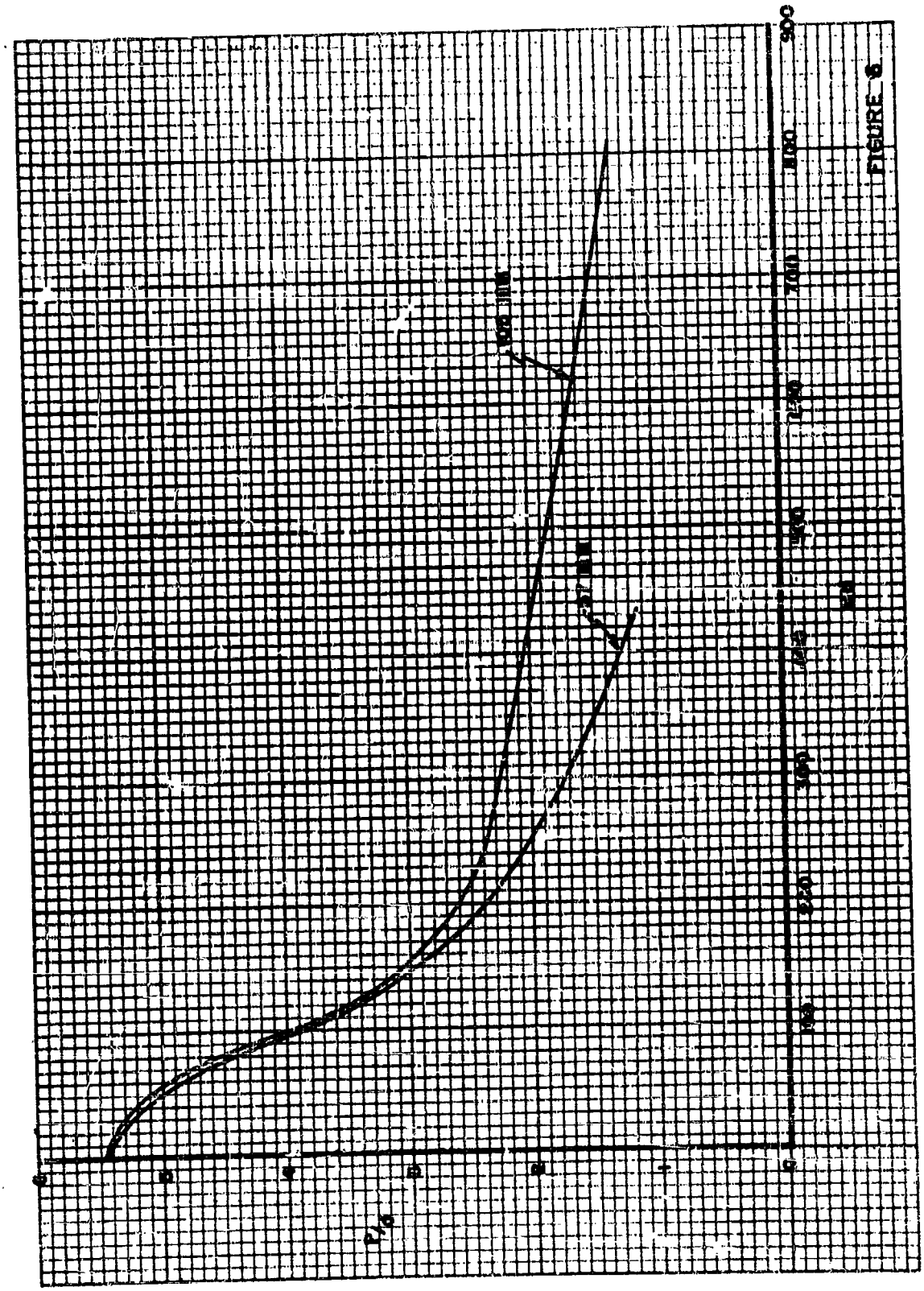
FIGURE 6
300
700
P/D

Remark 2. The hole volume is harder to predict theoretically. "Helie's Law" of the proportionality of hole volume to available energy (jet energy) is approximately valid* at low speeds. According to the hydrodynamical theory (64) infinite volumes could be obtained, but the yield-stress limits the growth of the hole.

§ 10. Effect of Rotation

It was observed as early as 1943 that rotation caused a large decrease in penetration P, and that this effect was especially noticeable at large standoff.** Typical records of P/d as a function of ω d (cf. § 7 above, Ch. VII below) are plotted in Fig. 6. The reduction in penetration by spin may be attributed to lateral dispersion of the jet, which decreases its effective mean density. This lateral dispersion is also evident in X-radiographs.*** Thus, the jet velocity and momentum are about the same as for unrotated liners (77).

Assuming that jet particles move in straight lines, we may correlate with the penetration theory of § 9, since the mean density ρ will be proportional to the inverse square $1/S^2$ of the standoff S. Thus, at large standoff S, the penetration P should be proportional to 1/S, and one may expect a decrease in penetration as standoff lengthens.

The X-ray pictures sometimes show a bifurcation of the jet (78) and a theory of the instability of a lengthening rotating jet is in process of construction (see § 11 (iii) below).

§ 11. Spin compensation

Attempts have been made to improve the performance of spin-stabilized shell, by using various non-conical, axially symmetric liners (cf. Ch. VII below). However, such attempts have not been promising at high rates of spin**** and so the major emphasis has been on the design of fluted liners not having axial symmetry.

The idea underlying the use of fluted liners is that of "spin compensation" - i.e., of annihilating the angular momentum of the liner so as to inhibit the jet spreading already discussed (§ 10). This is not quite the same as the original idea of using "offsets" (cf. Fig. 7a) to make most of the liner collapse on the axis.

---

* Relevant data for particle impacts have recently been obtained at C.I.T. Earlier data reported by Roberts and Ubbelohde, (73) or (74) are consistent with Helie's Law. There is an interesting analogy with the cavities formed behind missiles entering water, cf. (75) and (39), p. 12.

** See (39), Sections V, XII, for World War II data and references.

*** See (76), where a good discussion of the preceding material may be found.

**** They may, however, be adequate for slowly spinning rounds. Adequate compensation for normal, spin-stabilized rounds at 2000 f/s has not yet been achieved by any means.

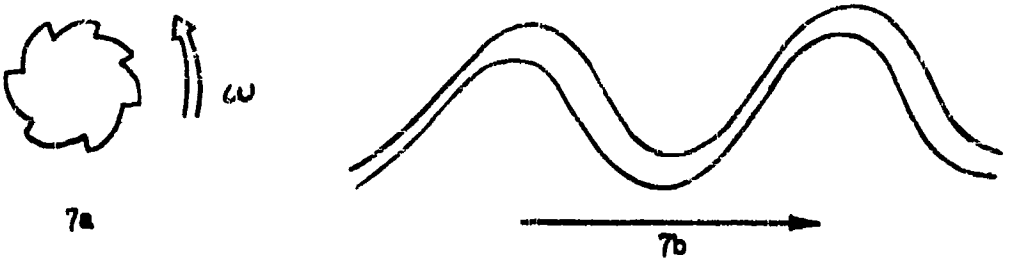

7a

7b

Generally speaking, one may hope to achieve some spin compensation by using wavy flutings, in which the wall is thicker on the forward side, as in Fig. 7b. This is because the momentum transferred is nearly normal to the liner surface, and proportional to its thickness.*

Near the base of the liner, where rotation effects are most serious, one may also hope to convert some of the axial momentum of the explosive behind the shock wave into rotational momentum, by using spiral flutings, whose angle with a meridian plane becomes progressively steeper.

However, the mechanism of spin compensation is not yet clearly understood. Thus, with several designs, even the direction of spin compensation is reversed by changing the number of flutings, and this seems hard to explain. Again, the consideration that uniform pressure of the explosive on the surface, however fluted, would produce exactly zero compensation, shows that a fairly sophisticated theory is required, which must probably include a detailed discussion of the explosive-liner interaction, perhaps by numerical methods (see § 12 below).

For the present, we must rely mainly on empirical data. Any successful theory must explain not only the direction of spin compensation but also its magnitude for the shapes discussed in detail in Chap. VIII.

§ 12. Perturbation methods

When a problem is too complicated for exact analytical solution, it is often possible to start with an exact solution of a special case or of a simplified problem, and to consider the effect of small departures ("perturbations") from this solution. To the first order in the perturbation, we have a linear problem, which will, however, usually still be too difficult for analytical solution. If further the linear problem turns out to have separable variables, in general or in special cases, or if some special cases, on account of symmetry, involve only one variable, one may be able to obtain analytical solutions.

In general, in order to carry out such a program, one must make drastic restrictions on the properties of the materials involved, or on the initial conditions, to obtain an exact solution from which to start. Also, one can often solve the linear perturbation equations analytically, by separating variables, only for special cases or configurations. In the end, we usually have the further approximation that the perturbation is taken into account only to the first order.

*See (79). A qualitative discussion of this was given in (80).

We must therefore be very cautious in making applications of the results of perturbation calculations for shaped charges, especially since we do not have at all exact knowledge of the properties of the materials under the actual conditions. They do, however, where they can be made, give insight into the stability of the exact solutions.

It would be encouraging if we could obtain perturbation solutions starting from the steady state two-dimensional flow or axially symmetrical three-dimensional flow described above (§ 2) so as to estimate the effects of departure from steady state conditions on account of geometrical factors or of the continuing pressure of the explosive gases as well as the effects of the actual compressibility and of the internal stresses in the material, but only some very special cases, of which we shall give three examples, have been treated with any success.

(i) If we suppose the liner to be very thin and weak (one-dimensional), and neglect its internal stresses completely, even the hydrostatic pressure, we may obtain* simple equations for its motion under continuing explosion gas pressure. If a denotes the Lagrangian mass variable, and $x(a,t)$, $y(a,t)$ denote the position of a point on the liner, the equations of motion are

$$(7)\quad \partial^2 x/\partial t^2 = -p\,\partial y/\partial a,\quad \partial^2 y/\partial t^2 = p\,\partial x/\partial a,$$

where $p(t)$ denotes the pressure at time t supposed constant in space. These equations are essentially unstable, in the sense that any waviness increases exponentially, and it is tempting to relate this to the extreme sensitivity of performance to initial departure from symmetry (Chs. III IV, V). It should, however, be remarked that constant pressure could not be maintained by the gases against exponentially increasing waviness, and in the limiting case of the flow of gas into a vacuum, a definite smooth boundary may be maintained.

(ii) By perturbing the exact solution, due to Rayleigh, for a collapsing spherical or cylindrical cavity surrounded by incompressible fluid, one can show that the inner wall tends to be stable while it is being accelerated radially, and unstable while it is being decelerated. These are the well-known conditions of Taylor instability. In addition, in the case of a spherical cavity having inward radial acceleration, there is an instability due to negative damping.** (81), (82)

(iii) The stability of a very long uniform uniformly extending jet may be investigated by perturbation theory (83). If we suppose the material incompressible, the steady motion remains geometrically similar to itself under longitudinal extension and lateral contraction even if rotation and internal stresses of plastic type are taken into account. The yield stress may even change with time, as by work hardening.

*See footnote * page 23, with references.

**The instability due to negative damping was first pointed out by one of us.

In terms of time t and coordinates x, y, contracting transversely and z extending longitudinally (so that $x/\sqrt{t}$, $y/\sqrt{t}$, and z t, are unscaled coordinates), the equations for small changes in velocity proportional to $u\sqrt{t}$, $v\sqrt{t}$, and w/t, take the form

$$\rho\left(\frac{\partial u}{\partial t} - 2\gamma t\, v\right) = t\left(\frac{\partial p_{xx}}{\partial x} + \frac{\partial p_{yx}}{\partial y}\right) + \frac{1}{\sqrt{t}}\frac{\partial p_{zx}}{\partial z}$$

$$\rho\left(\frac{\partial v}{\partial t} + 2\gamma t\, u\right) = t\left(\frac{\partial p_{xy}}{\partial x} + \frac{\partial p_{yy}}{\partial y}\right) + \frac{1}{\sqrt{t}}\frac{\partial p_{zy}}{\partial z}$$

$$\rho\frac{\partial w}{\partial t} = \frac{1}{\sqrt{t}}\left(\frac{\partial p_{xz}}{\partial x} + \frac{\partial p_{yz}}{\partial y}\right) + \frac{1}{t^2}\frac{\partial p_{zz}}{\partial z}$$

where γt is the angular velocity of rotation and p_{xx}, ... p_{zz} are components of stress.

The perturbation equations are separable in suitable variables, but we still have to determine the rate of change of amplitude of various modes in a complicated linear system whose coefficients are variable in the time. The frequently observed bifurcation under rotation may perhaps be understood qualitatively, when the solution has been carried through.

In jet break-up problems, the initially high internal hydrostatic pressure rapidly drops to zero and, for a rotating jet, becomes negative, so the assumption of incompressibility may be not too far from the truth.

§ 13. Numerical methods

Most unsolved shaped charge problems are highly non-linear, and cannot be solved analytically or by perturbation methods. Hence they must be solved numerically.

For numerical solution, problems can be roughly classified according to the number of independent variables involved, and to whether they are of elliptic, hyperbolic, parabolic, or mixed type. Elliptic problems in n variables involve about as much work (84) as hyperbolic problems in n + 1 variables, provided steps in the space-like variables are about $c\,\Delta t$, where Δt is the time step, and c is the analog of sound velocity (85).

Thus the simplest shaped charge problems for numerical solution concern the collapse of plane, cylindrical and spherical cavities under appropriate detonation waves, and involve only one dimension of space, and time. The order of difficulty is the same as for problems concerning the propagation of plane, cylindrical and spherical blast

waves, on which much numerical work has been done using desk machines (86). The principal difficulty comes in knowing the right equation of state. Once this is known, rapid progress may be hoped for, especially in the initial phases of collapse, when the differential equation is hyperbolic.

Most other unsolved shaped charge problems are too laborious for desk machines, and require large-scale computing machinery. The newer automatically sequenced computing machines are fast enough to make practical the solution of problems requiring 10^9 or fewer arithmetical operations. This permits the solution of problems of elliptic type in two variables, or provided the natural mesh-ratio $\Delta x/\Delta t$ giving good information is about c, of hyperbolic type in three variables. We shall now outline some problems which fall within these limitations.

§ 14. Some possible problems

The first class of such problems concerns "steady state" plane or axially symmetric jet formation and penetration (§§ 2,8). These are, in general, problems of mixed hyperbolic-elliptic type involving two space dimensions. When actual time variation is taken into account, we have a problem of hyperbolic type involving two space dimensions and time.

The axially symmetric case includes the general problem of a smooth conical liner. The plane case includes the general problem of a wedge-shaped liner. This case also includes the collapse of a cylindrical detonation wave on a fluted cylindrical liner, which may furnish us some information about the mechanism of spin compensation.

More generally, a steady state solution exists if the initial distribution of matter is two-dimensional and if the detonation wave travels in the third space dimension. The most general case will give us the spin-compensation for a fluted cylindrical liner, and we may hope that the earlier part of the motion will be of hyperbolic type. When, however, the geometrical interference leading to the production of a slug and jet has to be taken into account, the problem must become of elliptic type. The line of demarcation should be similar to the sonic line in fluid flow partly supersonic and partly subsonic, and may well include a strong shock.

It is tempting to do the hydrodynamical (incompressible, non-viscous) case first, because the differential equations are simpler. Thus the two-dimensional jet can be compared with the analytical solution (§ 2 above), while the axially symmetric case has also been solved approximately by relaxation methods (84).

However, the compressible case may actually be easier to solve in the initial phases of collapse than the incompressible case, because it reduces the problem to one of hyperbolic type. Indeed, low compressibility is probably a disadvantage, because it leads to a high sound

velocity c, and necessitates using a very short time step.

It is to be hoped that the introduction of plastic forces in the liner will have the effect of viscous forces in hydrodynamics of smoothing over shock fronts, so that we will not need to complicate the numerical work to take them into account (87); to do so would probably take problems involving two space dimensions and time out of range. At the same time, to follow a motion started nearly impulsively from initial rest should not get one into trouble with turbulence. (The actual observed formation of Mach Y's including slip streams at oblique reflections of shocks in fluids may warn us not to put too much trust in this hope.)(90)

The general problem of the impact of the detonation wave on a fluted conical liner and the subsequent collapse of the liner and formation of a jet and slug involves three space variables and time. Hence it is probably too complicated for presently available machines.

REFERENCES

1. J. E. Ablard, "Detonations," N. O. L. Report.

2. R. H. Kent, Jour. Appl. Phys. 13 (1942), p. 350.

3. W. G. Penney, and others, Proc. Roy. Soc. A-204, 1950.

4. W. G. Penney, Nature, Feb. 11, 1950, p. 214.

5. R. Courant and K. Friedrichs, "Supersonic Flow in Shock Waves," Chapter II.

6. J. M. Walsh, R. Shreffler, and F. V. Willig, "Limiting Conditions for Jet Formations in High Velocity Collisions," Jour. Appl. Phys. 24 (1953), 349-59.

7. Carnegie Institute of Technology, CIT-ORD-28, Part B, p. 3.

8. Carnegie Institute of Technology, CIT-ORD-37, pp. 14-68.

9. F. Charlton, "A Theoretical Treatment of the Misnay-Schardin Effect," ADE 10/50.

10. Rostoker and Murray, Carnegie Institute of Technology, CIT-ORD

11. Friedrich, Keller, and Lax, "Remarks about the Effect of the Detonation Wave on the Liner of a Shaped Charge," Institute for Mathematics and Mechanics, New York University.

12. Carnegie Institute of Technology, CIT-ORD-36, p. 29.

13. Carnegie Institute of Technology, CIT-ORD-38.

14. Carnegie Institute of Technology, CIT-ORD-40, pp. 30-48.

15. G. I. Taylor, R. C. 193.

16. R. W. Gurney, "The Initial Velocities of Fragments from Bombs, Shell, and Grenades," BRL Report 405, Sept. 1943.

17. L. H. Thomas, "Theory of the Explosion of Cased Charges of Simple Shape," BRL Report 475, July 1944.

18. T. E. Sterne, "A Note on the Initial Velocities of Fragments from Warheads," BRL Report 648, Sept. 1947.

19. R. G. Shreffler and W. E. Deal, Jour. Appl. Phys. 24 (1953), 44-9.

20. G. Birkhoff, E. M. Pugh, D. P. MacDougall, and G. Taylor, Jour. Appl. Phys. 19 (1948), pp. 563-582.

21. E. M. Pugh, R. J. Eichelberger, and N. Rostoker, Jour. Appl. Phys. 23 (1952) pp. 532-536.

22. L. M. Milne-Thomson, "Theoretical Hydrodynamics," § 11.43.

23. E. M. Pugh, "Theory of Lined Hollow Charges," Transactions of Symposium on Shaped Charges held at the Ballistic Research Laboratories Nov. 13-16, 1951, BRL Report 837, p.30, Fig. 14.

24. Reference (23) pp. 11-31.

25. Carnegie Institute of Technology, CIT-ORD-27, Part B.

26. W. H. Evans, A. R. E. E92 (1948).

27. H. Dean Mallory, "The Pin Technique for Velocity Measurements," Transactions of Symposium on Shaped Charges held at the Ballistic Research Laboratories Nov. 13-16, 1951, BRL Report 837, pp. 175-80.

28. G. E. Hudson and C. Gardner, "Generalisations Concerning the Motion of a Thin Shaped Charge Liner With an Arbitrary Initial Contour," Transactions of Symposium on Shaped Charges held at the Ballistic Research Laboratories, Nov. 13-16, 1951, BRL Report 837, pp. 61-74.

29. Carnegie Institute of Technology, CIT-ORD-44.

30. Carnegie Institute of Technology, CIT-ORD-31.

31. H. I. Breidenbach, "The Evaluation of Jets From Cavity Charges as Shown by Flash Radiographs," BRL Report 808, April 1952.

32. R. J. Eichelberger and E. M. Pugh, Jour. Appl. Phys. 23 (1952), p. 537.

33. Carnegie Institute of Technology, CIT-ORD-27.

34. Carnegie Institute of Technology, CIT-ORD-31.

35. References (23), pp. 22-31.

36. J. C. Clark, Jour. Appl. Phys. 20 (1949), pp. 363-370.

37. L. Zernow, S. Kronman, J. Paszek, and B. Taylor, "Flash Radiographic Study of Jets from Unrotated 105mm Shaped Charges," Transactions of Symposium on Shaped Charges held at the Ballistic Research Laboratories, Nov.13-16, 1951, BRL Report 837, pp. 119-132.

38. H. P. George, Frankford Arsenal Report R-667, Project 3/324.

39. G. Birkhoff, "Hollow Charge Anti-Tank Projectiles," BRL Report 623, Feb. 1947.

40. OSRD 2070, 2072, and 2815

41. A. C. 4130

42. P. W. Bridgeman, "Large Plastic Flow and Fracture, p. 282.

43. G. Birkhoff and J. M. Walsh, "Conical, Axially Symmetric Flows," to appear in the Riabouchinsky Anniversary Volume published by the French Ministere de l'Air.

44. Jour. Appl. Phys. (1948) p. 571.

45. OSRD 3752

46. G. Birkhoff, "Remark on the Hill-Mott-Pack Theory of Penetration of Monroe Jets." BRL Report 497, October 1944.

47. Reference (23), p. 14.

48. Reference (37), esp. Fig. 8

49. OSRD 5754, pp. 88-9.

50. Reference (23), p. 16.

51. Reference (37), pp. 128-9

52. Evans and Ubbelohde, ARD Expl Rep. 412/43.

53. N. F. Mott, A. C. 4035.

54. A. Nadai, "Theory of Flow and Fracture of Solids," 1950.

55. G. I. Taylor, R. C. 36.

56. Barrett - Structure of Metals
L. Zernow, J. Simon, "High Strain Rate Plasticity of Liner Materials and Jet Behavior," Transactions of the Symposium on Shaped Charges held at the Ballistic Research Laboratories, 7-9 Dec. 1953, BRL Report 909.

57. Reference (39), Section VI, and references given there.

58. A. C. 6366.

59. G. Birkhoff, "Hydrodynamics," Ch. III.

60. H. Winn, "Minimizing The Effect of Rotation Upon the Performance of Lined Cavity Charges," Transactions of Symposium on Shaped Charges held at the Ballistic Research Laboratories, Nov. 13-16, 1951, BRL Report 837, p. 340, Fig. 1.

61. Carnegie Institute of Technology, CIT-ORD-R30.

62. R. Hill, N. F. Mott, and D. C. Pack, Theor. Res. Rep., 2/44, Jan., 1944.

63. Carnegie Institute of Technology, CIT-ORD-26, p. 16.

64. Reference (59), Ch. II.

65. OSRD 3752, May 1944.

66. NDRC Symposium, pp. 79-102.

67. Carnegie Institute of Technology, CIT-ORD-9.

68. OSRD 1338.

69. A. D. Solem, and W. T. August, "Performance of Peripherally Initiated Shaped Charges," Transactions of the Symposium on Shaped Charges held at Ballistic Research Laboratories, Nov. 13-16, 1951, BRL Report 837, pp. 83-96.

70. Carnegie Institute of Technology, CIT-ORD-40.

71. Reference (23), p. 15.

72. OSRD 6384.

73. A. E. D. Expl. 606/66

74. H. C. 7434

75. G. Birkhoff and R. Isaacs, NAVORD Report 1490.

76. L. Zernow, S. Kronman, F. Rayfield, J. Passek, and B. Taylor, "Flash Radiographic Study of Jets From Rotated 105mm Shaped Charges," Transactions of the Symposium on Shaped Charges held at the Ballistic Research Laboratories, Nov. 13-16 1951, BRL Report 837, pp. 133-50.

77. Bruceton report SC-8.

78. L. Zernow, J. Regan, J. Simon, and I. Lieberman, "Study of the Effects of Rotation Upon the Penetration of Jets from 105mm Shaped Charges," Transactions of the Symposium on Shaped Charges held at the Ballistic Research Laboratories, Nov. 13-16 1951, BRL Report 837 pp. 319-330.

79. L. H. Thomas, "A Zero Order Theory of the Initial Motion of Fluted Hollow Charge Liners," Transactions of the Symposium on Shaped Charges held at the Ballistic Research Laboratories, Nov. 13-16 1951 BRL Report 837, pp. 353-358.

80. Carnegie Institute of Technology, CIT-ORD-R6 (1949) pp. 24-5.

81. Cole, "Underwater Explosions," p. 311.

82. A. S. Binnie, Proc. Camb. Phil., 49 (1953), 151-5.

83. G. F. Carrier, "On the Stability of an Elongating Metal Jet," BRL Report 862 April 1953.

84. L. H. Thomas and J. Sheldon, Jour. Appl. Phys. 24 (1953).

85. Courrant, Friedrichs, and Lewy, Math. Annolen. 98 (1927) p. 179.

86. G. I. Taylor, "The Air Wave Surrounding An Expanding Sphere," Proc. Roy. Soc. A186 (1946), pp. 273-292.

87. Becker, Zeits, F. Phys. 8 (1922), 321-62.

88. L. H. Thomas, Jour. Chem. Phys. 12 (1944), 149.

89. Von Neumann and Richtmyer, Jour. Appl. Phys. (1952).

90. Reference (5), p. 332.

CHAPTER III

LINER PERFORMANCE

John E. Shaw

Ballistic Research Laboratories
Aberdeen Proving Ground, Maryland

A. Introduction

1. Measures of liner performance

The performance of a shaped charge liner would logically be expressed in terms of the characteristics of the jet produced: velocity, length, velocity gradient, density, and mass distribution. What this jet accomplishes in penetrating a given target depends as much on the target as on the jet. However, it is difficult to determine some of the jet characteristics, while penetration into a given target is readily measured, and the ability to perforate a given target and to cause damage behind the target is the end result actually wanted in most cases. For this reason, liner performance is measured in terms of penetration into some homogeneous reproducible material, usually mild steel. Both mild steel and homogeneous armor are used, but the two are not equivalent. Different grades or types of mild steel all give about the same average penetration for a given shaped charge design but this is not true for homogeneous armor. It is reported (1) that the penetration of a given jet into steel at a fixed standoff varies essentially linearly with the Brinell hardness of the steel. Recent work at Ballistic Research Laboratories and Firestone indicate that the relative penetration into mild steel and homogeneous armor is also affected by standoff (2). The data show that the homogeneous armor is more effective at the longer standoffs. For convenience in measuring depth of penetration, targets are often made of stacks of plates 1/2" - 3" in thickness. There does not seem to be any objection to this practice if the plates lie flat on each other.

For some purposes, a better measure of liner performance is given by the volume of the hole or its smallest diameter. For most purposes the best measure would probably be some factor which indicates the amount of damage done behind a given target plate by the residual jet and spalled material from the back face of the plate. It has so far been difficult to define such a measure and more difficult to determine it from the test. In this discussion total depth of penetration into mild steel will be used as the measure of liner performance, except where stated otherwise.

2. Factors affecting liner performance

Shaped charge liners have been made in a variety of shapes, including hemispheres, spherical caps, cones, trumpets and combinations.

Cones have become almost standard, with hemispheres and trumpets occasionally used for special purposes. The results given in this chapter will be confined to simple cones except for some brief remarks in Section F 3 on double angle cone and other unusual shapes. The gross factors affecting liner performance are the explosive charge, which will be discussed in Chapter V the standoff, and the diameter, angle, thickness, and material of the cone. It is generally assumed that a linear scaling relation exists for shaped charge performance (Chapters II and VIII) and there is a considerable amount of evidence that a linear relation is valid.(3) For this reason, liner dimensions in this chapter will be given in terms of cone diameters - the inside diameter of the base of the cone - and the diameter of the cone can be eliminated as a factor affecting the liner performance. Details of liner design which affect liner performance include tapered walls, the base flange and the presence of a spit-back tube. When a spit back tube is not used, the configuration of the apex - whether sharp or rounded - seems to make little difference.

The effect of accuracy of the liner will be discussed in Sections C and D of this Chapter. The effect of accuracy of the complete round assembly will be discussed in Chapter IV.

3. References

Where numerical data are given, references to the source of the data are usually provided. The references most commonly used are coded as follows:

NDRC Division 8 references are to interim reports for the period given.

E. I. DuPont de Nemours and Co. - DuPont - references give the date of the report.

Carnegie Institute of Technology reports are the "Fundamentals of Shaped Charges" series, labeled CIT-ORD-No.

Firestone Tire and Rubber Co. reports are monthly progress reports, labeled FTRC No.

B. Methods of Manufacture

Cones may be made by any of a number of processes. The most common methods used in the past are spinning, drawing, casting, machining from bar stock, and electroforming followed by machining.

1. Spinning In the early days of shaped charge work, when the demands for cones were small, they were made by cutting a sector from sheet metal and rolling it to the desired shape, or by spinning. Such methods did not produce very good cones and were soon abandoned. However,

it is reported that spun cones which compare very favorably with drawn cones can now be obtained. The poor performance of some of the early spun cones can now be better understood in the light of recent work (4) which shows built-in spin compensation.

2. Drawing When the demand for cones became sufficient to justify the cost of dies, cones were made by drawing and this is the method usually used today for production quantities. Its advantage is low cost. Its disadvantage is the relatively lower accuracy in the finished cone than can be obtained by machining in those cases where extreme accuracy is required. Since the accuracy required is relative, it is sufficient for large cones but may not be sufficient for small ones. This method is not usually suitable for small quantities of a given design on account of the cost of the dies.

3. Casting Various methods of casting have been used. For a metal which shrinks when it freezes, casting by itself usually gives poor accuracy. If a suitable metal, probably an alloy, which yields accurate and homogeneous castings is found, casting may become an important method of manufacture for cones. It has been reported by Mr. G. C. Thronen, formerly of the Naval Ordnance Test Station, that cones cast with Zamac 5, a zinc alloy, gave 6.2 cone diameters penetration in mild steel targets, which compares very favorably with copper cones. (5) Work on this type of alloy is continuing at Firestone and at B.R.L.

4. Machining For a few cones of very high accuracy or where the cost per cone is not of primary importance, machining from bar stock is preferable to the methods mentioned above. Annealing the bar before machining may be desirable. There may be some difficulty in the machining near the apex, especially on the inside. Because a cone is machined it does not necessarily follow that it is accurately made; what is meant is that accurate cones can be made by this method if the required care is exercised.

5. Electroforming Electroformed cones are deposited on an accurately made mandrel and so have an accurate inner surface. If machined on the outside, means must be provided for accurately chucking, and checking, the mandrel when it is put back in the lathe to insure that the outside runs true with the inside. Carnegie Institute of Technology has reported favorable results with cones electroformed and peened, without machining (6).

C. Desirable Properties of a Liner

Aside from the fact that a given method of manufacture may be suitable for use with one material and not suitable for another, the method of manufacture affects the quality of the cone in two ways:

The accuracy of the cone
Its metallurgical properties

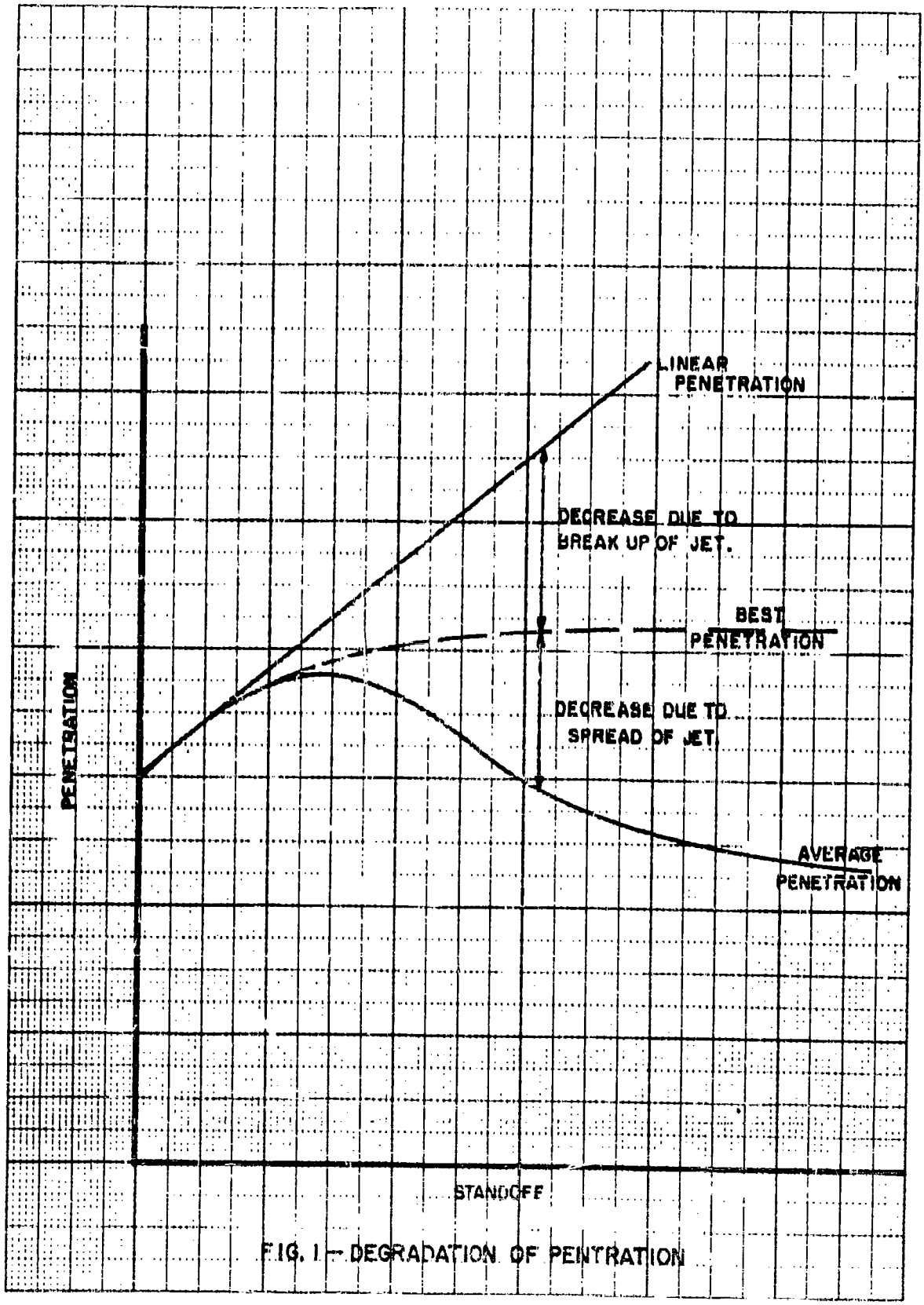

FIG. 1 — DEGRADATION OF PENTRATION

1. Geometrical Accuracy The formation of a shaped charge jet from the collapsing cone is a critical process. Ideally, the walls of the cone collapse and meet exactly on the axis of the cone. If, for any reason, one side of the cone collapses at a faster rate than the opposite side, they will not meet on the axis. This results, generally, in a crooked jet and the point of contact of the jet wanders on the surface of the target, giving impaired penetration. Thus, it is very important that sections of the cone perpendicular to its axis be true circles with centers on the axis and that the walls be of uniform thickness around a circumference. Uniform density of the metal is also required. Monotone variations in wall thickness along a slant height do not seem to be so important. Waviness along a slant height appears to be an undesirable characteristic. This is discussed in greater detail in Section D2. Axial symmetry in the explosive charge and the assembly will be discussed in Chapters IV and V.

2. Metallurgical Properties The metallurgical properties of the liner depend strongly on the method of manufacture as well as on the material and heat treatment. The metallurgical problem is difficult to analyse on account of the extremely high pressures and rates of strain and the excessive amount of plastic strain. For these reasons it cannot be said that the properties of the jet are the same as the properties of the cone. Also it must be remembered that the properties of importance are those under the high pressures and rates of strain mentioned above. That these may be very different from the properties under ordinary conditions is emphasized by the fact that glass cones give penetrations in concrete targets greater than might be expected from the "metallurgical" properties of glass. Nevertheless, it has been found possible to make some very interesting and important correlations between properties of the liner, principally crystal structure and melting point, and behavior of the jet. One of the most interesting features is a [illegible] factor in certain cases, due, apparently, to an unusual crystal structure which gave poor penetration in static firings (7).

Theory indicates that for the fast moving portion of the jet the penetration obtained is proportional to the length of jet and to the square root of the jet density. (8) The assumption that the jet density is the same as that of the cone is about as good a guess as any, if the jet is a continuous one. On account of the velocity gradient the jet lengthens as it travels. The stretching of the jet causes it eventually to break up into a series of particles. Thus, if the jet did not break up into particles, its length would increase linearly with time and so its penetration would increase linearly with time and consequently, with standoff. Penetration standoff data show (9) that penetration increases with standoff up to a maximum value of penetration, the corresponding standoff being called the "optimum" standoff, Figure 1. Beyond the optimum standoff the average penetration decreases with standoff, while the best values of penetration approach an asymptotic value. The decrease in penetration from the linear value to the asymptotic value may be ascribed to breakup

of the jet, while the decrease from the asymptotic value to the average value is due to increasing spread of the jet. Thus, for good penetration the jet should be capable of attaining a great length before breaking up. The ability to do this will be affected by the metallurgical properties of the jet. If experimental penetrations are adjusted for the effect of density of the jet (cone), the following comparison is obtained:

Copper	100%
Aluminum	110%
Steel	75%
Zinc	65%
Lead	50%
Glass	40%

The above figures were obtained as follows. The best penetrations for the different cone materials were divided by the square root of the jet (cone) density to get penetration for unit density. These penetrations for unit density were then divided by the penetration for unit density for copper and multiplied by 100%. The figures were rounded off to 5%. The best penetrations, regardless of standoff and cone thickness, were used. The NDRC and DuPont data were used since these covered the desired range of materials and the relative accuracy of the cones was approximately the same. Penetrations for the given metals were taken from curves given later in this Chapter. Penetrations for glass cones are given in the DuPont reports for February, May, October and November, 1943, and those dated 3 February 1943 and 18 September 1943. These figures are necessarily rough. For most materials except copper and steel the number of tests was small and optimum conditions of cone thickness, etc., were probably not obtained. The tests were conducted during the war and the accuracy of some of the cones was probably poor. However, one may conclude that copper and aluminum have metallurgical properties superior for shaped charge cones, while lead and glass have inferior properties. A desirable material would have properties similar to copper and aluminum and a high density.

D. Experimental Results of Inaccuracies in the Liner

Two series of tests designed to determine the effect of inaccuracies in shaped charge liners will be mentioned.

1. Tests by Ballistic Research Laboratories. (10) Two kinds of cones were used in these tests. Those designated "1" M9A1" were M9A1 steel cones (45°, 0.037" thickness) cut down to 1" base diameter and loaded with Composition C-3 in 1/16" cardboard tubes 1 1/4" x 4". The average variation in wall thickness of these cones was 0.007" around a circumference and 0.0018" along a slant height. The average penetration in mild steel targets for the undeformed cones was 3.5 cone diameters. Cones designated "electroformed" were of copper, electroformed and machined to a high degree of accuracy (about ± 0.0002"). Base diameter was 0.750", thickness 0.050" and apex angle 46°.

Due to the poor accuracy of the particular drawn cones, the aberrations described below were necessarily large to prevent their effect being masked by statistical fluctuations. For this reason the tests were not of much value in establishing tolerances. Their principal interest is thought to lie in the effects on the jet as shown by the radiographs.

a. Warping For this series 1" M9A1 cones were warped by flattening opposite sides. When the width of the cone between flat sides was reduced to 15/16" the penetration dropped to 2 9/16". For a width of 7/8" the penetration was 1 1/8".

b. Variations in Wall Thickness For this series 1" M9A1 cones were ground to various depths on different parts of the surface. For Figures 2 and 3 the thickness was reduced to 0.020" over the shaded portion. For Figure 2 the penetration was negligible in each case. For Figure 3-1. the penetration was 1.0 cone diameter; for Figure 3-3, 2.4 cone diameters. For Figures 4 and 5 the amount by which the wall thickness was reduced is shown on the photographs. Penetrations were as follows:

Amount Ground Out	Penetration
0.001"	3.5 Cone Diameters
.002	3.25
.003	3.38
.005	1.94
.007	1.69
.009	1.75
.012	0.87

c. Shallow Grooves The jet shown in Figure 6 was obtained from an electroformed cone having 5 wide shallow rounded circumferential grooves 0.005" deep machined in the outer surface. It is thought that the thin thread like portions of the jet came from the grooved portion of the cone and the "beads" in the jet correspond to the lands between the grooves. Apparently the thin portion of the jet is stretching greatly, while the beads are not stretching at all. Penetration of this jet was not obtained. These tests seem to bear out the common assumption that variations in wall thickness around a circumference, which disturb axial symmetry are more important in causing decreased penetration than variations along a slant height, but the latter can become very important, especially at long standoff. Since every effort is now being made to improve penetration at longer standoff, the requirement for accuracy along a slant height should not be relaxed.

d. Deep Grooves The cone from which the jet shown in Figure 7 was obtained was electroformed. A groove 1/32" wide and 0.025" deep was cut half way around a circumference 0.270" (approximately 1/4 of the height) from the base. The deflection of the jet away from the thinned side is

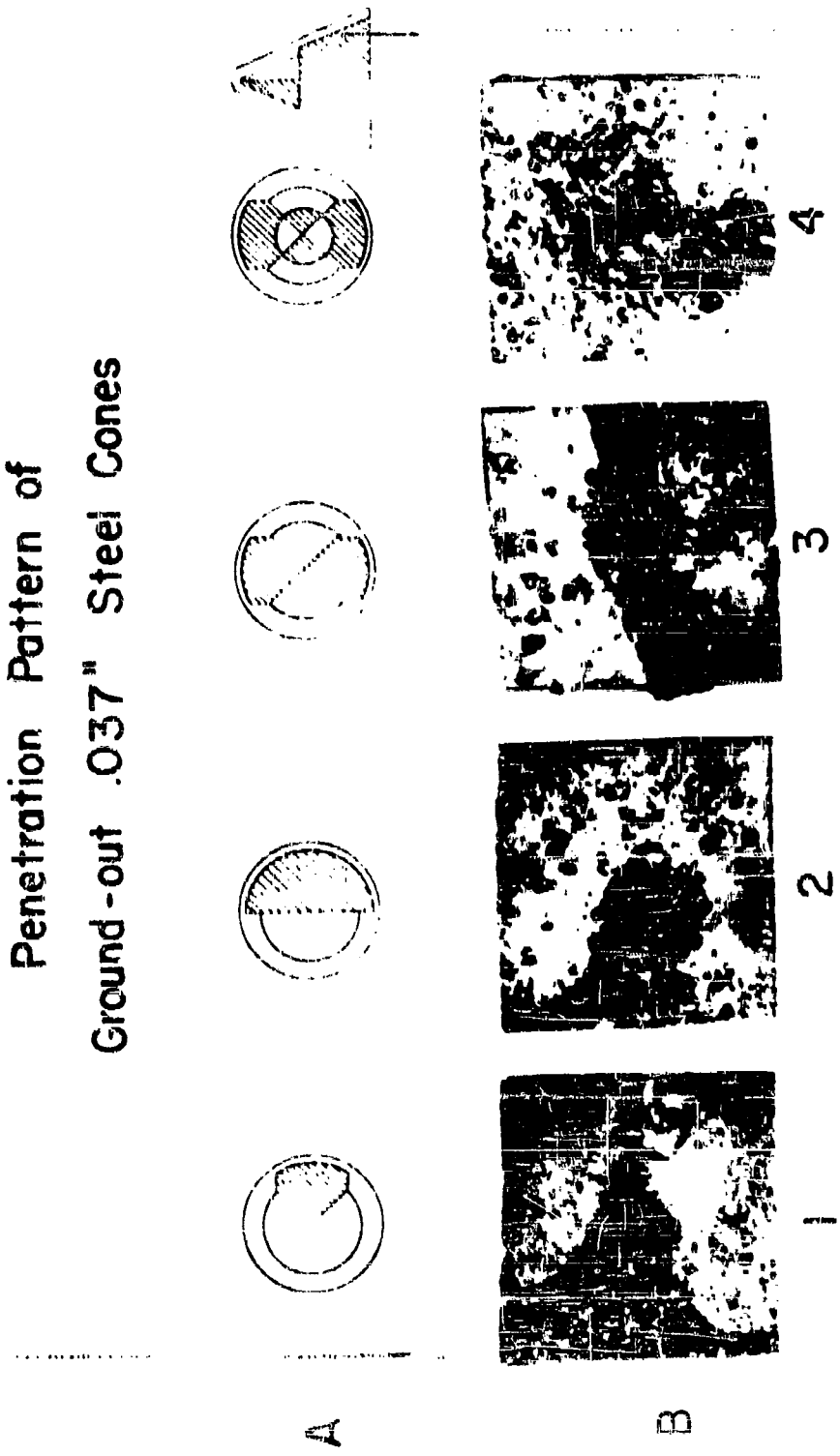

FIGURE 2

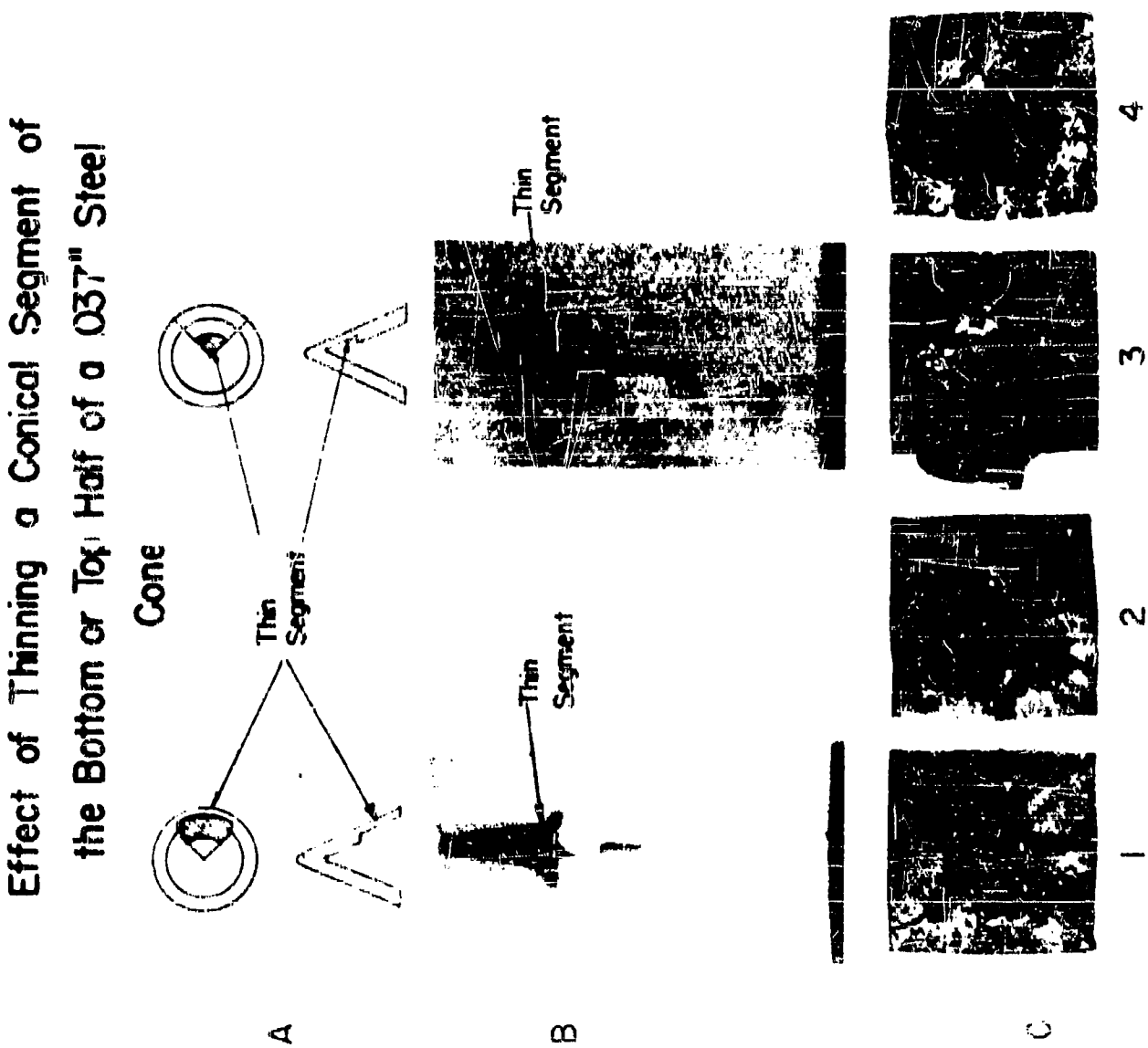
Effect of Thinning a Conical Segment of the Bottom or Top Half of a .037" Steel Cone
Thin Segment
Thin Segment
Thin Segment
A
B
C
1
2
3
4

FIGURE 3

CONFIDENTIAL

Effects of Controlled Wall Thinning on .037" Steel Cones

Amount ground out is noted below each target.

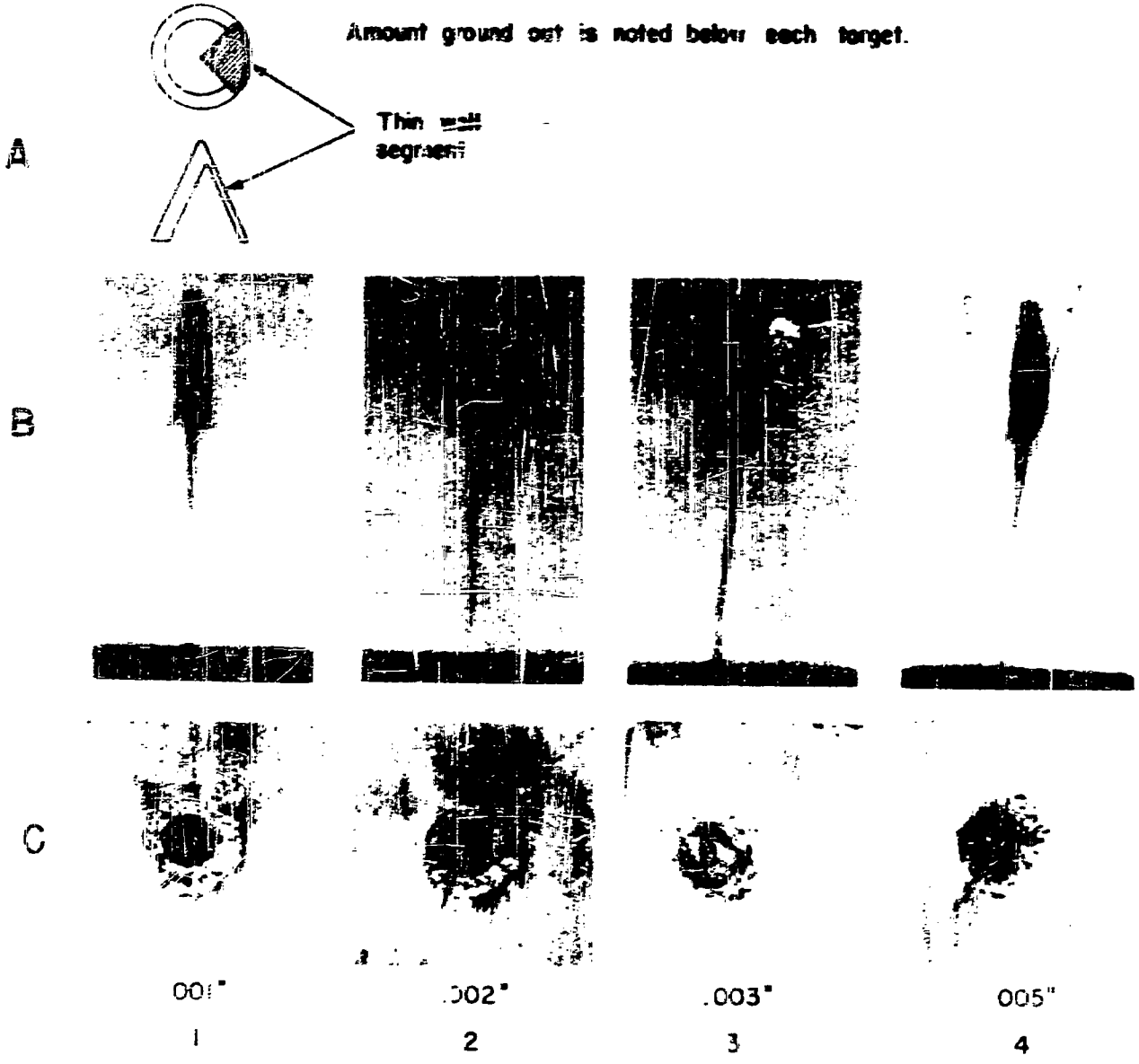

FIGURE 4

CONFIDENTIAL

Effects of Controlled Wall Thinning on .037" Steel Cones

Amount ground cut is noted below each target.

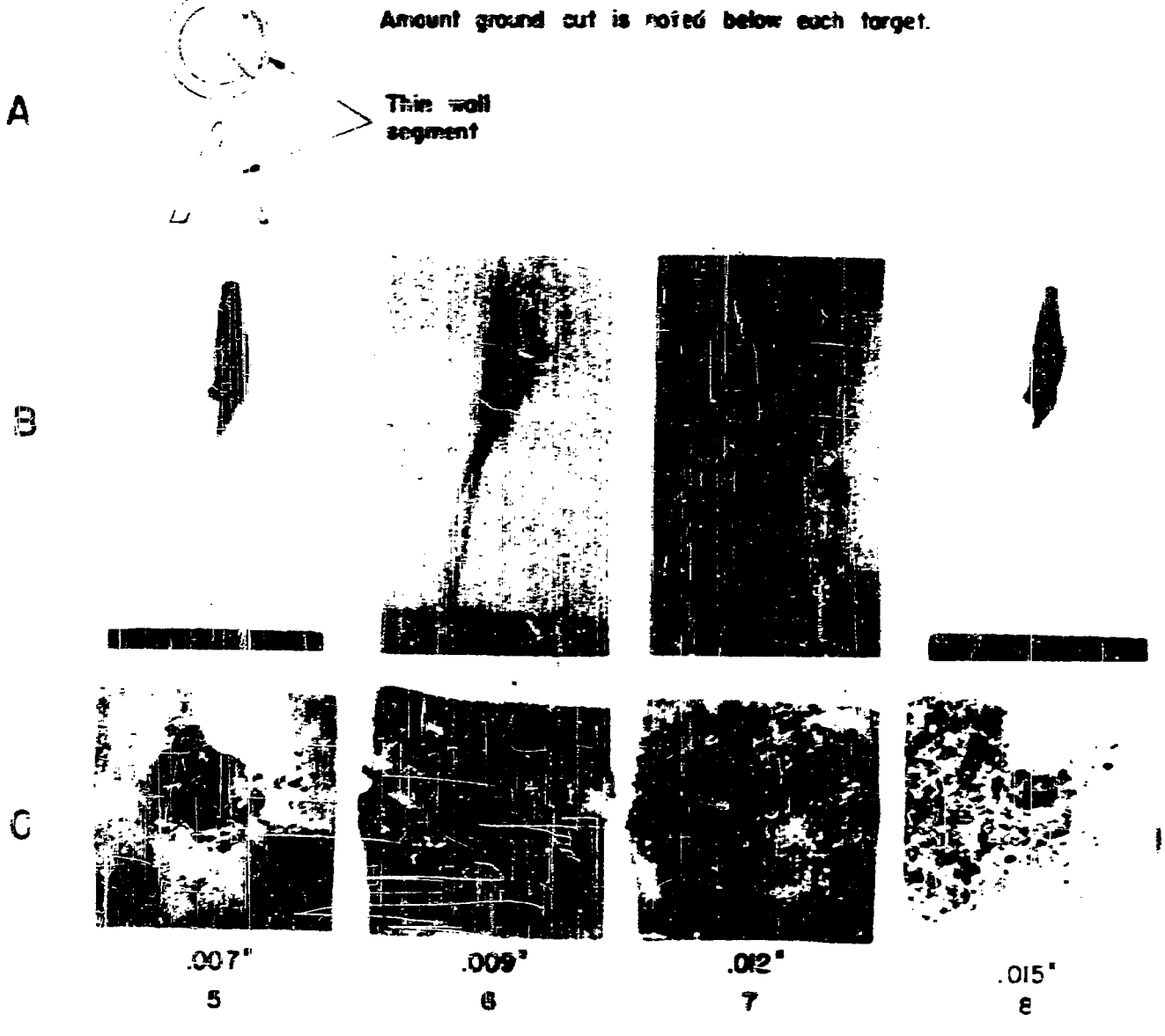

FIGURE 5

DEFORMED JETS FROM CONES WITH HALF CIRCUMFERENTIAL GROOVES

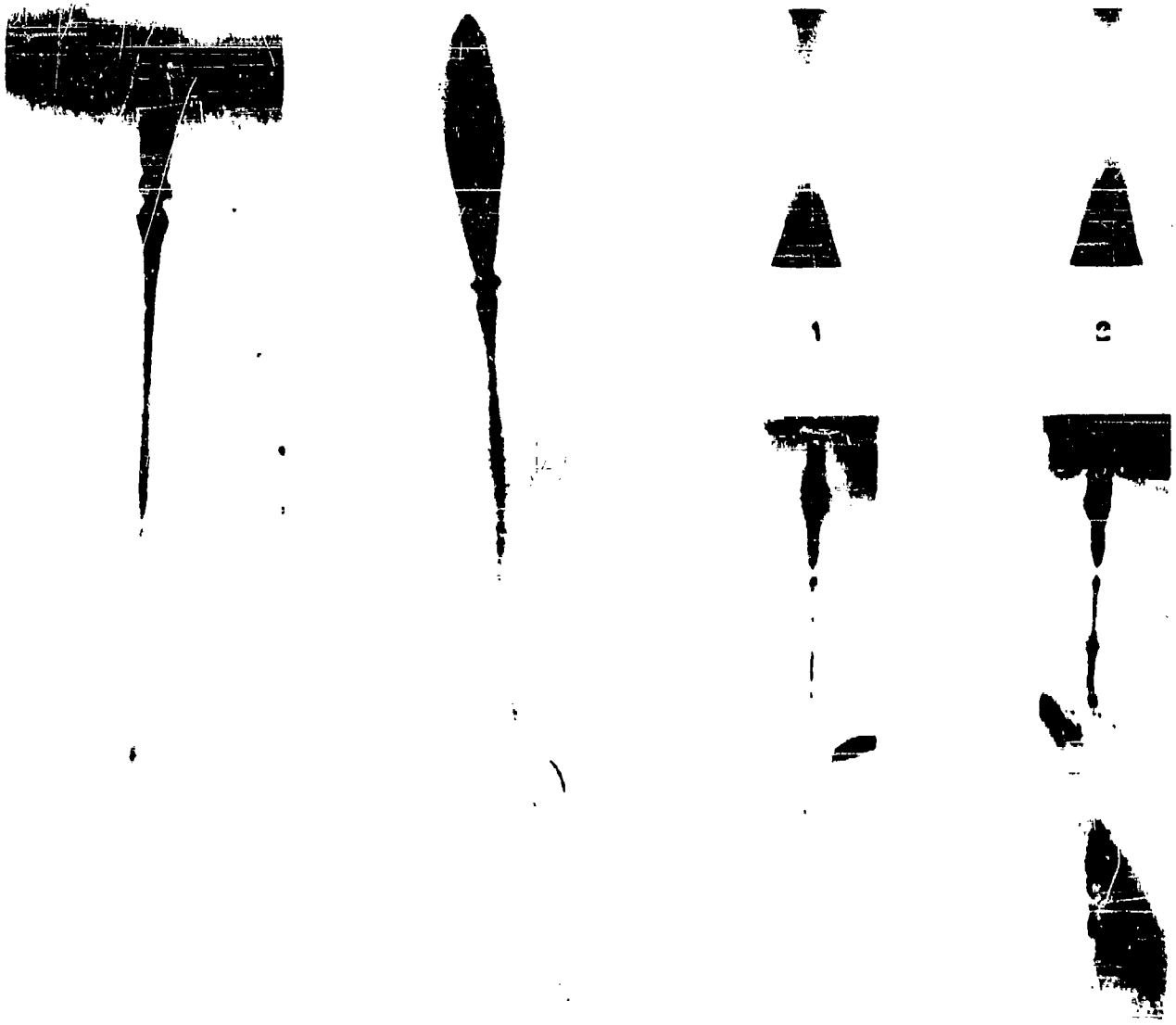

FIGURE 8

FIGURE 6

FIGURE 7

easily seen. Considering the length of the affected portion of the jet in relation to the width of the groove, it would seem that the effect of the groove is much greater than its width would indicate.

Figure 8 shows results from two 1" M9A1 cones. On each cone, a groove 1/32" wide and 0.018" deep was cut half way around a circumference. For Figure 8-1 the groove was 2/3 of the height from the base; for Figure 8-2, 1/3 of the height from the base. The groove can be seen on the left side of the cones in the static shots at the top of the figure. The effect of the groove on the jet is easily seen in Figure 8-2 and is severe. The effect on the jet in Figure 8-1 is hard to see, since it is at the very tip of the jet. From these radiographs (Figures 5 and 8) one surmises that the apex end of the cone produces very little jet. In Figure 8-2, the jet from 2/3 of the cone at the apex end is not as long as that from 1/3 of the cone at the base end. This result is in agreement with the generalized Theory of Jet Formation (11). As a result of this, imperfections near the base of the cone affect a greater length of jet than those near the apex and so are more important in decreasing penetration. This fact is emphasized by the results of the Budd Company work described in the next section.

2. Experiments by the Budd Company (12) In tests made in connection with the development of the 90mm HEAT round T108, the Budd Company used standard liners machined to give controlled inaccuracies. The standard liner was of copper, about 2 3/4" inside base diameter, 0.062" thick, 45°. The variation in wall thickness was of the order of 0.001", both circumferentially and longitudinally. For one series, a circumferential variation of about 0.005" was machined on the outer surface; for another series, maximum variations of 0.010" (0.006"-0.016") were machined on the outer surface. The variation was zero near the base and a maximum near the junction of the cone and spit back tube, so that it was both circumferential and longitudinal. A third series was machined on the outer surface to give four 0.010" waves simulating the surface resulting from drawing operations. Other series with eccentricities in the spit back tube were also made. The targets consisted of 9" of green armor, followed by mild steel, at 6" (2.2 cone diameters) standoff. Results were as follows:

No. Rnds.	Avg. Pene.	Std. Dev.	Cone
20	13.2"	0.92"	Control
10	13.1"	1.46"	0.010" longitudinal variation
10	10.8"	0.98"	0.005" Circumferential variation
9	10.1"	0.91"	0.010" Wavy wall

In conclusion, one can say that, for maximum penetration from simple cones the axial symmetry of the liner should be as nearly perfect as can be obtained especially near the base of the cone. Deviations from axial symmetry not only reduce penetration, but, in a lot with random deviations, even small average deviations may result in a large dispersion. Variations in wall thickness along a slant height are also important, but their effect is not as serious as those around a circumference. The requirement of axial symmetry extends also to the explosive charge and the assembly as well as to the cone.

E. Tolerances

As a result of general observation and of tests similar to those described in Section D2, tolerances on cone dimensions have been recommended for some designs. This does not imply that there exists a tolerance within which the cone performs properly and beyond which it does not perform properly. Any deviation of the cone from axial symmetry will, in the long run, result in a degradation in performance, either in average penetration or variability, or both. However, it must be remembered that extreme accuracy in cone manufacture is very expensive. The tolerance allowed must be a compromise between the desire for top performance from the round and what one is willing to pay for it.

For the 90mm T108 round mentioned in the previous Section the following tolerances were recommended in the Aberdeen Proving Ground Memorandum Report: (12)

0.001" Maximum wall variation in transverse plane

0.005" Maximum wall variation in longitudinal plane

0.003" Maximum waviness

These were simple copper cones, 45° apex angle, 2 3/4" diameter, 0.062" wall thickness.

Recommended tolerances for wall thickness of the blank for 57mm and 105mm cones (fluted cones, rotated) are given on page 243, Chapter VIII. The 57mm liners are about 1 11/16" diameter, 0.054 thickness; the 105mm, 3 1/4" diameter, 0.100" thickness. These tolerances seem a little more liberal than those quoted for the 90mm. Since the latter were determined from firings with inaccuracies of 0.004" - 0.005" in wall thickness, it might be possible to bring the 90mm tolerances in line with the 57mm and 105mm. General observations of miscellaneous tests indicate that, for 3/4" diameter 45° electroformed cones, variation in wall thickness should be less than 0.001" for 0.025" thick cones and not more than 0.002" for 0.050" thick cones.

One might expect tolerances on wall thickness to increase with the thickness. Experience with small cones (3/4" diameter) has indicated that a 4% inaccuracy on 0.025" cones is more damaging than a 4% inaccuracy on 0.050" cones. However, this may be due to the ease with which thin cones

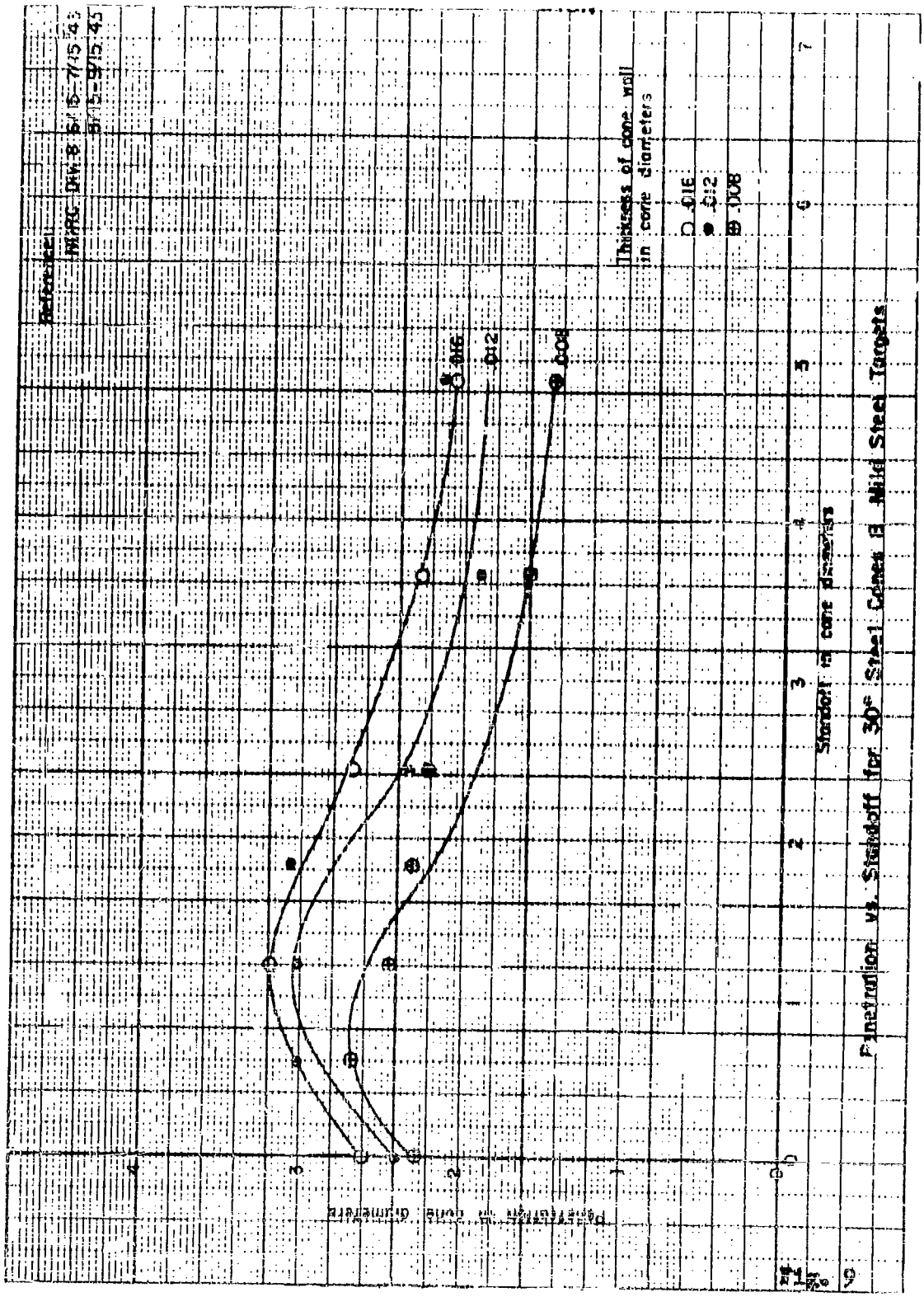
Penetration vs. Standoff for 30° Steel Cones in Mild Steel Targets
Standoff in cone diameters
Thickness of cone wall in cone diameters
.016
.012
.008
Penetration in cone diameters

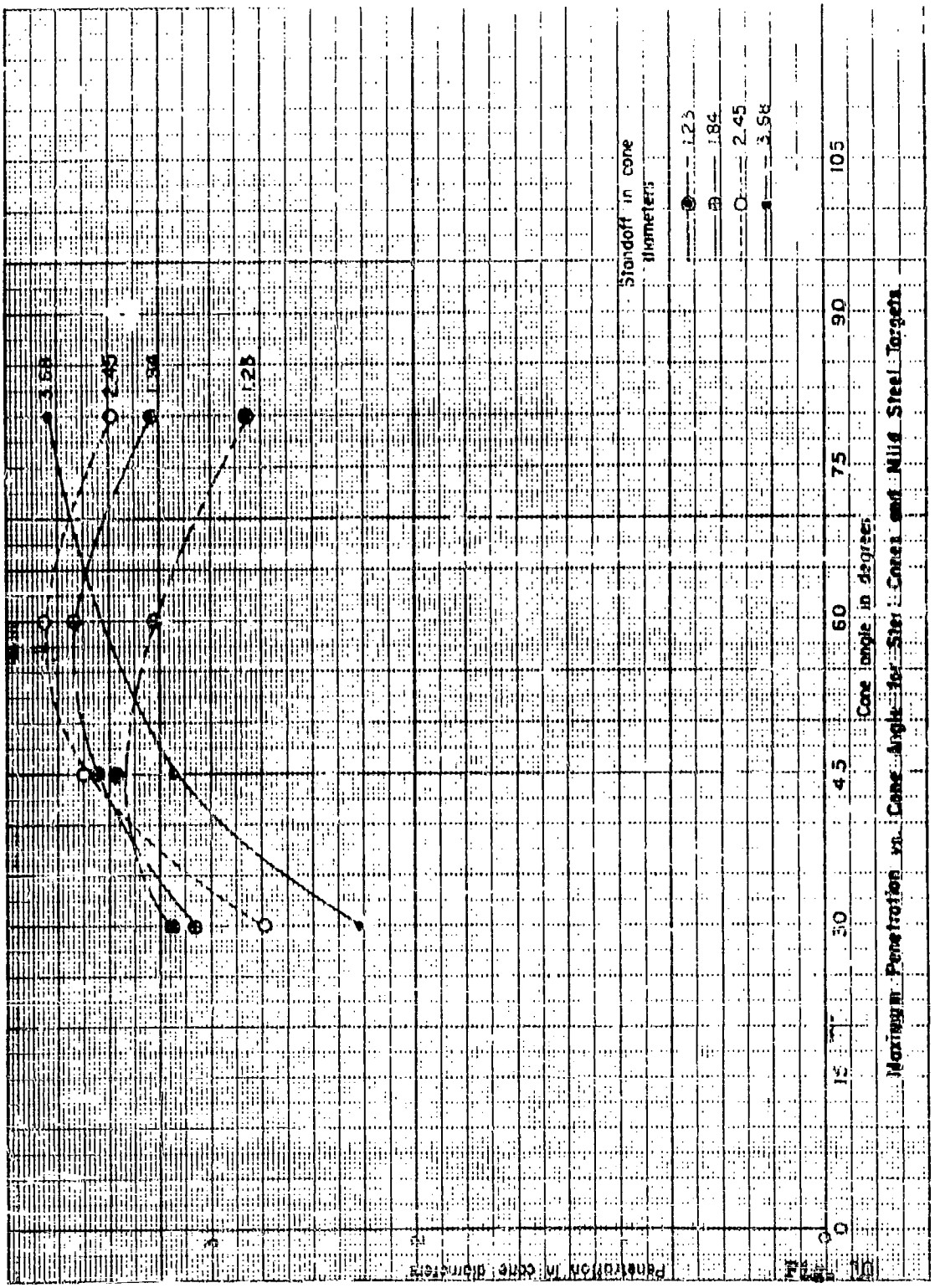
Maximum Penetration vs. Cone Angle for Steel Cones and Mild Steel Targets
Cone angle in degrees
0
15
30
45
60
75
90
105
Standoff in cone diameters
1.23
1.84
2.45
3.68
Penetration in cone diameters
3.68
2.45
1.84
1.23

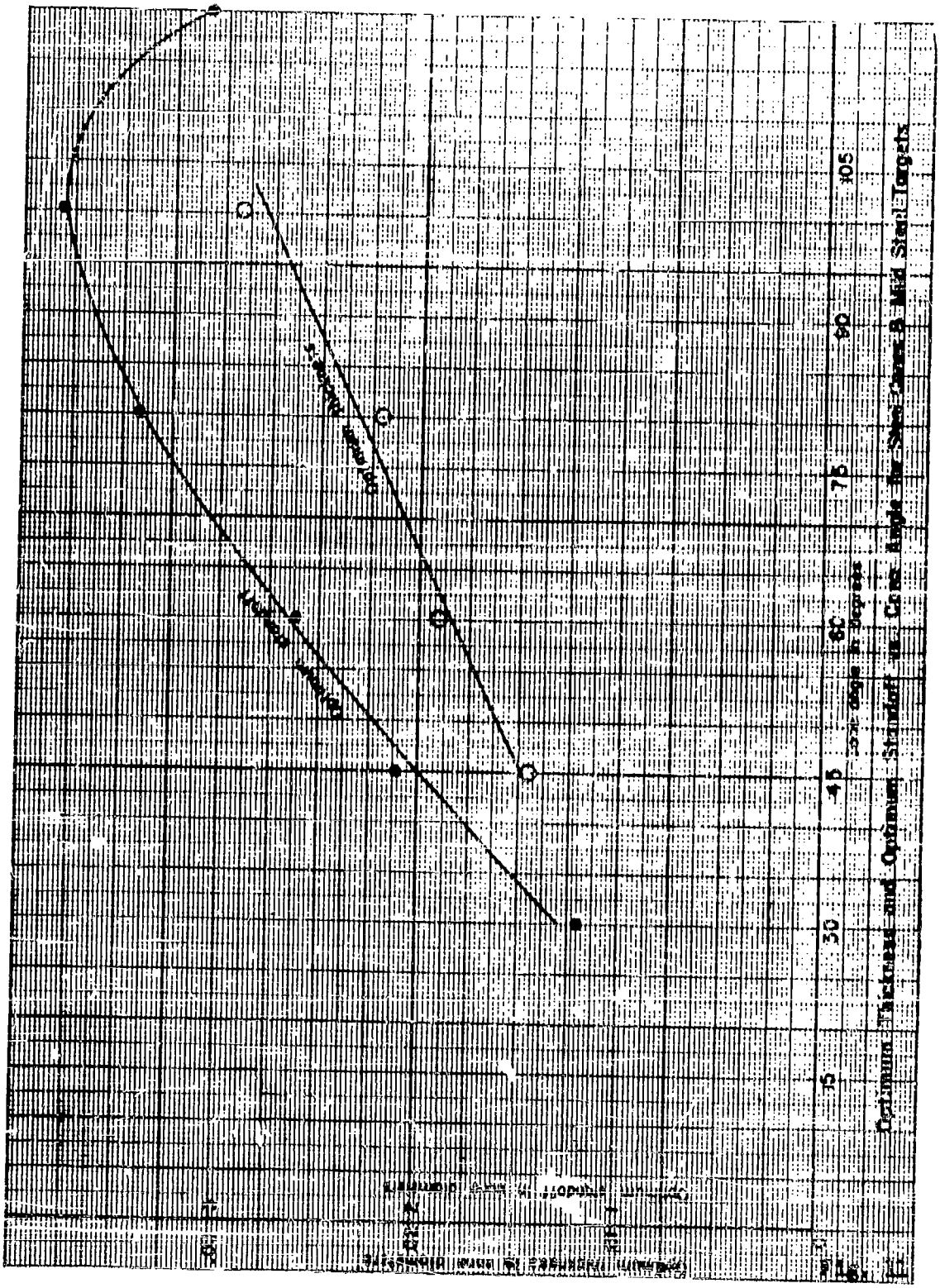
Optimum Tracking and Optimum Standoff vs. Case Angle for Non-Class B Mid Stage Targets
Case angle in degrees
15
30
45
60
75
90
105
Optimum standoff in nautical miles
Optimum tracking range in nautical miles

become out of round due to handling. It was found that particular care must be taken with 0.015" cones to prevent this. The writer has seen no discussion about whether large diameter cones require smaller percent tolerances than small diameter cones, though this question merits consideration.

F. The Effect of Design Parameters on Penetration

The effect of standoff, cone thickness and cone angle will be presented in the form of graphs. These curves are based on data published by various groups of investigators working at different places and different times. Under these conditions, differences in results are to be expected. It is to be remembered that cones available in the early days of shaped charge investigation were of relatively poor manufacture. As the importance of accuracy became known and methods of manufacture improved, the quality of cones improved and this resulted in increased average penetrations and smaller dispersions, especially at the longer standoffs.

This subject is most readily divided into early work and recent work. Where cyclotol and pentolite are quoted as the explosive, the usual compositions, 60/40 RDX/TNT for cyclotol and 50/50 PETN/TNT for pentolite, were used, unless otherwise stated.

1. Early work with simple cones - Figure 9 shows penetration of steel cones into mild steel targets for 30° cone angle and various cone thicknesses. This work was done in the early part of the war and the quality of the cones was probably not too good. Cones were, generally, 1 5/8" diameter, cast in 1 5/8" unconfined pentolite charges of 4"-5" length and fired statically at zero obliquity. Each point was the average of 5 shots except where shown on the graph. Curves were drawn by eye, with some attempt made to keep all curves of one family of the same general form. For most of this work, the dispersion, especially at long standoffs, was large.

The general characteristic of penetration-standoff curves for cones of early manufacture is a maximum penetration at a small optimum standoff, the penetration decreasing sharply for larger standoffs. The optimum standoff increases with the cone angle.

Similar curves can be plotted for larger angle cones from the data given in the NDRC Div. 8 interim reports and the DuPont reports.

From these data, the maximum penetration for any standoff is plotted in Figure 10 for the different cone angles. Figure 11 shows the optimum standoff and thickness as a function of the cone angle. Since steel is not regarded favorably as a liner material, this data is of limited usefulness, but material shortages in an all out war may force the use of steel again. The data do show that standoff, cone thickness, and cone angle are inter-related and that if any of these is changed it may be

necessary to change the others for best results. As an example, a comparison of cones of different angle may not be unbiased unless the thickness is also changed.

Figures 12 and 13 show penetration as a function of standoff for 45° copper cones. Here there is a distinct difference between the two sets of data at the longer standoffs. The reason for this difference is not known positively but it is probably due to a difference in quality of the cones, since recent work with cones of high accuracy tend to confirm the DuPont data.

Figures 14 and 15 give the results for aluminum cones. They show the characteristic property of aluminum, the fact that penetration holds up well at long standoff. Due to its low density one might expect that aluminum liners should be thick as compared to steel or copper, but Figure 14 does not show any advantage for the thicker liners.

Figures 16 and 17 show the performance of zinc and lead cones, neither of which are at present of considerable importance. However, as mentioned previously, the Naval Ordnance Test Station has recently reported, informally, excellent results from a castable zinc alloy.

2. Recent work with simple cones Figures 18-21 show penetration as a function of standoff for copper, steel and aluminum cones of a constant thickness for cone angles of 22°, 44°, 66° and 88°. The tendency of aluminum to maintain its penetration with increasing standoff is evident, as is also the tendency for optimum standoff to increase with cone angle. These curves do not necessarily show optimum results as the thickness may not be the best for some angles.

Figures 22-24 show results obtained under conditions very different from those for the previous data. These charges were fired in shell bodies or cases closely simulating shell bodies. Thus, the explosive charge was short, in comparison with its diameter, and fairly heavily confined. The accuracy of the cones was very good. Figure 22 shows a very good penetration, fairly flat penetration-standoff curve, and a long optimum standoff. Figure 23 shows an optimum cone thickness of 3%, which is somewhat heavier than that for unconfined charges. This is in agreement with the general observation that, if the charge diameter is increased or the charge is confined, the thickness of the cone should be increased for optimum penetration (13). Figure 24 gives the results of varying the cone angle under different conditions of constant explosive loading. The results are, therefore, not of general application. A penetration standoff curve obtained from firings at the Ballistic Research Laboratories is given in Figure 25. These were drawn 105mm cones of good accuracy confined in shell cases and fired against mild steel targets. Penetrations were unusually good and held up well at long standoff.

Figures 26-28 give the results of recent firings at the Ballistic Research Laboratories and not yet reported. These were small cones, 0.750" inside diameter, of electroformed copper machined on the outside to about .0005" tolerance. They were fired in unconfined pentolite

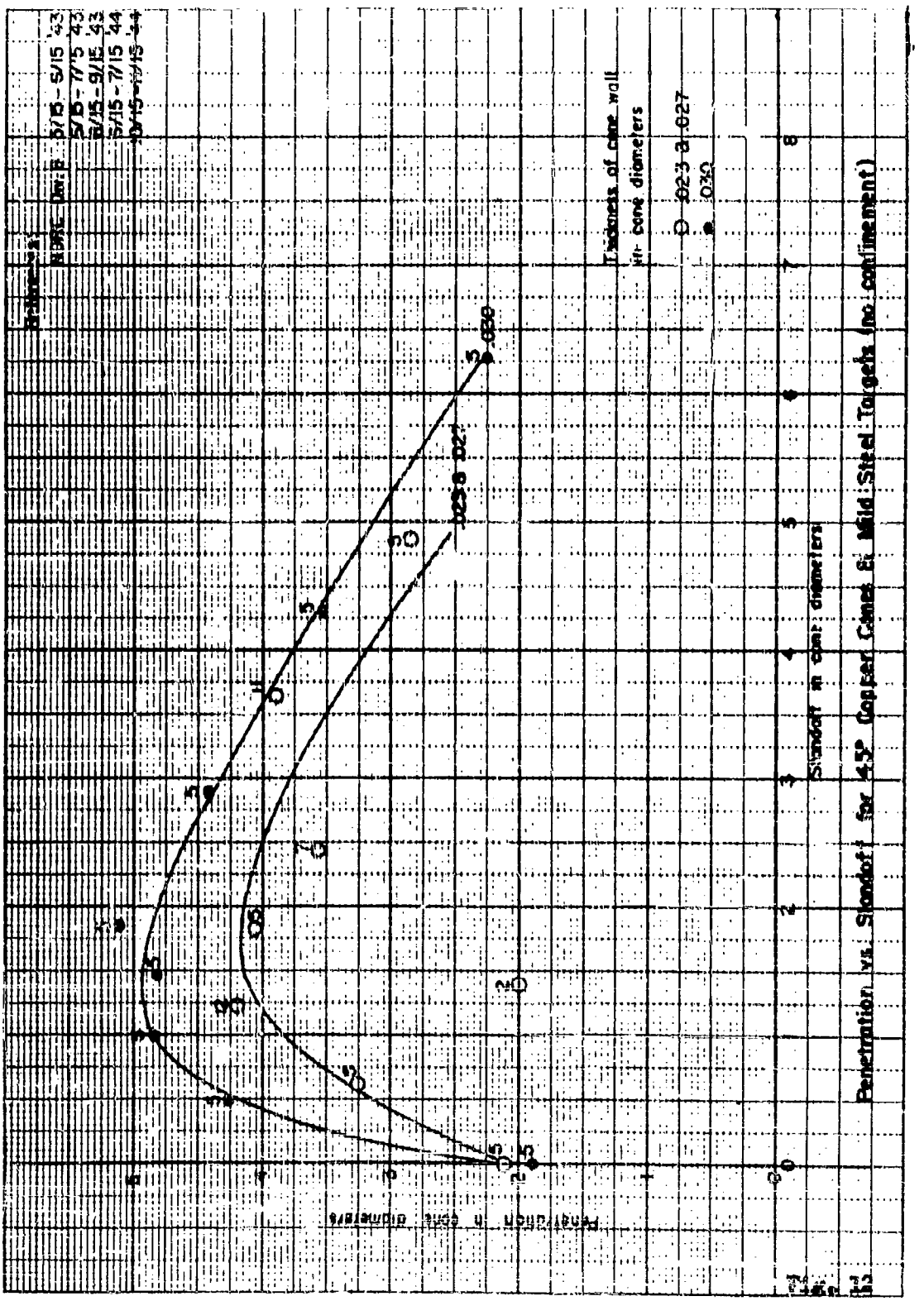
Penetration in cone diameters
Standoff in cone diameters
Thickness of cone wall
in cone diameters
Penetration vs. Standoff for 42° Copper Cones & Mild Steel Targets (no confinement)

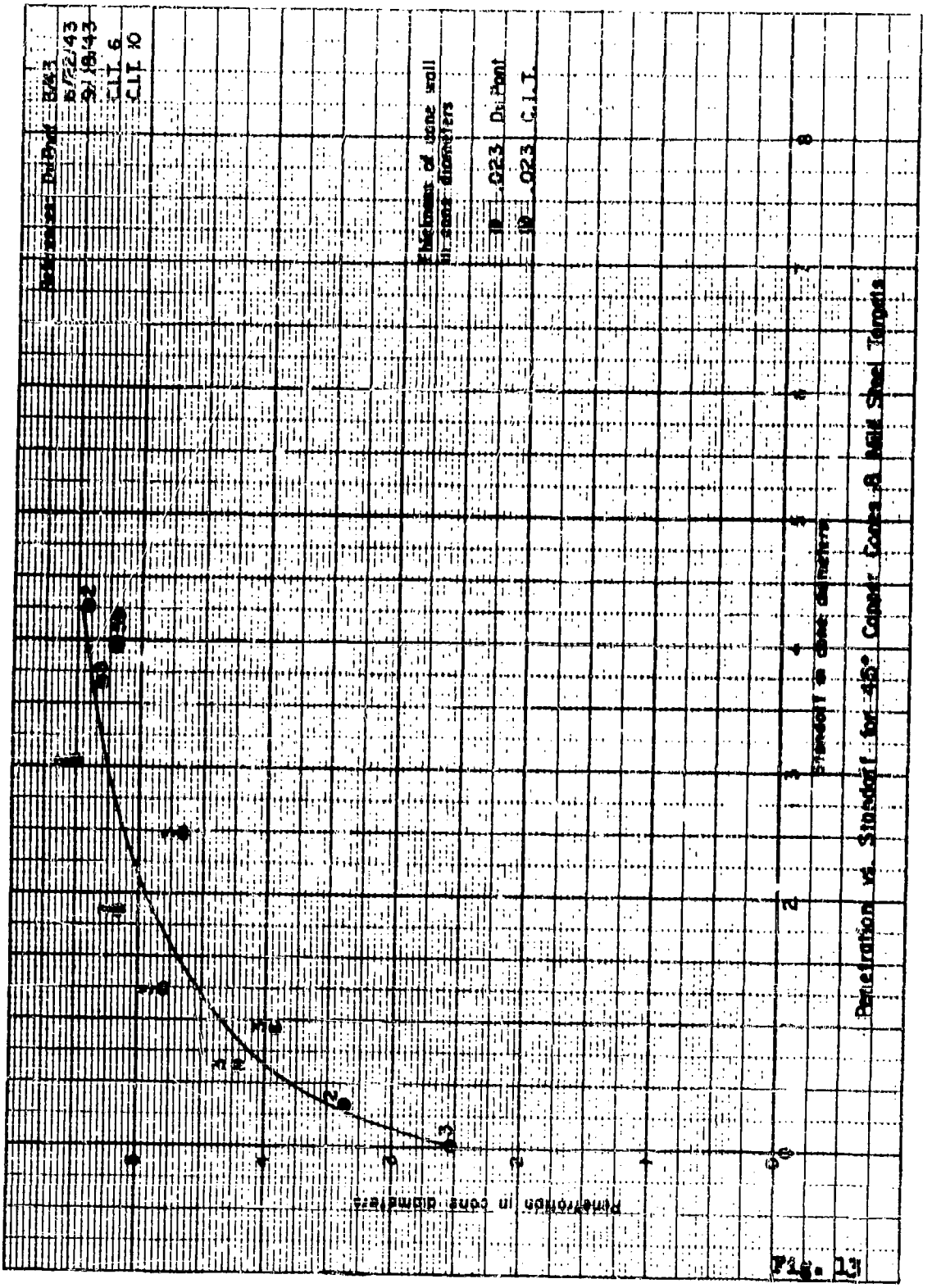
Penetration vs. Striking V for 45° Cone Tools & Mild Steel Targets
Striking V in feet per second
Penetration in cone diameters
Thickness of cone wall in cone diameters
.023 Dia Pt
.023 C.I.T.
Ballistic Bal'd 8/12/43
9/18/43
C.I.T. 6
C.I.T. 10

Fig. 13

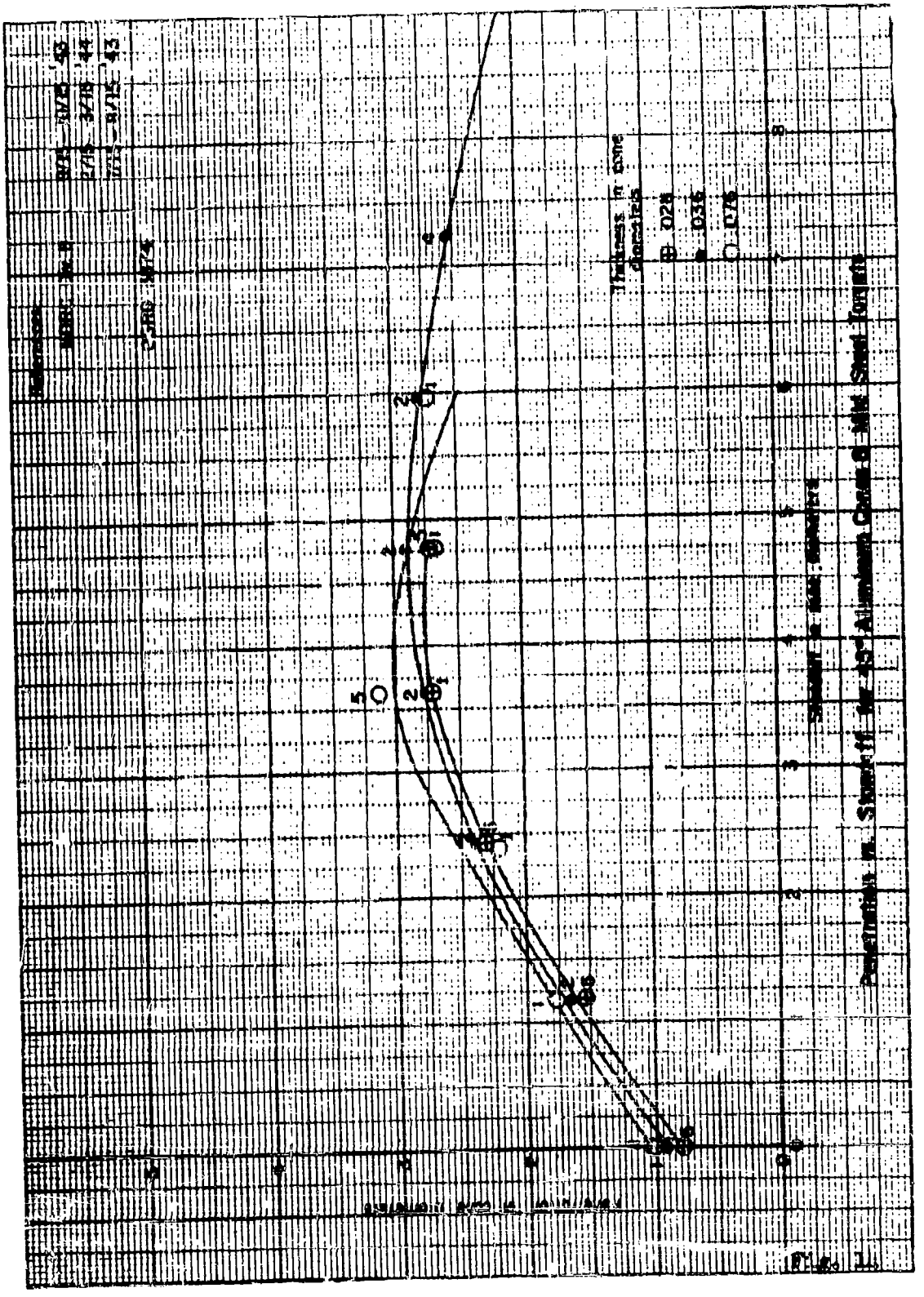
Thickness in cms
density
.024
.036
.076
Penetration in Standard Aluminum Cms of Mat. Shad Through

Fig. 1.

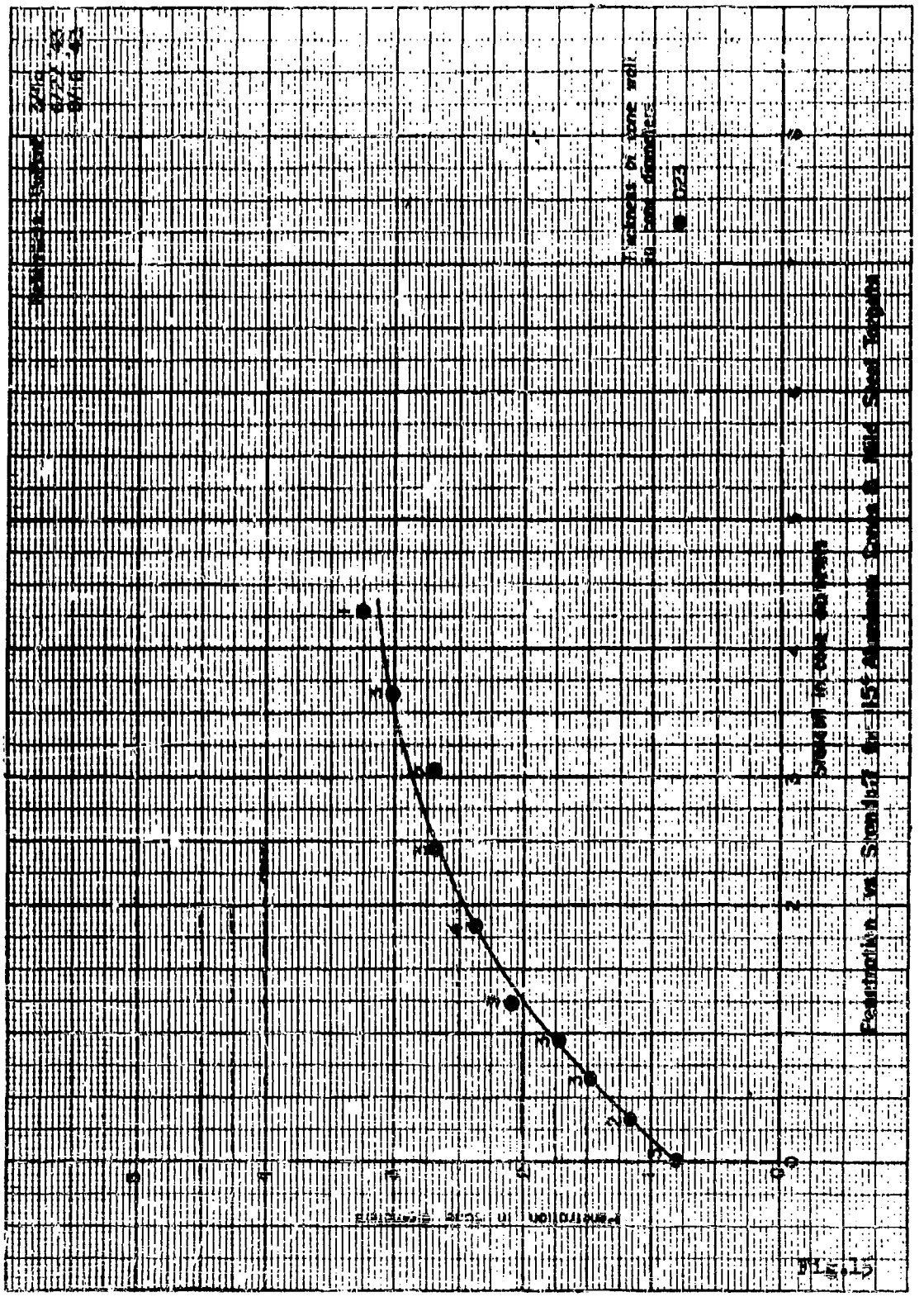

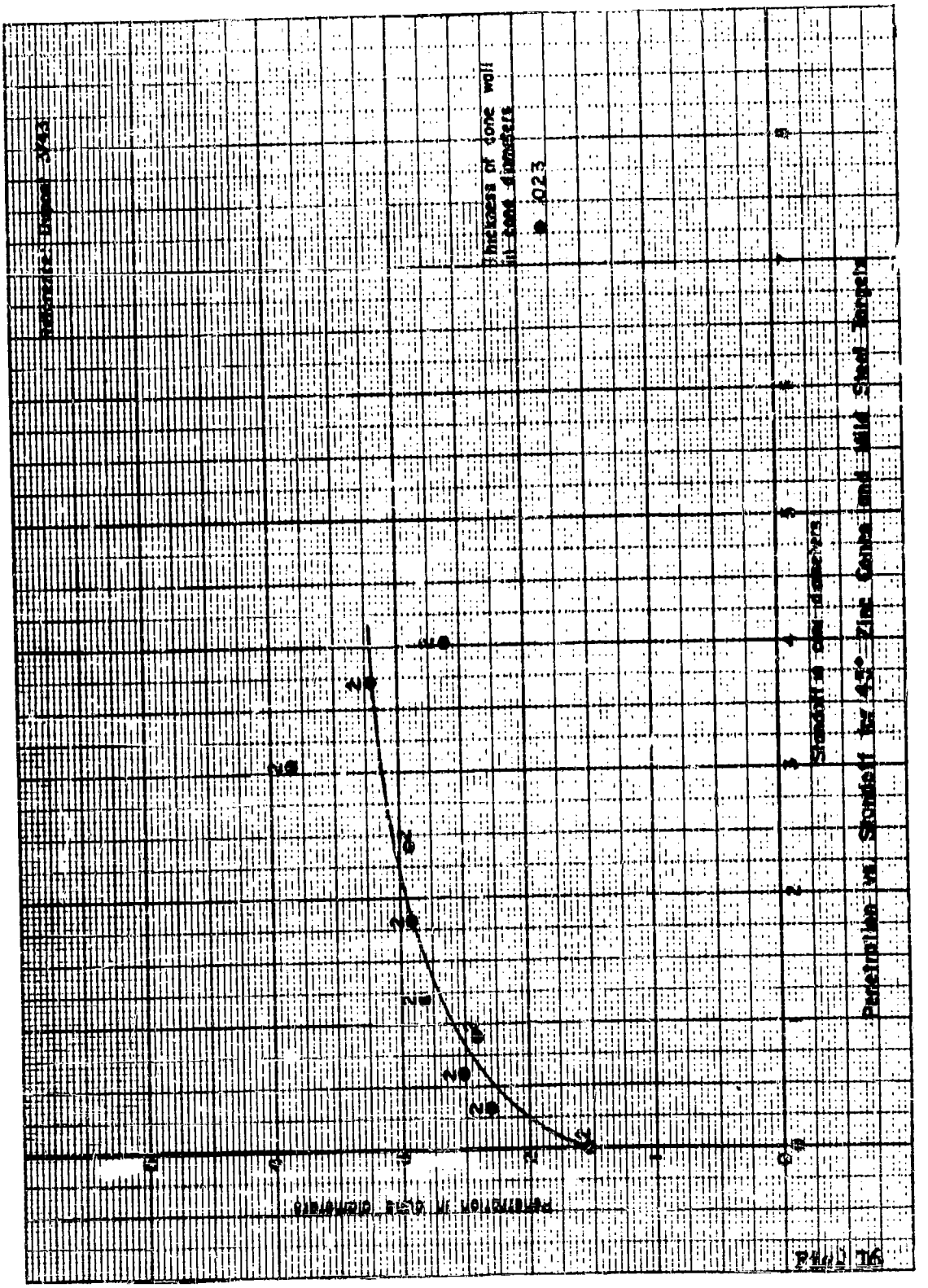
Potential vs. Standoff for 45°-Zinc Cone and Mild Steel Target
Standoff in cone diameters
Thickness of cone wall in cone diameters
.023
Potential in millivolts

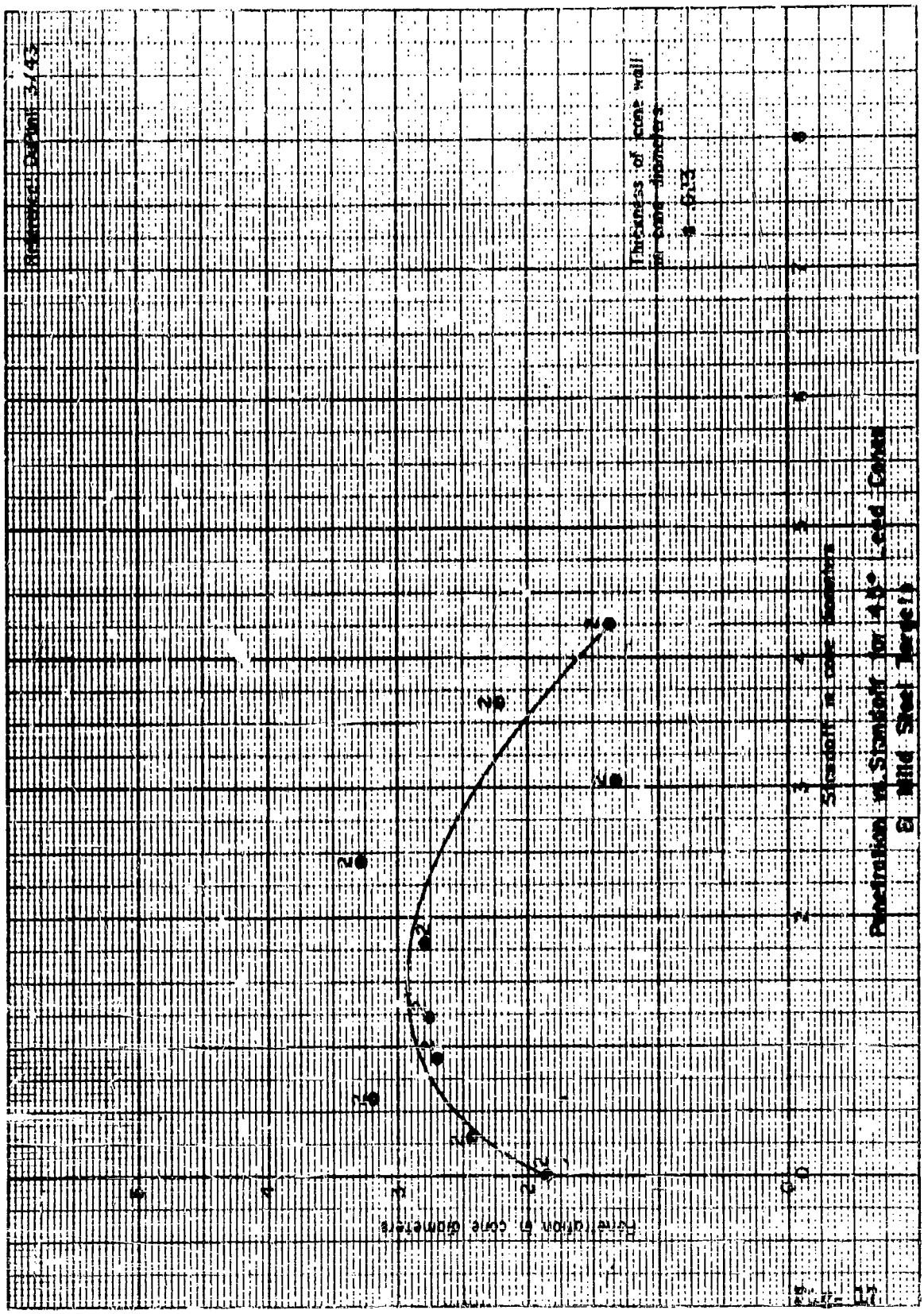
Penetration vs Standoff for 45° cold Cone
& Mild Steel Target
Standoff in cone diameters
Penetration in cone diameters
Thickness of cone wall
in cone diameters
= .033

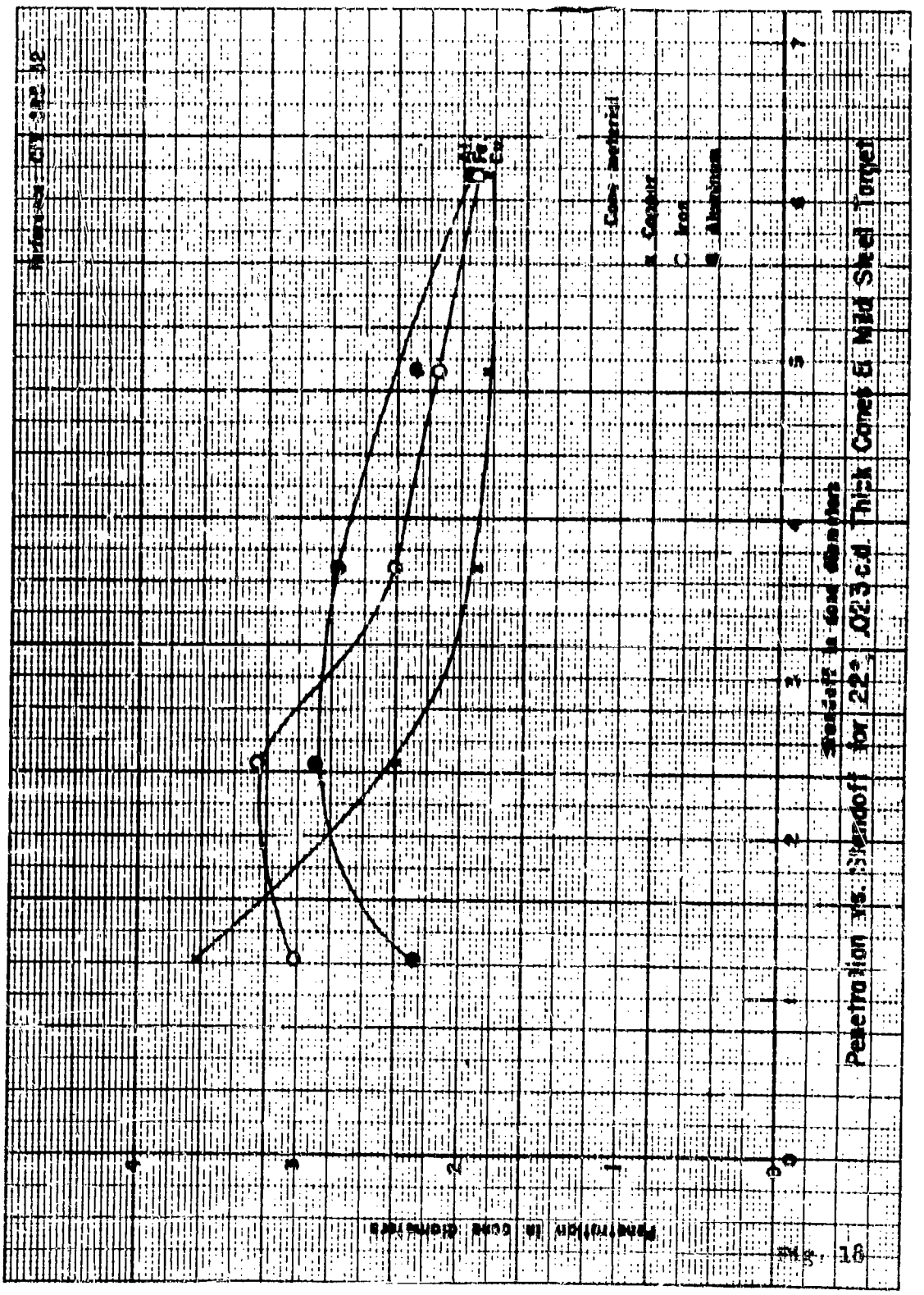
Penetration vs. Standoff for 22s .023 c.d. Thick Cone & Mild Steel Target
Penetration in cone diameters
Cone material
Copper
Iron
Aluminum

Fig. 16

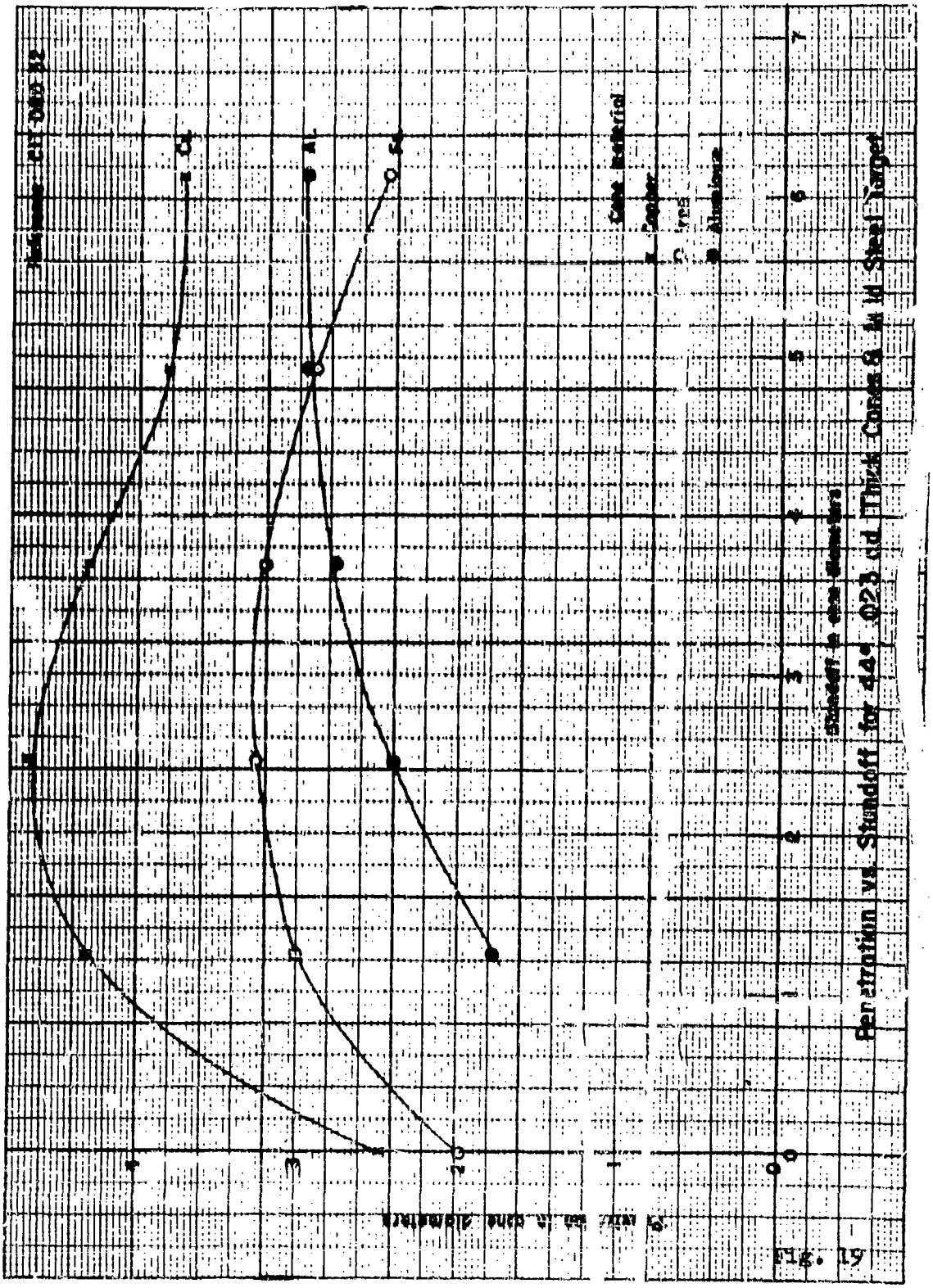
Penetration vs. Standoff for 44° .023 cd. Thick Cones & ¼ id Steel Target
Cu
Al
Fe
Cone Material
Copper
Iron
Aluminum

Fig. 19

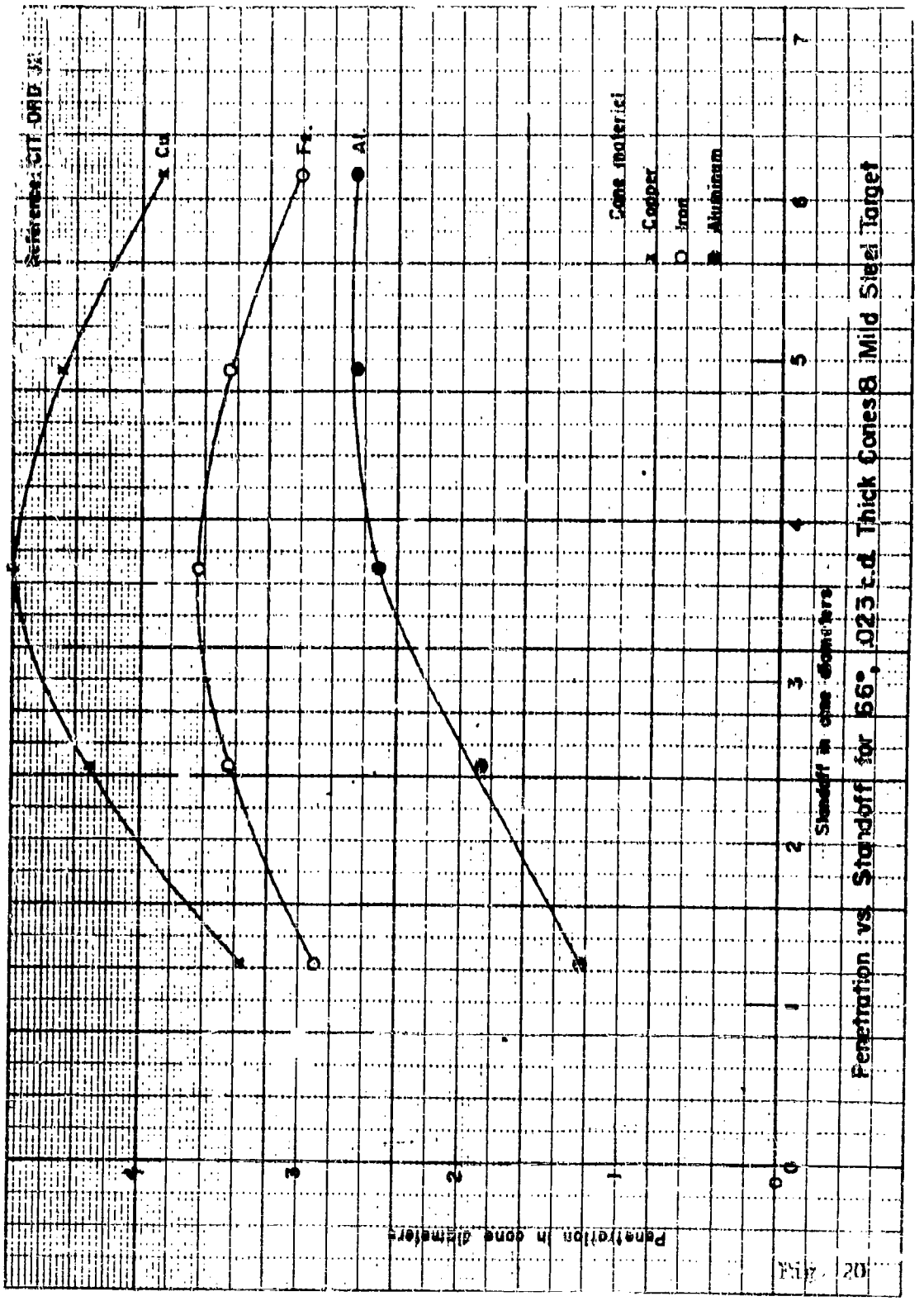
Penetration : vs Standoff for 56°, .023 t.d. Thick Cones in Mild Steel Target
Standoff in cone diameters
Penetration in cone diameters
Cone material
x Copper
O Iron
■ Aluminum
Cu
Fe
Al
Reference: CIT ORD 33

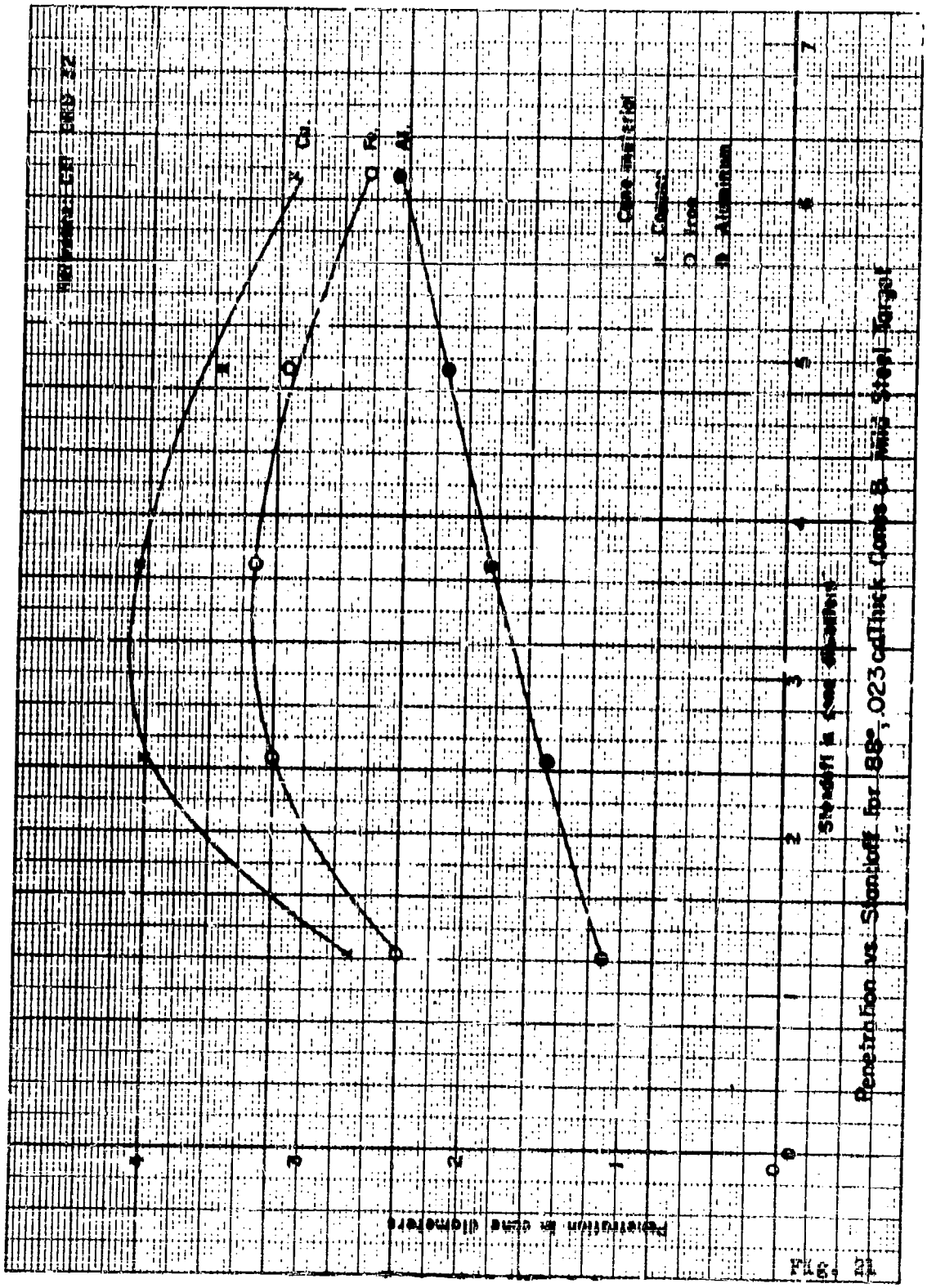
Penetration vs. Standoff for .88", .023 calthick Comp B, Mild Steel Target
Standoff in Cone diameters
Penetration in cone diameters
Cone material
C Iron
A Aluminum
Cu
Fe
Al
FIG. 23

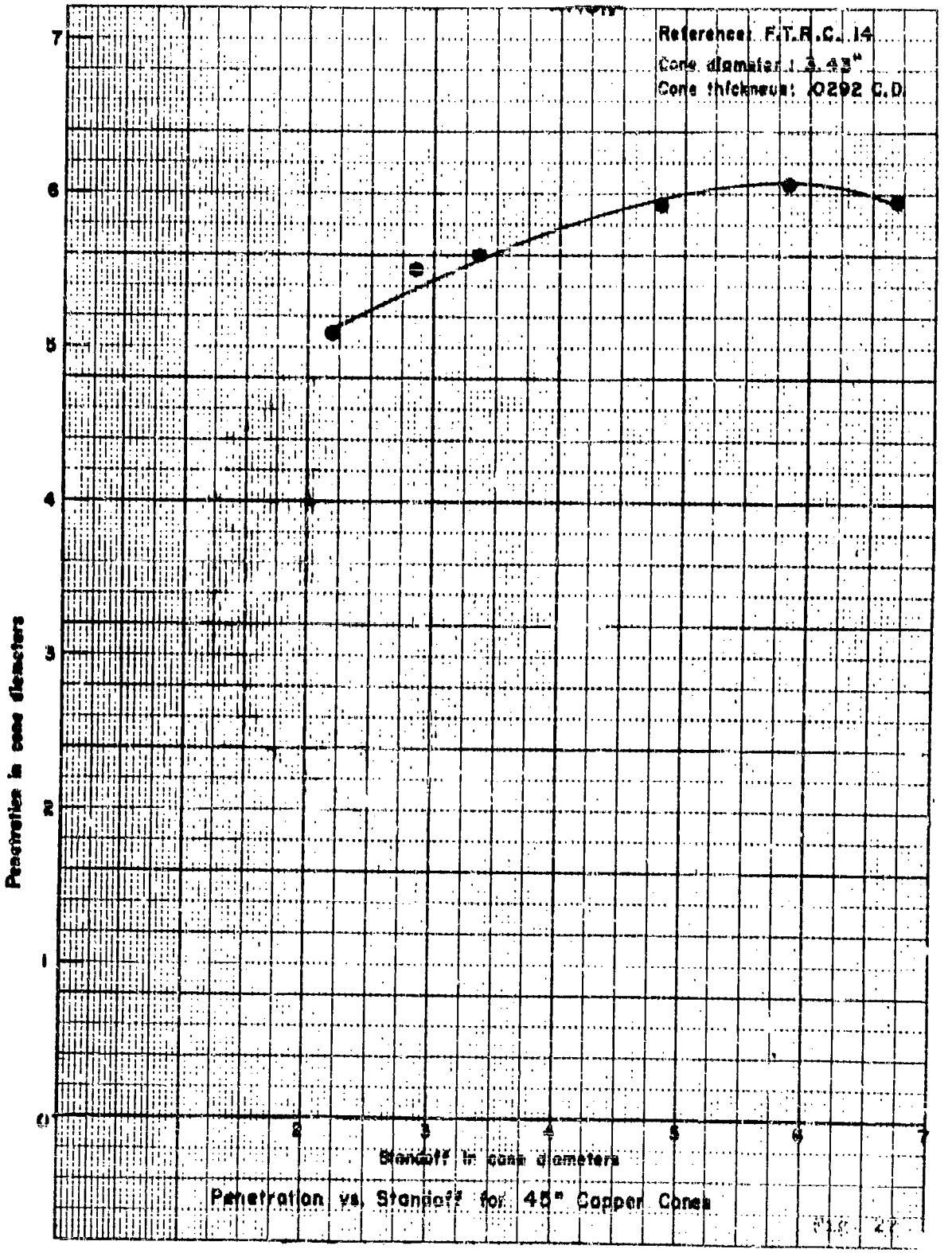
Reference: F.T.R.C. 14
Cone diameter: 3.43"
Cone thickness: .0292 C.D.
Penetration in cone diameters
Standoff in cone diameters
Penetration vs. Standoff for 45° Copper Cones
FIG. 27

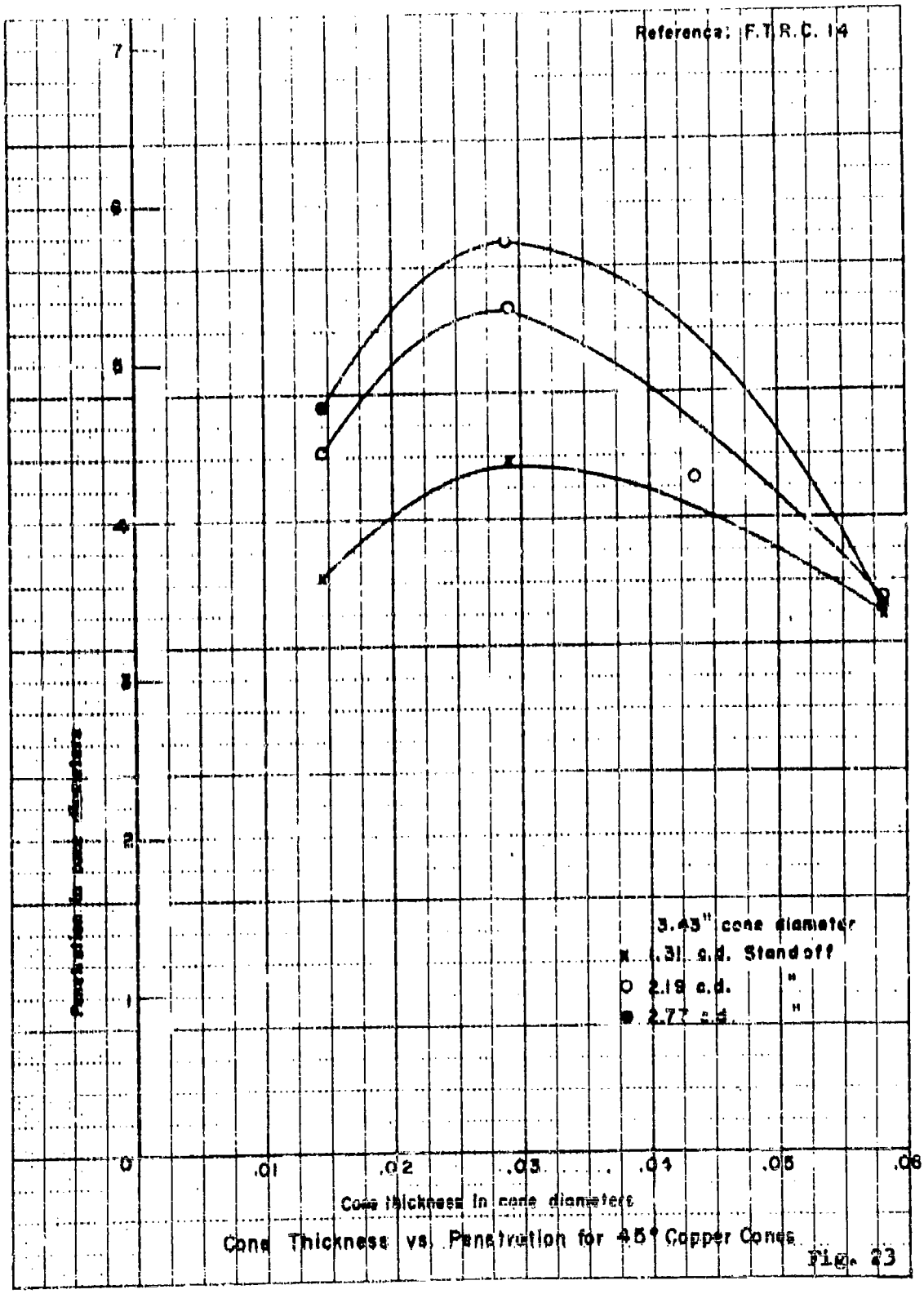

Cone Thickness vs. Penetration for 45° Copper Cones

Fig. 23

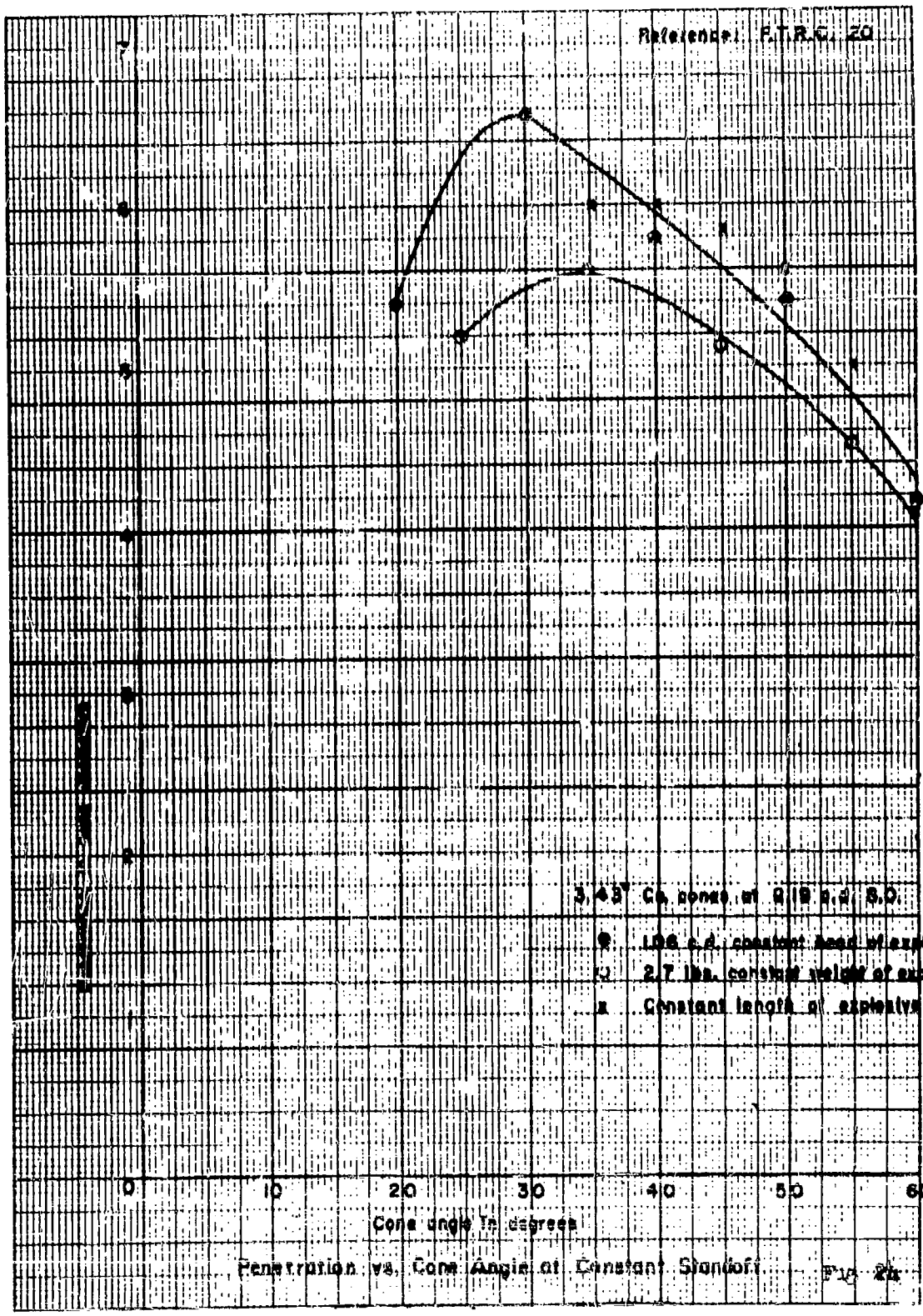

Penetration vs. Cone Angle at Constant Standoff. Fig. 24

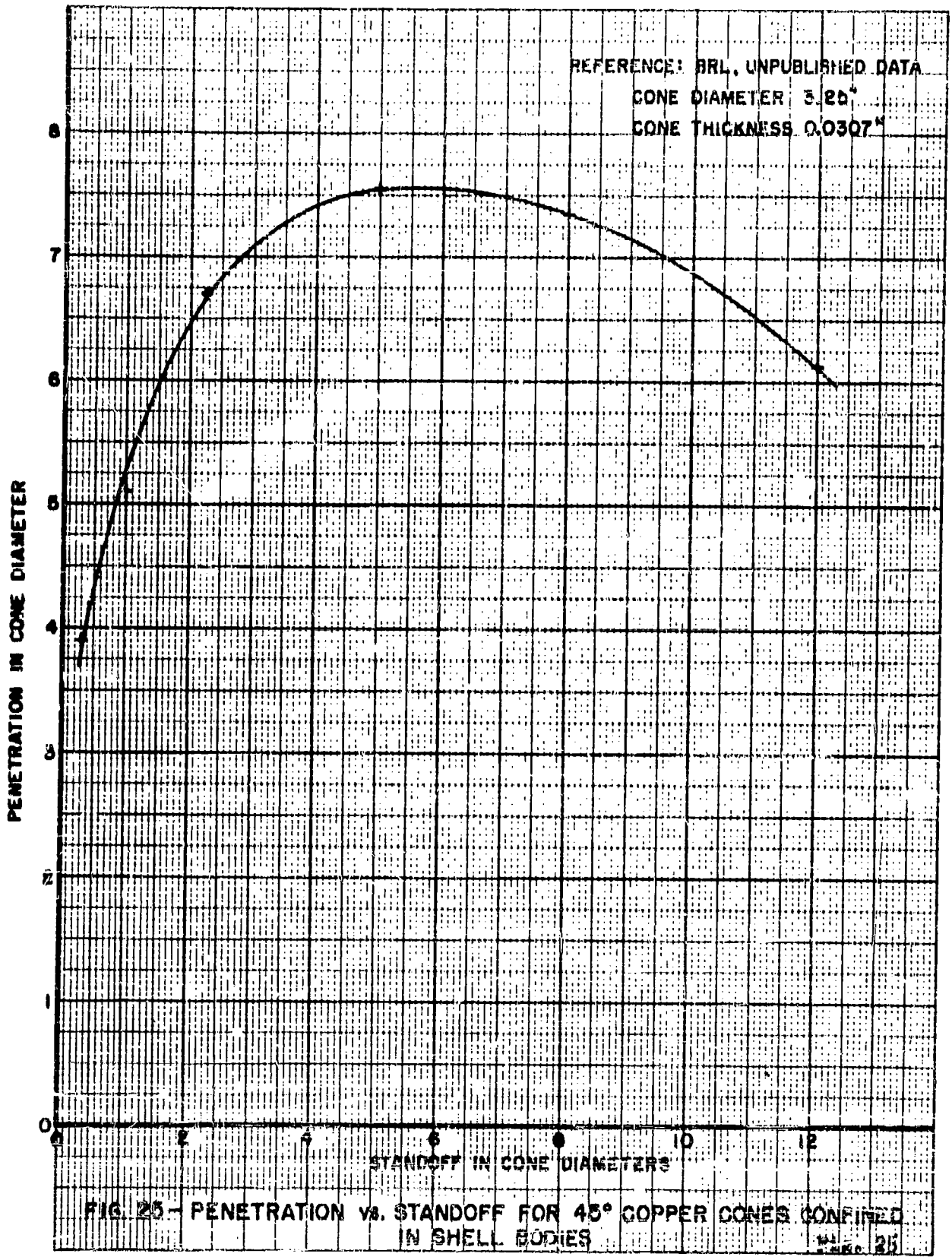

FIG. 25 – PENETRATION Vs. STANDOFF FOR 45° COPPER CONES CONFINED IN SHELL BODIES

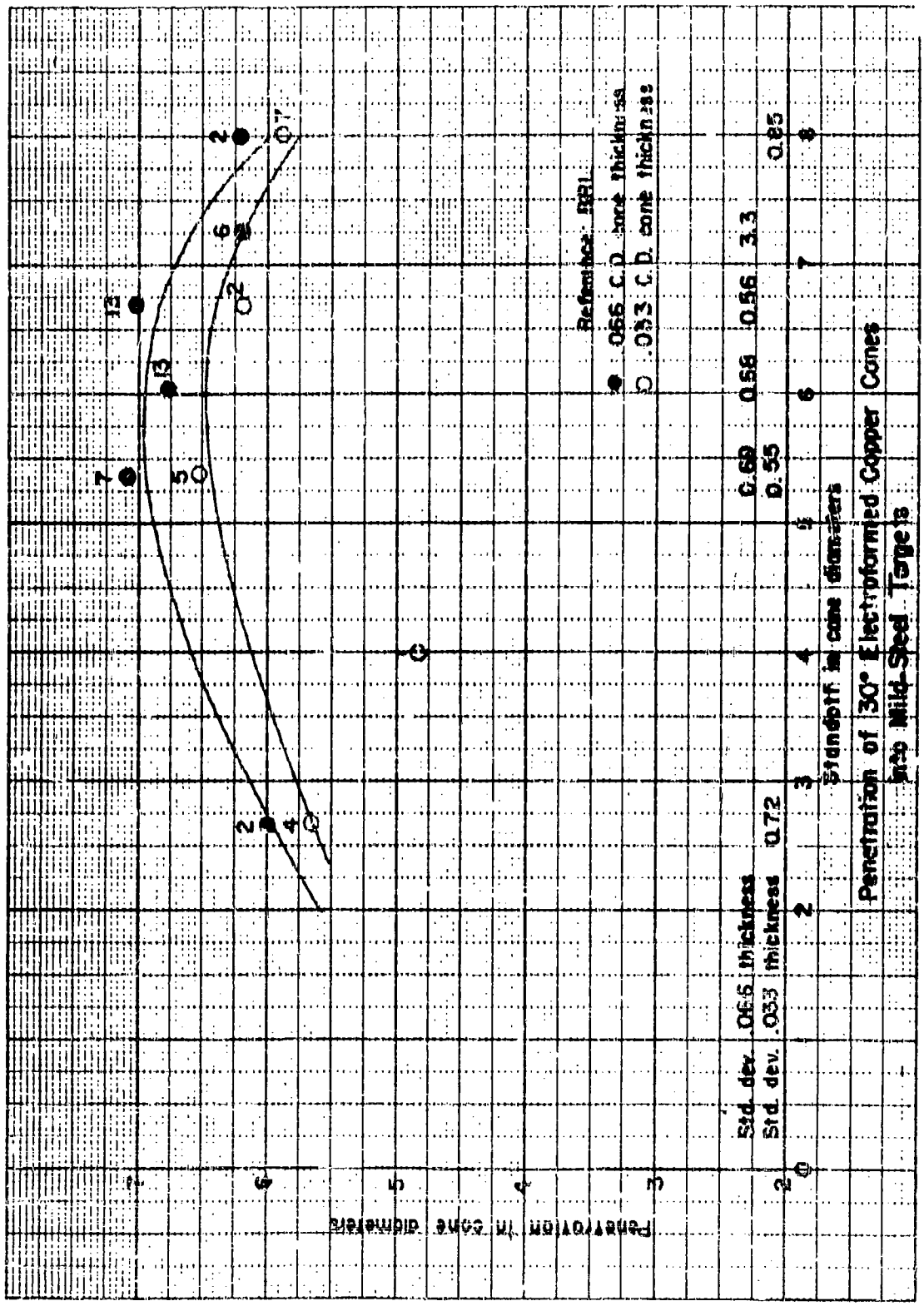
Penetration of 30° Electroformed Copper Cones
into Mild Steel Targets
Standoff in cone diameters
Penetration in cone diameters
Reference: BRL
● .066 C.D. cone thickness
○ .033 C.D. cone thickness
Std. dev. .066 thickness 0.72
Std. dev. .033 thickness 0.85
0.69 0.56 0.56 3.3
0.55

Fig. 20

charges whose diameter was 20% greater than the cone diameter, and of a sufficient length (2 cone heights above the apex) to insure that penetration was not restricted by short charge length. The cone thickness was much greater than that usually used. Figure 26 gives penetration as a function of standoff for 30° cones. Similar curves were obtained for 20°, 46°, and 60° cones. The results of most interest are those for the small angle cones, which gave excellent penetration and a large optimum standoff. This is at variance with previous results for steel cones of smaller wall thickness and with charges the same diameter as the cone, for which both optimum standoff and maximum penetration decrease with cone angle (Compare Figs. 10 and 11 with Figs. 27 and 28). However, Figure 9 does show the penetration increasing with cone thickness even up to the maximum thickness fired. Figure 27 shows that the cone thickness is not critical for 46° cones, but this is not true for other angles especially 20° cones. Figure 28 shows maximum penetration as a function of cone angle. It is thought that the differences in optimum standoff given are not of any significance, since no definite trend is shown and the penetration standoff curves are fairly flat. The optimum thickness for 46° seems a misfit. It is possible that a trend in thickness might be shown if intermediate thicknesses between 0.033 and 0.066 had been used.

3. Bimetallic cones and non-conical shapes The term "bimetallic cones" will be applied to cones consisting of an inner layer of one metal with an outer layer of another metal. It does not include cones the apex end of which is of one metal, the base end being of another metal. In most cases the composite cone consists of two separated cones nested in intimate contact. However, in the case of copper clad steel, the two metals are bonded together. The following penetrations into mild steel targets by 45° cones 1.63" diameter are reported. For comparison, results from single metal cones as reported elsewhere in this Chapter, are given in each case.

	Cone Thickness Outside	Center	Inside	Total	Standoff	Penetration	Reference
St.	0.017"	---	Al 0.040"	.035 C.D.	7.4 C.D.	2.6 C.D.	NDRC Div 8 12/15/43
		Aluminum		.036	7.4	2.6	
St.	.036"		Al 0.036"	.044	5.5	3.5	Du Pont 9/18/43
		Aluminum		.036	5.5	2.9	
*St.	.018"		Cu .012"	.018	0.9	4.0	Du Pont 2/5/45 and 10/1/45
*Cu.	.005"	St. .018"	Cu .018"	.025	1.0	4.0	
		Copper		.024	1.0	4.3	
**Cu.	.010"	St. .029"	Cu .025"	.031	1.2	4.3	Du Pont 10/1/45
		Copper		.031	1.2	4.6	
St.	.036"		Cu .036"	.044	2.5	4.7	Du Pont 9/18/43
		Copper		.030	1.4	5.0	
St.	.018"		Cd .006"	.015	.9	3.0	Du Pont 8, 9/43
		Steel		.015	1.3	3.5	

* Copper Clad
**Copper Clad, 46°, 2.07" dia.

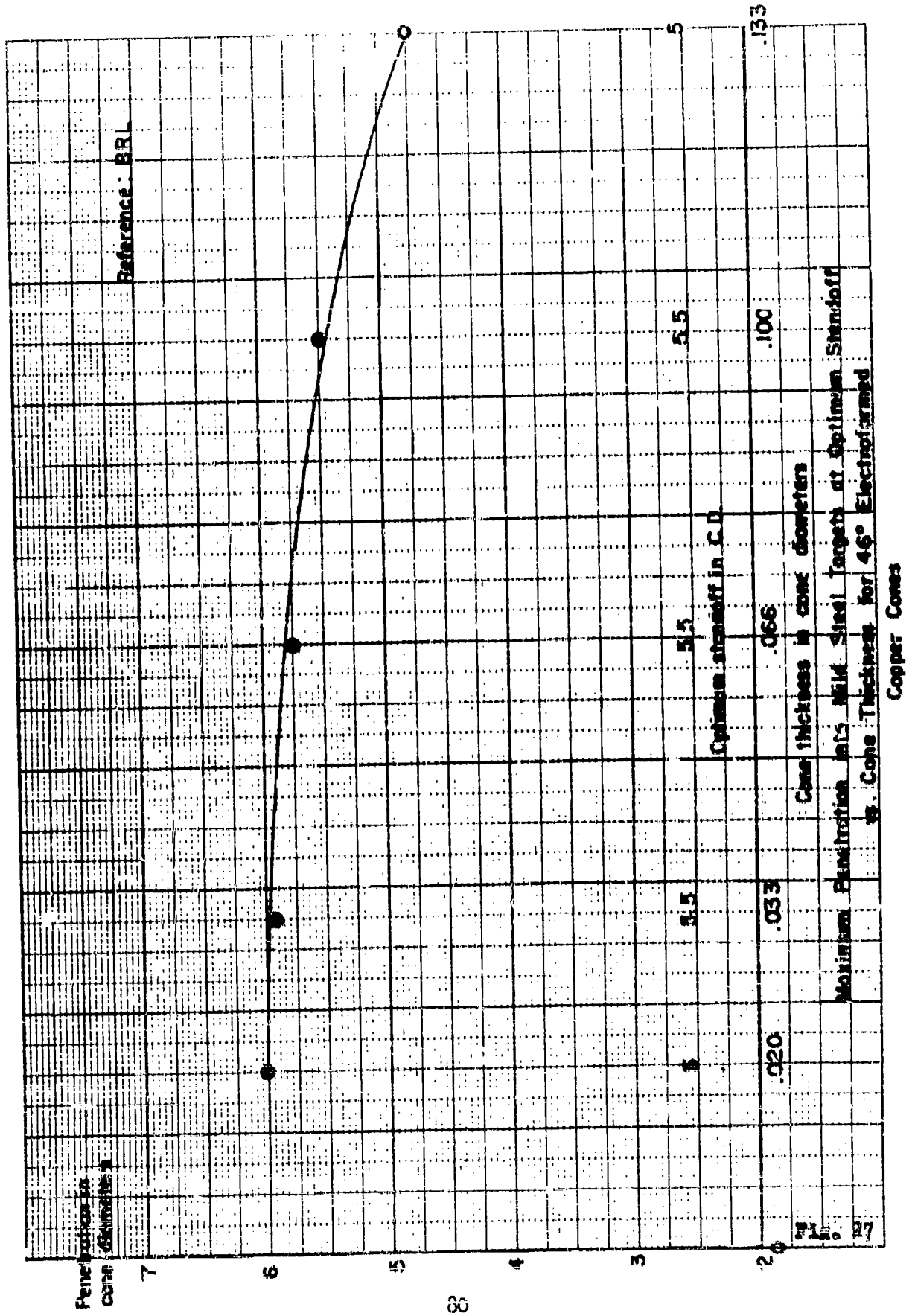
Reference: BRL
Penetration in cone diameters
7
6
5
4
3
2
0
5
5.5
5.5
5.5
5
.133
.100
.066
.033
.020
Optimum standoff in C.D.
Cone thickness in cone diameters
Molybdenum fluorination at 5 Mild Steel Targets at Optimum Standoff
Cone Thickness for 46° Electroformed Copper Cones
Fig. 27

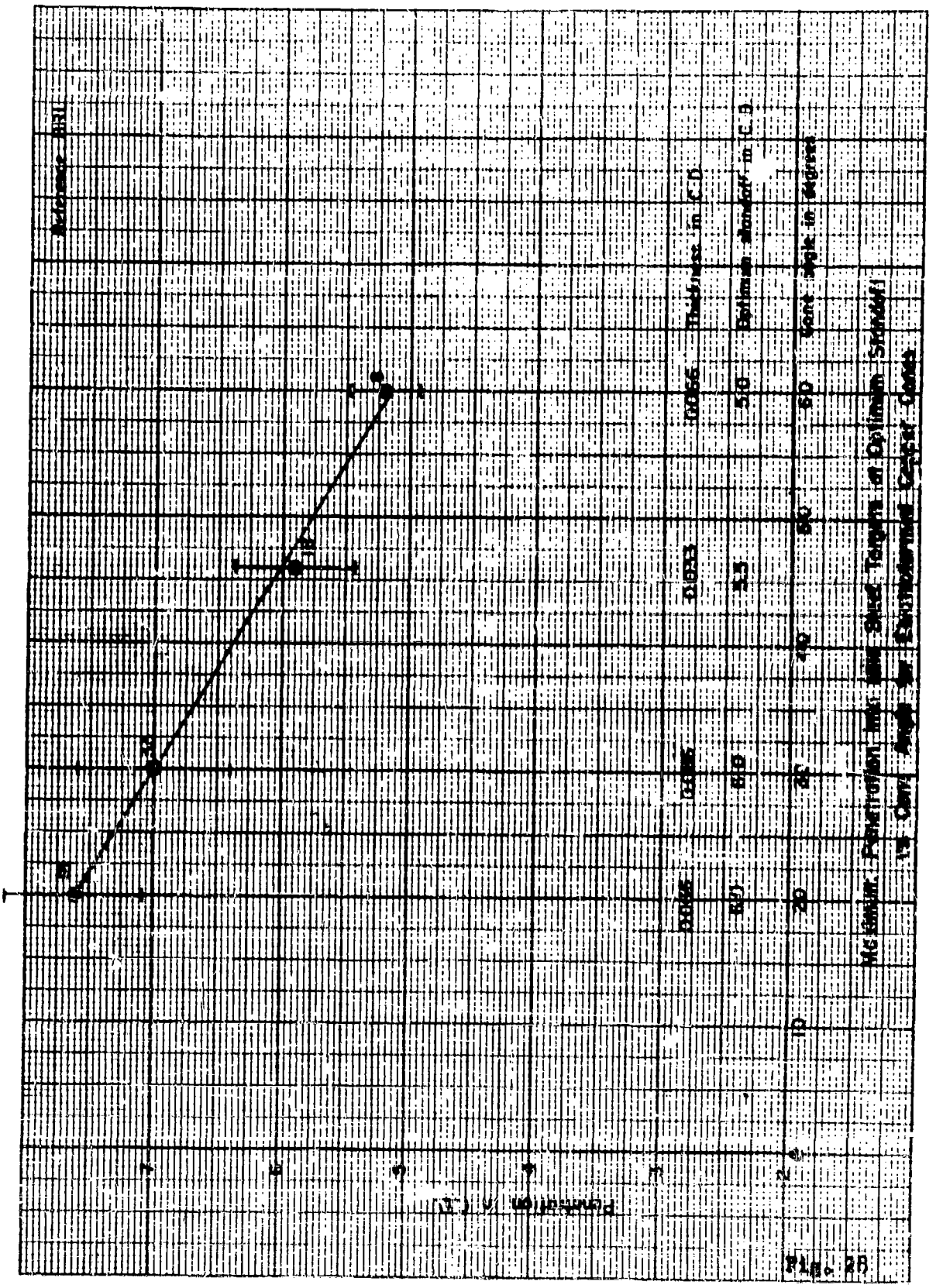
Fig. 28

Non-conical shapes include hemispheres and spherical caps, trumpets, and combinations.

Radiographs indicate that hemispheres do not collapse, with the formation of a jet, as do cones; they turn inside out before collapsing, the whole liner being projected as a stream of particles. Spherical caps (segments) are fragmented and projected as a cluster of particles which may be more or less focused, depending on the curvature. The following data have been reported for hemispheres:

Material	Dia.	Thickness	Standoff	Penet.	Confinement	Reference
Brass	2.375"	0.021 Dia.	2.5 D	3.0 D	3" OD St.	NDRC Div 8,6/15/44
Steel	1.37"	.033 D	.4 D	2.9 D		**ARD/Expl 172/43
		.052 D	.9 D	1.9 D		
	1.63"	.020 D	3.7 D	3.1 D	2" OD St.	OSRD 5598
	1.88"	.027 D	4.3 D	2.6 D	$2\frac{1}{4}$" OD St.	
	*2.38"	.021 D	3.8 D	2.9 D	3" OD St.	NDRC Div 8,7/15/44
	2.38"	.026 D	3.8 D	3.0 D	3" OD St.	
Cu	1.63"	.015 D	3.7 D	2.0 D		CIT-ORD-16
	1.88"	.022 D	4.3 D	3.3 D	$2\frac{1}{4}$" OD St.	OSRD 5598
	1.88"	.027 D	3.2 D	3.2 D	$2\frac{1}{2}$" OD St.	NDRC Div 8,6/15/44
Al	1.38"	.056 D	9 D	1.6 D		ARD/Expl 172/43
		.058 D	18 D	1.5 D		
Cd	1.38"	.033 D	9 D	1.7 D		ARD/Expl 172/43
		.049 D	18 D	0.8 D		

* With Spitback tube
** British Report

Some work has been done with spherical segments especially by the British. The results were, generally, poorer than those from hemispheres.

The following results have been obtained for trumpets:

Material	Dia	Thickness	Standoff	Penet.	Shape	Reference
Fe	1.63"	.021 D	1.2 D	2.6 D	Flare from 20° to 120°	NDRC Div 8, 8/15/43
			2.5 D	3.4 D		
	1.90"	.032 D	1.1 D	3.7 D	Ht 1.81" Rad. 2.85"	OSRD 5598
Cu	1.63"	.031 D	2.5 D	2.9	Rad. 1.50" 3/8" Dia.	CIT-ORD-R3
			3.7 D	3.7 D	2.50" flat	
			5.2 D	5.2 D	2.50" apex	
	1.63"	.031 D	1.2 D	4.0 D		OSRD 5598
	3.40"	.028 D	2.1 D	4.9 D*	Rad. 4.85" = $\frac{1}{4}$" Dia.	BRL unpublished
				6.4 D**	Rounded apex	

* Point initiation
**Peripheral initiation

Electroformed liners of doubtful quality.
The penetration of similar 45° cones was 5.1 Dia.

Interest in double angle cones has been revived recently, due largely to certain advantages shown for the French 73mm round. Early firings of double angle cones, in which the change from one angle to the other was made abruptly, did not show any increase in penetration for the double angle (14). In the French 73mm round, the change from one angle to the other was made smoothly and the liner wall was tapered. This round gave peak performance at normally available standoffs. (15)

An almost infinite variety of combinations is possible. Complete coverage would be too lengthy for this Chapter, especially since, generally speaking, the penetrations achieved from them are inferior to those from cones. The following references are suggested:

Combinations of cones, hemispheres, and cylinders:

DuPont, 18 September 1943

CIT-ORD-16

OTIB 1146a (Translation of German Report)

OSRD 5598

BRL 848

Helmet and bottle shapes (German Work)

OTIB 1148

OTIB 1149

NEC 2587

NEC 5919

G. The Effect of Liner Details on Penetration

1. Tapered walls The British suggested (16) that, since the thickness of liners should scale as the diameter, a cone would logically be thicker at the base than at the apex. This idea has been followed up by several groups of investigators. Only a few results will be mentioned.

Reported by NDRC, Div. 8

45° Steel Cones

Thickness at Base	Thickness at Apex	S. O.	Penetration	
C. D.	C. D.	C. D.	C. D.	
0.006	0.025	1.2	2.6	11-15-43
.025	.006	1.2	2.9	
.055	.007	1.4	2.6	
.017	.029	1.4	3.0	5-15-44
.027	.043	1.4	2.5	
.018	uniform	1.4	3.4	from
.022	uniform	1.4	2.5	Fig. 11

45° Copper Cones

Reported by Firestone

.037*	.027*	2.2	5.6	FTRC 21
.029	uniform	2.2	5.2	

*Thickness measured at reference points 0.14 C. D. and 0.84 C. D. from base.

Reported by Carnegie Institute of Technology

45° Copper Cones

Thickness at Base	Thickness at Apex	S. O.	Penetration	
.030	.020	3.0	5.70 **	
.030	uniform	3.0	5.37	CIT-ORD-46
.037	.029	3.7	5.53 **	
.037	uniform	3.7	5.85	
.023	uniform	3.7	4.75	
Double Taper		3.0	3.07	
.031	uniform	3.0	3.43	

**Machined from drawn liners.

In general, it does not seem likely that any very appreciable improvement in performance can be obtained by the use of tapered wall cones, within the range of the above data. However, it is possible that if the right combination of thickness and taper can be found, improved results may be obtained.

2. Wires and other obstructions within the cavity A very large number of tests have been conducted to find the effect of wires, coils, simulated firing pins, etc. placed within the cavity of the cone or on the axis in front of the cone. Practically all of these items were in connection with fuzing. All such obstructions almost invariably cause very serious impairment of the penetration, often as much as 50%. Details will not be given here, but those interested may refer to NDRC Div. 8 Interim reports 15 February 1944, and 15 February 1945, DuPont reports for April and May 1943, Firestone Reports No. 16 and 19, and OSRD 5599.

3. Flanges The effect of the base flange of the cone on the jet formation is somewhat curious. The DuPont workers reported (17) the following data for M9A1 steel cones 45°, 1.63" base diameter, flange 2.0" diameter, unconfined:

Dia. of Explosive	Penetration in MS at 1" S.O.	No. Rds.
1.63"	5.45"	4
1.75	5.70	5
1.88	4.50	5
2.00	4.00	5

As the diameter of the explosive is increased beyond the cone diameter, there is a slight increase in penetration followed by a decrease. NDRC Div. 8 (18) followed this up, with the following results: M9A1 steel cones unconfined at 2" S.O. penetration in mild steel targets.

Dia. of Explosive	With Flange	Without Flange
1.63"	5.39"	
1.75	6.00	5.49"
1.88	5.39	5.35
2.00	4.30	5.34

For 1 3/4" diameter charges in 1 3/4 x 2" steel tubing:
With flanges 4.12"
Without " 5.33"

For 1 3/4" diameter charges in 1 3/4" x 2 1/4" steel tubing:
With flanges 4.33"
Without " 5.07"

Firestone reported 2 series of tests as follows: (19)

Explosive backed flange	10.45"	Penetration
No explosive on flange	18.14	Penetration
Explosive backed flange	8.50	Penetration
No explosive on flange	16.21	Penetration

These were for heavily confined charges.

Recently, Carnegie Institute of Technology has reported the following: (20)

M9A1 steel cones, penetration into mild steel targets, 4" standoff.

	Not confined		Confined, 1/4" steel	
Dia. Explosive	With Flange	Without Flange	With Flange	Without Flange
1 5/8"	5.9	5.4	6.6	6.5
2	6.4	6.7	5.5	6.4
2	5.1	4.4	3.6	3.6

The CIT data are in partial disagreement with those from DuPont and NDRC. The figures for the unconfined charges, with flanges, suggest that the disagreement may be due to the change in standoff.

The CIT explanation of the flange effect is briefly as follows:

The velocities and the velocity gradients along a jet are quite sensitive to the times of arrival of the release wave at the liner. Since the release wave is initiated at the charge boundary, any change in the geometry will consequently cause a change in the velocity and in the velocity gradient. With the larger diameter charge, which has an explosive belt, the major portion of the release wave is initiated on the lateral surface, but a small portion is initiated along the base of the explosive shoulder during the later stages of the cone collapse process. This small portion of the release wave produces a greater gradient in the velocities of the rear elements of the jet, which contain a large fraction of the jet mass. To be of benefit, the magnitude of this gradient should be neither too great nor too small. If it is too large, this portion of the jet will break up quite rapidly and become ineffective. If it is too small, proper lengthening will not be achieved for efficient penetration. This, in essence, explains the observed optimum charge diameter for a liner of given base dimension.

Consider the 2" diameter charges, completely unconfined. As explained above, most of the release wave has been initiated along the side of the charge. The part of the wave originating from the base affects only a small portion of the cone, thus, the short delay caused

by the confining action of the thin flange is a second order effect and can be neglected, as the penetration depths indicate. When 1/4" steel tubing is used as lateral confinement, the shock conditions are altered, in that the release wave from the lateral surface is delayed considerably. Under these conditions, the position of the release wave propagating from the base of the charge affects a greater portion of the liner and plays a more important role. The slight delaying action caused by the base flange is enough to increase the magnitude of the velocity gradient at the rear of the jet to the point where break-up begins to occur. The effective length of the jet will then be somewhat greater for the charge without the flange than for the charge with the flange. The observed penetrations show that this is the case. With the charges having the heavy base confinement but no lateral confinement, the effect will be to nearly eliminate the initiation of a release wave from the charge base. The consequence will be very little gradient in the velocities of the rear elements of the jet, which will lead to a shorter jet and less penetration. When both lateral and heavy base confinement are introduced we alter the shock conditions so that there is the combined effect of an increase in the impulse available to the liner and the absence of any release wave initiated from the base of the charge. This results in a still shorter jet. The penetration data substantiate this. BRL 585 gives a radiographic study of the effect of the flanges, as a follow up to the NDRC penetration study. When the diameter of the explosive is the same as that of the base of the cone. (See Fig. 29) The radiographs show that, near the end of the collapse process, the cone proper pulls loose from the flange at a point near the base. The flange ring appears to remain stationary while jet and slug move forward through the ring. When the flange is backed by explosive to half (See Fig. 30) or all of its width, the portion of the flange so backed is projected forward as a cylinder of fragments, converging toward the axis at its front end. There has been some tendency in the past to interpret these radiographs as indicating that the cloud of fragments interrupted the jet. That a target so nebulous as the cloud of fragments could interrupt the jet seems somewhat incredible. The only thing the radiographs show is that when the flange is backed by explosive, the jet either is interrupted or is very short, and when the flange is not backed by explosive, the jet is normal. No evidence substantiating any explanation is given by the radiographs.

4. Effect of spit-back tubes For some types of fuzing, a small tube called a spit-back tube, is attached to the apex end of the cone, extending away from the cavity. The portion of the apex inside the spit-back tube is removed. For M9A1 steel cones in unconfined charges, the presence of the spit-back tube caused little change in penetration or a slight decrease. (21) For copper liners in confined charges, there was no change or an increase up to 20% (22).

5. Effect of annealing Results of tests to determine the effects of annealing and of hardening steel cones (23) show that the penetration from drawn M9A1 cones is not changed by annealing but that it becomes

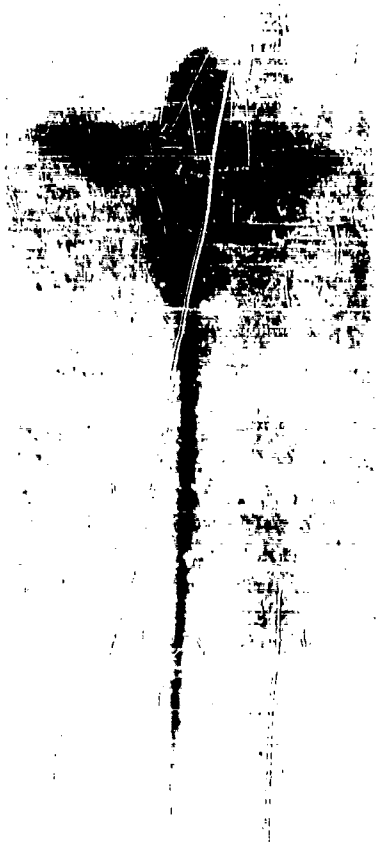

FIGURE 29

FIGURE 30

progressively less as the hardness is increased. Drawn copper cones (24) show no change with annealing. Results at the Ballistic Research Laboratories show that cast beryllium copper cones, whose normal penetration was low, were improved by annealing; electroformed copper cones were not affected by annealing, except that, when the annealing temperature was increased to 1400°F, the cones blistered on the inner surface, with a decrease in penetration; and that cones made by a shear forming process, which worked the metal so severely that its structure was impaired, were improved by annealing. A complete and interesting discussion of the effects of annealing on copper cones are contained in a BRL report (29).

These results may be summarized as follows:

Annealing, if not carried to high temperatures, is neither harmful nor beneficial unless the metallurgical condition of the liner is very poor.

If the metallurgical condition of the liner is very poor, annealing is beneficial.

Hardening of steel liners is detrimental.

H. Jet Velocities

1. Initial velocity The velocity of the head of the jet is usually obtained from streak camera records. What the camera actually photographs is the luminous shock in air associated with the head of the jet. Often the head of the jet is ill-defined in that it is surrounded by a shroud, the exact nature and cause of which is not completely understood. Initial velocities are apt to have a large dispersion.

Figure 31 shows the variation of jet velocity with cone thickness for 45° and for 80° steel cones. Some data are available for 60°, 100° and 120° cones, the results being similar to those shown. Figure 32 shows the variation with cone angle for 0.020" thickness and for 0.037" thickness. All rounds were 1.63" diameter, cast in pentolite charges, unconfined. In drawing the curves, the points for 100° were ignored. It should also be mentioned that, for some of the data, it was necessary to infer the thickness from the weights given and this may have introduced small errors in some of the points.

Figures 33 and 34 are from unpublished data recently released by Carnegie Institute of Technology for cones of steel, copper and aluminum. These data, especially for copper and aluminum, are a valuable addition to our knowledge of jet characteristics.

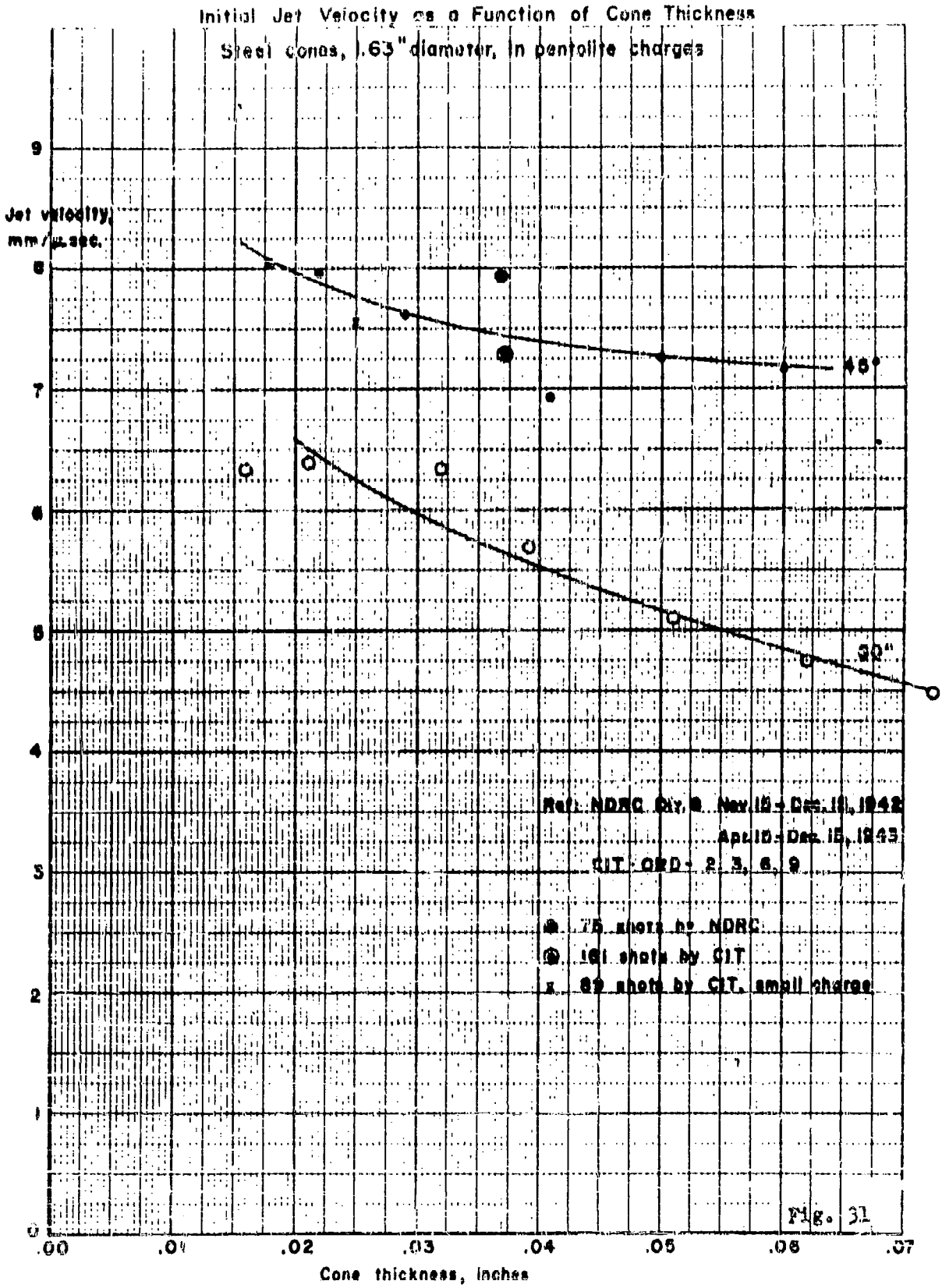
Initial Jet Velocity as a Function of Cone Thickness
Steel cones, 1.63" diameter, in pentolite charges
Jet velocity, mm/μ sec.
9
8
7
6
5
4
3
2
1
0
45°
60°
Ref: NDRC Div. 8 Nov. 15 - Dec. 15, 1942
Apr. 15 - Dec. 15, 1943
CIT - ORD - 2, 3, 6, 9
75 shots by NDRC
161 shots by CIT
89 shots by CIT, small charge
.00
.01
.02
.03
.04
.05
.06
.07
Cone thickness, inches

Fig. 31

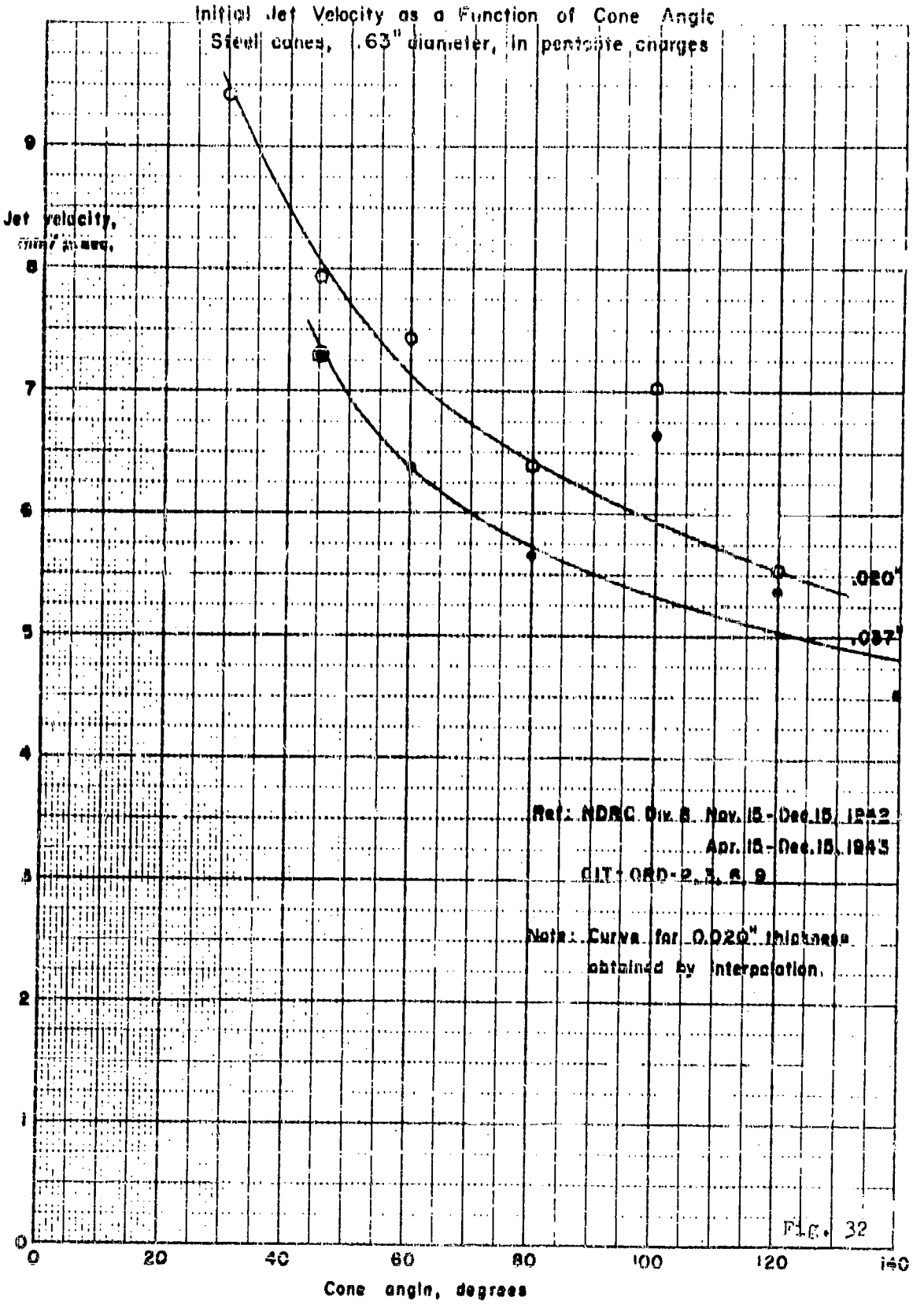
Initial Jet Velocity as a Function of Cone Angle
Steel cones, .63" diameter, in pentolite charges
Jet velocity,
mm/ μsec.
9
8
7
6
5
4
3
2
1
0
0
20
40
60
80
100
120
140
Cone angle, degrees
.020"
.037"
Ref: NDRC Div. 8. Nov. 15 - Dec. 15, 1942
Apr. 15 - Dec. 15, 1943
CIT - ORD - 2, 3, 8, 9
Note: Curve for 0.020" thickness
obtained by interpolation.

FIG. 32

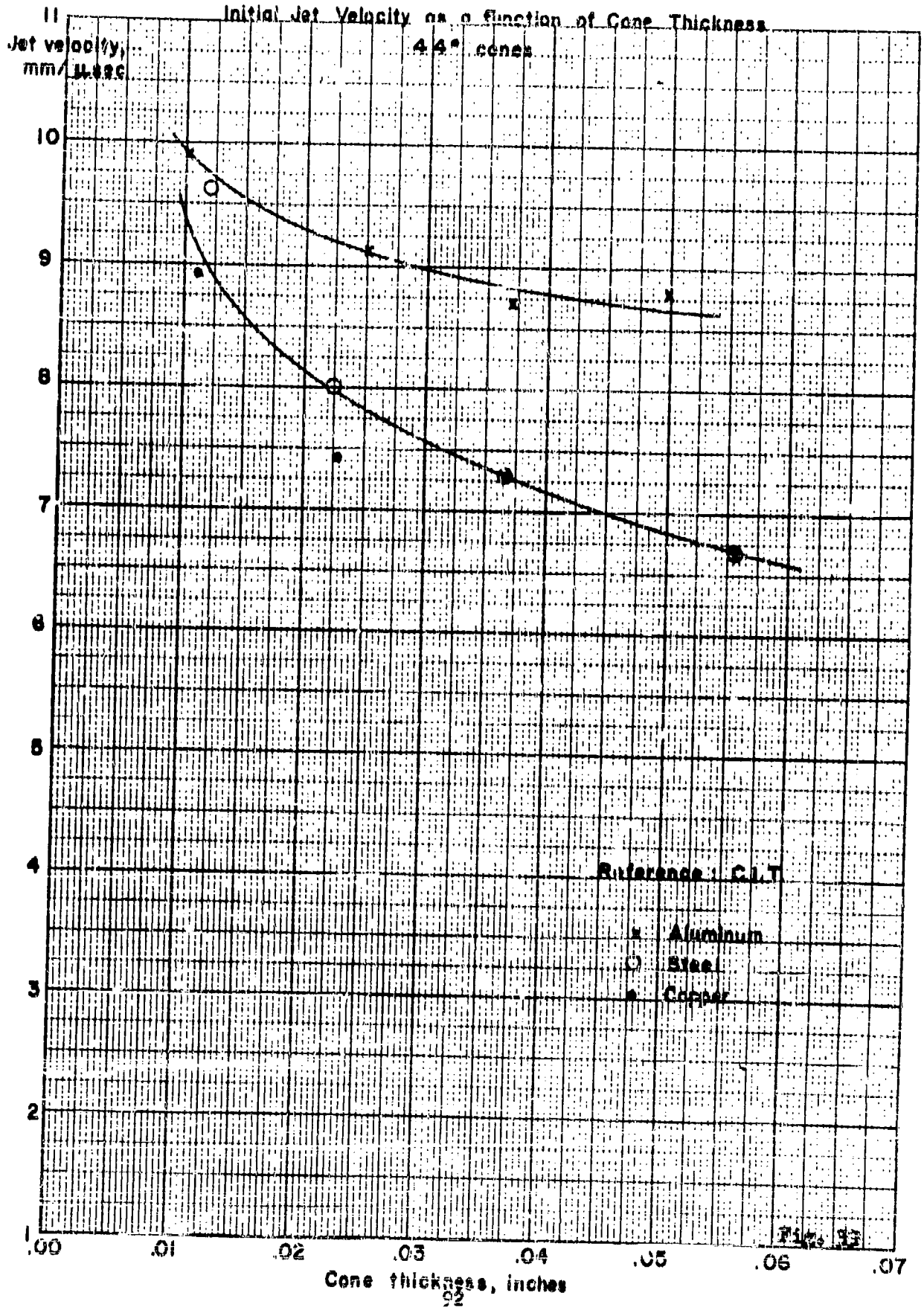
Initial Jet Velocity as a function of Cone Thickness
44° cones
Jet velocity, mm/μsec
11
10
9
8
7
6
5
4
3
2
1
.00
.01
.02
.03
.04
.05
.06
.07
Cone thickness, inches
Reference: C.I.T.
Aluminum
Steel
Copper
Fig. 33

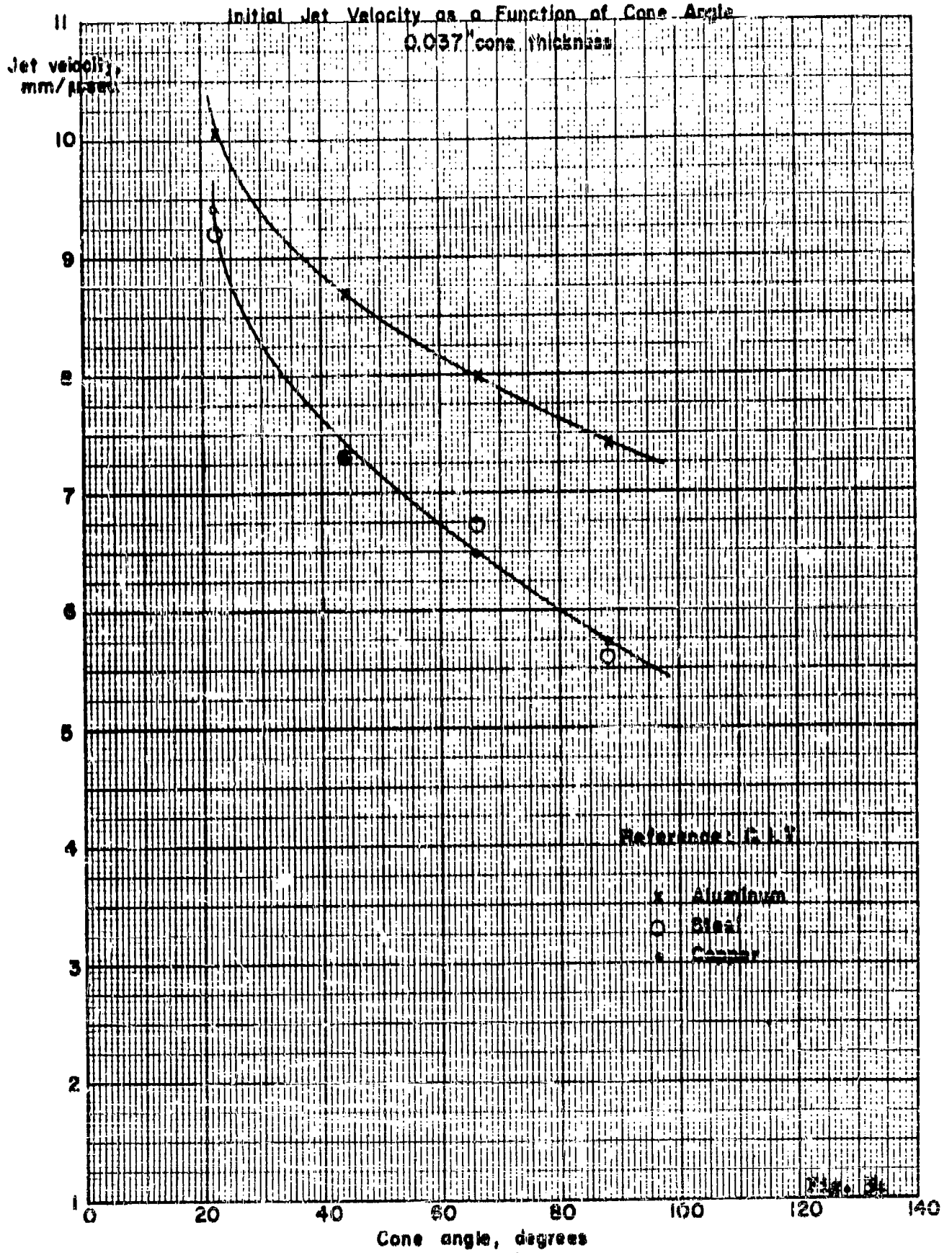
Initial Jet Velocity as a Function of Cone Angle
0.037" cone thickness
Jet velocity, mm/μsec.
11
10
9
8
7
6
5
4
3
2
1
0
20
40
60
80
100
120
140
Cone angle, degrees
Reference: G. I. T.
x Aluminum
○ Steel
• Copper

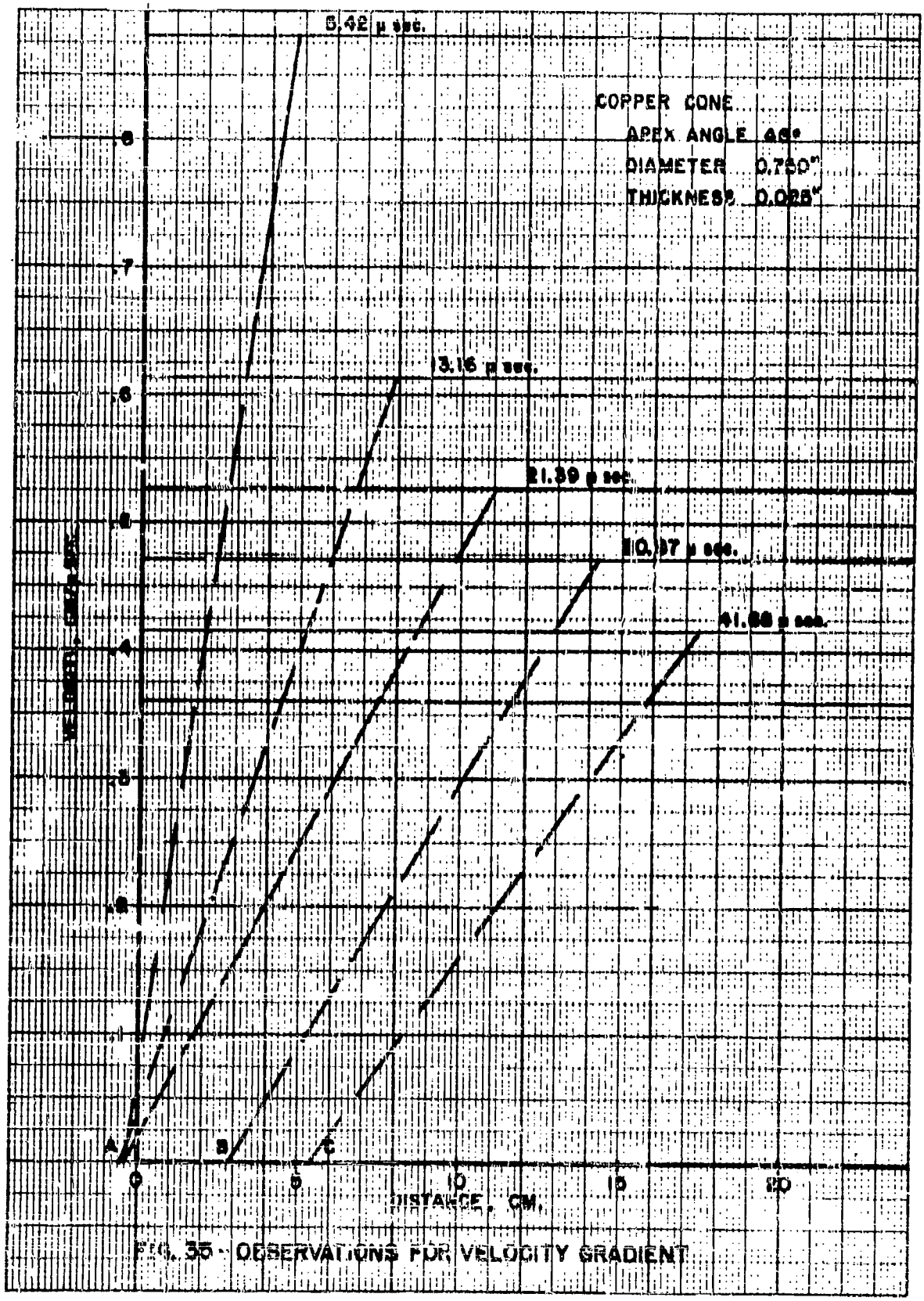

FIG. 35 - OBSERVATIONS FOR VELOCITY GRADIENT

The following miscellaneous data are available.

Material	Cone Dia.	Angle	Thick.	Explosive	Jet Vel. MM/μSec.	No. Rounds	Reference
Al	1.63	45°	0.046"	Pent	8.39	8	NDRC, Jul. 15-Aug. 15 1943
Cu	1.63	45°	0.029"	Pent	7.39	3	Same
Pb	1.5	45°	0.037"	Cyclotol	8.50	5	Aug 15 - Sep 15 1942
Pb	1.5	80°	0.037"	Cyclotol	5.82	4	Same
Pb	1.5	120°	0.037"	Cyclotol	4.85	4	Same

There is also an interesting set of data on 3/8" diameter cones of copper and aluminum, 45°, 60° and 80° angles, in NDRC Div. 8, 15 February - 15 June 1944. These were tested for use in spit-back fuses.

2. Velocity gradient The velocity gradient of a jet is the rate of change of velocity with respect to length. Since the length is changing with time, the gradient must be given for some specified time, or distance. Ideally, the determination of the gradient would be made by measuring the velocity and position of a series of points in the jet at the desired time. For particle jets, approximate results can be obtained from successive flash radiographs. For solid jets results can not be obtained by the usual method of instrumentation available at the present time. By firing jets through targets of different thicknesses or through spaced targets, the length and the velocity of the tip and tail of successive elements of the jet can be obtained. Thus, the mean gradient of these elements can be determined, but each gradient is for a different time (the time at which the tip of the element contacted the target). To adjust the gradients of all elements to the same time, it is necessary to make some assumption about the variation of the velocity with time. It is usually assumed that the velocity of any point in the jet is constant in time and this has been done in computing the gradients given below. The validity of this assumption will be discussed later in this section.

As an example, Figure 35 shows the results of firing the jet from a 46° copper cone 0.750" diameter and 0.025" thick through 5 spaced targets. The figure is a plot of jet velocity vs position or distance from the base of the cone for the 5 elements of jet wiped off by the 5 targets. The mean gradient for any element is the slope of the straight line shown and is determined for the time shown on the plot, time being measured from the instant the tip of the initial element passed the base of the cone. As mentioned above, the calculations are based on the assumption that the velocity of any point in the jet is constant. If the curves are extrapolated to the horizontal axis the points A, B, C, which the CIT writers have called the origin of the jet, are obtained.

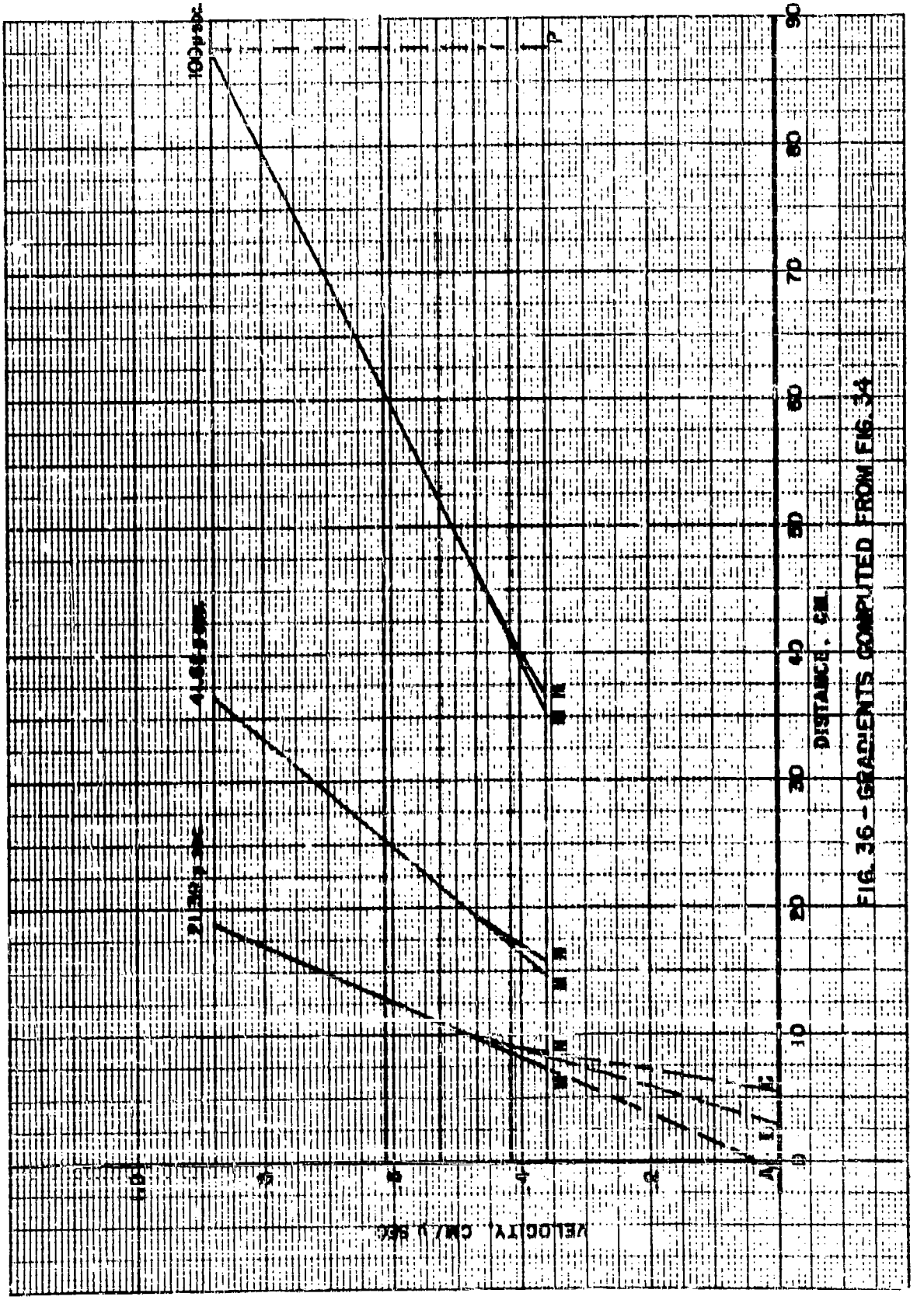

FIG. 36 - GRADIENTS COMPUTED FROM FIG. 34

For the 5 elements shown, the coordinates of the origins were -0.41, -0.50, +2.89 and +5.41 cm., the first 3 values being essentially the same. It follows from simple considerations that the location of the origin for any element is independent of the time at which its length is measured, so that, if one point, say the tip of the leading element, is determined for any time, the curve for the first 3 elements can be drawn by passing it (extended) through the origin A; as shown in Figure 36; the parts of the curve for the 4th and 5th elements are then added, passing through B and C respectively.

Figure 36 shows the plots for 3 different times: 100 μsec, which was chosen arbitrarily; 41.68 μsec., the time at which the last element was measured; and 21.39 μsec., the time at which the mid element was measured. It is seen that, as the time increases, the line tends to become straight, so that the gradient tends to become linear with increasing time. If the gradient at any time t is V_{gt}, then the gradient at any later time $t + \Delta$ is given by $V_{g(t+\Delta)} = 1/1/V_{gt} + \Delta$ and, if Δ becomes large compared with $\frac{1}{V_{gt}}$, the latter term can be neglected and the gradient becomes essentially $\frac{1}{\Delta}$.

The length of the jet, Figure 36 is $\overline{NP}$. For a strictly linear gradient the length would have to be $\overline{MP}$. The distance $\overline{MN}$ (or $\overline{AC}$) may be taken as a measure of the non-linearity of the gradient. Percentage-wise, $\overline{MN}$ decreases with the time but its absolute value is independent of time. Strictly speaking, the condition that a gradient become linear at some later time is that it be linear to start with, and the condition that the numerical value of the gradient be 1/t is that the origin of the jet lie at the origin of coordinates.

Most of the work on velocity gradients was done by Carnegie Institute of Technology. (25) Figure 37 (26) is a plot showing the results of a large number of firings of M9A1 steel cones reported in NDRC Div. 8 summary reports. However, the time of 100 μsec. was chosen merely for convenience in calculation and it must not be assumed that the jets remain continuous for this length of time. It is seen that the gradient is the same for cyclotol or Comp B and pentolite, and is independent of the target material used. The following values of the velocity gradient computed for a time of 100 μsec. after the tip of the jet reached the base of the cone, have been obtained.

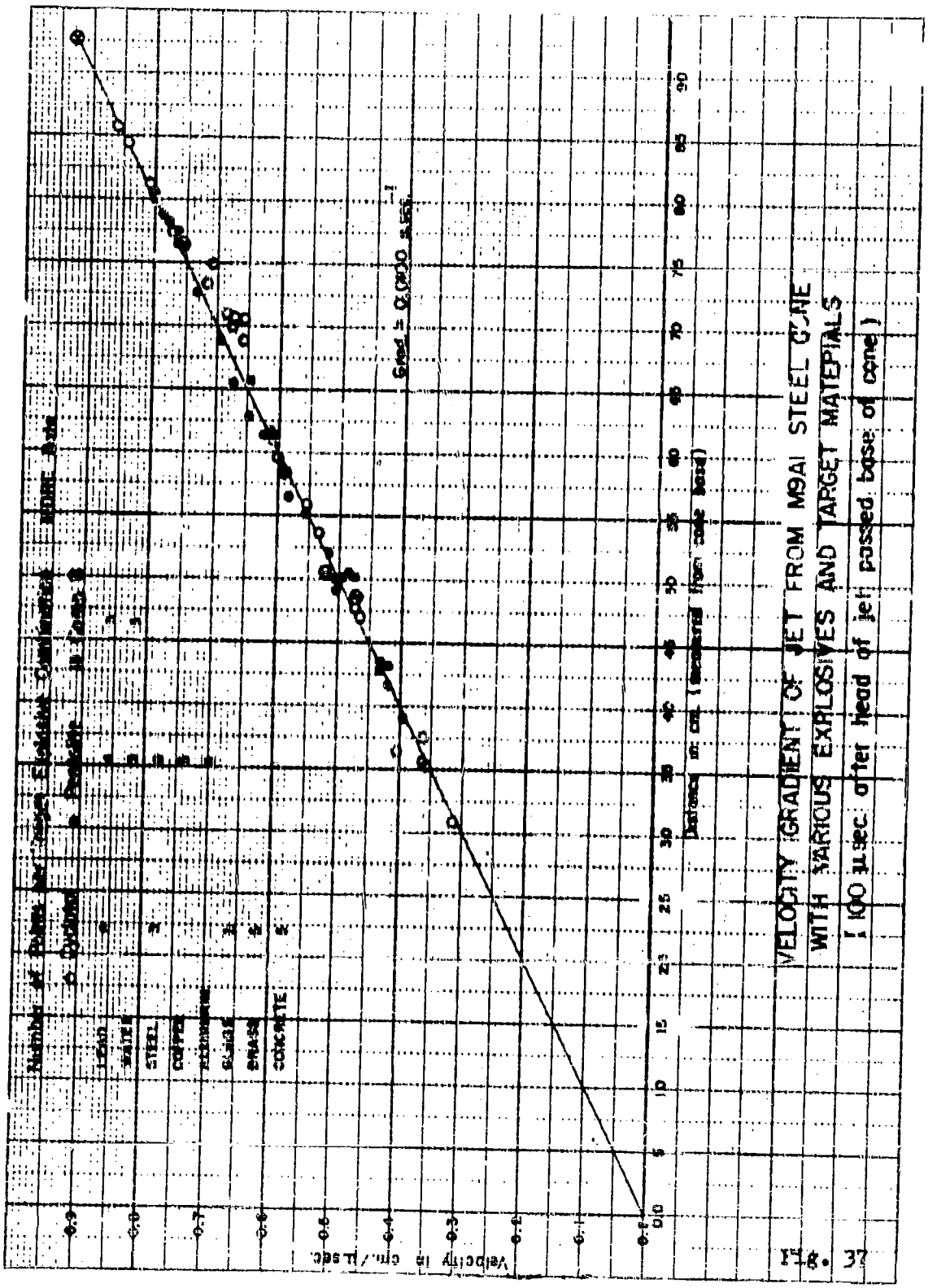
VELOCITY GRADIENT OF JET FROM M9A1 STEEL CASE
WITH VARIOUS EXPLOSIVES AND TARGET MATERIALS
1100 μsec. after head of jet passed base of cone)
Distance in cm. (measured from cone base)
Velocity in cm./μsec
Grad = 0.0020 μsec⁻¹
Number of Points for Each Explosive Combination
Cyclonite
Pentolite
Tetryl
LEAD
WATER
STEEL
COPPER
ALUMINUM
GLASS
BRASS
CONCRETE

FIG. 37

Material	Dia.	Angle	Thick	Gradient		Reference
Steel	1 5/8"	120°	0.022"	0.0111	sec.	NDRC Div. 8, 15 June 1943
Steel	1 5/8	45	.025	.0102		CIT-ORD-3
Steel	1 5/8	45	.037	.0097		CIT-ORD-9
Copper	1 5/8	45	.037	.0112		CIT-ORD-6
Magnesium	3/4	46	.050	.0107		BRL Data
Steel	3/4	46	.050	.0106		Same
Copper	3/4	46	.050	.0104		Same
Copper	3/4	20	.025	.0100		Same
Copper	3/4	30	.025	.0099		Same
Copper	3/4	46	.025	.0103		Same
Copper	3/4	60	.025	.0103		Same
Copper	3/4	46	.015	.0102		Same
Copper	3/4	46	.075	.0104		Same
Copper	3/4	46	.100	.0104		Same

When plotted the data summarized above gave essentially straight lines except that when velocities below about 0.3 cm /μ sec were obtained the curve usually dipped toward the horizontal axis as shown in Figure 36. It should also be noted that the total length of jet cannot be obtained from the plot since the tail elements may be too low in velocity to penetrate the target or to register on the film.

That the gradient should be linear, if the observations on each element of the jet are made after the element has traveled for a sufficient time, follows from elementary considerations. A uniform gradient implies a uniform tensile strain with uniform stresses in the jet, and a non-uniform strain would set up non-uniform stresses which would alter the velocities in such a way as to make the strain and gradient uniform.

For the data given above, the origin was close to the base of the cone in each case and the gradient was practically the same for the range of cone materials, angles and thicknesses covered by the data. If the velocity of the tail of the jet can be increased, the tip velocity and length remaining the same, the gradient will be decreased and the origin moved to some point behind the base of the cone. That this can be done by an appropriate explosive geometry is shown by results with the Carnegie Institute of Technology "explosive compensated" charge (27), which gave a gradient reduced by a factor of 2. Since the tip velocity was unchanged, the origin of the jet must have been far behind the apex of the cone. However, if increasing the velocity of the tail of the jet results in a shortened jet, the gradient may not be changed greatly.

The origin concept implies that, if the velocities of the elements of the jet are constant, then all of that part of the jet which was formed behind the origin was massed at the origin at some time. Since this is not true it may be concluded that, in the early stages after

their formation, the velocities of the various elements of the jet are not constant. Thus, the method of determining velocity gradients outlined above, is not valid for very early times. Some theoretical calculations made at the Ballistic Research Laboratories suggest that, when first formed, the front elements of the jet have a negative velocity gradient. After a short time, the leading elements are overrun by those following, forming a bead or mushroom head, sometimes seen in radiographs. There is other indirect evidence supporting this view and some direct evidence (28).

It may be conjectured that, for a jet penetrating at optimum stand off or less, the penetration could be improved by giving the forward elements a larger gradient, thus permitting them to attain a greater length before being wiped off. Whether this result can be achieved and maintained for the required time is an open question.

1. FTRC 38, Firestone Tire & Rubber Co., Sept. 1953.

2. Minutes of the Second Meeting of the Shaped Charge Research and Development Steering & Coordinating Committee, 22-23 April 1954 Ballistic Research Laboratories, Aberdeen Proving Ground, Md. FTRC 43, Firestone Tire & Rubber Co., Akron, Ohio, Feb. 1954

3. FTRC 37, Firestone Tire & Rubber Co., Akron, Ohio, Aug. 1953

4. FTRC 41, Firestone Tire & Rubber Co., Akron, Ohio, Dec. 1953

5. FTRC 37, Firestone Tire & Rubber Co., Akron, Ohio, Aug. 1953

6. CIT-ORD-42, Carnegie Institute of Technology, Dec. 1952

7. This subject is too lengthy to discuss here. See "The Present Status of the Artillery Program at FTRC" and "High Strain Rate Plasticity of Liner Materials and Jet Behavior" in "Transactions of The Second Symposium on Shaped Charges," Ballistic Research Laboratories, Aberdeen Proving Ground, Maryland, Dec. 7-9, 1953. See also FTRC 41, Dec. 1953

8. Chapter II Sec 8 Equation (4) of this publication. Many other references might be cited, especially from The Carnegie Institute of Technology literature.

9. OSRD 3752, May 1944
OSRD 6384, Feb. 1946

10. BRL Report No. 811, Ballistic Research Laboratories, Aberdeen Proving Ground, Md., March 1952.

11. CIT-ORD-21, Carnegie Institute of Technology, June 1949, Journal of Applied Physics, Vol. 23, p. 532 May 1952.

12. Engineering Progress Reports, The Budd Company, Project No. TM-1451R and Ordnance Contract DA-36-034-ORD-62 for the period 6 Dec. 1950, 15 Jan. 1951 and 15 June 1951 - 15 July 1951.

13. DuPont Reports, August and September 1943 NDRC, Aug. Sept. Nov. Dec. 1943 and Feb. 1944.

14. BRL Report No. 848, Ballistic Research Laboratories, Aberdeen Proving Ground, Md. Feb. 1953.

15. Minutes of the Second Meeting of the Shaped Charge Research & Development Steering & Coordinating Committee, Ballistic Research Laboratories, Aberdeen Proving Ground, Maryland.

16. AC6366, Apr. 1944

17. DuPont, May 1943

18. OSRD 5604, Jan. 1946

19. FTRC 18, Firestone Tire & Rubber Company, Jan. 1952
FTRC 20, Firestone Tire & Rubber Company, Mar. 1952

20. CIT-ORD-42, Carnegie Institute of Technology, Dec. 1952

21. NDRC Div. 8, July 1943 & March 1944

22. FTRC 11 Firestone Tire & Rubber Co., June 1951
FTRC 13 Firestone Tire & Rubber Co., Aug. 1951
FTRC 22 Firestone Tire & Rubber Co., May 1952

23. NDRC, Div. 8, Oct. 1943
DuPont, May 1943

24. FTRC 14 Firestone Tire & Rubber Co., Sept 51
FTRC 15 Firestone Tire & Rubber Co., Oct 51
FTRC 27 Firestone Tire & Rubber Co., Oct 52

25. CIT-ORD-2 Carnegie Institute of Technology, April 1946
CIT-ORD-3 Carnegie Institute of Technology, June 1946
CIT-ORD-6 Carnegie Institute of Technology, Dec. 1946
CIT-ORD-7 Carnegie Institute of Technology, Feb. 1947
CIT-ORD-9 Carnegie Institute of Technology, June 1947
CIT-ORD-10 Carnegie Institute of Technology, Aug 1947

26. This figure is practically a duplicate of Figure B-13 in CIT-ORD-10, Aug. 1947

27. CIT-ORD-34, Carnegie Institute of Technology, Aug. 1951

28. CIT-ORD-3, p. 16, Carnegie Institute of Technology, June 1946

29. BRL Report No. 837, p. 43, Nov. 13-16, 1951, Ballistic Research Laboratories, Aberdeen Proving Ground, Maryland

CHAPTER IV

THE UNFUZED WARHEAD

Hugh Winn

Defense Research Division
Firestone Tire and Rubber Co., Akron, Ohio

Introduction

The modern shaped charge projectile is intended as an instrument of destruction whose principal objective is the defeat of enemy fortifications and armored vehicles. To satisfactorily accomplish its mission the projectile must be capable of defeating its assigned target, and of flying accurately enough to assure a high probability of striking the target with the first or second round fired. While flight of the projectile is properly the problem of the exterior ballistician and the destructive capacity that of the terminal ballistician, the requirements of accuracy and of destructive capacity are so often at variance that the designer is compelled to make compromises and to attempt to arrive at the best overall balance of accuracy and destructive potential. The effect of various design parameters upon shaped charges has been described in some detail in other portions of this volume (Chapters I, II, III, V, VII and VIII) and will be discussed here only in relation to the limitations imposed upon the designer by the realities of practical shell design. An effort will be made to trace the development of a typical warhead and to point out the general areas where compromises have been made successfully.

Selection of Weapon Type and Size

The design for a specific type of shaped charge missile begins with the performance specifications for the weapon system. The range, accuracy and mobility requirements determine the velocity of the projectile and the type of weapon required, while the maximum penetration determines the minimum size of liner and charge.

Table I contains typical accuracy, range and velocity data for existing shaped charge projectiles. The range shown in the table is that which offers a fairly high probability for a first round hit on a small target (such as a tank) and is not to be confused with the maximum range of the missile.

TABLE I

Type	Range (Yards)	Velocity (fps)	Typical Ballistic Accuracy (Probable Error)
Bazookas and Grenades	100 to 400	150 to 250	± 2 mils
Rockets (fixed launchers)	1000 to 4000	1000 to 4400	± 1 to 2 mils
Recoilless Rifles	500 to 2000	500 to 2200	± .5 mil
Guns and Howitzers	1000 to 2000	1000 to 4000	±.15 to .30 mil.

The caliber or size of the missile depends upon its required destructive capacity, its peak acceleration and the type of weapon from which it will be fired. Although perforation of the target is a necessary condition for the defeat of a target it is not sufficient. Unfortunately, very little is known about the effect of shaped charge design parameters upon the extent of damage beyond penetrable armor and the work which has been reported is insufficient for establishing adequate criteria for shaped charge effectiveness (57), (63), (Chap. X). It has become customary, therefore, to evaluate shaped charge effectiveness upon the basis of depth of penetration and relative hole volume, and to trust that a provision for some arbitrary "residual" penetration-usually 2 inches of homogeneous armor - will be enough to assure the defeat of the target. Additional studies of shaped charge effectiveness should certainly prove to be fruitful avenues for further research.

The maximum thickness of the armor to be penetrated, without provision for any "residual" penetration, quite clearly establishes the minimum diameter of the liner and charge. Based upon present standards of shaped charge performance the minimum diameter of an unrotated copper cone (D inches) required to penetrate a given thickness of armor (T inches), 90% of the time, without provision for residual damage effect, may be estimated quite well by equation (1).

$$D = \frac{T + 2}{5} \text{ inches homo. armor, BHN 300} \quad (1)$$

The following tabulation shows the penetration level above which 90% of the rounds would fall for cones and charges of various diameter.

TABLE II

D (inches)	T (inches armor)	Approx. Proj. Cal.(mm)
2.5	10.5	75
2.6	11.0	
2.7	11.5	
2.8	12.0	
2.9	12.5	
3.0	13.0	90
3.1	13.5	
3.2	14.0	
3.3	14.5	
3.4	15.0	
3.5	15.5	105
3.6	16.0	
3.7	16.5	
3.8	17.0	
3.9	17.5	
4.0	18.0	
4.1	18.5	120
4.2	19.0	
4.3	19.5	
4.5	20.0	

After selecting the type of weapon and velocity from the accuracy and portability requirements, and the minimum size of cone and charge from Equation (1) and Table II, the caliber of the missile may be determined from the thickness of the projectile walls required to withstand the stresses of firing.

Before proceeding with a more quantitative discussion of the effect of the various design parameters upon the penetrating potential of the charge, we summarize the present state of the development of the hypothetical projectile. The type of weapon, peak gun pressure, acceleration forces, muzzle velocity, projectile caliber, cone size, projectile wall thickness and the material of construction of the projectile body have been tentatively defined. All have been fixed as a result of a consideration of the specifications for weapon weight, weapon accuracy and range, and by the projectile penetration requirements. The type, shape, material, wall thickness, apex angle and method of mounting of the cone, the amount and distribution of the explosive, the size and positioning of the booster, provision for the fuze, and the manufacturing precision required for obtaining the shaped charge performance predicted in Table II remain to be determined.

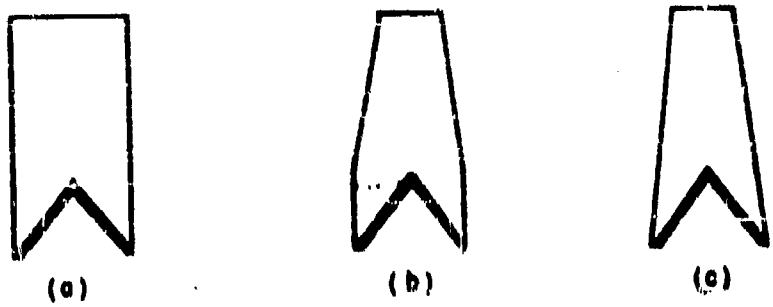

FIG. 1

CONSIDERATION OF LINER PARAMETERS

Although the effect of various liner parameters - shape, material, wall thickness, cone angle, etc., - are described in detail in Chapter III, the projectile designer is not free to treat these parameters independently. He must be guided in his choice by the projectile parameters fixed by the requirements for projectile accuracy. It is therefore quite appropriate to treat each of these parameters here in order to illustrate the manner in which a judicious choice of each of these parameters may be related to the boundary considerations of the projectile design.

Standoff Distance

In a real projectile the effective standoff distance is determined by the length of the ogive, the velocity of the projectile and the fuse functioning time. Although the optimum standoff distance for a well made conical liner is usually more than four cone diameters (36), (39), (41), (44) (Chap. III) (Fig. 22, 25, 28), the actual standoff is usually limited to from one to three cone diameters by aerodynamic considerations involved in ogive shape and size. However, this standoff may be enough to permit the attainment of about 90% of the penetration expected at optimum standoff and the shorter standoff has advantages in certain instances. For example, if the shell must be rotated at some low spin rate, 10 to 15 rps, in order to achieve projectile accuracy, the optimum standoff may be reduced from four to two cone diameters. (44) Also, if the enemy employs spaced armor in an effort to reduce the efficiency of shaped charge projectiles, the spaced armor itself may provide the increased effective standoff required for maximum penetration (24).

Charge Length

The length of the projectile body, and hence of the charge, is most frequently limited by aerodynamic performance and projectile weight specifications. In general, the penetration and the hole volume obtained increase with increasing charge length and reaches a maximum at about 2 or 2.5 charge diameters for heavily confined charges or 4 charge diameters for lightly confined or unconfined charges. (55) (Chapter V, page 127). In most cases involving rockets or projectiles a charge length of 2 charge diameters can be provided and this is sufficient if the charges are subjected to close quality control during manufacture and loading. The usual effect of reduced charge length is a lowered average penetration, reduced hole volume and an increased number of rounds with below normal penetration. (55),

Charge Shape

Existing shaped charge designs usually have one of the shapes shown in Figure 1. Although each can be made to perform satisfactorily, 1 (a) has the advantages of a somewhat greater ease of manufacture, of high explosive loading and of blast effect (because of the larger amount of explosive); 1 (b) or 1 (c) are sometimes necessitated by the requirements for accuracy. There is some slight evidence that a tapered charge has a shorter optimum standoff and a slightly lower maximum penetration than the cylindrical charge. (58). The greater amount of explosive in the cylindrical

charge makes it more valuable than the tapered charge for the secondary effects of blast and fragmentation damage.

Selection of Liner Material

Although depth of penetration is not the only criterion for judging the maximum damage to the target, there is only limited information available as to the relative damage beyond the target caused by target penetration by liners of different material. Such information as there is (63), (57) indicates that the relative damage decreases in the order aluminum, steel, copper. The relative penetrating ability of various materials is described in Chapter III and has been the subject of many investigations (11), (40), (38), (15), (17), (22). If the type of weapon is such that the caliber of the projectile overmatches the penetration requirement for the defeat of the prospective target, a most desirable circumstance, it may be possible to select aluminum or steel in preference to copper. But if, as is most frequently the case, the penetration requirement taxes the penetrating ability of the projectile only copper can be considered seriously. In this case aluminum sleeves (45) or bimetal cones (43), (36) should be considered.

Having reached a decision as to the type of cone material to be used it is necessary to specify the composition or alloy. Although only very scanty evidence can be cited for evidence it is the considered opinion of those most closely associated with the art of shaped charge design that the purity of the material, or the type of alloy to be specified, should be that which has the greatest ductility. This conclusion is deduced from the fact that potential depth of penetration is governed by the length and density of the jet. The density of the jet is of course characteristic of the type of material used and is only slightly influenced by impurities and alloying ingredients. The length of the jet is determined not only by the size of the cone but also by the velocity gradient resulting from the design of the charge and by the ability of the ductility of the jet material to support the velocity gradient, during elongation of the jet, without rupturing. This effective jet ductility is of course dependent upon the inherent ductility, the strength and the melting point of the material. Much more work needs to be done before the influence of these factors is understood. At this time, however, the best choice of material for shaped charge liners is believed to be oxygen free electrolytic copper.

Liner Shape

Liners of many different geometric shapes have been tested for penetrating efficiency (Chapter III) but experience in the United States seems to indicate that the best and most consistent results can be obtained with conical liners of appropriate apex angle and wall thickness. Some very recent data, yet unpublished (65), indicate that "double angle" conical liners may offer certain advantages, but the performance of these liners has not yet been determined sufficiently well for a complete evaluation of their true worth.

Cone Wall Thickness

For each type of cone material, standoff, projectile wall confinement, type of explosive, shape of charge, and apex angle there is an optimum wall thickness. From the practical consideration of projectile design, however, projectile confinement and cone apex angle are most determining.

Figure 2 shows reasonable values of liner wall thickness for copper cones with apex angles between 40° and 45° plotted as a function of the confinement. As an approximate guide for liners of different apex angles, or for shapes other than conical, an approximately correct wall thickness may be obtained by maintaining the thickness constant in an axial direction (55), (12), (Chap. III, Figure 11, 23).

Curves of penetration vs wall thickness are frequently unsymmetrical (58). A thicker wall generally is to be preferred over a thinner wall. The performance of the latter is typified by an excessive variability from charge to charge, the former by good reproducibility with only a tolerable decrease in penetration. It would, therefore, seem to be good practice to select a wall thickness about 5% greater than the optimum to assure that in production the wall thickness will not be less than optimum.

Cones with tapered wall thickness have been studied from time to time. (Chapter III),(42), (53). Though more work in this field is desirable the available evidence indicates that tapered walls offer slight, if any, real improvement in the performance of conical liners. The data do show, however, that rather wide tolerances may be placed upon the variation in wall thickness between apex and base without reducing penetration, providing the wall thickness is held constant at each transverse section of the cone.

For liners of shapes other than conical - double angle, hemispheres, trumpets, etc., the observation that optimum wall thickness depends upon the inclination of the surface indicates that in such cases tapered wall cones may be advantageous.

Cone Apex Angle

The choice of cone angle is quite important both from a performance and a manufacturing point of view. Data are abundantly available to show that reducing the apex angle may decrease the optimum standoff, and that the optimum angle is dependent upon the cone material, wall thickness and charge length. (Ch. III, Figures, 18, 19, 20, 21, 28). As with most other cone parameters, the effect of apex angle becomes less important as the spin rate of the projectile increases. For example, at 0 rps a 45°, 3.4 inch copper cone penetrates 3 inches deeper than a 60° cone of the same wall thickness, but at 45 rps the difference is less than 1 inch. (16).

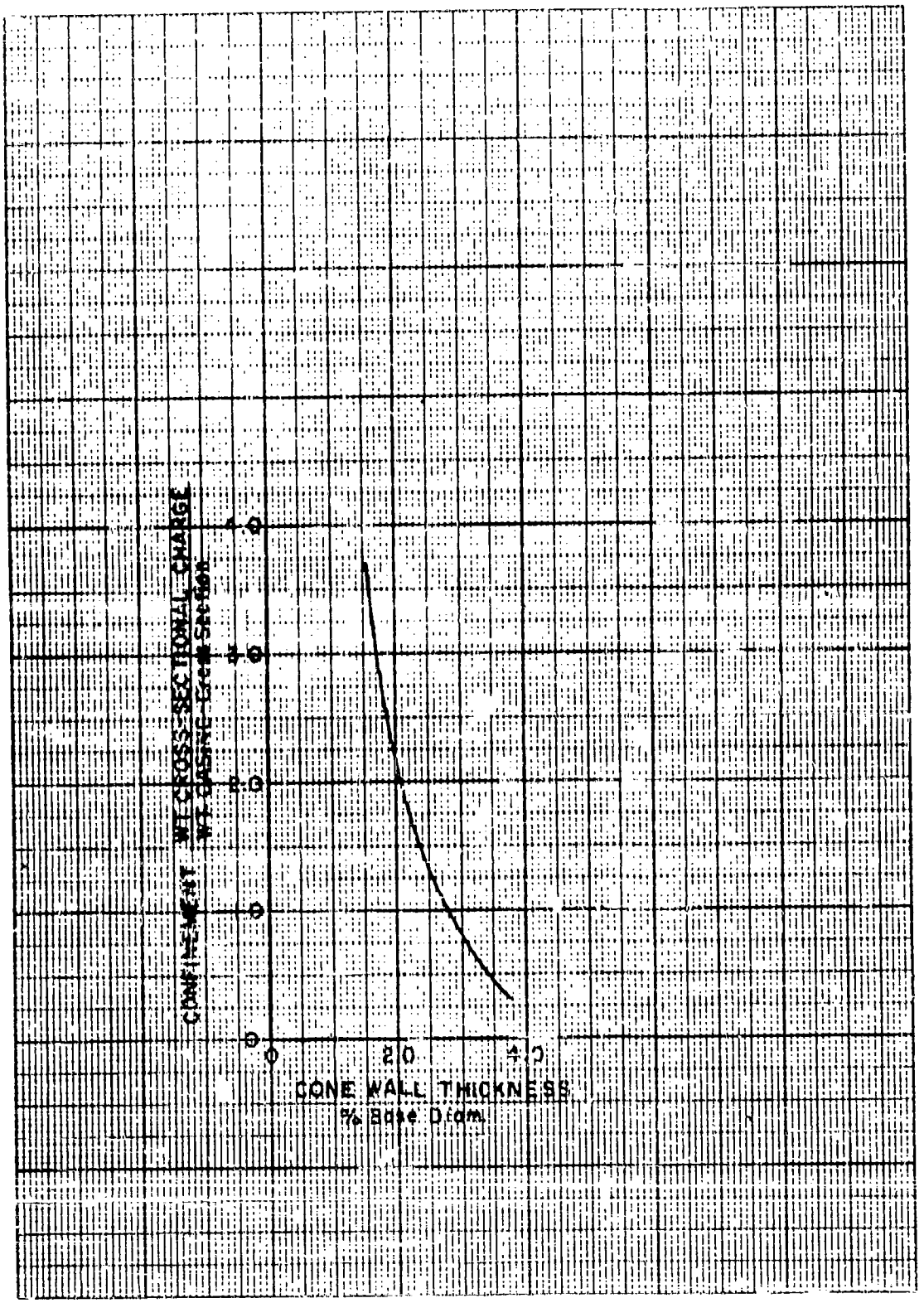
CONFINEMENT WT CROSS-SECTIONAL CHARGE
WT CASING-Cone Section
1.0
.8
.6
.4
0
2.0
4.0
CONE WALL THICKNESS
% Base Diam.

Fig. 2

The penetrating performance of small apex cones (20°) is characterized by lowered efficiency and increased deviation or scatter of the data. (33), (50) It is probable, however, that this merely reflects the difficulty of manufacturing good cones of very small angle. (Ch. III,, Fig. 28). With the precision of modern manufacturing methods the optimum cone angle for projectiles with copper cones is close to 40° or 45°. In some cases best penetration performance has been observed with 20° (Ch. III, Fig. 28) cones and in others with 60° cones((3) Fig. 4).. As a first choice a cone angle of either 40° or 45° may be selected and will give good performance in projectiles with an ogive length of two calibers.

Sharp Apex VS Spitback Tube Cones

In most reported cases involving copper cones where charges differing only in the presence or absence of a spitback tube have been compared, equal or slightly better penetration is obtained with a spitback tube. (5), (19), (23), (39), (66). There is no effect upon optimum standoff, rotation or optimum wall thickness. In addition to the usually better performance of spitback tube cones, it is easier to manufacture cones with a short spitback tube section and maintain close tolerances than it is a sharp apex cone, and less difficulty is encountered in obtaining sound charges when spitback tube cones are used.

It is standard practice to specify hard drawn copper tubing with a wall thickness of .060-.065 inch for spitback tubes. The effect of tube diameter has received only limited attention but satisfactory results have been obtained with tubes having a diameter between 20% and 30% that of the cone (27).

Little information is available upon the effect of method of attachment of spitback tubes to cones. The tubes may be integral with the cone, or may be attached by means of soft solder, brazing, buttress threads, cementing or crimping. Although all methods have been used only the first and last three are both relatively inexpensive and do not require the application of heat to the cones with the consequent danger of cone warpage. In any soldering or cementing operation great care must be exercised to see that any excess material is removed from the tube and cone. Even a small amount of cement smeared on one side of a cone has been shown to be enough to reduce penetration by 40%. (6).

ASSEMBLY OF THE LINER

Method of Attaching

Four different methods of cone attachment are commonly employed; (1) crimp cone flange between ogive and body flanges (M9A2 Grenade), (2) braze or cement (M28A2 or T205 Rockets), (3) cone flange registers in body and is clamped firmly by a threaded ring or ogive (M67, T108, T184 HEAT Projectiles), (4) cone is pressed into the ogive and held in place by a locking groove (T119, T130 Projectiles). Although each method has certain advantages in manufacture the last two methods have demonstrated

consistently good performance and may be used satisfactorily (62).

Alignment of Cone and Charge

For best and most reproducible performance the axis of the charge and cone should coincide. In actual practice, however, the axes may be parallel but displaced, or may not be parallel. A large number of experiments have been described in which the importance of these variables is treated (1), (4), (46), (49), and the importance of extremely careful control over this type of imperfection cannot be overemphasized.

Tilt of the liner results in a reduced average penetration. The lowered average is the result of a larger number of "poor" shots. There are some good shots even with angles of tilt as high as 2.0°, but in general the average penetration is reduced by 50% when the cone is tilted 1°, about 20% at .5°, 10% at .3° and a difference in the spread and average penetration can be detected between tilts of .05° and .15° (2), (59).

The second type of misalignment, in which the cone charge axes are parallel but offset slightly must be controlled just as carefully. In one experiment an offset of only .015 inches (1% of the base diameter) reduced the penetration significantly, approximately 20% (2).

From the standpoint of manufacturing, however, it is not difficult to maintain the coincidence of the charge and liner within .010 inches provided the cones are properly registered and clamped in place. It is much more difficult to maintain alignment in brazed, welded or cemented assemblies. However, regardless of the method of cone attachment and the care exercised in maintaining proper alignment it is very important to be able to inspect the alignment after the cone and charge are assembled. Every effort should be made to avoid blind assemblies of the projectile.

BOOSTERING OF THE CHARGE

The size, shape, location and alignment of the booster have all been studied (4), (28), (19), (64). In most cases electric detonators have been used to initiate the booster. In one experiment the thickness of the booster was varied from 0 to 1" without any indication of a detrimental effect upon performance (45) and it was concluded that the detonator was sufficiently powerful to initiate the charge. In a real projectile, however, the detonator is enclosed in a rotor in the fuse and even though a tetryl lead may be employed the probability of being able to initiate the charge satisfactorily without a booster is not high. Nevertheless, experience with several projectiles has shown that the booster does not need to be large; a pellet 1 inch in diameter and .4 inch high appears sufficient for 3.5 inch charges. (T208 E7 base element).

The effect upon penetration of the "head"of explosive, or the distance between the booster and the apex of the cone has been examined. (26), (28), (33), (58). The head of explosive required seems to vary with the "order" of the initiation. If the main charge is satisfactorily initiated in a symmetrical fashion the booster may be placed directly above the liner. If, however, the initiation is borderline satisfactory performance will be obtained only if the booster is from one to 2 cone diameters above the cone. If the detonator and booster are adequate it is believed that satisfactory shaped charge effect will be obtained if the booster is not less than 1 inch above the cone. It does seem likely, however, that the effect of misalignment of the cone will become increasingly severe as the booster is moved toward the cone. Therefore, the booster should be placed as far rearward in the charge as other design considerations permit.

Eccentric initiation of the charge has been studied extensively. (47), (61). For point initiation it has been shown that the detonation wave front is essentially spherical with the detonator at the center of curvature. (48). If the detonator is moved off-center a decrease in penetration is observed but the effect is relatively small. Placing the detonator .5 inch off-center, in a charge length of two cone diameters, resulted in a loss in penetration of 20% (7). Since it is not difficult to hold booster and detonator alignment to within .060 inch, off-axis initiation is not an anticipated problem with electric or magnetic fuses, but some difficulty might be experienced with a spitback type fuse. In the latter case initiation at a point .5 inch off-center can occur unless care is taken in assembly of the spitter cone.

CONFINEMENT

The relationships between cone wall thickness and projectile wall thickness were described earlier in this chapter. There are, however, other effects of confinement of considerable interest to the designer. Increasing the confinement increases the hole volume greatly (8), (51). This effect is noted whether the confinement is provided by increased wall thickness or by a "belt" of explosive (25). The presence of explosion products at high pressure within the explosive belt retards the expansion of the products in much the same manner as does a steel casing. The "confining" effect of different inert materials is, of course, proportional to their density.

In early experiments with charges of diameter larger than that of the cone, a significant effect was noted in those cases where the cones were flanged. (9), (10). It was observed that when an explosive belt is in contact with the flat flange of a cone the penetration was lower than when the flange was removed. The loss in penetration was considerably greater when the charges were heavily confined. With the typically heavy confinement of a 105mm projectile a loss in penetration of 40% resulted when a .10 inch flange was backed by explosive (25), (26). Recently the results of an extensive study of the effect of confinement

upon the performance of flanged and unflanged cones have become available. (51). The data are summarized in Chapter III.

From these data the author drew the following conclusions:

1. The addition of a small explosive belt obtained by increasing the charge diameter from 1.63 to 2.00 inches has produced very nearly the same effect on penetration and hole volume as the addition of .25 inch of steel confinement.

2. When heavy base confinement has been added to the 2 inch charge, the penetration is decreased about 27%.

3. The addition of both lateral and heavy base confinement to the 2 inch charge causes a drastic reduction in penetration performance of about 45%.

4. When the larger charge is confined laterally, the presence of the flange has caused a relatively small but significant decrease in penetration, as compared with a similarly confined charge lined with a deflanged cone.

5. The hole volume produced by the 2 inch charge is increased by about 50% when lateral confinement of .25 inch steel is used (compared with the 100% increase which occurs with the 1.63 inch charges); boundary conditions at the base of the charge have little or no effect on hole volume in spite of the large changes in depth of penetration.

This experiment illustrates how an apparently superficial change in charge design can cause profound changes in charge performance. While it is possible to explain these changes satisfactorily in the light of fundamental information, and to predict qualitatively what might have been expected, great care should be exercised in designing experiments so as to be sure that the variable being evaluated is indeed the only variable under test.

INTERNAL OGIVE SHAPE

The internal shape of a conical or tangent ogive does not interfere with the normal collapse process of the shaped charge liner. However, a number of HEAT shells now being developed for the Ordnance Corps employ a tee, boom, or spike ogive which can reduce penetration greatly. Ogives of this shape are of interest because they have a low lift and therefore a smaller restoring moments are required for projectile stability. While such ogives do have a much higher drag than conical or tangent ogives at projectile velocities up to 2000 fps, the advantage of lower drag possessed by the latter is much less marked at velocities of 3500 and 4000 fps.

The effect of internal tee configuration upon shaped charge effect has been given a great deal of attention. Figure 3 shows six of the many configurations which have been tested and the penetrations each of these

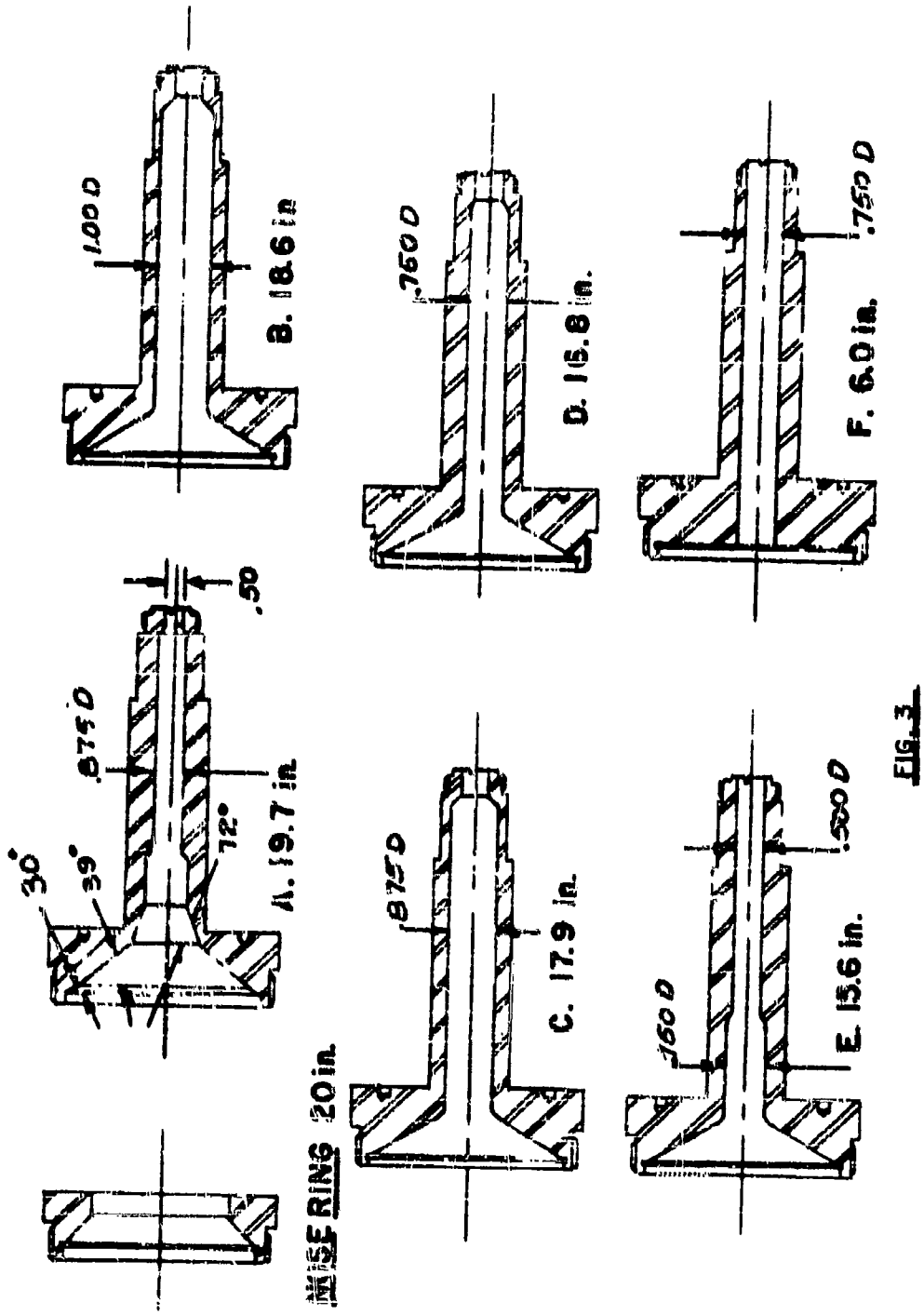
1.000 D
B. 18.6 in
.750 D
D. 15.8 in.
.750 D
F. 6.0 in.
.50
.875 D
30°
39°
72°
A. 19.7 in
.875 D
C. 17.9 in.
.500 D
.160 D
E. 15.6 in.
RISER RING .20 in.

Fig. 3

booms permit. (13), (14), (17), (18), (20), (22), (29), (30), (31), (37) (35), (34), (32), (38). A consideration of designs A to F disclose two important design requirements: (1) a free space not less than 0.6 cone diameters must be provided in front of the cone, and (2) the bore of the boom must be as large as the maximum diameter of the slug. It seems clear that near the base of the cone the collapsing elements follow a forward curved path (52) and that cone collapse is not complete until the cone has moved forward a distance of nearly one cone diameter, and that useful jet elements are formed during the time the slug is moving forward a second cone diameter. If the bore of the boom is not at least as large as the major diameter of the slug, the jet will be pinched off when the slug jams in the bore and a portion of the potential penetration will be lost. The tests reported above were static tests and it is reasonable to suspect that in dynamic firings the boom may be jammed rearward toward the cone by the impact velocity and that this will reduce the effective free space. Therefore, some additional free space must be provided and the actual amount required will probably depend upon the maximum impact velocity of the projectile.

REFERENCES

Explosive Research Laboratories: Bruceton, Penna.

1. OSRD No. 1681
2. OSRD No. 1681 - p. 3, 5
3. OSRD No. 1861 Figure 4
4. OSRD No. 5599
5. OSRD No. 5601 - p. 11
6. OSRD No. 5601 - p. 74
7. OSRD No. 5601 - p. 55
8. OSRD No. 5604 - p. 14
9. OSRD No. 5604 - p. 18
10. NDRC Div. 8, SC-4 p. 12, 42

E. I. duPont de Nemours & Co., Contract No. W-670-ORD-4331

11. March 1943 - Section VII
12. March 1943 - Section IV

Firestone Tire & Rubber Co., Contract No. DA-33-019-ORD-33

13. No. 2 p. 32
14. No. 3 p. 29
15. No. 4 p. 46
16. No. 5 p. 40
17. No. 10 p. 31, 32
18. No. 11 p. 36
19. No. 11 p. 28, 29
20. No. 12 p. 24
21. No. 12 p. 31
22. No. 13 p. 36, p. 37
23. No. 13 p. 41
24. No. 16 p. 21
25. No. 18 p. 22, 23
26. No. 20 p. 21, 24
27. No. 22 p. 26
28. No. 24 p. 18
29. No. 24 p. 15
30. No. 25 p. 25
31. No. 26 p. 22
32. No. 27 p. 11
33. No. 28 p. 20
34. No. 29 p. 18
35. No. 30 p. 12
36. No. 32 p. 2, 22
37. No. 33 p. 27
38. No. 37 p. 39, 47
39. No. 37 p. 34, 37
40. No. 38 p. 30, 39
41. No. 39 p. 31
42. No. 39 p. 12
43. No. 40 p. 30
44. No. 42 p. 23

Carnegie Institute of Technology

45. CIT-ORD-15 p. 40
46. 27 p. 39
47. 28 p. 61
48. 28 p. 69
49. 31 (Part II) p. 39
50. 32 p. 3
51. 42 p. 12, 13
52. 44 p. 1
53. 46 p. 8

Ballistic Research Laboratories, Aberdeen Proving Ground

54. No. 585
55. Memorandum Report No. 607, p. 6, 8
56. Memorandum Report No. 607, p. 36
57. No. 837 p, 359 to p. 371
58. No. 837 p, 256, 257, 258
59. No. 837 p. 77
60. No. 846
61. Advance Release No. 0.0.400.112/1108 (s) p.33
62. In Preparation Transactions of Symposium on Shaped Charges held Dec. 6-8 1953

63. Naval Ordnance Test Station (Inyokern, Calif.) TM No. 443 Chapter 10
64. Naval Ordnance Laboratories "Ordnance Explosive Train Designers Handbook, "NOL - R-1111- Section VII

65. Picatinny Arsenal Report of Shaped Charge Committee Meeting for Nov.6, 1953. p. 4
66. Picatinny Arsenal Report of Shaped Charge Committee Meeting for Nov.6, 1953 p. 5

CHAPTER V

THE EXPLOSIVE COMPONENT OF SHAPED CHARGES

A. D. Solem
W. T. August
Naval Ordnance Laboratory
Silver Spring, Maryland

Introduction

The shaped-charge effect depends upon the pressure impulse of a detonated explosive to accelerate the liner walls in the collapse process which produces the jet. The explosive is therefore fundamental to the phenomenon and it is essential that charge parameters be carefully selected. This means that proper distribution, initiation, and explosive, or an adequate compromise of these factors be made.

Fortunately, considerable experience has been gained from which it is generally possible to make adequate shaped-charge designs. The effect of compromises with the ideal design can also be estimated reasonably well. However, the problems of explosives in shaped charges have not all been solved. Conditions arise wherein minor variations cause an appreciable performance change which can be attributed only to the explosive. Small modifications in charge preparation technique or a change in explosive distribution about the liner may affect the penetrations significantly. The exact bearing non-uniformity of the explosive charge has on performance requires further investigation. Proper shaping of the detonation wave in the explosive has shown promise of large increase in penetration performance but has introduced additional difficulties which must be overcome before it can be considered seriously for applications (1-3).

Practically all studies of explosives in shaped charges have been experimental. This does not mean, however, that the basic studies have been neglected. Detonation theory is being actively pursued, as is also the study of explosive-metal interactions (4). Direct application of these research studies are being carried out by the CIT group in their work on a release wave theory as applied to liner collapse (5).

Detonation Theory

While detonation theory is fundamental to the study of explosives, only a brief summary is needed for the present purposes of shaped charges. Details can be found in references (6), (7), (8), (9) and (10). The connection between detonation and shaped charge theories is given in Chapter I, for instance. Consider the simplified one-dimensional case with the reaction zone Z stationary with respect to the observer, Figure 1. Assume the unreacted material (p_1, v_1, T_1) enters the reaction zone with a velocity D and the products (p_2, v_2, T_2) leave the zone Z with a velocity $(D-u)$. The quantities p, v, and T are the pressure, specific volume, and temperature respectively and the subscripts 1 and 2 refer to the media ahead of and behind the reaction zone. Also the symbol u may be defined as

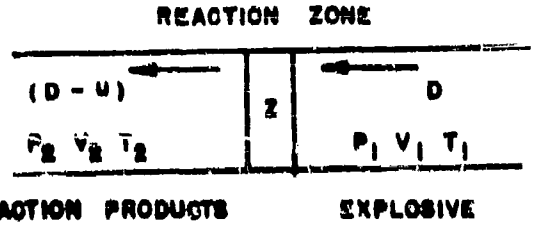

FIGURE 1- THE DETONATION PROCESS AT REST WITH THE DETONATION FRONT.

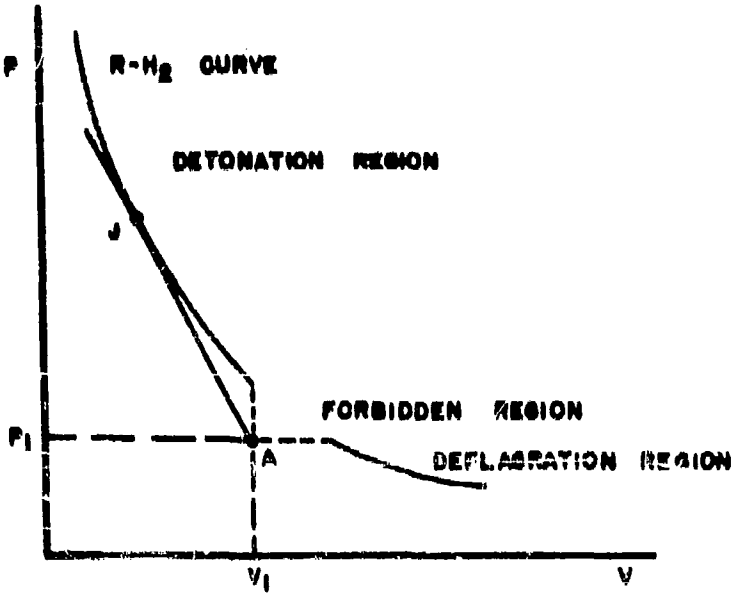

FIGURE 2 - RANKINE-HUGONIOT CURVE SHOWING THE CHAPMAN-JOUGET CONDITION.

the particle velocity, that is, the difference between inflow and outflow velocities.

The conservation equations are:

Mass
$$\frac{D}{v_1} = \frac{D - u}{v_2} \tag{1}$$

Momentum
$$\frac{D^2}{v_1} + p_1 = \frac{(D - u)^2}{v_2} + p_2 \tag{2}$$

Energy
$$E_1 + \frac{D^2}{2} + p_1 v_1 + Q_1 = E_2 + \frac{(D - u)^2}{2} + p_2 v_2 + Q_2 \tag{3}$$

Terms involving the gradient of temperature ahead of and behind the reaction zone are neglected. E_1 and E_2 are the internal energies of media 1 and 2 respectively and the quantity (Q_2-Q_1) is the energy evolved in the reaction. These equations yield

$$D = v_1 \left(\frac{p_2 - p_1}{v_1 - v_2}\right)^{1/2} \tag{4}$$

$$u = (v_1 - v_2)\left(\frac{p_2 - p_1}{v_1 - v_2}\right)^{1/2} \tag{5}$$

$$E_2 - E_1 = \tfrac{1}{2}(p_2 + p_1)(v_1 - v_2) + Q_1 - Q_2 \tag{6}$$

This last equation is the Rankine-Hugoniot relation and is represented by a curve shaped about as shown in Figure 2. Starting with the unreacted material at A (this point will be below the Rankine-Hugoniot curve) the shock and reaction will carry the process so that the state of the reacted material lies on the Rankine-Hugoniot curve $(R-H)_2$ to the left of A as the products emerge from the detonation front. Transitions to lower pressures and higher volumes are deflagrations and are not to be considered further herein.

In the model, steady-state might exist anywhere along the $(R-H)_2$ curve above the point of tangency. But in practical three-dimensional situations, rarefactions from the boundaries always reduce the process to this point of tangency. It is the only stable propagation velocity and this condition leads to the equation for the sound velocity in the products (the Chapman-Jouguet condition),

$$C_2 = v_2 \left(\frac{p_2 - p_1}{v_1 - v_2}\right)^{1/2} \tag{7}$$

the detonation velocity is then related to sound speed by:

$$D = u + c_2 = v_1 \left(\frac{p_2 - p_1}{v_1 - v_2}\right)^{1/2} \tag{8}$$

Also

$$p_2 - p_1 \approx \frac{1}{v_1} Du = \rho_1 Du \tag{9}$$

for the detonation pressure. As can be seen these considerations are intimately connected with the subject of equation of state of explosion products which will not be discussed in detail because of its length although it is of primary importance. For gaseous explosives the ideal gas law works reasonably well. For solid or liquid explosives this is not the case. Several equations of state have been used such as:

$$\text{Abel:} \quad p(v - b) = \frac{RT}{n} \tag{10}$$

$$\text{Jones:} \quad pv = RT + f(p) \tag{11}$$

and the more complicated ones of Wilson-Kistiakowsky, Leonard-Jones-Devonshire with modifications, etc. Observations of detonation velocities with different loading densities, plus assumptions concerning the chemical reactions involved and the use of the hydrodynamic equations permit evaluation of the constants entering the equations of state. Present efforts are being directed toward obtaining better equations of state (or better parameters) to predict detonation phenomena.

For shaped-charge work accurate values of particle velocities of the product gases and detonation rates are required to get good estimates of detonation pressures. A theory of H. Jones (9) permits placing limits on the range of detonation pressures and particle velocities which will prevail for a given detonation velocity (10). Jones has shown that for a one dimensional detonation in a charge large enough to have the infinite stick rate:

$$\frac{D}{u} = (2 + \alpha)\left(1 + \frac{\rho_1}{D}\frac{dD}{d\rho_1}\right) = r \tag{12}$$

where

$$\alpha = \left(\frac{K C_v}{v_2\left(\frac{\partial p}{\partial T}\right)_v} - 1\right)^{-1} \tag{13}$$

and

$$K = -\frac{v_1}{v^2}\left(\frac{\partial v}{\partial p}\right)_s \tag{14}$$

The quantity α is approximately equal to 0.25. Here ρ_1 is the loading density of the explosive and $(dD/d\rho_1 = B)$ is the slope of the detonation velocity vs loading density curve at density ρ_1. The detonation velocity can be represented by

$$D = D_{1.0} + B(\rho_1 - 1)$$

where $D_{1.0}$ is the detonation velocity at a density of 1 gram/cm^3. Thus detonation velocity data can give a good estimate of D/u and an estimated accuracy of 5-10 percent based on an assumed error of 50 percent in c. As a consequence, many of the parameters needed for hydrodynamic treatment of shaped charge jet formation can be derived from known detonation velocity data with reasonable accuracy.

This discussion has been brief. It was given to point out the accuracy with which the detonation parameters that enter shaped charge considerations are known.

Effect of Different Type of Explosives

In shaped-charge development considerable work has been performed on standard charges to evaluate the relative performance of various explosives (11-15). Only a few of these have found ordnance application. Some explosives with low detonation pressures are marginal and form very poor jets, but no upper limit to performance has been found i.e., as the detonation pressure is increased the penetrations increase. The trend in explosives research is the development of new compounds with higher detonation velocities and pressures. Thus small additional improvement in performance might be anticipated.

Table 1 lists various high explosives, their properties, and shaped-charge penetrations (16). The list is not complete, and some are unacceptable for wide application because of sensitivity, compatability, stability or production difficulties. The densities given are those actually obtained in the charges used for penetration comparisons. The detonation velocities given are computed on the basis of experimentally derived density-detonation velocity slope data for the explosives (17). Sensitivities are taken from impact studies at NOL only to avoid introducing calibration constants for different testing machines. The penetrations are from NOL work on point initiated, unconfined charges 4.0 inches in height, 1.63 inches in diameter with M9A1 steel cones and fired with 4.0 inches standoff into mild steel plates (14, 15). A few similar explosive comparisons performed at DuPont's Eastern Laboratories are also given. This furnishes a reasonable comparison of different explosives.

Formulas or correlations relating penetrations and cavity volumes to parameters of the explosive have been developed. They do not take into account, however, the properties of the liner or the nature of jet formation and penetration processes.

a. The first was developed by DuPont Laboratories in 1943-44 (11) wherein the penetrations obtained from M9A1 steel and glass conical liners for different explosives were correlated with the calculated hydrodynamic detonation pressure.

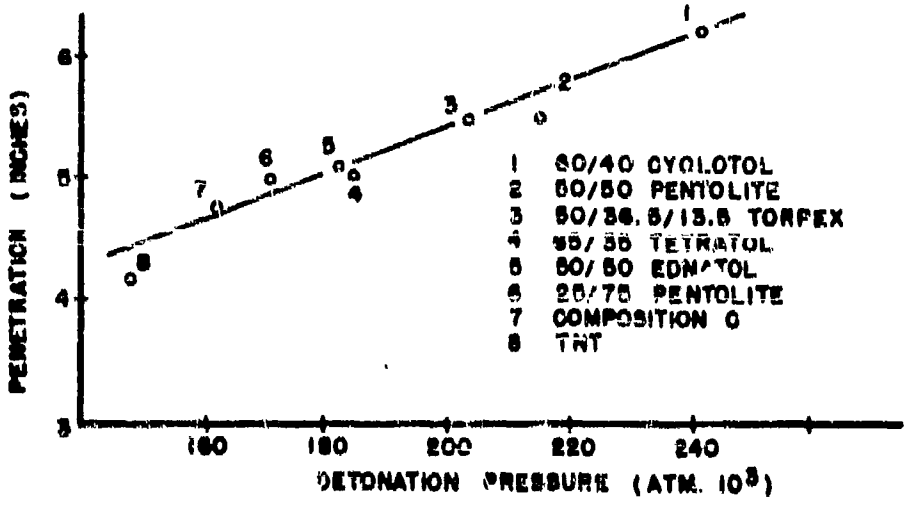

FIGURE 3 - SHAPED CHARGE PENETRATIONS AS FUNCTION OF DETONATION PRESSURE FOR M9A1 STEEL CONES.

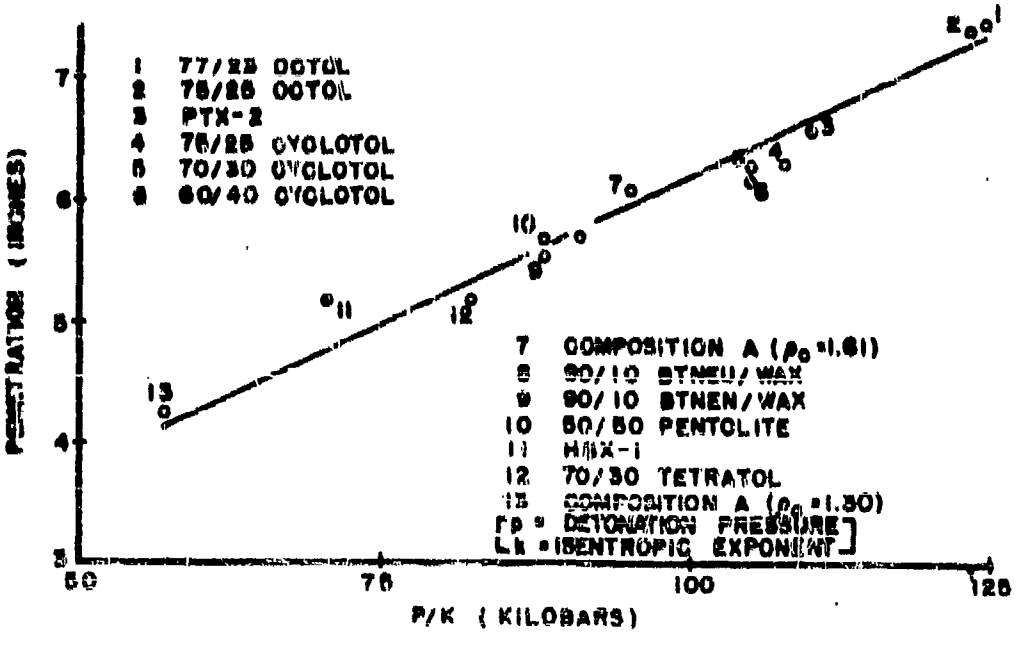

FIGURE 4 - SHAPED CHARGE PENETRATIONS AS FUNCTION OF P/K FOR M9A1 STEEL CONES.

Detonation pressure = $\rho_1 Du$

A modified Abel equation of state was used to establish an average value of u/D as 0.21 so that

$$\text{Detonation pressure} = 0.21\ \rho_1 D^2. \qquad (16)$$

Figure 3 shows the correlation obtained.

b. To improve the prediction of performance for higher energy explosives the following formulas were developed at the Naval Ordnance Laboratory based on Jones' formulation of detonation theory for solid explosives (18). These were based on NOL penetration data obtained with M9A1 steel cones.

$$\text{Penetration} = \frac{P_{2/K} + 31.19}{71.31}$$

or

$$\text{Penetration} = \frac{\rho_1 D^2/K + 73.58}{73.99}$$

where D and p_2 are defined as before.

$$P_2 = \rho_1 D^2/r$$

where r is defined in equation (12) and p_1 is neglected.

K = isentropic (exponent) as defined in equation (14).

$$K = R - 1 = D/u - 1$$

ρ_1 = explosive loading density

and $\alpha = 0.25$

Figure 4 shows the correlation for various explosives using equation (1) above. To be applicable these formulae require some knowledge of the explosive, namely D and B.

c. A correlation of cavity volume with detonation pressure was also attempted from the same tests (a) by the DuPont Laboratories (11). It was found that the volume was approximately proportional to the detonation pressure as indicated in Figure 5.

Extrapolating these results to other shaped-charge configurations might lead to considerable error. The results can be generalized somewhat, if exact predictions are not required, by applying as corrections the known effect of changing the variables which affect penetration for a given explosive. These formulae can also be used to predict relative performance for a class of explosives.

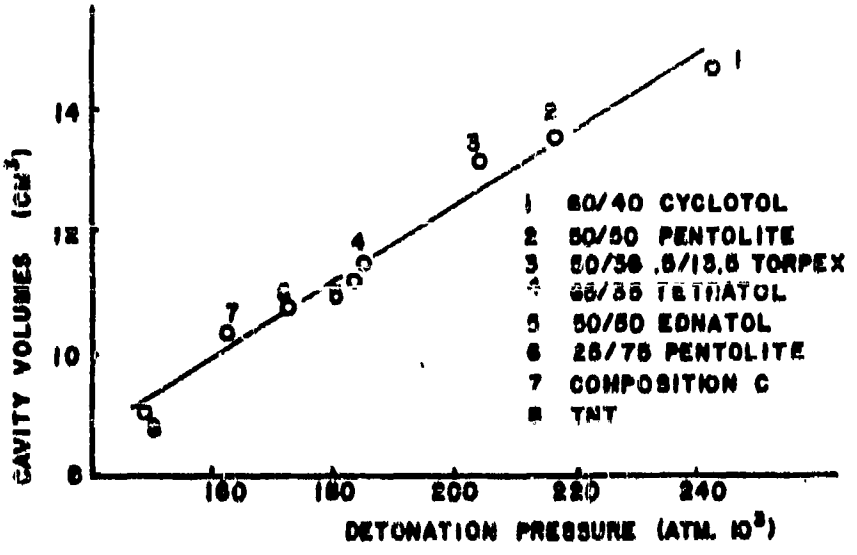

FIGURE 5. SHAPED CHARGE CAVITY VOLUMES AS FUNCTION OF DETONATION PRESSURE FOR M9A1 STEEL LINERS.

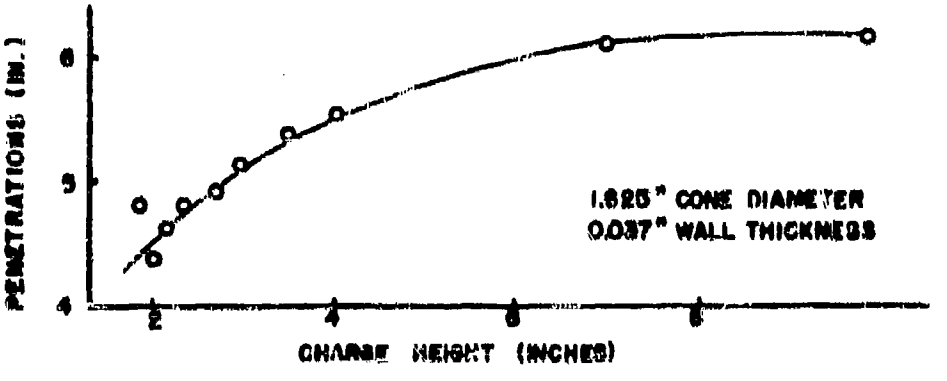

FIGURE 6. SHAPED CHARGE PENETRATION AS A FUNCTION OF CHARGE HEIGHT FOR M9A1 STEEL CONES AND 50/50 PENTOLITE EXPLOSIVE.

Several exceptions have been noted experimentally from these correlation formulae--specifically some aluminized explosives and ammonium perchlorate compounds. Several reasons have been advanced for their deviation but no positive evidence has been obtained to support them. Despite these cases for all practical applications the use of these correlation formulae will give adequate answers.

Explosive Distribution and Initiation

The distribution of the explosive about the liner and the type of initiation used to detonate the charge have a very marked influence on the performance of a shaped charge. Distribution as discussed in this section is concerned only with the geometrical arrangement of the explosive. Inhomogeneities or variations from a uniform charge will be considered later. The parameters which describe the explosive geometry for cylindrical or near cylindrical charges are height and diameter. The dependence of performance on the distribution is closely related to the manner in which it controls the pressure impulse delivered to the liner walls.

It is not possible to generalize much on the effect of the explosive distribution parameters without first defining certain supplementary conditions. If one takes an unconfined and point initiated charge, the mean penetration will increase with increasing charge height. Penetration is very sensitive for heights up to several cone diameters after which it shows only small changes with increase of the explosive column. However, it is still observable at lengths up to 6 or 7 cone diameters. Figure 6 is indicative of the normal behavior of penetration as a function of charge height under the conditions previously enumerated. Actually varying the length of explosive above the liner apex affects the shape and magnitude of the high pressure region in the explosive reaction zone and also varies slightly the direction of the wave front which interacts with the liner, especially at short charge heights.

Under similar conditions the effect of varying the explosive to liner diameter ratio results in a penetration relation as shown in Figure 7. Varying the explosive diameter with a fixed cone diameter results in a performance similar to that for changes in the confinement wall thickness.

The hole volume increases with increasing length and also increasing diameter of explosive within the range normally observed. A limiting value is approached and, of course, it becomes more difficult to observe the smaller increases which are hidden by the spread in the data.

Although the preceding paragraphs would indicate a relatively simple correlation for performance with explosive length and diameter, in reality it is a complex problem. It should be noted that the results presented were for the simplest case and under restricted conditions. The shape and magnitude of these curves might be greatly changed by any one of the

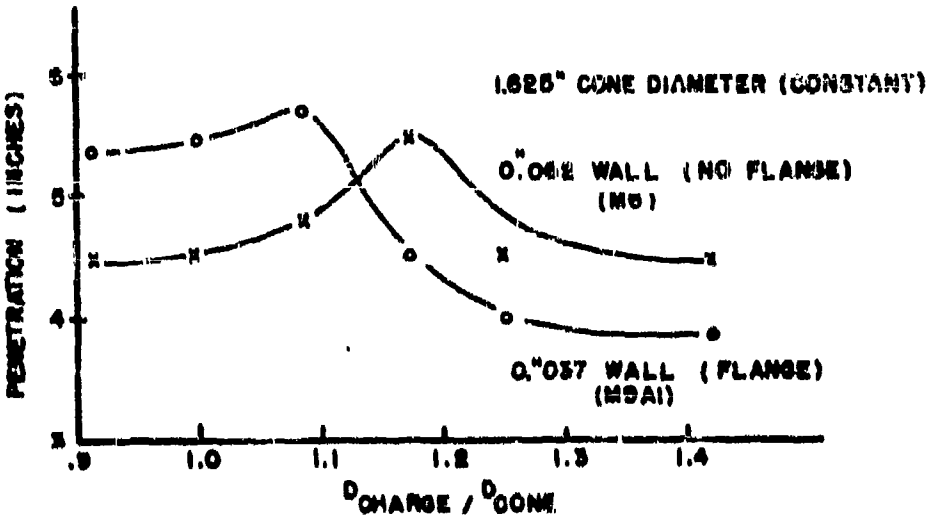

FIGURE 7 - SHAPED CHARGE PENETRATIONS AS FUNCTION OF CHARGE DIAMETER. (UNCONFINED)

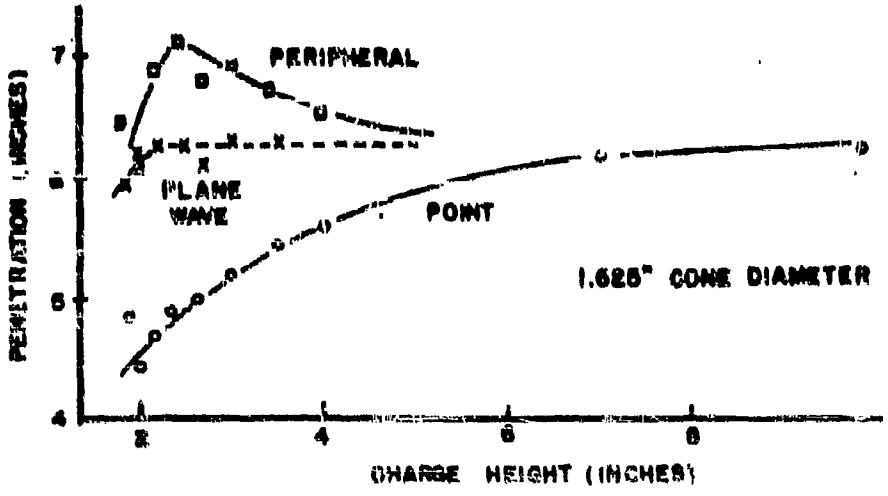

FIGURE 8 - SHAPED CHARGE PENETRATIONS AS FUNCTION OF INITIATION FOR M9A1 STEEL CONES AND 50/50 PENTOLITE EXPLOSIVE.

large number of variables not considered in the discussion up to this point. In general unless experimental results are available for the particular situation at hand, it is difficult to predict the effect of variation of charge height or explosive diameter with any certainty. This is also true if the shape or contour of the explosive charge deviates from cylindrical symmetry. Some hope is offered, however, in the way of qualitative predictions by application of the "Release Wave" considerations being developed by the CIT group (5).

So far only point initiation has been discussed. Plane wave, peripheral, or other types of initiation which shape the detonation wave may change the penetrations obtained. Figure 8 compares point, plane wave, and peripheral initiated standard charges for different charge heights (3). These results are for steel liners. Limited tests for other liner materials indicate an increase in penetrations with peripheral initiation but the percentage improvement varies considerably with the material of the liner (20). These special results are given to indicate what might be achieved with proper wave shaping. Penetrations from point or plane wave initiation are fairly reproducible. However, small asymmetries anywhere in the system will produce large variability with peripheral initiation. Application of such an initiation system must be made with caution if increased penetrations are to be achieved. Experience with a large number of shots under well controlled conditions has shown that increased penetration for steel cone lined charges and peripheral initiation is real (21). However, the large increase (25-30 percent) reported here has been shown to depend critically upon the liner used (22). Furthermore the cavity volume may be reduced by as much as one half.

Charge Preparation

In charge preparation the problem is to produce an explosive loading which will result in maximum shaped charge performance. The method should insure: a) uniformity of the explosive; b) axial symmetry and c) maximum density. Radial uniformity and axial symmetry are highly important to jet formation, and small deviations from these conditions may produce a significant decrease in mean penetration. Maximum densities are required to obtain the highest possible detonation pressures and hence deepest penetrations. Lack of uniformity in the charge does not always result in poorer performance. Increased penetrations have been reported when composition and density gradients along the charge length were changed inadvertently. Increased penetrations have also been reported which could be attributed to charge imperfections in the form of axial pipes that produced some shaping of the detonation wave.

Explosive charges may be prepared by pressing or casting. In pressing, maintenance of uniform density throughout the charge is difficult. Composition uniformity is assured by adequate blending in the case of a multicomponent system. Pressing the charge in a single operation will surely result in considerable density variation if the charge is not short. Usually for experimental work, the charge is made by pressing a

number of short sections which are assembled to give the required charge height. Even then density changes occur in the section containing the liner since it generally is much longer than the other pieces. The mold for this section must be designed so the liner will be well supported or it will suffer deformation. Preparation of the other sections is not difficult but the problem of assembling the charge still exists. If the interfaces are clean and smooth, performance will not be influenced by the manner in which the sections are joined. Of course, axial alignment must be maintained. The problem of obtaining maximum overall density also arises with pressing. Unless high pressures are used the charge will not approach crystal density. Definite variation across the charge, or axial pipes may be formed if care is not taken to insure uniform distribution of the explosive powder in the pressing mold. Densities comparable to the cast material may be obtained with proper care. With the same densities and compositions pressed charges perform as well but no better than cast charges. However, pressing permits the use of explosives which cannot be cast; such as high RDX or HMX content mixtures. Pressures of 20,000 to 25,000 psi will produce densities within 6 to 8 percent of theoretical.

For cast charges the problem is to obtain a solid free of voids, low density regions, composition gradients and large crystals. The methods presently in use vary considerably in detail from laboratory to laboratory but all fundamentally involve the following steps:

a. The explosive is melted at a temperature slightly above the melting point and then slowly stirred to maintain composition uniformity and to remove entrapped air.

b. The melt is then poured into a heated mold. A riser is placed on top of the mold body and filled with liquid explosive so that as the explosive charge contracts on cooling the shrinkage cavities will be filled.

c. Cooling is usually by convection but sometimes may be forced by a water bath.

The explosive is kept in the liquid phase at as low a temperature as possible, so that the melt will go through the freezing point rapidly after pouring. This encourages the formation of small crystals and in the case of multicomponent systems minimizes segregation. With TNT the melt is usually seeded (creamed) to obtain small crystals. The mold is heated to prevent too rapid initial cooling with associated entrapment of air or formation of low density regions. Sometimes the explosive reservoir in the riser is poured at a temperature 10-15 degrees higher than that in the body. A steam finger is frequently placed in the riser to keep the explosive molten during solidification of the charge. When this method is not used to prevent the riser surface from freezing over, the crust is broken at frequent intervals and the charge may even be probed to increase downward flow of the molten

explosive. Cooling, if forced by a water bath should progress from the bottom up toward the riser. This is done to prevent formation of low density regions. The use of insulation which retards cooling increases the probability of low density regions.

Cast charges have not been entirely satisfactory and there has been considerable effort spent attempting to improve them. The following techniques are the major ones which have been proposed for improvement:

a. Vacuum melting: It is being used with some success to produce more uniform higher density charges. Both the melting and stirring must be done under a vacuum. The cooling may be done under a vacuum, but it does not appear to be important in further improvement of the charges.

b. Vibration or agitation of the poured charges: An attempt to help free the entrapped air. This has not shown much promise.

c. Centrifuging: Spinning the poured charge during the cooling period has been tried at NOL as a means for reducing voids or low density regions. For a single component explosive it was found that no improvement in appearance or performance could be noted. However, with a multicomponent system, a long conical pipe was seen in the radiographs along the charge axis which no doubt produced the increase in penetration which was observed. The method did not offer much encouragement for producing a homogeneous charge.

d. Machining the explosive charge: Casting a large billet of explosive from which several smaller charges are machined permits discarding of the low density core and other questionable regions. This would produce good high density charges but would involve an operation which is difficult to carry out.

The first three of these techniques have been tried in shaped charges, at least to see if they would be feasible. Vacuum melting offers the best method for improving density and uniformity of the charge. Machining the cavity in the charge and fitting the shaped charge liner in the explosive billet appears promising, but intimate contact of explosive with liners from a production lot is hard to achieve. In general it can be said that any improvement from these methods will not be large. A maximum of a 5-10 percent increase in mean penetration might be expected. The spread of penetrations might be reduced up to 50 percent.

At this time the optimum cast-charge preparation would appear to be melting and stirring under vacuum followed by a differential cooling bath (23) after casting. Exact details cannot be given because they would depend upon the explosive, the charge size, the mold, and the ambient conditions in the casting house.

Charge Imperfections

What influence does imperfections or inhomogeneities (cracks, voids, bubbles, density, or composition variation) introduced in charge preparation have on performance? No overall assessment of the importance of these items has been made; however, there are considerable data to indicate the importance of specific deviations. The imperfections may range widely in size. The larger ones are easily visible on radiographs or on the surface of the charge. Small inhomogeneities appear as a change in average density. Some idea of the relative importance of the explosive may be gained from the shaped charge results using liquid explosives. A liquid charge should have near ideal uniformity and therefore less spread in the penetration should be expected, if explosive inhomogeneities are of any consequence. A reduction in the standard deviation of the mean penetration has been observed using a liquid explosive (Nitromethane) with precision cones (24). This is the basis for estimated ultimate improvement in reproducibility which was quoted earlier. Only recently additional investigations with Nitroglycerine (25) confirmed the conclusions based on the earlier tests. Practical considerations make the use of liquid explosive undesirable. Those which conform to sensitivity requirements produce small penetrations. Charge assembly is also complicated. However, the results are indicative of the value of a uniform explosive in reducing the round to round variability in shaped charge tests.

Since solid explosives have positive coefficients of thermal expansion there is always a tendency for cast charges to crack upon cooling. Pressed charges may crack in expansion after release of pressure. The techniques used to insure high densities for the explosive enhance the tendency for cracking. This imperfection may occur anywhere in the charge and in any direction. There is no direct evidence that it adversely influences performance.

Voids and bubbles have the same appearance on radiographs. Bubbles form when the cooling is too rapid to permit entrapped air to escape to the top of the charge before the melt solidifies. They also result when dissolved air is separated out in the crystallization process. Voids occur as a result of shrinking as the explosive cools. It is not scientifically conclusive that small bubbles or voids in regions far removed from the liner have appreciable influence on performance (25). Bubbles or voids at or near the liner are important. Single cavities have been introduced into charges 1 5/8 inches in diameter by removing the liner, drilling a hole in the charge and then replacing the liner (26). Control shots in which the liners were removed and replaced indicated no deterioration in performance due to the operation, hence

any change in penetration could be attributed primarily to the hole in the explosive.

Cavity Location	Decrease in Penetration 3/16" x 3/16" Cavity	1/8" x 1/8" Cavity
At apex	10%	5%
1/3 length from apex	20%	25%
2/3 length from apex	30%	10%
5/6 length from apex	---	5%

These percentages are approximate, but they indicate that the bubble effect may be appreciable. Small bubbles or voids distributed uniformly throughout the charge reduce the density. From a consideration of detonation pressure a 2 percent density change may produce as much as a 5 percent variation in penetration.

Pipes are low density regions parallel to the axis of the charge produced because the explosive does not flow into this region in the final solidification. They can be controlled to a certain extent by using sufficient riser, or they can be removed by drilling or remelting this region of the charge and repouring. In some cases when the casting mold is insulated a pipe may occur as a thin cylinder displaced from the axis. Wide spreads in penetrations or the reduction of mean penetrations have been attributed to the cylindrical pipe. On the other hand slight increases in penetration also have been attributed to the wave shaping action of small symmetric pipes on the charge axis. In general pipes are considered undesirable because they are uncontrolled variations contributing to the lack of charge uniformity.

The influence of localized inhomogeneities is hard to determine. Their occurrence has the effect of tilting or otherwise disturbing the uniform detonation front needed for ideal liner collapse. A considerable amount of the spread in results obtained from a group of supposedly uniform shaped charges may be caused by this irregularity. As indicated previously the use of a liquid explosive, which is assumed gradient free, resulted in a 50 percent decrease in the coefficient of variability for the mean penetration. In these considerations one is concerned with the ultimate performance which might be expected from an ideal charge. This has not been established. It is therefore not possible to indicate how far one must go toward improving charge uniformity before negligible gain in reproducibility of performance results.

Summary

In summarising it is noted that the explosive detonation parameters are fairly well known. Those of interest in shaped charges may be computed with an accuracy of 5 to 10 per cent for a given explosive. In the present state of the theory this is satisfactory although further refinements may be needed. Shaped charge performance at least in part may be correlated to detonation parameters so that the best explosive may be selected from detonation data. Explosives with high detonation velocities and densities are preferred. Of the existing explosives Composition B is good, but improvement is possible by going to a higher RDX content cyclotol or an octol (HMX/TNT). Up to 20 percent increase in penetrations over Composition B can be realized by the proper substitution.

The effect of explosive distribution may be explained qualitatively and in some instances quantitatively. General rules for optimizing the explosive distribution are not available but there is a considerable experimental background to guide further designs. The method of initiation is important. Improvement may be realized in shifting from the standard point initiation system, but such a shift must be made with caution.

The problem of charge preparation must also be considered carefully if maximum uniform performance is to be achieved. The present methods for producing cast charges give reasonable uniformity and density but can be improved at least for experimental charges. The extent which an improved charge preparation will help performance or general reproducibility is not known. It may be small. The use of pressed charges should be considered since it is possible to obtain density and uniformity comparable to cast charges. Pressing permits use of high performance explosives that are not castable.

Charge imperfections resulting from the preparation techniques have been discussed in detail. Many of the results are inconclusive. Local irregularities in the region of the liner are undesirable and contribute to lack of reproducibility in penetrations. Uniform distribution of very small bubbles reduces the overall density of the charge. However, this may have only a small influence on general performance.

TABLE 1

Explosive	Composition	Density (gms/cc)	Detonation Velocity (m/sec)	Sensitivity (Drop Height in cms.)	Penetration HOL (inches)	Other
TNT	Trinitrotoluene	1.60	6960	162	4.25	(DuPont) 4.2
Composition B	59.5 39.5 1.0 RDX/TNT/Wax	1.69	7930	60.4	6.17	(DuPont) 6.2
Composition A*	91 9 RDX/Wax	1.60	8230	58.8	6.22	
50/50 Pentolite	50 50 PETN/TNT	1.65	7560	23.5	5.56	(DuPont) 5.5
HBX-1	40 38 17 5 RDX/TNT/Al/D-2	1.72	7350	95.7	5.16	
PTX-2	43.2 28.0 28.8 RDX/PETN/TNT	1.68	8000		6.57	
70/30 Tetratol	70 30 Tetryl/TNT	1.64	7310		5.12	(DuPont) 65/35/Tetratol/ 5.0
70/30 Cyclotol	70 30 RDX/TNT	1.70	8100	37.6	6.27	
75/25 Cyclotol	75 25 RDX/TNT	1.71	8160		6.56	
75/25 Octol	75 25 HMX/TNT	1.78	8350	45.6	6.98	
77/23 Octol	77 23 HMX/TNT	1.81	8480		7.45	

*Pressed (all other explosives listed were cast)
DuPont charges were similar except chg. height was 6.0 in.

CONFIDENTIAL
CONFIDENTIAL

REFERENCES

1. E. Schumann and G. Hendrichs; "Increase of Hollow Charge Effect Through Ignition Control"; Second Ballistic Institute of the University of Berlin; OTIB N. 1471; 30 March 1943.

2. M. Paul and J. F. Lemons; "Improvement in the Performance of Cavity Charges"; Explosives Research Laboratory, OSRD 3443; 3 April 1944.

3. B. E. Drimmer and W. T. August"; "Peripherally Initiated Shaped Charges"; Naval Ordnance Laboratory; NavOrd 1722; 1 November 1950.

4. H. Dean Mallory; "The Measurement of Detonation Pressure in Explosives"; Naval Ordnance Laboratory; NavOrd 1883; 5 March 1953.

5. E. M. Pugh, R. J. Eichelberger, C. T. Linder, and F. Allison; "Fundamentals of Shaped Charges"; Carnegie Institute of Technology, Fourth Bimonthly Report. (CIT-ORD-35); 31 October 1951.

6. H. Eyring, R. E. Powell, G. H. Duffy, and R. B. Parlin; "The Stability of Detonation"; Chemical Reviews, 45 No. 1 69, August 1949.

7. R. J. Finkelstein and G. Gamow; "Theory of the Detonation Process"; Navy Department, Bureau of Ordnance, NavOrd 90-46; 20 April 1947.

8. H. G. Snay, E. A. Christian; "Analysis of Experimental Data on Detonation Velocities"; Naval Ordnance Laboratory; NavOrd 1508, 1 February 1951.

9. H. Jones; "The Properties of Gases at High Pressures Which can Be Deduced from Explosion Experiments"; Third Symposium on Combustion, Flame and Explosion Phenomena; Williams and Wilkins Publishers; 1949.

10. S. J. Jacobs; "Remarks on Some Fundamental Features of Detonation"; Transactions of Symposium on Shaped Charges; Aberdeen Proving Ground, Ballistics Research Laboratories, BRL Report 837; 13-16 November 1951.

11. W. R. Burke; "Investigation of Cavity Effect Section III-Variation of Cavity Effect with Explosive Composition"; Army Contract W-672-ORD-5723; 3 February 1943.

12. C. O. Davis et al; "Investigation of Cavity Effect" Final Report; DuPont de Nemours & Co. Eastern Laboratory (Army Contract W-672-ORD-5723); 18 September 1943.

13. G. M. Hopkins; "Evaluation of Explosives for Shaped Charges"; Picatinny Arsenal; 3 January 1945.

14. A. D. Solem, W. T. August and S. R. Walton; "A Comparison of Various Explosives with Respect to Shaped Charge Efficiency;" Naval Ordnance Laboratory, NavOrd 1853; 1 April 1951.

15. W. T. August and A. D. Solem; "Shaped Charge Performance with Various Explosive Loadings"; Naval Ordnance Laboratory NavOrd 2767; 16 February 1953.

16. C. Keenan and D. Pipes; "Table of Military High Explosive (Second Revision); Navy Department, Bureau of Ordnance, NavOrd 87-46; 26 July 1946.

17. N. L. Coleburn and T. P. Liddiard; "The Rates of Detonation of Several Pure and Mixed Explosives"; Naval Ordnance Laboratory, NavOrd 2611; 22 September 1952.

18. N. L. Coleburn; "A Correlation of Explosive Properties with Shaped Charge Performance; Naval Ordnance Laboratory NavOrd 2721; 19 January 1953.

19. M. A. Cook and P. A. Coombs; "Theory and Application of the Cavity Effect"; Report for May 1943 Contract W-670-ORD-4331 duPont de Nemours & Co. Eastern Laboratory; 17 June 1943.

20. A. D. Solem and W. T. August; "Performance of Peripherally Initiated Shaped Charges"; Transactions of Symposium on Shaped Charges; Aberdeen Proving Ground, Ballistic Research Laboratories; BRL Report 837; 13-16 November 1951.

21. W. T. August and A. D. Solem; "Peripheral Initiation of Shaped Charges II, Penetration Patterns for Different Shaped Charge Parameters and Initiator Barriers Using Steel Liners"; Naval Ordnance Laboratory, NavOrd 2681; 1 October 1952

22. R. J. Eichelberger, C. T. Linder, and F. E. Allison; "Fundamentals of Shaped Charges"; Carnegie Institute of Technology, Fifth Bimonthly Report (CIT-ORD-40), 31 August 1952.

23. D. L. Laskowski and W. C. McCrone; "Casting of TNT Final Report"; Armour Research Foundation of Illinois Institute of Technology; 25 June 1952.

24. E. E. Drimmer; "Performance Uniformity of Shaped Charges, Effect of Liner and Explosive Uniformity on ---"; Naval Ordnance Laboratory, NOLM 9790; 24 June 1948.

25. G. D. Clift and Charles E. Jacobson; "Determination of the Effect of the Use of a Homogeneous Explosive and of Liners made in Various Ways to Close Tolerances on the Performance of Experimental Shaped Charges;" Picatinny Arsenal, 16 October 1953.

26. S. Fleischnick; "Investigation of Factors Entering into Design of Shaped Charges (Loading and Testing of High Explosives in Shaped Charges)"; Picatinny Arsenal; 14 October 1948.

27. M. A. Paul, E. P. Meibohm, and H. L. Bachrach; "The Effects of Various Aberrations on the Performance of Cavity Charges"; Explosives Research Laboratory, OSRD 5599, 16 October 1945.

CHAPTER VI

FUZES FOR SHAPED-CHARGE MISSILES

J. Rabinow and Wm. Piper

National Bureau of Standards
Washington, D. C.

Introduction

This chapter is concerned with contact fuses for shaped-charge projectiles. While experiments have been conducted with proximity fuses for such applications, and the fuses have proved particularly suitable for the very large rounds, at the present writing it appears that the complexity and expense of a proximity fuse for rounds smaller than 8-inch in diameter is warranted only in special cases.

A fuse for a shaped-charge round has some elements in common with other types of fuses, and some features which are unique. A fuse, in general, consists of two essential elements which are somewhat mutually contradictory. It must possess a safety system that keeps the fuse inert under all conceivable conditions until such time as it is considered to be at a safe distance from the launcher, and then the fuse must execute a technical somersault and become a very sensitive and lethal device. In some of the simpler fuses these two separate functions are so intermingled that the distinction is sometimes lost. In the more sophisticated fuses this distinction between the trigger and the arming system is very marked and, particularly in devices like the proximity fuse and the fuses for guided missiles, these two components consist of separate and distinct physical entities.

Because of special requirements in designing a fuse for a high-velocity shaped-charge round, the triggering and the safety devices are separate devices. In some of the fuses which have been and are being designed for low-velocity rounds, however, the physical separation is not well defined. The reasons for this will be explained in detail below.

General Requirements

Because the shaped-charge explosion must be initiated from the base of the round, the main detonator's location is immediately fixed. In locating the target-sensing element, however, the designer has some latitude. It may be well to consider a difficult case first. A 90mm fin-stabilized gun-fired projectile may travel at a velocity of some 2500 feet per second. The distance from the nose of the round to the location of the detonator is approximately 1 1/2 feet. This means that if the round is to be detonated a very short time after the nose contacts the target (the time being limited arbitrarily by the requirement that the nose must collapse not more than 1/4 inch before the initiation of

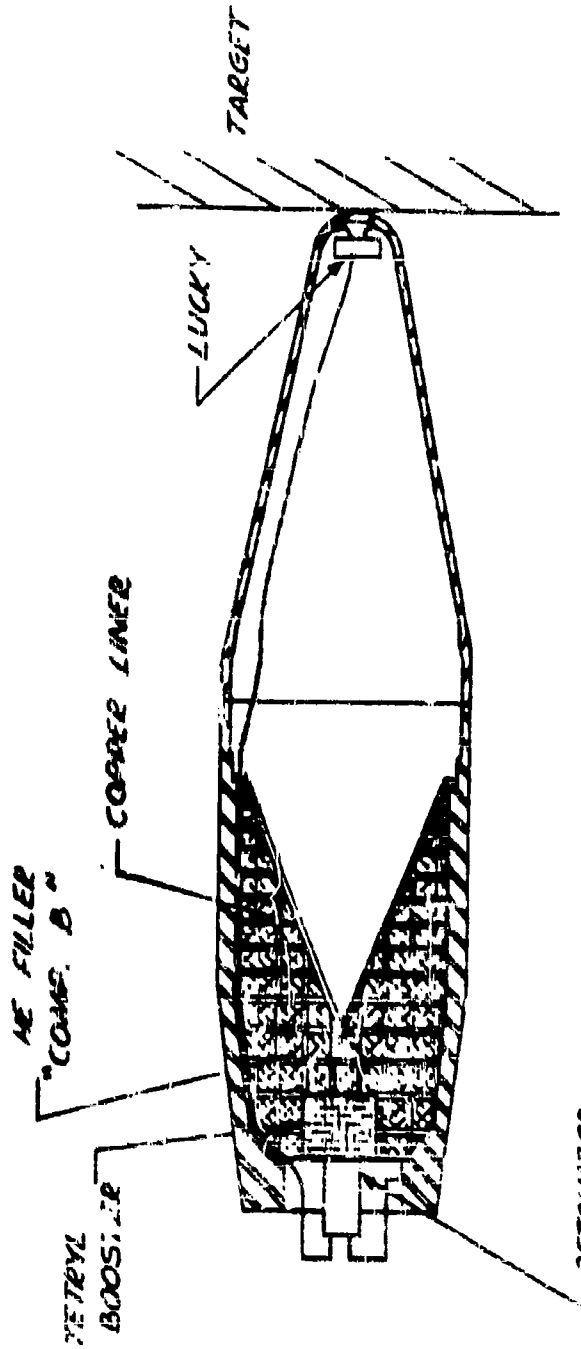

Figure 1 Barium titanate firing principle.

explosion), the following requirements of time exist: The initiation must be started in 8 microseconds, because that is the time required for the shell to travel 1/4 inch. If the detonator requires 6 microseconds to detonate after receiving the signal, it follows that the information must travel from the tip of the shell to the detonator in 2 microseconds. This immediately rules out any mechanical means of transmitting the information from the front to the base of the shell, and it is because of this consideration that an electrical system was adapted for the T208 fuse which will be described later.

In the case of a subsonic round such as the 3-1/2-inch rocket grenade or, even better, the T37 rifle grenade, the requirements for speed of initiation of the explosion are far less stringent. A rifle grenade travels at some 150 feet per second. Again, if one permits the round to deform a 1/4 inch before setting off the high-explosive charge, the time available is 140 microseconds, and a mechanical transmission of information from the nose to the rear element becomes at least theoretically possible. Two general methods are employed to provide mechanical transmission: One is the so-called "spit-back" fuse where a small shaped-charge explosive in the nose of the round is initiated by a percussion primer and fires a jet backwards through a passage provided in the main charge into a base booster. Since the velocity of such a small jet is very high, this provides an extremely rapid method of transmitting the trigger action from the front to the rear. Another approach used in rocket grenades is to have an inertia weight located at the base of the round. When the round contacts a target it decelerates, the inertia weight slides forward and fires a percussion cap. The disadvantage of this type of fuse is that it is inherently slow and that the shell is required to have a very rigid nose section so as to prevent collapse while the fuse is going through its triggering cycle.

Electrical Fusing

In order to fuse a high-velocity round, several electrical methods have been tried. One is to use a power supply such as a battery, a switch in the nose (which may be a simple double shell), and a detonator at the base with an appropriate arming system. The second, which is really a modification of the first, is to use a source of electrical energy which is inert until firing, such as a simple impulse generator that charges a capacitor on firing. This capacitor can be made to hold its charge for the duration of the flight of the projectile and can be discharged by a switch as in the previous case. This last approach was used in the first model of the T208 but was abandoned in favor of the simplicity of the piezoelectric generator. A third possible electrical method is to use a generator located in the nose of the projectile which is energized by the impact with the target; either an electromagnetic or an electrostatic device can be used.

Driving a small magnet through a coil can be made to generate enough energy to fire a detonator. This has been tried but there are certain difficulties in actuating such a device at various angles of impact and also keeping it small enough to be put into the nose of a shell and not interfere with the formation of the jet. The method now being employed in several fuzes makes use of the piezoelectric effect of a barium titanate element. The barium titanate crystal as used in this fusing system has been given the coded terminology of "Lucky" fuze and should be so referred to whenever possible. Figure 1 shows the general arrangement of such a fuse.

A small disk of this material, approximately 1/16 inch thick and 3/8 inch in diameter, is located at the forward end of the round. The disk is silvered on both sides, and electrical connections are brought out from the two silvered surfaces. One side of the disk is usually "grounded", and a wire lead is brought from the other surface through a suitable arming switch to the detonator. In the high-velocity rounds, a rubber cushion is placed between the barium titanate disk and the metal ogive of the projectile. This is done so that rough handling will not break the crystal. The rubber, however, transmits high-velocity shocks with very little attenuation, so that upon contact with the target it acts as a solid and the barium titanate disk is subjected to a large and sudden compressive force. When subjected to shock large enough to crush the element, such disks deliver as much as 1200 volts on open circuit and will fire a nominal 1000-erg detonator within 10 microseconds. Because they are essentially high-impedance devices, barium titanate generators are generally used in conjunction with carbon bridge detonators.

Because of the simplicity of such a fuse, this system is also being used in the T2030 for 3-1/2-inch rocket, T205; the T224 for the 75mm recoilless round, T188; the T2028 fuse for the high velocity rocket, T2017; and the T1014 fuse for the T37 rifle grenade. Experiments are now under way with low velocity rounds, with the intention of locating the barium titanate element at the base of the projectile, in the same package with the arming system and the detonator, and to transmit a mechanical shock to it through the body of the projectile. As stated previously, this is possible where sufficient time after impact is available.

Arming Systems

The arming systems for the shaped-charge rounds can be of many types acceptable for other high-explosive rounds. Bore riding pins, pull wires, and other externally operated devices may be used. External electrical systems can be connected to the fuze, air pressure devices may be employed, etc. The systems generally being adopted at the present time make use of acceleration of the round in such a manner that arming will occur only at some time after the round has reached a predetermined minimum velocity and, if required, after a specific

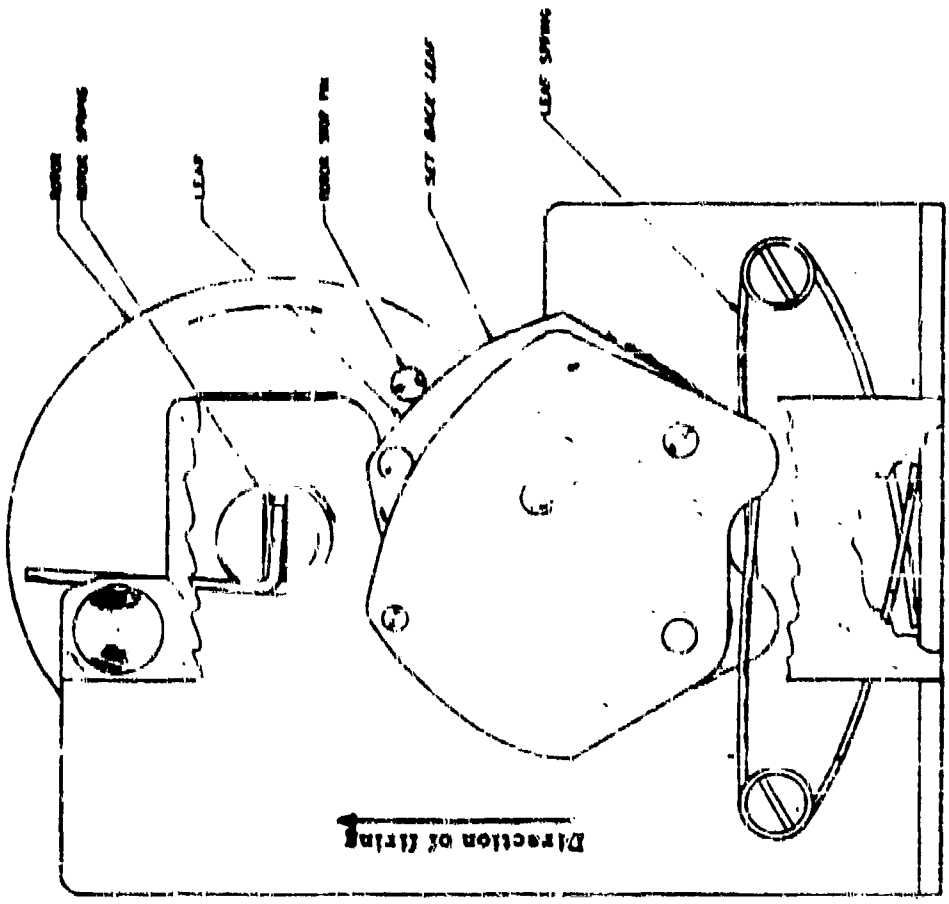

Figure 7. Typical acceleration device (schematic).

additional time has elapsed after firing. Since hermetic sealing of the fuze is always desirable, the use of acceleration is particularly attractive since this is the only effect that can operate in a completely sealed system. The specific method that is used is to integrate acceleration over a certain time so as to distinguish between proper firing and accidental acceleration such as shock in handling, and particularly in accidental dropping of the round.

A typical acceleration device is shown schematically in Figure 2. It consists of several set-back weights held forward by springs and so arranged that they must move back in sequence. The device is further so arranged that if only some of the weights have moved back under the action of acceleration, and the acceleration ceases, they all return forward so that the fuse cannot remain partially armed. The restoring springs also serve to increase safety because they set the threshold acceleration that is required before the elements will respond at all. Details of some of the arming systems will be described under the appropriate fuse heading. An out-of-line detonator is universally employed because it is generally considered that detonators are less stable than other components of the explosive system. The evidence that electric detonators are, in themselves, dangerous is very scanty. The writer knows of no case where an electrical detonator was exploded by any means other than applied electrical energy. This does not mean that heat due to a fire could not fire a detonator, but because the detonator is normally surrounded by high explosive, it is doubtful that this presents any additional hazard over that generally obtained when high-explosive shells are subjected to a fire. The electrical detonators, as used in shaped-charge rounds, need not be of the very sensitive type. This should make them safer to handle than others of that general class.

The above remarks relative to electric detonators should be considerably qualified in the case of certain rounds. In several shaped-charge fuses, grase action is achieved by a mechanical stab-primer which explodes a relay of lead azide which, in turn, explodes the main electrical detonator. Because of the sensitivity of such an arrangement, out-of-line mechanisms are required. It is also possible that high-velocity impact will function an electric detonator. In the field, therefore, light-wall ammunition may be seriously jeopardized by stray fragments. This may not be true in the case of rounds with very thick walls, in which the detonator is amply protected from any fragments but those of the highest velocities.

A simple method of obtaining both electrical and mechanical arming is to place the detonator into a movable member such as a small cylinder. Then, with a single motion, it is possible to align the detonator with the rest of the explosive train and at the same time to close the electrical circuits. In the "safe" position, the detonator can be short-circuited or left unconnected. It has been stated that it would be desirable to keep the detonator short-circuited when in the "safe" position. The writers are of the opinion that if the fuse is contained in a metal case, this is a superfluous requirement because there is no possible way in which an electrostatic charge, due to external causes,

can be accumulated inside a completely shielded enclosure. It is assumed, of course, that the electrical arming system is adequate to prevent galvanic currents, or piezoelectric currents due to set-back, from reaching the detonator.

Specific Fuses

T208

This is one of the early piezoelectric fuses. In the original model, an impulse-generator-capacitor system was employed. A photograph and schematic of the original version are shown in Figures 3 and 3a. The generator consists of a coil approximately 1 inch in diameter and 3/8 inch thick, wound with very fine wire. An alnico magnet, 3/8 inch in diameter and 1/2 inch long, is placed inside the coil. On set-back, a multi-element device releases the magnet, which moves rapidly out of the coil. This produces a high-voltage pulse that charges a capacitor. To prevent the capacitor from subsequently discharging back through the coil, a breaker switch is mounted in the path of the alnico magnet so that the charging circuit is timed to open just after the capacitor has been fully charged. The capacitor then holds its charge until impact, at which time the double-wall nose "switch" discharges the capacitor through the detonator. Although the very first fuse of this type worked, subsequent tests were extremely unsatisfactory and the fuse was abandoned because of its relative complexity as compared with the barium titanate design.

A photograph of the components of the barium titanate T208 fuse is shown in Figure 4. This is the latest model, designated T208A7. The safety of the fuses is based on the three-lead set-back device shown in Figure 4a. The leaves are made of aluminum for lightness because of the very high acceleration of the round, and are interlocked by small steel pins, which can be seen in the photographs. Each leaf is held in its forward position by a small spring, and the weight of each leaf and spring combination is such that a set-back force of 4,000 g is required for the leaves to move back. The third leaf of the series releases the arming rotor that carries the detonator. Friction between the rotor and housing prevents it from turning until setback drops to about 100 g. This assures bore-safety. Without any additional delay mechanism, the rotor turns in about 5 milliseconds and therefore arms the round 15 feet from the muzzle of the gun (in the 2800 fps T108 round). By the addition of a small flutter mechanism, the rotor can be delayed so that the round arms at 25 feet from the muzzle in a 1000-fps round. This is the lowest velocity contemplated for this fuse.

One side of the detonator is grounded to the rotor; the other is brought out to a contact spring which, upon arming, makes contact to a stationary terminal. This terminal is connected to the barium titanate nose element. The fuze is contained within a heavy steel wall to confine the detonator blast if it should explode in the out-of-line position. A small thinned-out section of the barrier plate separates the detonator from the booster and couples the explosive elements in the in-line

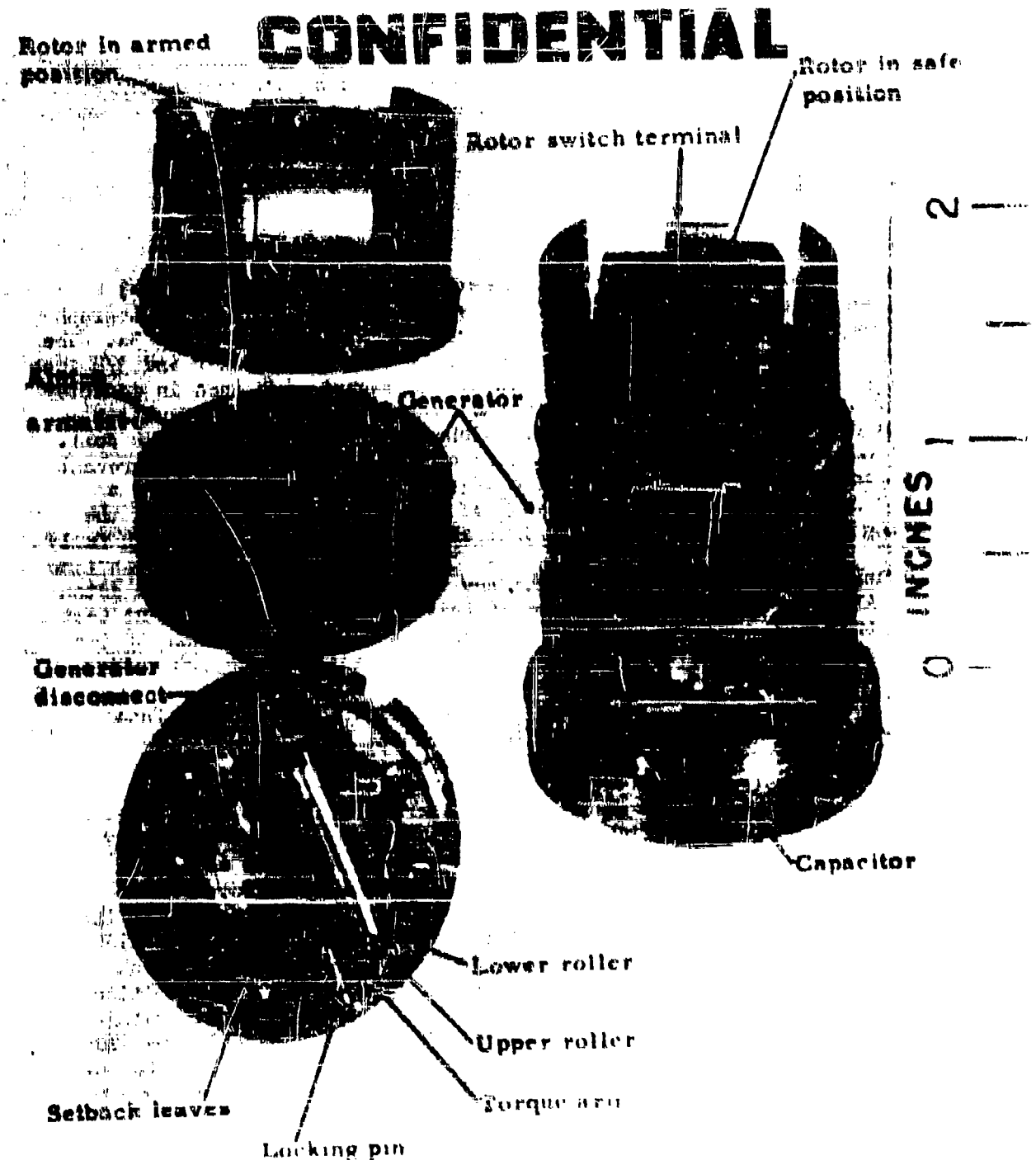

FIG. 3. T-206 fuse breakdown

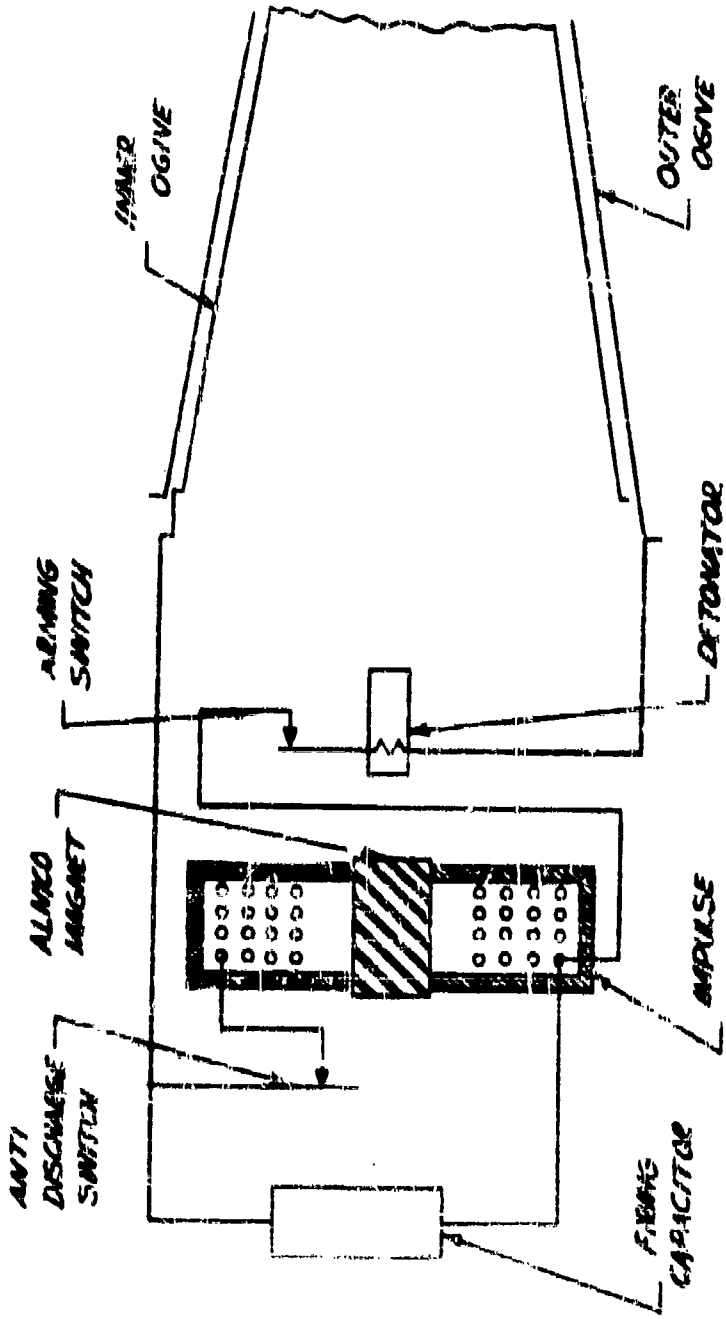

Figure 36. Firing diagram of T203 Fuze.

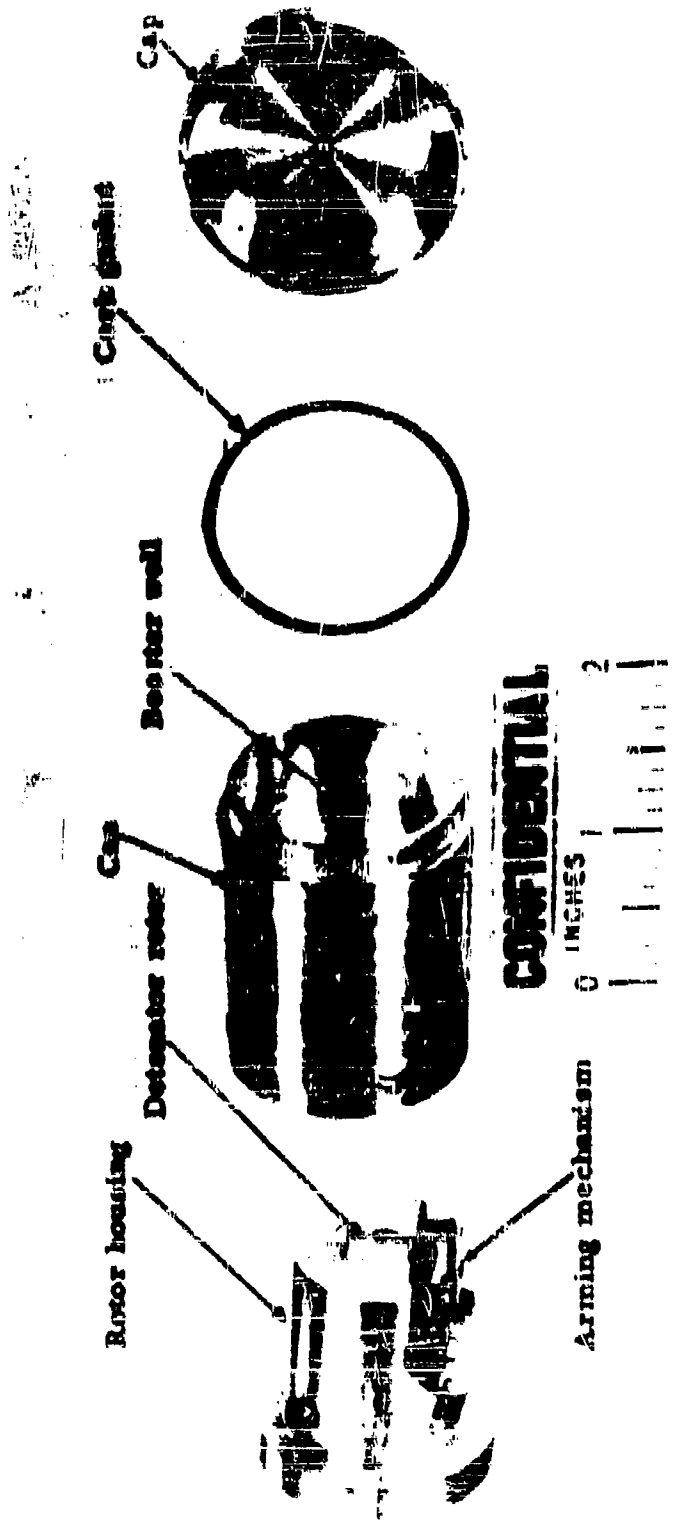

FIG. 4. Base element - Fuze, Pl, BD, T208E5

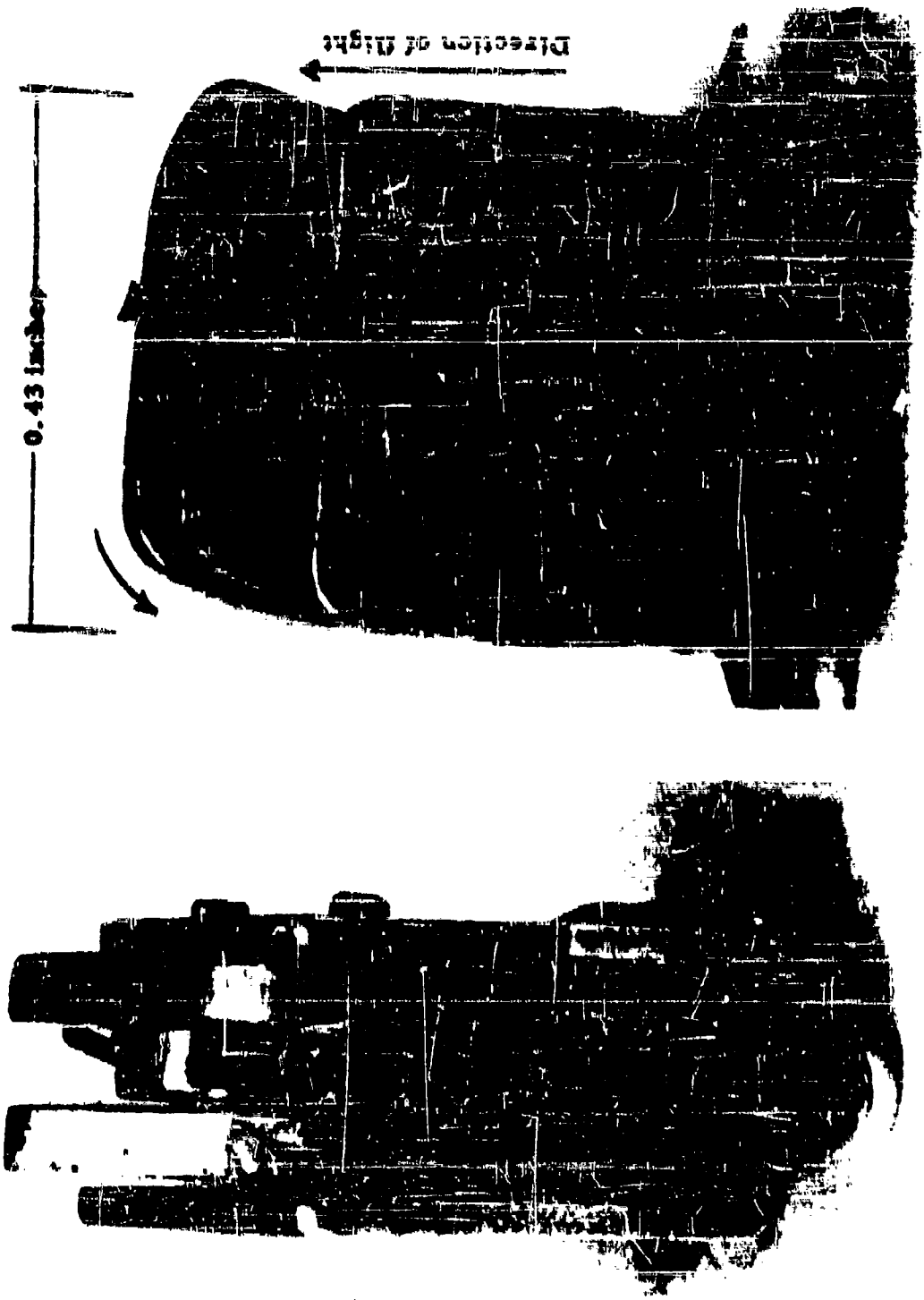

FIG. 4a. Enlarged view of setback leaf assembly for T203, arrows show directions of leaf movements

position. Originally a pellet of tetryl was placed in this depression, but subsequently the unit has been modified by making a through hole in the barrier plate and later pressing in a gilding-metal lead cup. The fuse-triggering element is a disk of barium titanate, 3/8 inch in diameter and approximately 1/16 inch thick. It is mounted as shown in Figure 5. A cap of rubber or similar material is placed over the barium titanate in such a way as to fill the space between it and the ogive. A flexible strip of metal is pushed through the rubber so as to form the electrical connection between the top surface of the barium titanate and this ogive. The rubber provides the tolerance take-up in assembly and serves to protect the barium titanate element in rough handling of the round. At high-velocity impact with a target, however, the rubber acts as a rigid element and transmits impact without substantial attenuation.

The lower surface of the lucky rests on the inner, insulated, cone which serves both as a support and as part of the electrical circuit. An insulated wire is connected to the bottom of this cone and passes through a metal conduit which is rigidly attached to the inner surface of the explosive cavity. This wire terminates at a connection on the base element. One of the difficulties encountered in providing an electrical connection from the front to the back of the round was that the high value of acceleration made a single-wire connection difficult to achieve. A rather strong wire, made of 7 #28 AWG strands of Alcoa 528 and covered with 0.010 inch nylon insulation, was finally developed and, by the use of the inner cone as part of the circuit, was kept as short as possible.

This fuse has given excellent performance in preliminary tests and at the present writing is in initial stages of large-scale production. Figure 6 shows several sequence photographs of the 90mm T108 round equipped with the T208 fuse impacting against 5-inch armor plate. The photographs were taken at approximately 8,000 frames per second so that the velocity of the round, the time for fuse function, and the velocity of the penetration of the jet can be estimated. The fuse works satisfactorily up to angles of impact of 65°.

A grase action of this round is now (early 1953) in the process of being developed and will be added to the production fuse in the near future. It consists of a weighted mass attached to a firing pin. (See Figure 7) On impact the inertia drives the firing pin into a stab-sensitive primer. The primer, in turn, initiates a flame-sensitive charge of lead azide. The lead azide relay explodes the electrical detonator, which in turn functions the round. The inertia weight is restrained from moving until the rotor moves to the in-line position. A small compression spring keeps the inertia weight from creeping forward during flight, and thus reduces the kinetic energy which the moving weight develops during the deceleration due to a grase impact. Alternately, the lead azide relay can be replaced by a barium titanate crystal which, compressed by the primer gases, produces an electrical

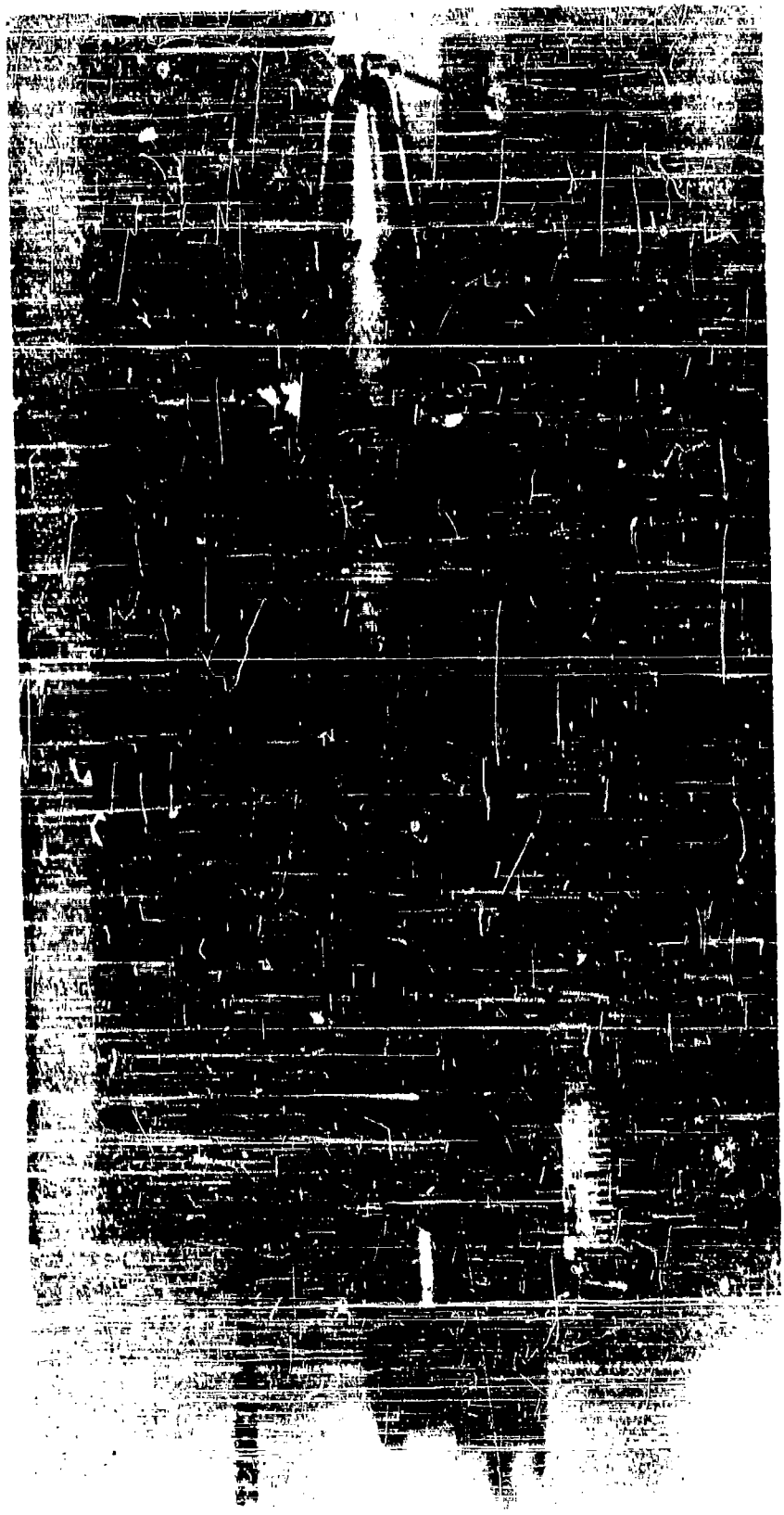

FIG. 5. T208E2 FIED fuze assembly in 90mm, M36B1 shell cutaway to show mounting details

FIG. 6. T108E16 90mm fin stabilized HEAT rounds with T208E2 fuzes fired against 5 inch armor plate, Aberdeen Proving Ground, December 1950 and January 1951

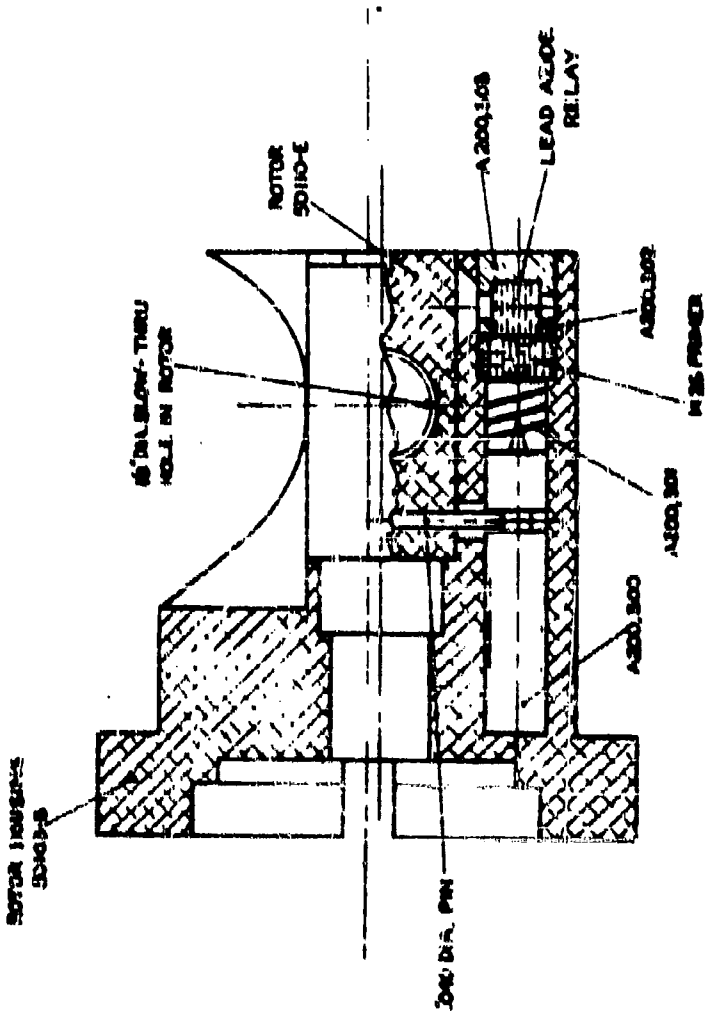

Figure 7. Grease system assembly for Item T20827.

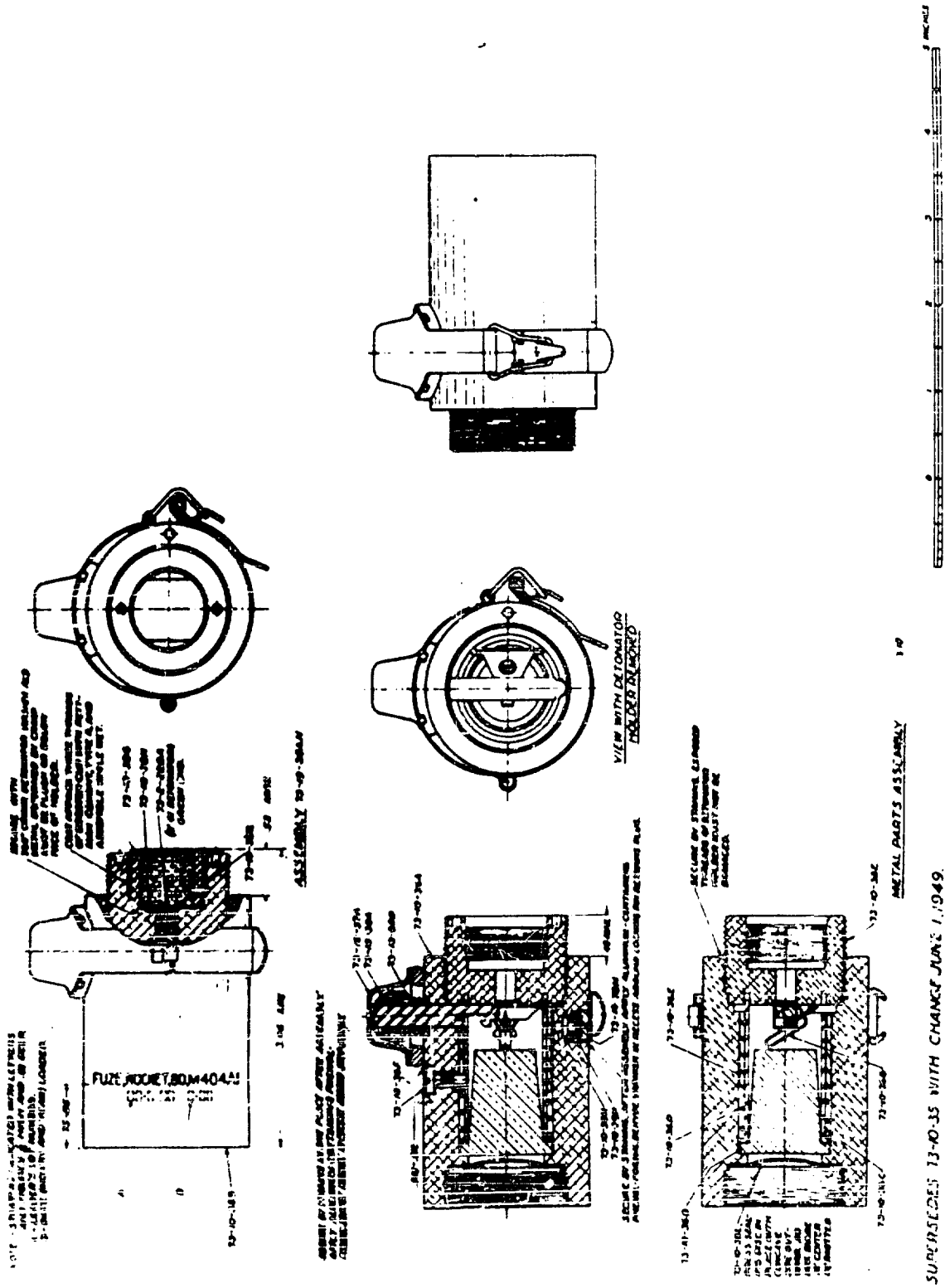

FIG. 8. Fuze, Rocket, BD M404A1 assembly

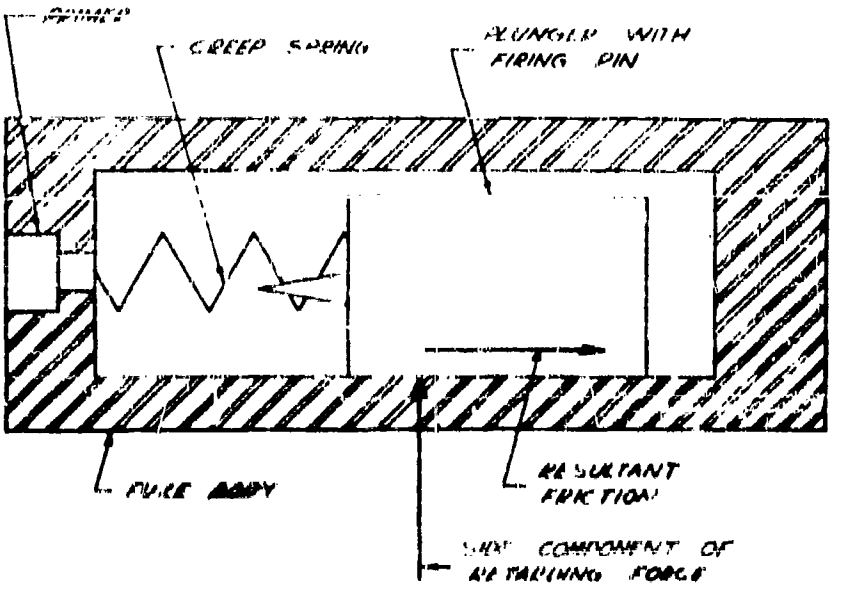

Figure 8 Slide type graze element.

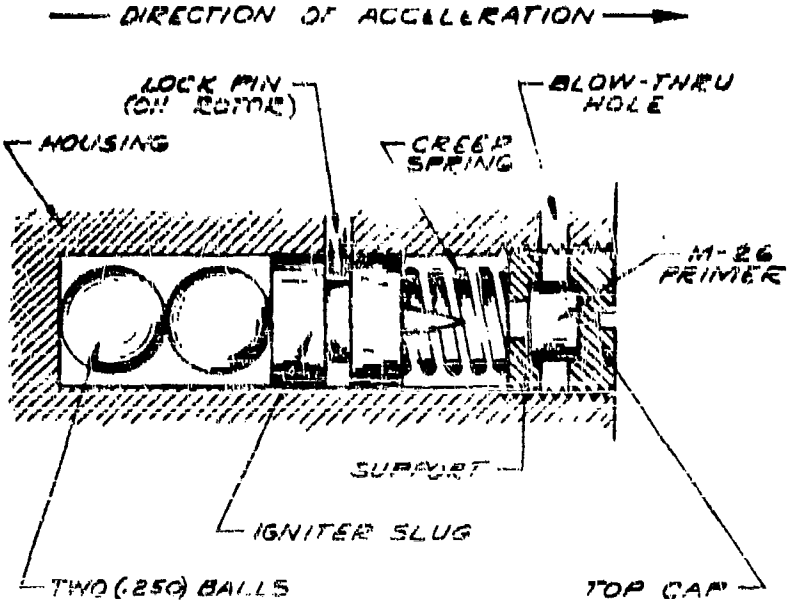

FIG. 10a- GRAZE ELEMENT- BALL TYPE

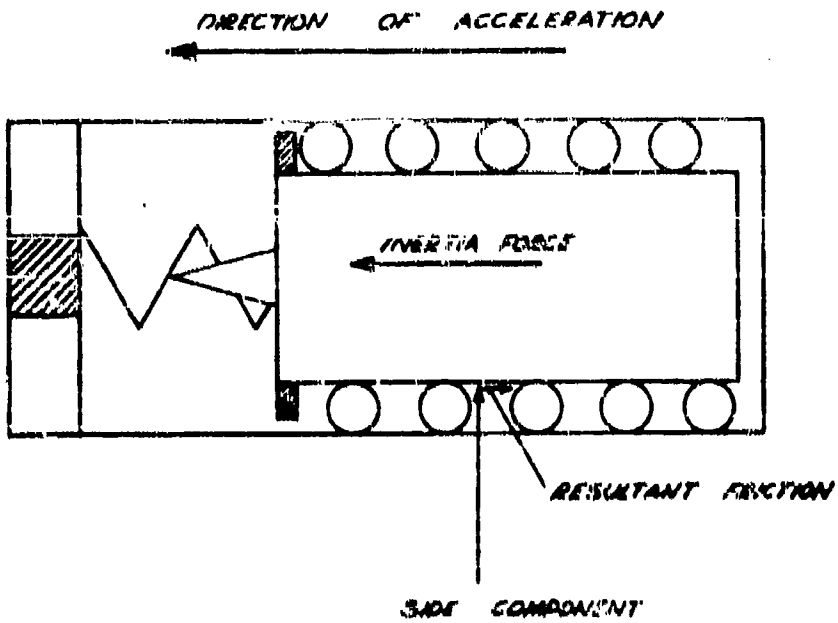

Figure 10b. Anti-friction grase element.

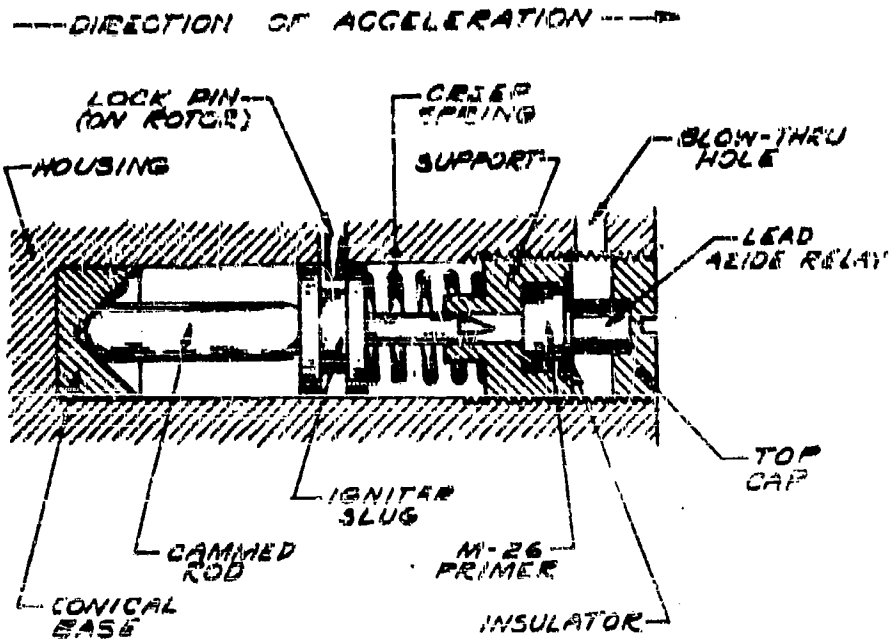

FIG. 10c GRAZE ELEMENT - CAMMED ROD TYPE

pulse that can fire the main detonator.

M10A1

The M10A1 bazooka fuze is typical of the bore-riding-pin arming, mechanical-inertia fuze. It is shown diagramatically in Figure 8. The bore-riding pin is held in place by an inertia weight when the round is in the launcher. Upon firing, the inertia weight releases the pin, which is then prevented from leaving the round by the wall of the launcher. As the round leaves the tube, the pin is ejected sideways by a spring, and the fuze is armed immediately after this. Upon impact with the target, the round is decelerated, and the inertia mass moves the percussion pin forward, fires the detonator, and thus initiates the explosion. The inertia weight is not fastened to the firing pin, but acts through a third-class lever system, multiplying the motion so that 1 motion increment of weight causes about 8 motion increments of the firing pin.

Fuzes of this general type have several inherent disadvantages. One is that there is no appreciable safety delay after firing; hence, contact with camouflage or the branches of a tree can cause an early function. The bore-riding pin, being an externally operated device, prevents the complete hermetic sealing of the fuze and while rubber gasketed caps are employed in shipment, moisture, ice and corrosion have to be continually fought in such designs. This type of fuze also suffers from the disadvantage that it is very difficult to make it operate properly upon grazing impact. Figure 9 shows what happens when such a round impacts very obliquely against the target. The force of deceleration under such conditions has a large component at right angles to the axis of the round, and under certain conditions the frictional force (due to the side acceleration) is sufficient to prevent the weight from sliding forward. This is also a difficulty encountered in providing graze action in electrical fuzes. Several methods of minimizing this frbtion have been tested. One is to use one or two steel balls in place of the sliding weight, as shown in Figure 10a. Another is to provide a linear ball-bearing as shown in Figure 10b; still another is the canned-rod type shown in Figure 10c. Such schemes, while reducing the frictional forces on the inertia weight, also increase the complexity and cost of the round.

The greatest disadvantage of an inertia-weight mechanical fuze, however, is its slow action. Assume, for example, that the weight has to move 0.1 inch to function the primer; the nose section has (in a typical case) an approximate strength in compression of 500 pounds; the grenade weighs 5 pounds and has a velocity of 200 fps. This means that on impact the shell decelerates at 100 g, or 3200 fps. The inertia weight, then, moves forward through the 0.1 inch in 0.0023 second. The shell is therefore detonated after the nose has crushed about 5 inches. This rough computation assumes that the velocity of the shell suffers negligible reduction during the impact.

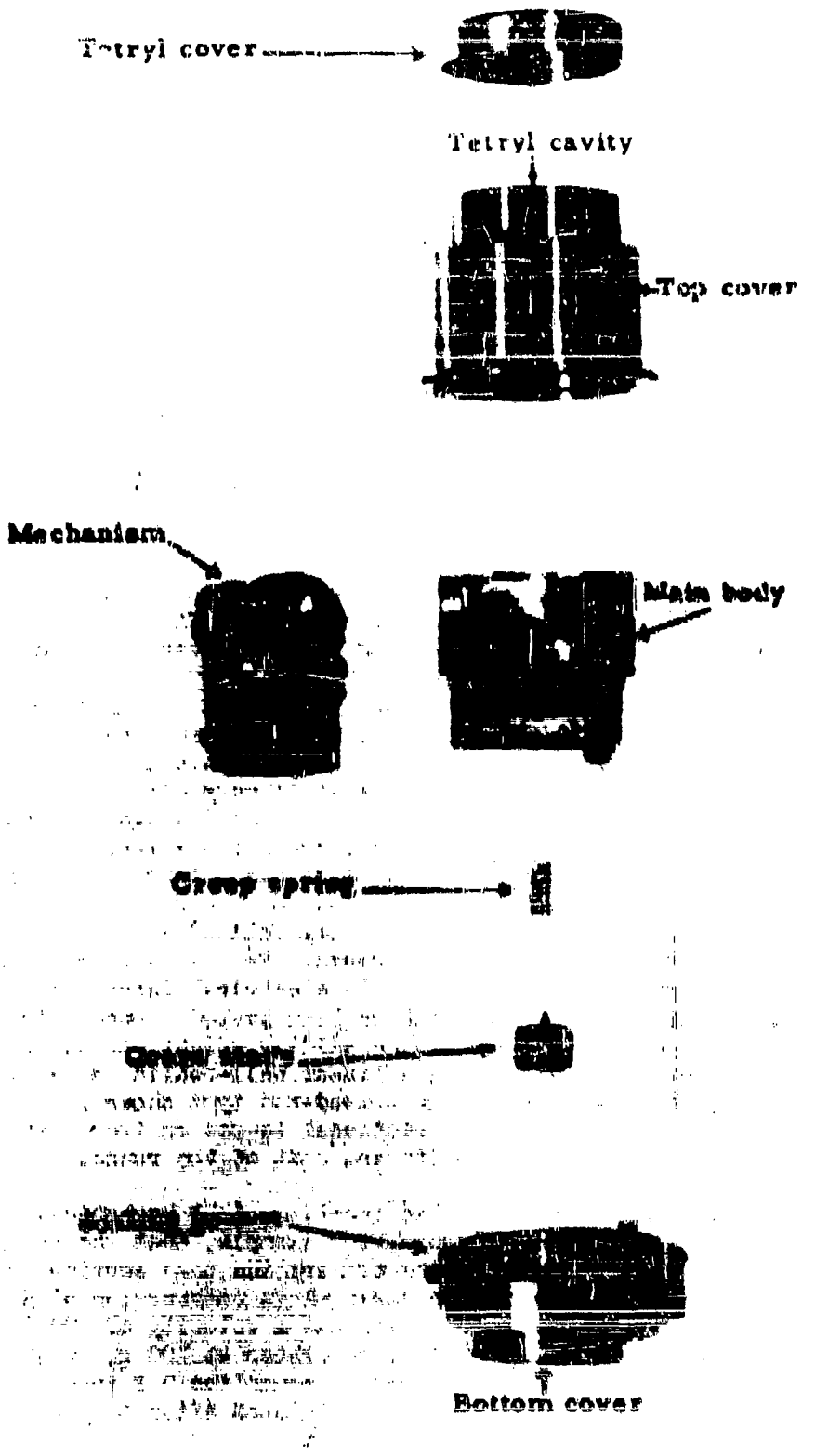

FIG. 11. T2030E2 Base element components

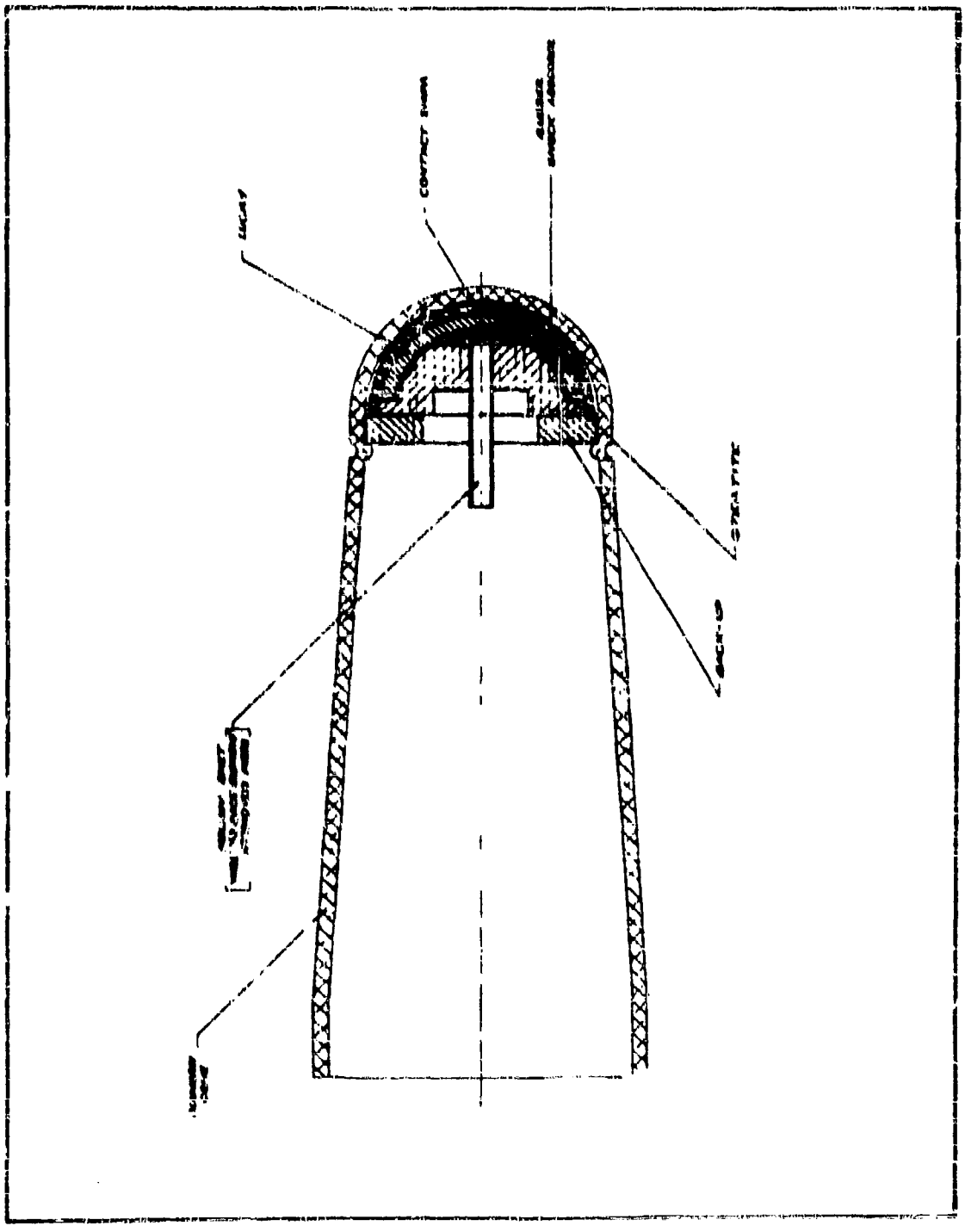

FIG. 11a. T295 Ogive assembly

An electrical fuze, the T2030, for this 3 1/2-inch rocket, is being developed (see photograph, Figure 11, and 11a). It is similar to the two electrical fuzes previously described except that the set-back weights are heavier and move through larger angles and are supported by relatively softer springs. This is because of the lower value of acceleration encountered by this round. Originally, the fuze was specified to initiate arming between 300 and 400 g. Complete arming was to take place between 20 and 35 feet from the launcher. Work was undertaken on an improved round which required release for arming between 900 and 1200 g. The acceleration period was shorter, necessitating a reduction in the number of set-back leaves. Once the set-back leaves release the rotor, and the acceleration drops to zero, the rotor is restrained by a delay system. The delay is provided by a starwheel and oscillating-pallet flutter mechanism which is geared to the rotor.

The lucky element is hemispherical so as to present a larger area at the point of impact and to align the mode of polarization most favorably to the impact stress. Subsequently, however, further study and tests reveal that a suitably mounted flat disk may be superior, since the ratio of strained area to total area at impact may be larger than in the corresponding hemispherical unit. The unstrained part of a lucky does not contribute any energy to the external circuit and behaves as a capacitive shunt, reducing the energy available to the detonator. The cost of the flat unit appears to be about 1/10 that of a corresponding hemispherical unit, making it particularly attractive.

The grase element which is being considered at the present writing is essentially of the inertia type, with two variations (See Figures 14 and 14a). Variation Number 1 is simply a sliding weighted firing pin, free to strike a primer when the round is decelerated. Variation Number 2 is similarly a weighted firing pin but resting on a canned surface so that the force normal to the axis of the round due to a glancing impact can assist in moving the firing pin into the primer. Because of space considerations it was necessary to locate the primer back-to-back with the detonator. A longitudinal blow-hole along the primer and detonator directs the primer flash to the lead aside relay located at the most sensitive spot of the detonator. This entire assembly could be replaced by a combination detonator, were one available. As yet, however, there are only experimental layouts of such an item.

At the present writing, this fuze has passed its laboratory tests but will not be put into production until work on the shaped charge head is completed and service board tests can be run.

T224

For the T184, 57mm fin-stabilized round to be fired from a recoilless rifle, a fuze very similar to the T208 has been developed. Because of space considerations, the base element is of smaller diameter and somewhat longer. Again a multiple-element set-back device is used as the safety, but in this case the set-back leaves are arranged in a single plane, as can be seen in Figures 12 and 12a. It is believed that this leaf arrangement is superior to the ones previously described in that no interlocking pins are employed, the angles through which the leaves rotate are greater, and visible inspection of the assembly is much easier.

In the matter of the electrical connection, however, a radical departure from the wiring system of the T208 is being tested. (See Figure 13). The copper liner is made with a flash tube and mounted so as to be insulated from the body of the round. Together with the inner cone supporting the lucky, it provides the electrical connection between the barium titanate and the fuze. The fuze is provided with a special terminal which plugs directly into the flash tube so that no other wiring is required in assembling the round and a very efficient assembling procedure is therefore provided. It is hoped that a similar change will eventually be incorporated into the T108 round as well.

The general specifications for the T224 fuze are as follows: The nominal acceleration of the round is 12,000 g; the fuze must release for arming at 4,000 g and arm not less than 25 feet from the muzzle, and must function at all angles of incidence up to 65°. It is also being provided with a graze action.

T101

This is a fuze designed for a low velocity round, the T37 rifle grenade (See Figure 16). Accelerations encountered by the fuze average 1200 g for 4 milliseconds and the final velocity of the round is about 150 feet per second. The fuze, shown in Figure 15, is similar to the other electrical fuzes previously described, with the appropriate set-back weights causing its arming. A wide variety of graze mechanisms have been proposed and tried for this round. Thus far most of them have failed to function the round consistently on the first impact, particularly when hits are made on soft earth with very little obliquity. This may be unrepresentative of service conditions, but is an excellent laboratory goal. The design that is most promising uses a spring-loaded firing pin that is triggered by an inertia-operated member. The energy necessary to fire the primer then can be predetermined, and the graze system can be made as sensitive as desired. Initially, it was intended to include delayed arming and a graze mechanism in the fuze. However, due to the urgent requirements for an armor-piercing round of this type, it was decided to release the basic fuze first and then prove out the additional features for incorporation in the

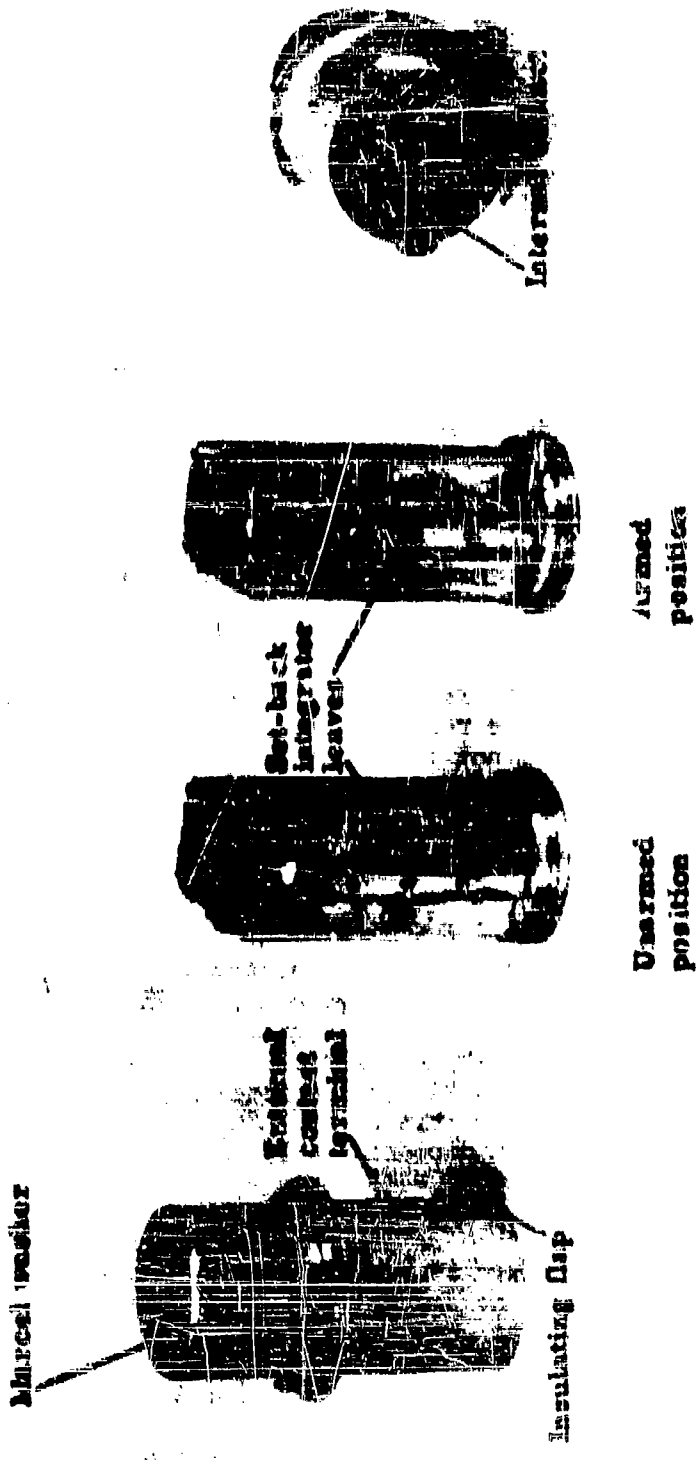

FIG. 12. T224 Fuze showing the integrator leaves

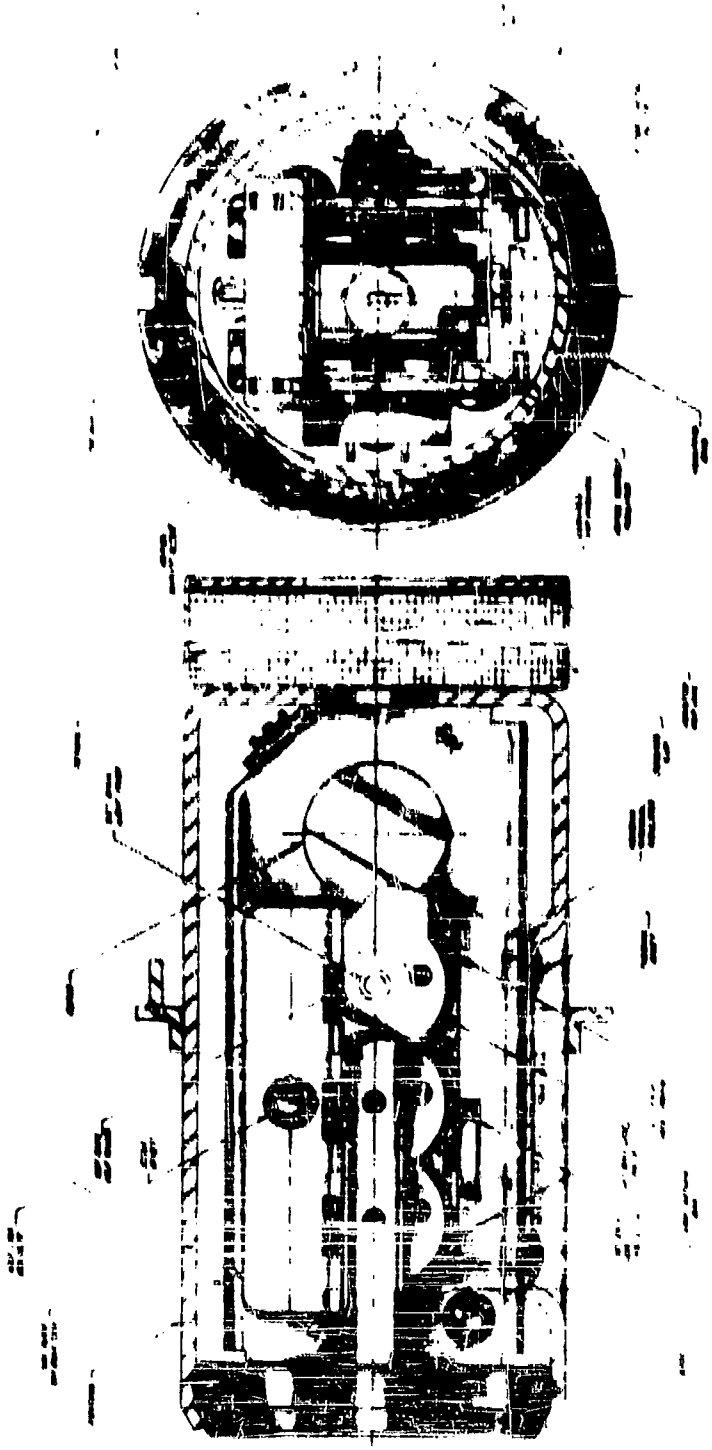

FIG. 12a. T224 Fuze showing the integrator leaves in the unarmed position

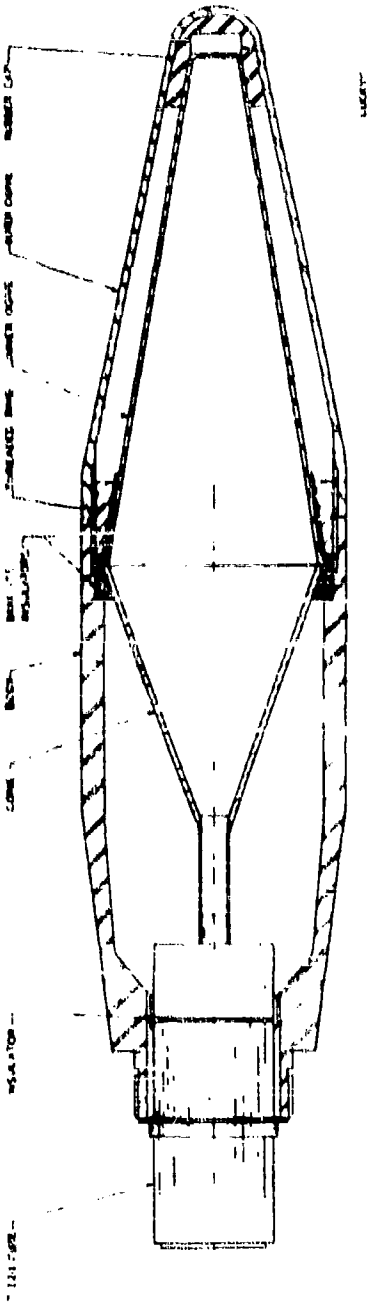

Figure 8. T224 Plug-in Fuze assembly for T186 HEAT shell.

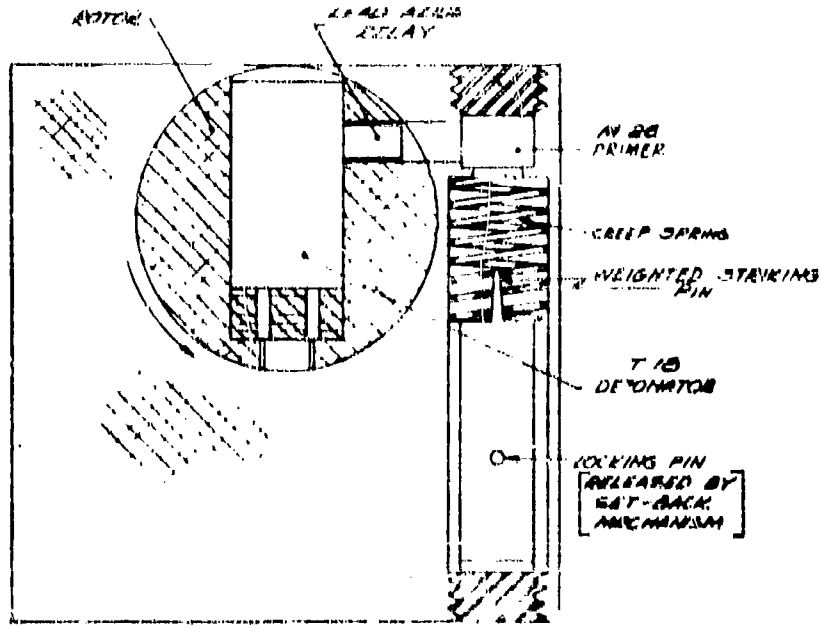

Figure 14. [illegible] Grazer Element

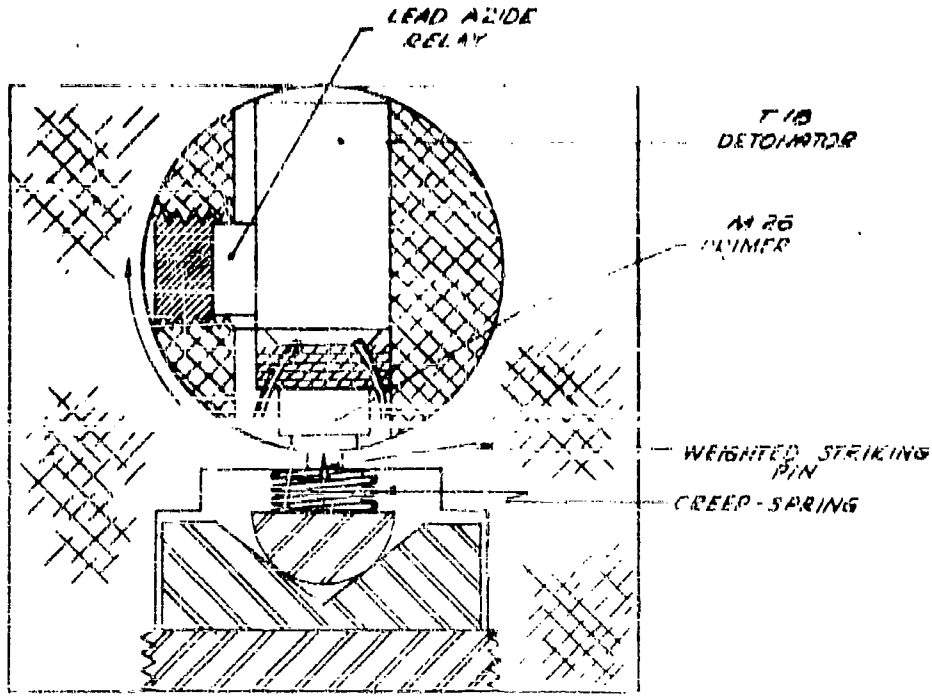

Figure 14a. [illegible] Grazer Element

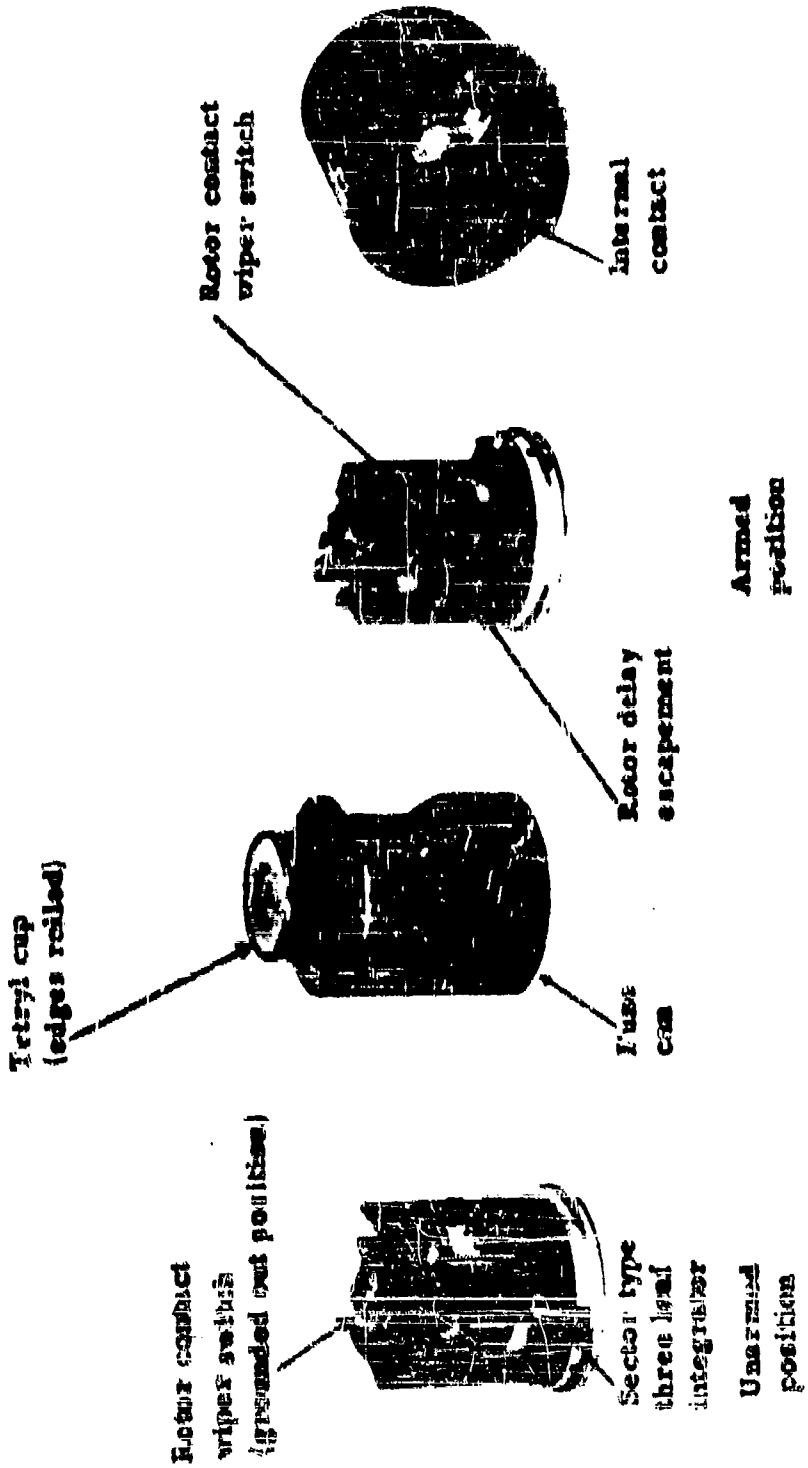

FIG. 15. T1014E, Fuze

fuze at a later date. Because of the very low velocity of the round, and the requirement for proper functioning at large angles of incidence, the rubber protective shield has been removed from the lucky and a rather large lucky is being used. The fuze performed well in the initial tests and is, at the present writing, going into large scale production.

Footnote

Barium titanate ($BaTiO_3$) is a hard, light-colored polycrystalline substance which looks very much like china. The composition which has found greatest use in fuzes contains lead titanate in controlled amounts for improved high-temperature performance. Its dielectric constant of approximately 1500 is somewhat lower than the material used for ceramic capacitors. It is prepared for use by mixing the component powders and pressing them, while slightly moist, into the desired shape. The green units are fired in a furnace at about 1300°C. A silver paint is applied and fired at about 690°C to form the electrodes. The units are then made piezoelectric or polarized by applying a high d-c voltage. Voltages of 70 to 80 volts per mil of thickness are used and the unit is immersed about a half-hour in an insulating liquid to prevent sparkover and corona. The units are then ready for use and remain active permanently as far as can be ascertained, deteriorating only with temperature in excess of the Curie point, which is about 120°C. The application of a stress produces a potential difference between the electrodes. If a load is connected, current will flow and produce electrical energy. The following general equations relate the energy, voltage, and physical characteristics of the material.

Voltage output, $V = 2.2P\ t$ where V = volts, P = pressure in psi, t = thickness in inches;

$$\text{Energy} = 1.1 \times 10^{-2} F^2 \cdot \frac{t}{A},$$

E = energy in ergs,

F = force in pounds,

A = area in sq. in.*

*Data from Franklin Institute Report 6-16-51, 7-15-51, p. 2247-4. Information compiled from Properties of Piezoelectric Barium Titanate Ceramics issued by Erie Resistor Corp., and article Journal Acoustical Society of America, Volume 24, No. 6, p. 709, Nov. 1952, Electromechanical Properties of $BaTiO_3$ by Brush Development Company.

Because of the low velocities of the rifle grenade and the 3 1/2-inch rocket grenade, experiments are being made with a view to the relocation of lucky to the rear of the round. It should be possible (theoretically, at least) to transmit a mechanical shock through these rounds fast enough to detonate the rounds before the nose is appreciably crushed. The relatively weak ogive in the case of both the rocket grenade and the rifle grenade is such that this is somewhat difficult to accomplish. However, preliminary tests using a fairly rugged structure are encouraging. By mounting a barium titanate crystal in the base element, backed by an appreciable mass of metal, it appears possible to generate enough current to detonate the fuze by a transmitted mechanical shock. If this arrangement proves to be practicable, it would make possible a single compact assembly of the entire fuze with the concomitant advantages of complete sealing, simple packaging, and simple assembly into the round. It is interesting to note that the T37 grenade itself was developed in conjunction with the fuze and has special features of assembly and construction for the support of the lucky and of the base element. This tendency to parallel and integrate the development of the round and the fuze is, in the writers' opinion, highly desirable and should be encouraged. Too often in the past the fuze designer has been confronted with an existing round which is far from optimum from the over-all engineering point of view, and has, therefore, been handicapped by inadequate space, poor location, or fastening means. Intelligent compromise between the vehicle and fuze parameters should always result in a more soundly engineered and integrated weapon.

FIELDS FOR FUTURE WORK

"One Piece" Fuzes

There is little question that a single compact unit fuze would be most desirable for the shaped-charge rounds. Many of the ordinary fuses were made as a single package and depend on the deceleration of the round for actuation. For reasons stated previously, such fuses were generally too slow for modern weapons. A promising field of work, therefore, is in the development of high-speed fuses which can be mounted at the base of the round and which will be actuated by nose contact with the target. Experiments conducted at NBS and elsewhere indicate that if a sufficiently sensitive fuze is designed, the mechanical shockwave produced by contact with the target can be employed for triggering. Unfortunately, there are many difficulties in this approach. If the ogive wall is thin, the amplitude of the shock is quite low, and it is difficult to derive enough energy from the resultant pulse to operate a simple fuze. Heavier and more rigid ogives are one possible solution, but may have the limitation of adding unnecessary weight to the round. More sensitive fuzes can be built, but they require much more sensitive detonators, and the best detonators presently available are probably not good enough. Electronic amplification, particularly with the use of transistors and very small

batteries, may be worthwhile, particularly in the larger rounds. In any case, the problem of triggering a base fuze by nose contact at very high speeds should be worked on intensively.

Fuzes with Long Standoffs

Because certain charges in combination with certain liners appear to give improved performance with very long standoffs, there is a fruitful field of work in fuzing for this application. In the case of bombs and other very large projectiles, VT fuzing is entirely possible and has been the subject of experimentation. While no fuzes are now completely engineered for this service, there is no doubt that fuze functioning can be obtained for any standoff from a few inches to many feet with fairly good accuracy, and if long standoffs prove to have the anticipated advantages, this should be a fruitful field of work. Other methods of obtaining long standoffs, such as extension probes, leader projectiles, and bouncing mechanisms, are at least theoretically possible.

Hand and/or Rifle Grenades

It is conceivable that shaped charges could be effectively applied to hand-thrown grenades. This would mean that special fuzing designed particularly for very low velocity impact would have to be developed. The experience with fragmentation hand grenades would, of course, be applicable here except that all-way fuzing may not be required because the shaped-charge grenade must necessarily be oriented at the time of impact.

The National Bureau of Standards is now experimenting with a combination rifle and hand grenade. While this grenade is not now designed for shaped-charge work, it would be fairly easy to modify it for this purpose, and it may serve as a starting point for the development of armor-piercing hand grenades. The fuze is of a simple inertia-weight type and should be entirely satisfactory because of the low velocity of the round.

Detonator Research

The study of initiators is of particular importance [illegible] problem of fuzing for shaped-charge rounds. In the writer's opinion, the present knowledge on detonators is far from sufficient although very rapid strides are being made to fill in the gaps. The design of the proper detonators is quite archaic, and a great deal of work is obviously indicated in simplifying, miniaturing, and reducing the cost of electrical detonators suitable for the mass production of shaped-charge fuzes. The present electric detonators, or initiators, are a throw-back to the blasting caps used in industry, and their design is such that the cost is 5 to 10 times as high as it should be. New detonators, designed specifically for automatic production, for

machine insertion into fuzes, for automatic connection to the circuitry, etc., should be developed.

The business of connecting a detonator into a circuit by bending two pieces of wire, tightening them under screwheads, or soldering them in place, is indefensible. A very appreciable saving in the cost, safety, and over-all elegance of a fuze can be achieved by radical redesign of electrical initiators. This work would also be very profitable not only to the shaped-charge field but to the field of VT fuzes, mines, bomb fuzes, and all ordnance where electrical initiation is employed.

Another important field of work that should be pursued is the investigation of the safety of electric fuzing. The arguments for using in-line and out-of-line detonators should be carefully reviewed. Considerations of safety against fire, shock, and accidental application of electrical energy, should be investigated without the bias that is present in the field today due to greater experience with mechanical initiators. Because many shaped-charge fuzes are buried inside the explosive cavity of a round, safety from fire may be easier to achieve than in other fuzes. It is, perhaps, possible to design electrical detonators which are as safe from shock as the main charge. If this is so, requirements for out-of-line detonation may be eliminated. If very large amounts of electrical energy are available on impact, such as is the case in certain lucky fuzes, the usual dangers with sensitive detonators may not exist. In any case, the requirements for a safety mechanism should always be examined so as to produce the best over-all fuze from the point of view of dependability as well as safety. This is particularly true in close-support weapons, such as a grenade round where a dud is much more serious to the using personnel than would be the equivalent condition in bombs dropped from aircraft. Also, the large quantities in which such fuzes are built make economics imperative. This may be particularly serious in the case of a major war when many of our facilities will probably be destroyed.

Production Engineering

Since "crash" programs are the normal mode of existence in the development work on new fuzes, relatively little opportunity exists for modifying, simplifying, or reducing the cost of fuzes for shaped-charge rounds. Too often, the first fuze that works ends up by being the production model. This is quite different from the conditions that obtain in industry, where basic designs are little modified over a period of years, and a great deal of effort goes into simplifying and reducing the cost of the production items. Efforts to simplify and improve existing fuzes are, of course, always being made, but it is the writers' opinion that the intensity of such efforts should be increased and that definite dollar or cents goals be set up in the redesign of existing fuzes. Perhaps contracts or special prizes could be awarded to industry for submitting the best redesigns of fuzes for production. If it is possible for suppliers of the automobile industry to engineer and produce a complete door-lock mechanism, a mechanism that

would meet all military specifications for corrosion resistance, vibration and shock tests, for something like 90 cents, it should certainly be possible for a shaped-charge fuze to be produced for less than one dollar. Modern methods of assembly should be emphasized, together with the avoidance, wherever possible, of slow operations such as lathe and milling-machine work.

It is difficult to understand why a present T208 fuze costs almost as much as what the industry pays for an electric steam iron which is constructed of aluminum, stainless steel and bakelite; which is provided with an electrical heating element and an adjustable thermostat; and must withstand temperature and corrosion conditions far in excess of those required of the fuze. The arguments that the military specifications are far more stringent than those employed by civilian industry are, in the writers' opinion, not borne out by the facts. This is not the place where the possible reasons for the high cost of ordnance should be discussed, but certainly a continual and thorough investigation of the cost factors is indicated.

THE ENERGA RIFLE GRENADE

The Energa rifle grenade is an anti-tank weapon provided for use by infantry and other rifle-armed troops. It is primarily a "close-in" weapon, using a .73 lb., 3 inch diameter conventional shaped charge. The overall grenade is 16 inches long, weighs 1 lb. 7 oz. and has a maximum range of 328 yards. (Fig. 16).

The fuzes used with this grenade are the percussion type and are known as "spitback" fuzes. Figure 17 shows a Model L9 Mark 1 of the fuze designed for direct action on impact and Figure 18 shows a Model L9 Mark 2 designed for direct and graze action on impact. On setback, referring to Figure 18 which appears to be the latest model, the arming sleeve overcomes the arming spring, forcing the steel balls which hold the striker away from the detonator. The striker is then held off the detonator by the striker spring only. Upon impact, the striker is driven into the detonator which fires and "spits" back a flash to the main detonator at the base of the grenade body through a central tube. The main detonator initiates the booster pellet, which in turn detonates the main HE filling. The striker head is of tungsten carbide and has a jagged edge which is claimed to dig into armor and function the fuze at angles up to 65°. On graze, if the striker is not contacted, deceleration of grenade body and fuze housing causes the detonator and striker guide assembly to set forward and function the detonator. The model shown in Figure 17 operates similarly to that in Figure 18, but the setforward force due to impact causes the detonator assembly to move and strike the firing pin.

An additional safety device is incorporated into the base of the grenade body. The shroud, shown in Figure 19, is assembled into the grenade body between the fuze and the main detonator. It fits over a central tube, and is located by raised studs which engage in zig-zag

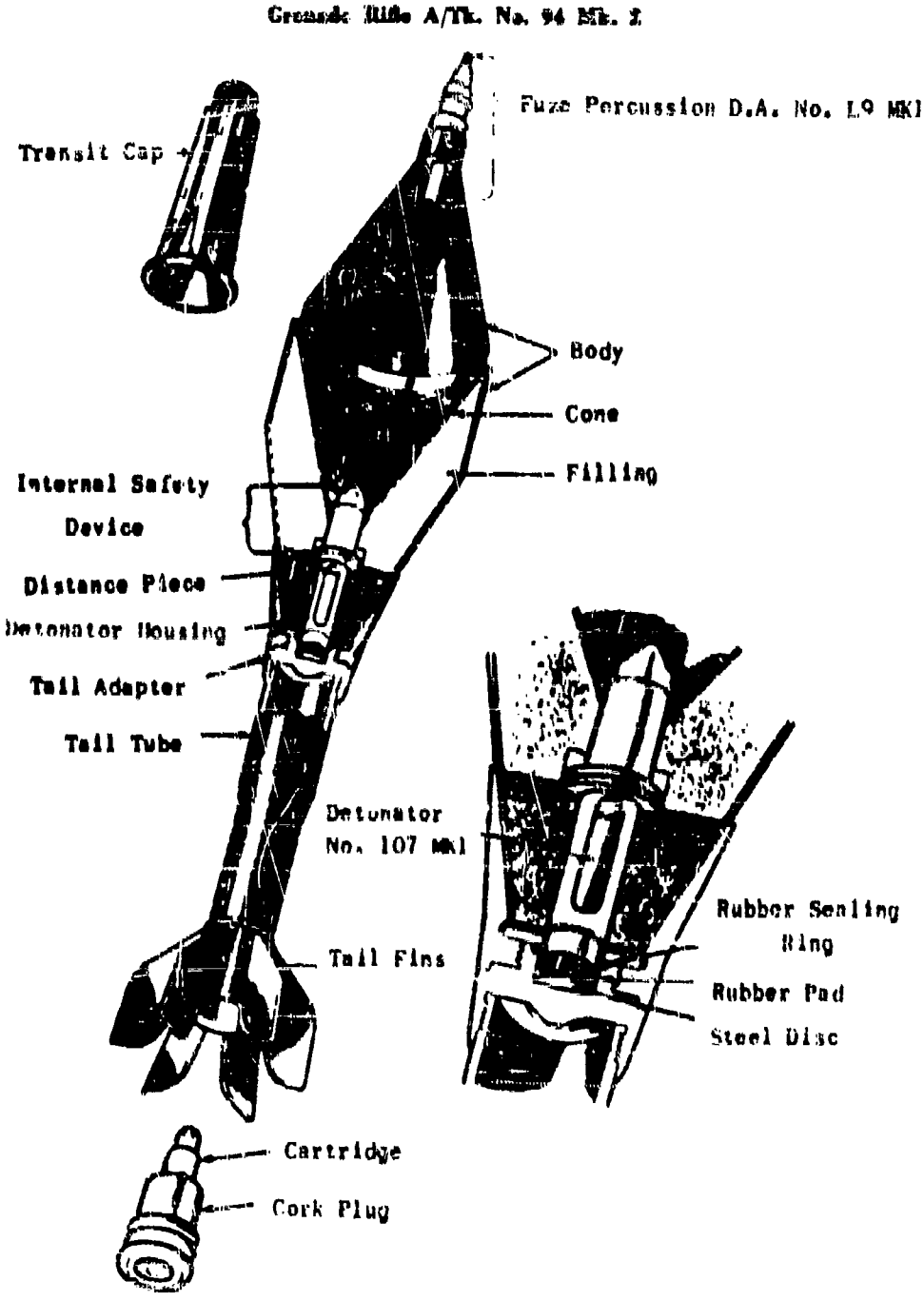

FIG. 16. Energa rifle grenade with percussion fuze

Fuze percussion, D.A., No. L9 Mk. 1

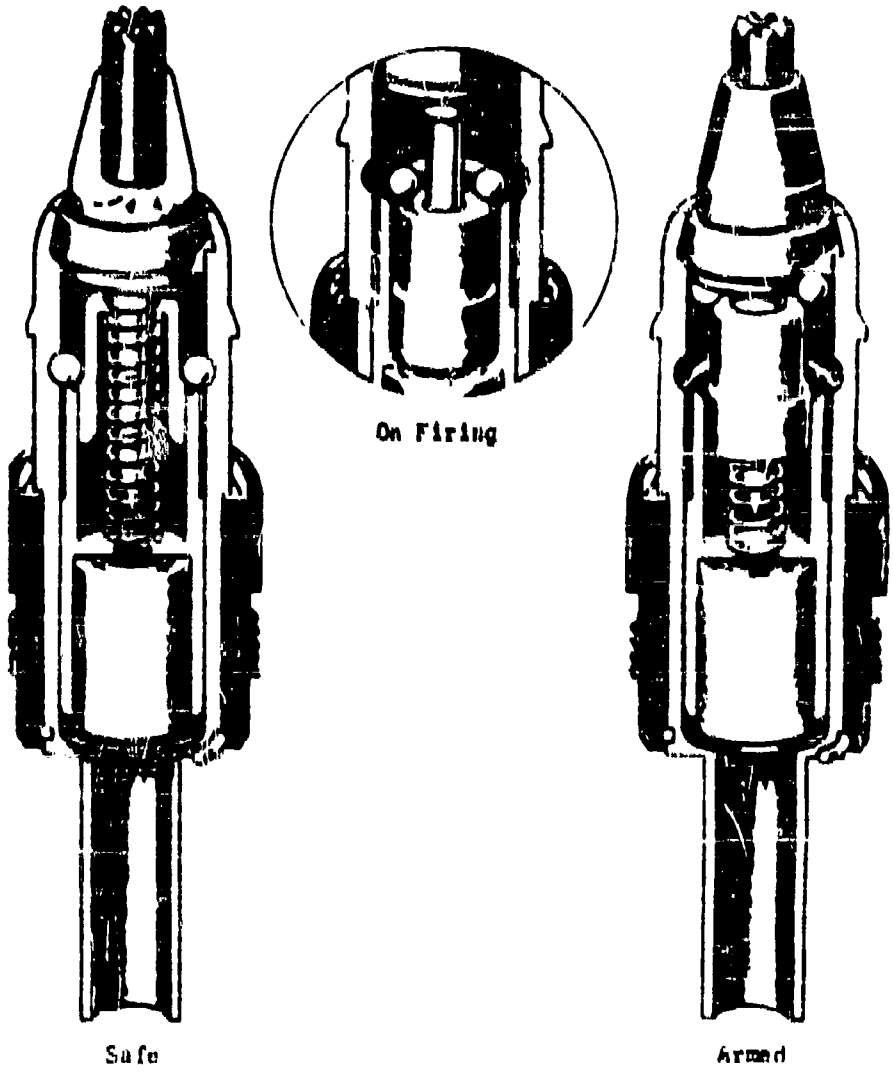

FIG. 17. Percussion fuze - direct action type

Fuze, percussion, D.A., No. 19 Mk. 2

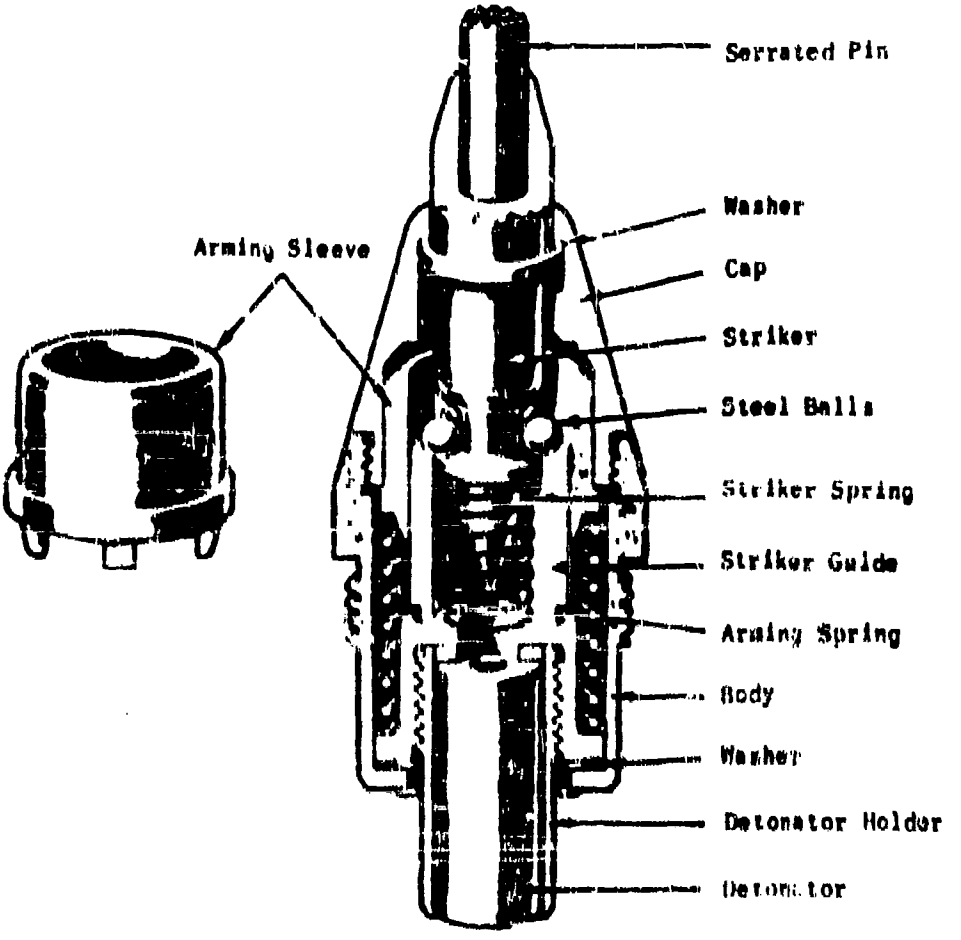

FIG. 15. Percussion fuse - direct and grase action type

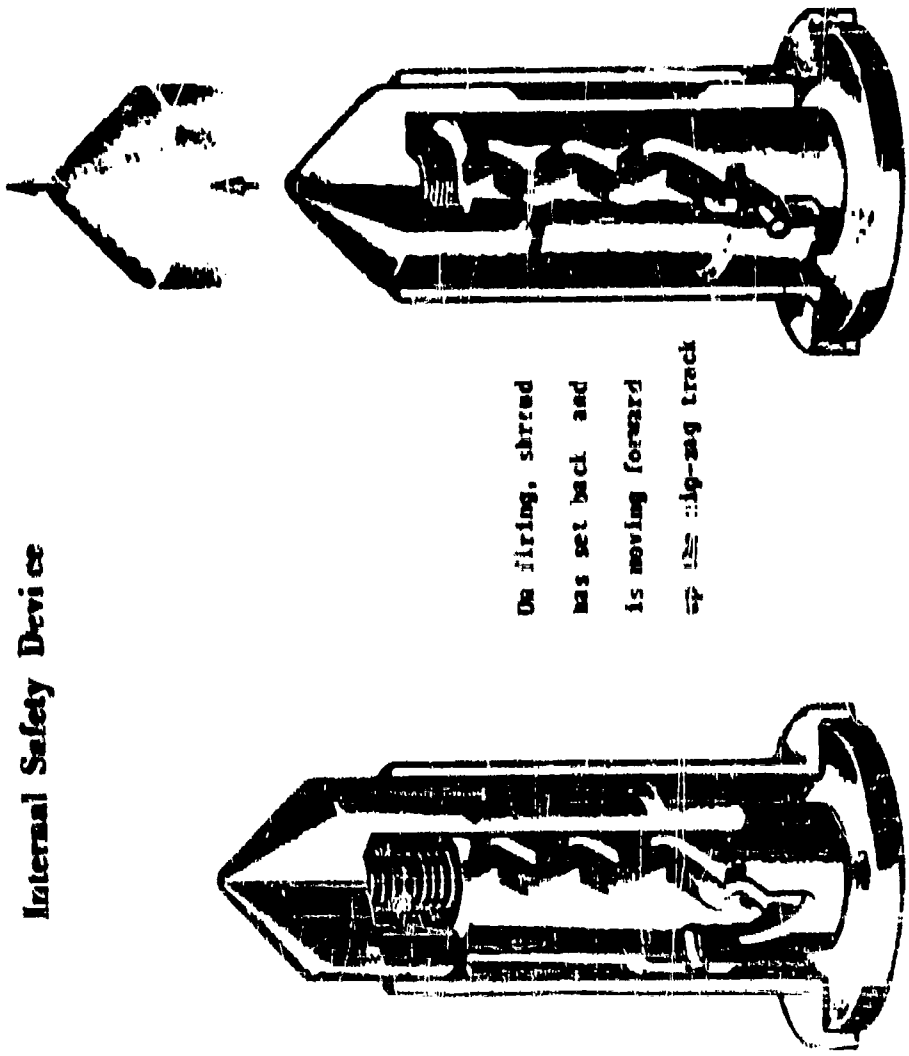

FIG. 19. Internal safety device

channels cut in the central tube. In the safe position the shroud is held by a spring which forces the studs to the dead end of the shorter channel. On setback, the shroud moves rearward against the spring and oscillates about its axis because of the stud engagement with the shorter zig-zag channel. This oscillation similar to the motion of a wheel and pallet escapement adds a time delay to the action of the force and therefore prevents operation on instantaneous shocks. Similarly when the shroud reaches bottom and setback ceases, it is moved back by the spring with a time delay controlled by the longer zig-zag path. When it reaches the end of the track, there is no further constraint and the spring ejects it into the front part of the body clearing the hole for passage of the nose detonator "spit".

CHAPTER VII

THE EFFECT OF ROTATION UPON SHAPED CHARGE JETS

Louis Zernow

Ballistic Research Laboratories
Aberdeen Proving Ground, Maryland

Historical Introduction

Although it was known before 1940 (1) that spin stabilized shaped charge projectiles gave much poorer penetration when fired dynamically than when fired statically, this was attributed for a long time to improper fuze functioning. It was not until 1943 that it became apparent almost simultaneously to the British (2) and the Germans (3) that this deterioration was in fact attributable to rotation. This was verified by both groups (4) (5) by means of static spinning experiments.

In the United States, the Explosive Research Laboratory, and OSRD, (6), (7), (8) took up the study of rotation after the British experiments were reported. They confirmed the British results and extended the work to include experiments to evaluate methods of overcoming and reducing the effects of rotation. Studies of trumpets and hemispheres were carried out by E.R.L. as well as the initial fluted liner experiments.

Following the end of the war, study of the rotation problem was continued by the group at the Carnegie Institute of Technology. In addition to C.I.T., the Firestone Tire and Rubber Company and the Ballistic Research Laboratories are the other two groups of investigators now putting sizeable efforts into the study of the effects of rotation.

The physical effects of rotation were found by the early investigators to consist generally of a "spreading" of the jet observed optically by the Germans (9) using multiple Kerr Cell photography and by the British (10) who fired rotated charges vertically at night. Clark and Fleming (11) were the first to study the effects of rotation by means of flash radiographic observations. Their radiographs of jets from rotated cones and hemispheres confirmed that the physical effects of rotation were dispersion and fragmentation of the jet.

In 1951 the development at the Ballistic Research Laboratories, of the wire driven rotator (12) and the application of improved flash radiographic techniques to 105mm charges (13) made possible the study of the effects of rotation on a scale large enough to show details of the physical effects of rotation upon the jet. It became clear at that time that the deterioration of a copper jet could be followed through several distinct stages as rotational frequency was increased. The evidence at that time was, however, based on single x-ray exposures. Since then the development of a triple-flash X-ray system (14) for studying jets from

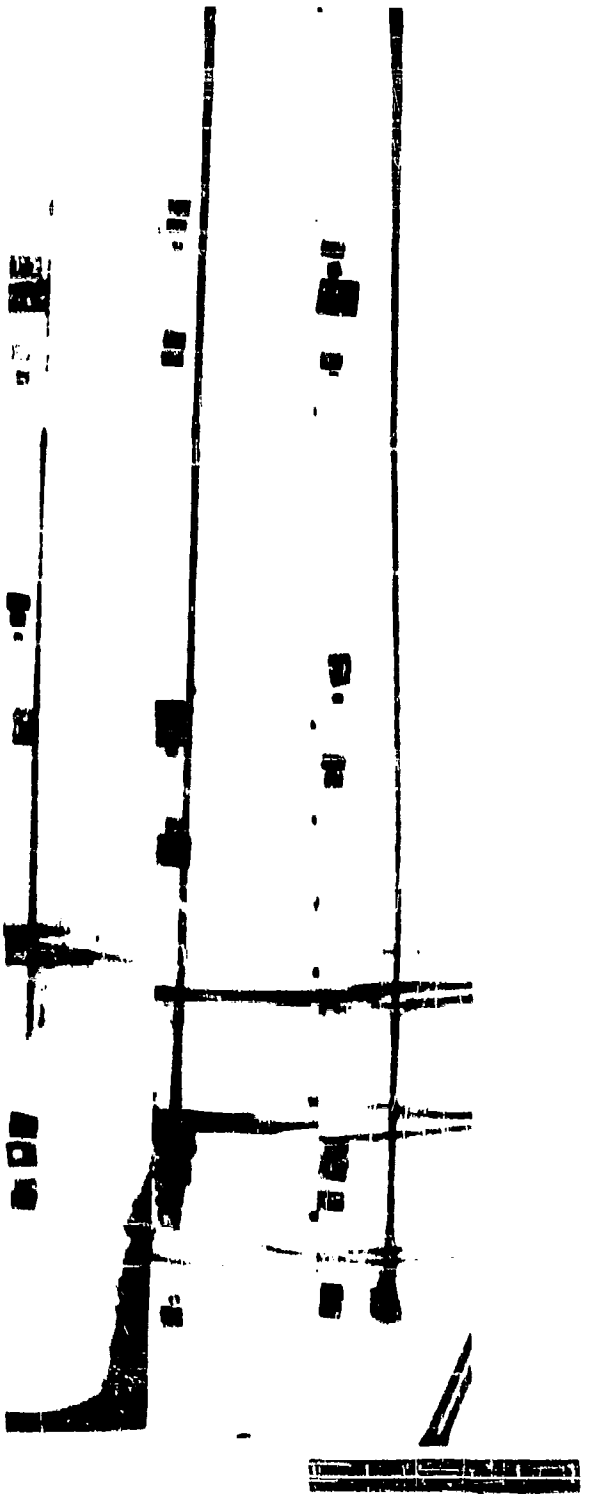

FIG. 1. Radiograph of jet from 105mm copper liner, unrotated

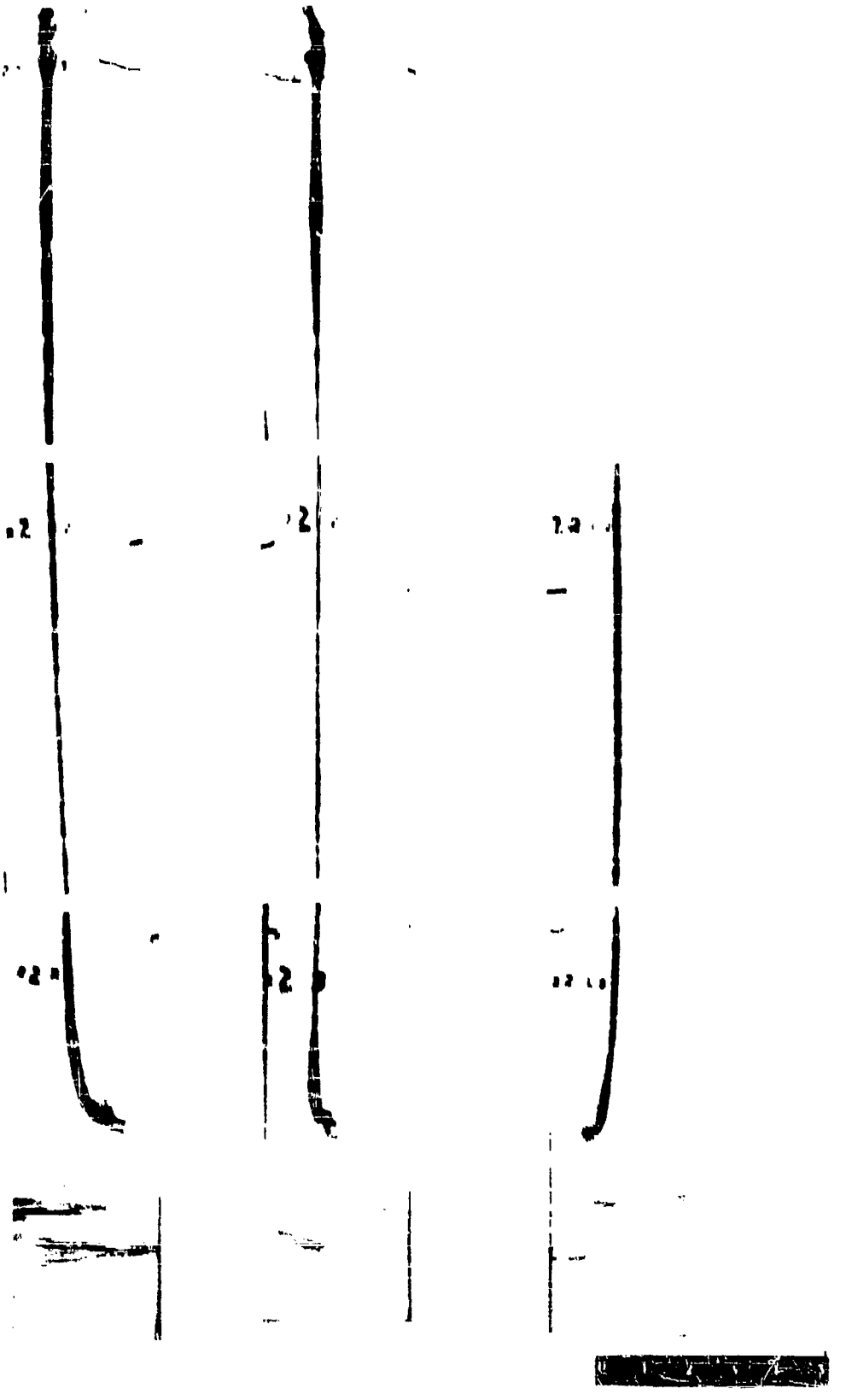

FIG. 2. Radiograph of jet from 105mm copper liner, rotated at 15 rps

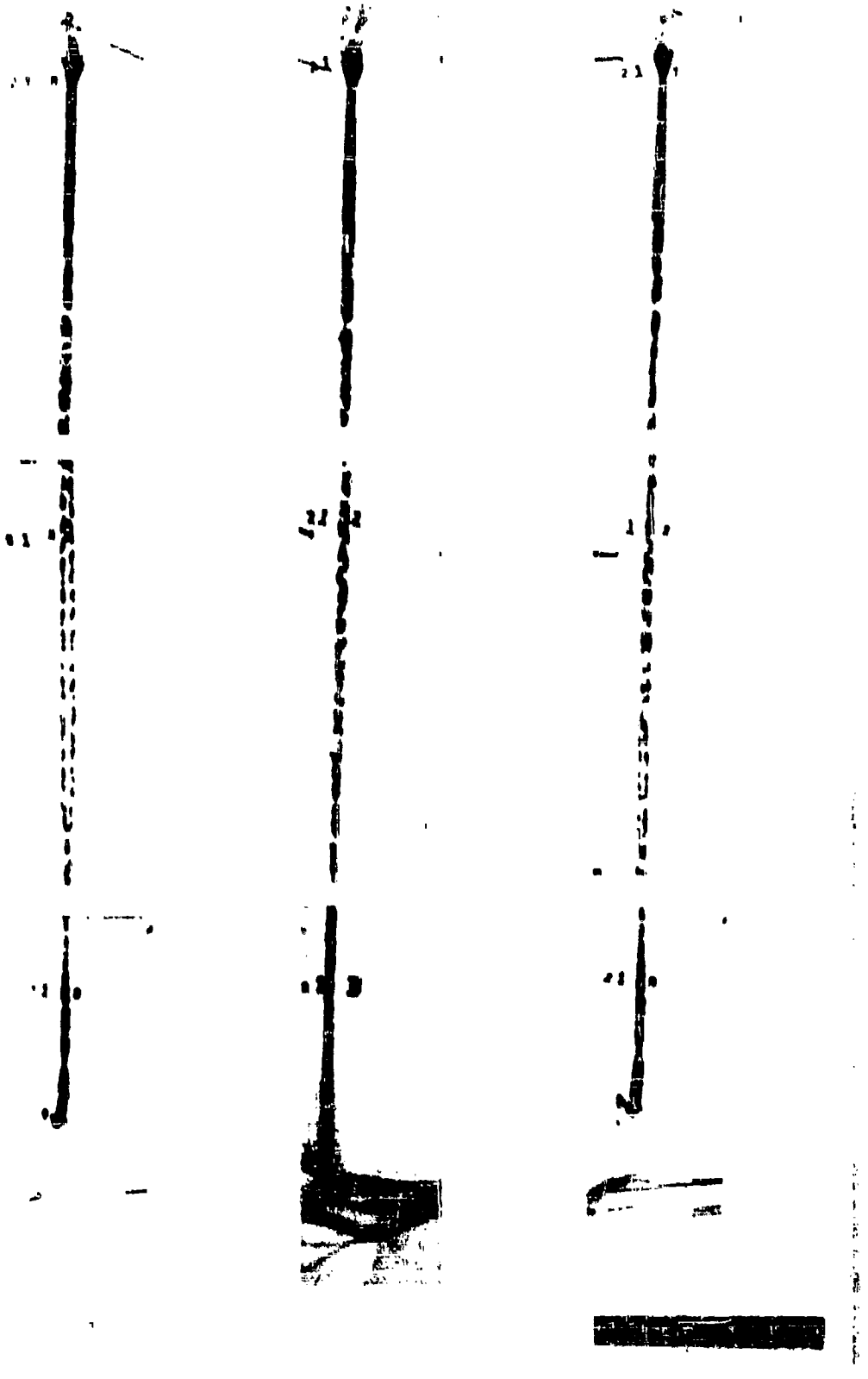

FIG. 3. Radiograph of jet from 105mm copper liner, rotated at 30 rps

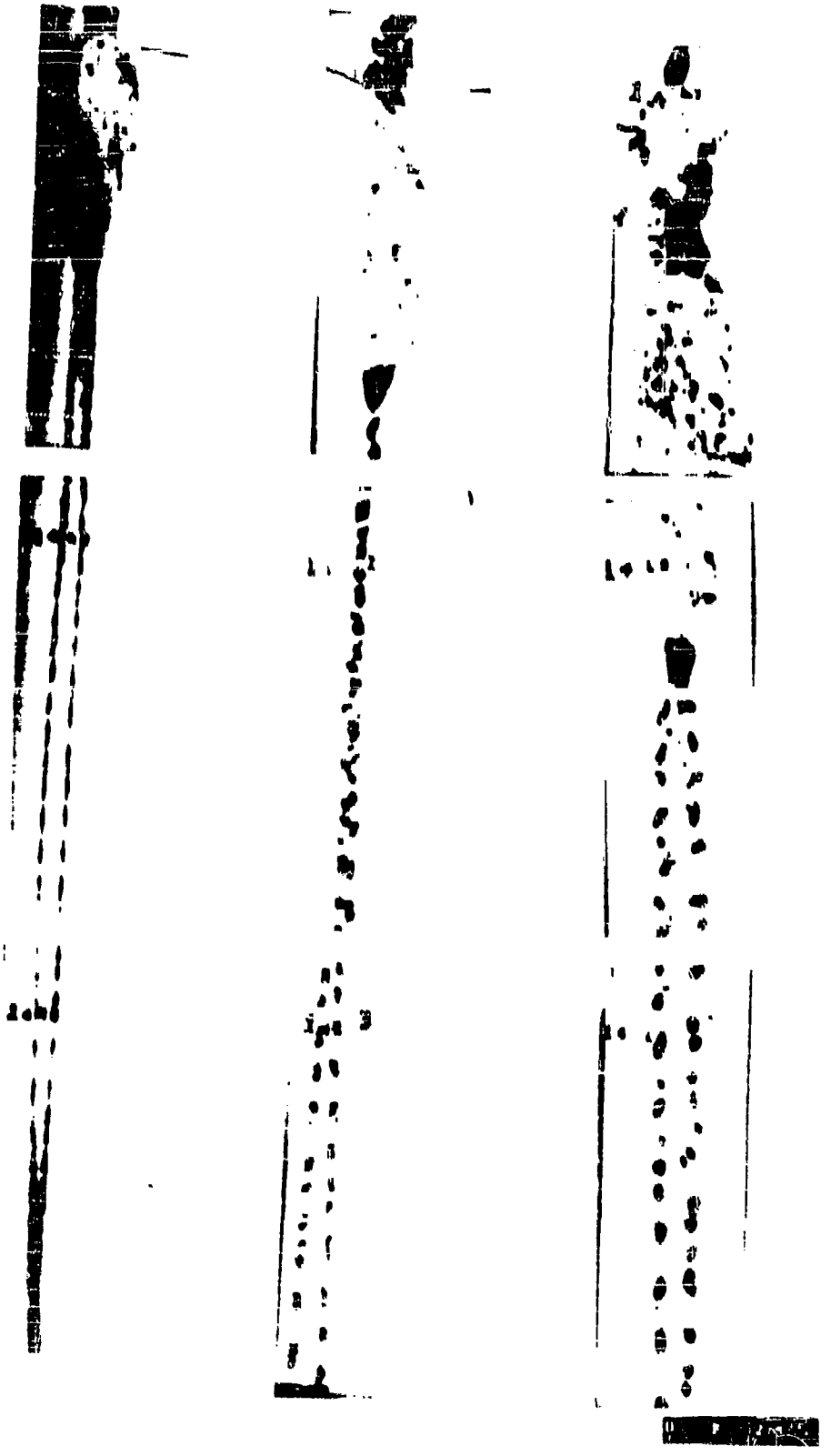

FIG. 4. Radiograph of jet from 105mm copper liner, rotated at 45 rps

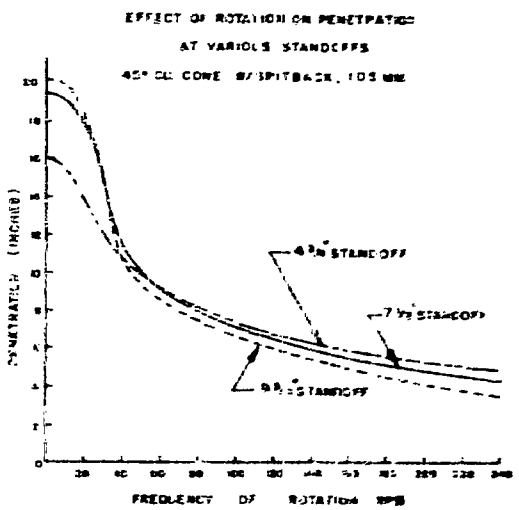

FIGURE 5

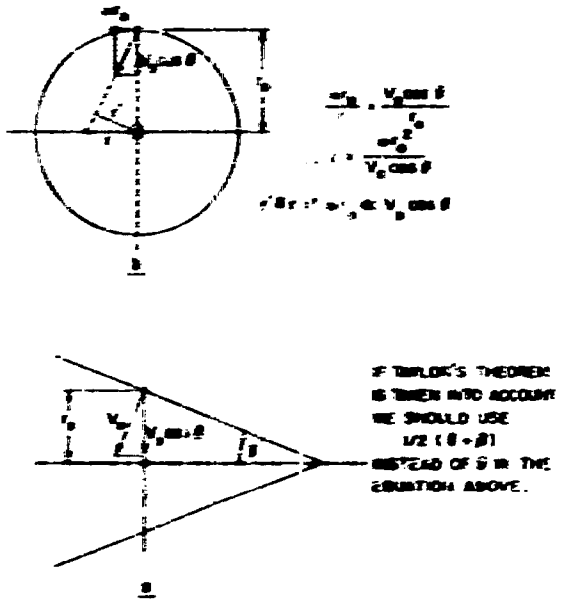

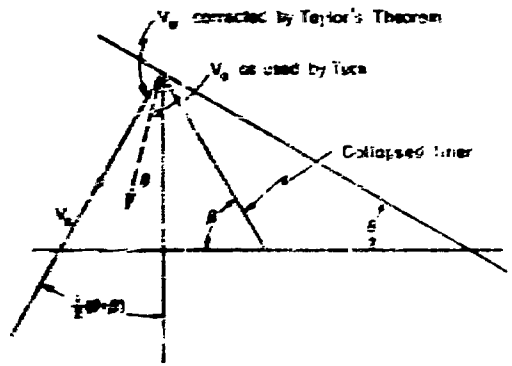

FIG. 6
DERIVATION OF TUCK'S
RELATIONSHIP FOR MASS

large rotated charges has made possible an extension of the previous work which has further clarified the details of the deterioration process. The sequence of events as the rotational frequency increases is shown in Figures 1, 2, 3, 4 which show the effects of increasing rotation upon the jet from a 105mm copper liner. The deterioration process can be broken down into the following distinct steps:

1. The jet which is normally continuous when unrotated, begins to break up into separate pieces along its length.

2. As the rotational frequency increases, the cross section of the jet starts to deviate more and more from a uniform circular shape and shows evidence of deformation into a ribbon-like structure.

3. There is finally a definite bifurcation or separation of the jet into two essentially parallel jets with each jet broken into separate pieces. When the bifurcation first appears, generally the two portions of the bifurcated jet seem to lie in a plane of bifurcation.

4. Increasing rotational frequency causes the plane of bifurcation to be distorted into a helical surface.

The bifurcation in the jet appears to be associated with a critical frequency which depends on the caliber. Thus, bifurcations have not been seen in jets from 105mm charges rotated at 15 rps, whereas all jets from 105mm charges rotated at 45 rps show bifurcation as do most jets from 105mm charges rotated at 30 rps.

The incidence of bifurcation is clearly associated with the steepening portion of the penetration fall-off curves. (Figure 5) Finally the plateau region associated with the highest spin frequencies indicates that the later modifications of the bifurcation process contribute very little to further reduction in penetration. It was originally conjectured (15) that the original bifurcation was perhaps followed by bifurcation of each of the new portions of the jet. This has not been ruled out, but the observations on the target plate (15) upon which this was based can also be explained by the distortion of the plane of bifurcation into a helical surface.

Theory

It was pointed out by Tuck in 1943 (2) that rotation could result in a malformed jet. Rotation of the liner would cause any element of the collapsing liner to miss the axis (Figure 6) of the cone by an amount

$$r' \cong \frac{\omega r_o^2}{v_o \cos \theta} \quad *$$

*This expression would be more accurately written $r' \cong \frac{\omega r_o^2}{v_o \cos\left(\frac{\theta + \beta}{2}\right)}$ cf. Figure 6.

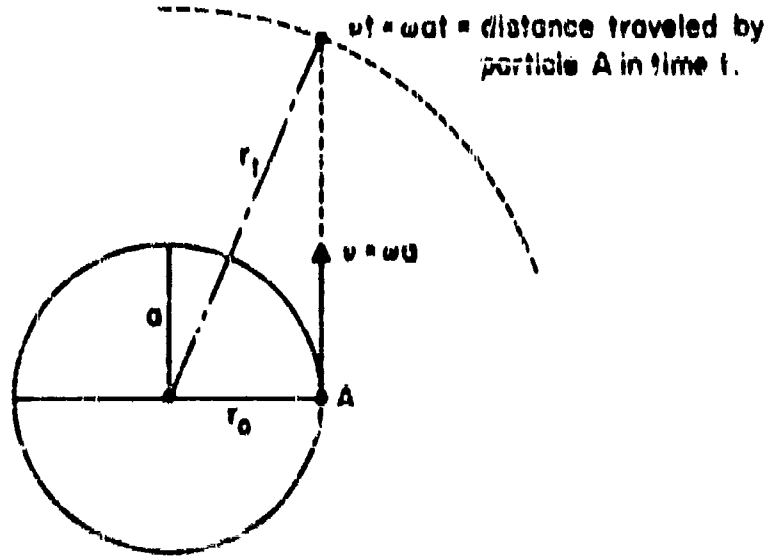

$$r_t^2 = r_o^2 + \omega^2 a^2 t^2$$

r_t = radius of jet at time t

r_o = initial radius of jet

FIGURE 7

VARIATION IN CROSS SECTION OF A DISC SHAPED SYSTEM OF NON-INTERACTING PARTICLES STARTED UNDER INITIAL ROTATION AT ω RADIANS PER SECOND.

where r' = the miss distance $\cong r$.

r_o = the radial distance of the liner element from the axis of the cone.

v_o = the collapse velocity of the liner element.

θ = the semi-angle of the cone.

ω = the angular velocity of the liner in radians/second.

This would result in a hollow jet. This malformation could cause a drastic decrease in penetration if r'became large enough. Thus on this basis, Birkhoff (16) estimated that a 3" dia. liner would show appreciable deterioration due to this malformation at 100 rps.

Birkhoff, using a different approach which neglects initial malformation of the jet, has estimated the decrease in the penetration from a given element of a properly formed jet due to the increase in cross sectional area resulting from the expansion of the jet due to rotation. A very useful discussion of Birkhoff's work has been given by Shofield (1). On the assumption of a fluid jet rotating initially with an angular velocity ω radians/second he finds that the cross sectional area (of the jet element) will grow with time according to the relation

$$A_t = A_o + \pi\omega^2 a^2 t^2 = A_o (1 + \omega^2 t^2).$$

where A_o = initial cross sectional area of the jet.

A_t = cross sectional area at time t.

a = initial radius of jet.

ω = initial angular velocity in radians/second.

t = time in seconds from start of jet spread.

This relationship is also valid for a disc shaped system of non-interacting particles and can readily be derived from the construction in Figure 7. The increase in cross sectional area is equivalent to a decrease in the average density of the particular jet element. This results according to penetration theory, in a decreased penetration by that jet element, since the penetration p is proportional to $\sqrt{\rho_j}$. Therefore, if the length of the element of jet is assumed to be unaffected by the rotation then

$\sqrt{\rho_j}$ is proportional to $\frac{1}{\sqrt{A_t}}$ and

the penetration at time t will be

$$p_t = \frac{\sqrt{A_o}}{\sqrt{A_t}} p_o$$

$$P_t = \sqrt{\frac{\pi a^2}{\pi a^2 + \pi a^2 \omega^2 t^2}}\ P_o$$

$$\frac{P_t}{P_o} = \frac{1}{\sqrt{1 + \omega^2 t^2}}$$

The elapsed time t, measured from the formation of a jet element and the start of jet spreading to final impact of that jet element on the target, is given by S/V where

S = the standoff for the particular jet element.

V = the velocity of the particular jet element assumed to remain constant.

Shofield, following Birkhoff, defines a constant, ω_o characteristic of a particular charge and standoff for which S and V for a particular jet element are thus defined.

Therefore letting

$$t = \frac{1}{\omega_o}$$

the final dimensionless expression obtained by Birkhoff becomes

$$\frac{P_t}{P_o} = \sqrt{\frac{1}{1 + \left(\frac{\omega}{\omega_o}\right)^2}}$$

Experimental data relating total penetration and rotation can be very readily fitted (17) by means of a Birkhoff equation. It was first specifically pointed out by Litchfield, Beitel and Eichelberger (18) that since the Birkhoff equation was derived for a given jet element, it is initially rather surprising that the total penetration data should be representable by such a functional form, since ω_o is clearly not a constant for all jet elements of a given conical liner undergoing collapse. They give the expression* for the "constant" ω_o, for a given jet element in terms of charge parameters as follows:

$$\omega_o = \frac{\tau v_j \sin^2 \beta/2}{RS}$$

*Because of the fundamental importance of this relationship, its derivation by Beitel of the Carnegie Institute of Technology group is given in Appendix I.

where

τ = the thickness of the element of liner.

v_j = the velocity of the element of jet coming through that element of liner.

β = the collapse angle.

R = radial distance of original liner element from cone axis.

S = distance traveled by the jet from point of formation to point of impact on the target.

Since ω_o is a function of the position of the jet element along the jet it is clear that the total penetration will have to be obtained by integrating the differential contributions due to elements with different characteristic ω_o's. Hence, in general (e.g. on the basis of steady-state theory) the integrated result will not have the simple form of the Birkhoff equation.

The C.I.T. workers have presented plausibility arguments (18) for the approximate constancy of ω_o on the basis of non-steady-state considerations in the following manner: For conical liners, v_j decreases as R increases from the apex to the base of the cone. Therefore $\frac{v_j}{R}$ should decrease, slowly at first and then very rapidly. Simultaneously $\sin^2 \beta/2$ should increase slowly at first and then very rapidly as one moves from the apex to the base. Thus, the compensatory variation of these two factors in the ω_o expression will tend to reduce the range of variation of ω_o over the liner in the case of non-steady collapse.

The fact that the simple Birkhoff equation actually does fit the observed data, is considered as evidence in support of the idea that ω_o does remain nearly constant.

SCALING UNDER ROTATION

Birkhoff has proposed (16) that for scaling comparisons of the effects of rotation to be applied to geometrically similar shaped charges, the correct measure of relative spin is ω d, where

ω = angular velocity of the projectile

d = cone diameter

and that a proper correlation of scaled experimental data would require the comparison of dimensionless variables like p/d and τ/d, where

$\frac{p}{d}$ = penetration in cone diameters

$\frac{\tau}{d}$ = thickness of liner in cone diameters

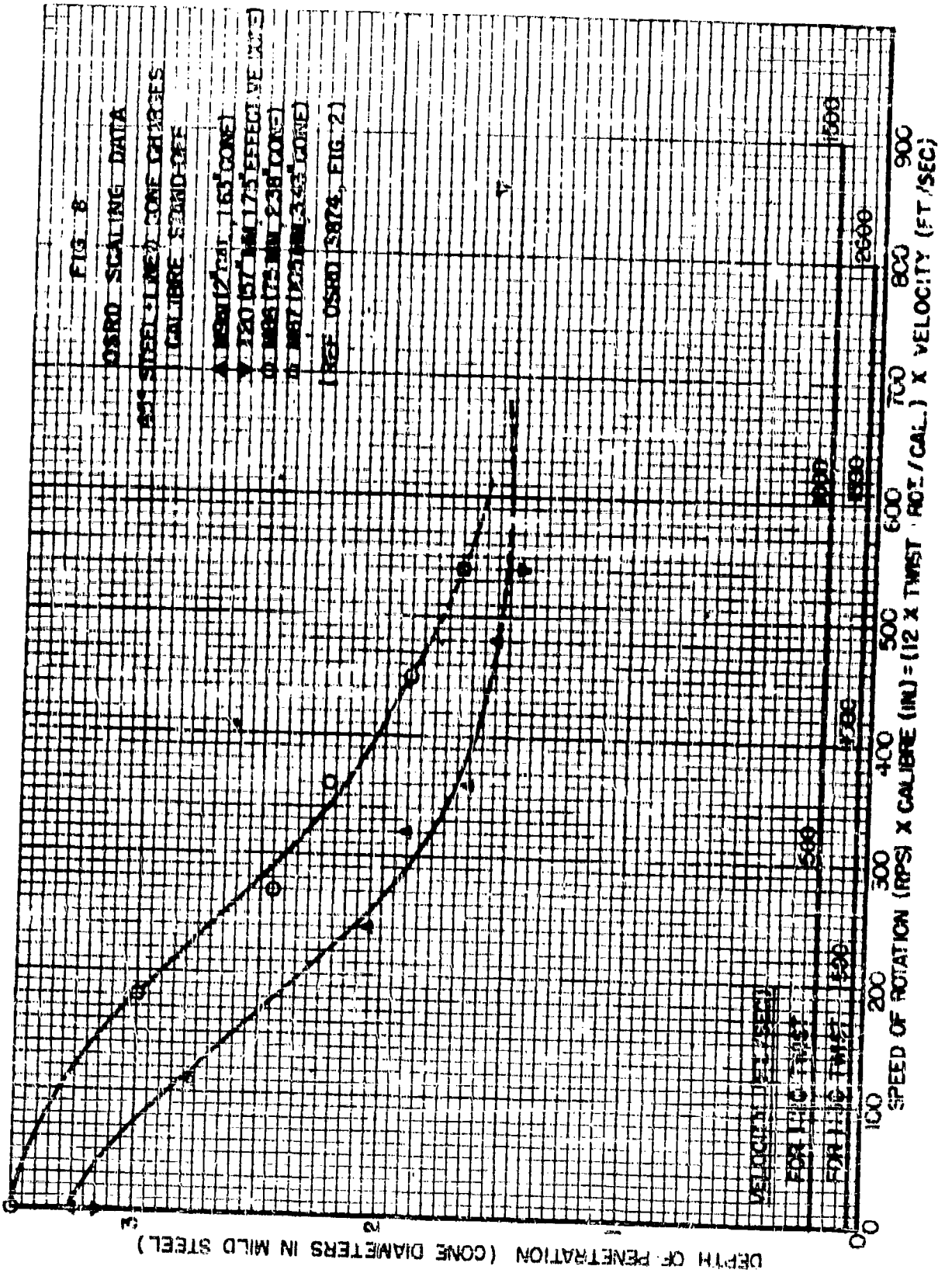
FIG. 8
OSRD SCALING DATA
SPEED OF ROTATION (RPS) X CALIBRE (IN.) = (12 X TWIST (CAL.)) X VELOCITY (FT/SEC)
DEPTH OF PENETRATION (CONE DIAMETERS IN MILD STEEL)
0
100
200
300
400
500
600
700
800
900
1000
1500
2000
2500

and the properly scaled relative spin, ωa. For an actual projectile ωd can be conveniently obtained from the relation

$$\omega D = v/n$$

in which

D = Kd, is the caliber of the projectile, K, the ratio of caliber to cone diameter being known for any given projectile

v = the muzzle velocity of the projectile

1/n = twist of rifling in turns/caliber e. g. 1/25

Thus, if ω is expressed in rev/sec., D in inches, and v in feet per second, then ωD (rps x in) = $12 \times v \times \frac{1}{n}$

Birkhoff (16) summarizes the arguments for scaling under the transformations

$X = \lambda x$ where λ = Scale Factor

$T = \lambda t$ X, x = position coordinates

$V = v$ T, t = time coordinates

V, v = velocities

The assumptions that support such an argument are:

a. The liner behaves like a fluid.

b. Thermal conduction and radiation are of minor importance.

c. Stresses do not depend on strain rates but only on strains.

Experimental evidence obtained by OSRD with 45° steel liners (7) generally favors this viewpoint. Figure 8 illustrates the OSRD results.

The disagreement evident in Figure 8 between the scaled penetrations at 0 rps as well as over the entire range of ωd, probably reflects, among other factors, the lack of geometrical scaling among the projectiles compared. It is evident that if p/p_o were plotted as the ordinate, instead of p, the agreement between the results for different sizes would be better than that shown in Figure 8. Hence, the similarity of the two curves suggests that ωd is indeed an appropriate scaling parameter.

Deviations which occur are at least in part attributable to the fact that comparisons in some cases were made with charges which were not properly scaled geometrically. There is a possibility, however, that scale effects,

such as greater instability of the jet from a thinner liner* as well as strain rate effects** may also contribute to the deviations observed in some experiments. More carefully designed experiments are needed to establish the scaling facts from the experimental viewpoint and improvements in the "art of scaling" may ultimately bring the experiments into complete agreement with the theoretical predictions. For the present the scaling correlations suggested by Birkhoff offer the safest guide.

An empirical scaling correlation has been proposed by Winn, (19) which does not use the Birkhoff scaling relation, but instead assumes the penetration law

$$L = K \omega \rho_o$$

where

L = relative loss in penetration $= 1 - \frac{p_\omega}{p_o}$

ω = rotational frequency

K = proportionality constant

p_o = penetration when $\omega = 0$

p_ω = penetration when $\omega = \omega$

This leads to the expression

$$1 - \frac{p_\omega}{p_o} = K \omega p_o$$

$$\text{or } (p_o - p_\omega) = K \omega p_o^2 \quad \therefore \quad p_\omega = p_o (1 - K \omega p_o)$$

Thus since $p_o - p_\omega$ is the actual loss in penetration this means that the assumption is being made that the actual loss in penetration at any spin rate is proportional to the square of the unrotated penetration p_o. On this basis there is drawn a set of curves of the form

$$p\omega = p_o (1 - K\omega p_o)$$

which relate the rotated penetration p_ω to the unrotated penetration p_o.

*There is scattered evidence that indicates a decreasing optimum standoff (in cone diameters) for smaller cones as well as incomplete evidence from flash radiographs that suggests the possibility of relatively earlier break-up for smaller cones. These notions should not presently be considered as firmly established. They do, however, warrant additional careful investigation.

**Since the tip and tail velocities of a jet should be independent of the caliber the strain rate($\Delta v/L$) at a given jet length, should vary inversely with the caliber, because the jet length should vary directly with the caliber.

In comparing penetrations from rotated 57mm cones with penetrations from 105mm cones, it is found that the proposed correlation is invalid beyond 45 rps so that predictions must be limited to this range of spin frequencies.

Unfortunately, Winn's 57mm data and 105mm data were not obtained at the same scaled standoff, the 57mm data having been obtained at 3.5 cone diameters standoff and the 105mm data at about 2.2 cone diameters. Therefore the ω d scaling relationship should not necessarily be obeyed, and indeed it is not, as can be seen from Figure 9.

A more rational scaling procedure would involve starting with the Birkhoff equation

$$\frac{p_\omega}{p_o} = \frac{1}{\sqrt{1 + \left(\frac{\omega}{\omega_o}\right)^2}}$$

and since

$$\omega_o = \frac{\tau v_j \sin^2 \beta/2}{R\delta}$$

ω_o should vary inversely with the cone diameter since the thickness τ, the radius R and the elemental standoff δ should all transform according to

$$X = \lambda x$$

whereas v_j is unchanged. Hence the functional form for ω_o as a function of the scale factor λ should be

$$\omega_o(\lambda) = \frac{\omega_o}{\lambda}$$

Thus for a 57mm cone, the value of ω_o should be 2 times the value for a cone with twice the 57mm diameter if their penetrations are compared at the same scaled standoff under rotation.

All the penetration rotation data, if it scales should then be correlated with a single expression of the form

$$\frac{p_\omega}{p_o} = \frac{1}{\sqrt{1 + \left(\frac{\omega_d}{\omega_o^*}\right)^2}}$$

where d = cone diameter

ω_o^* = the value of ω_o for a cone of unit diameter under the prescribed standoff conditions.

This expression contains the scaling relationship in the form required by theory.

FIGURE 9

CURVES ILLUSTRATING NON-SCALING ROTATION DATA WHICH MAY BE ATTRIBUTABLE TO FAILURE TO SCALE STANDOFF

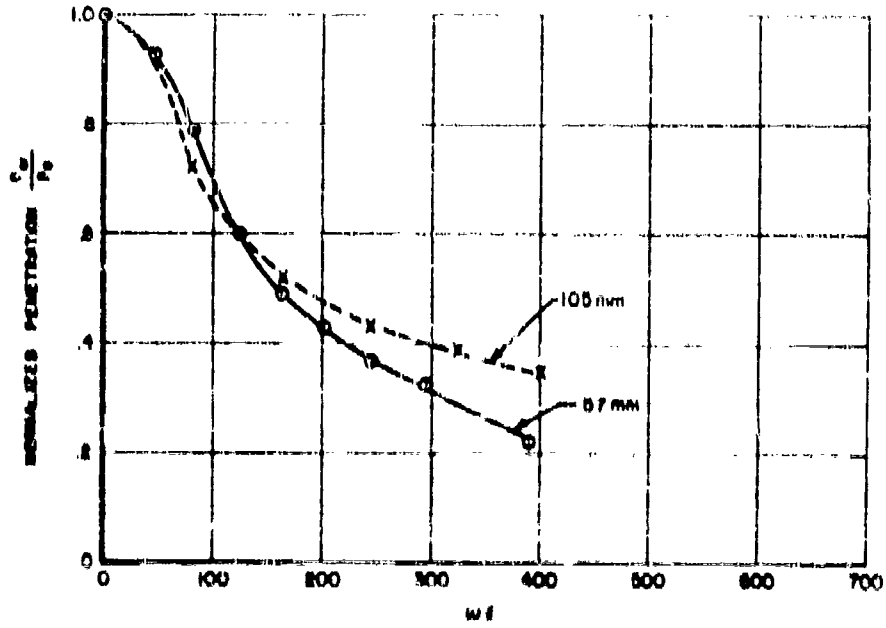

FIG 10

FIRESTONE TIRE & RUBBER CO SCALING DATA

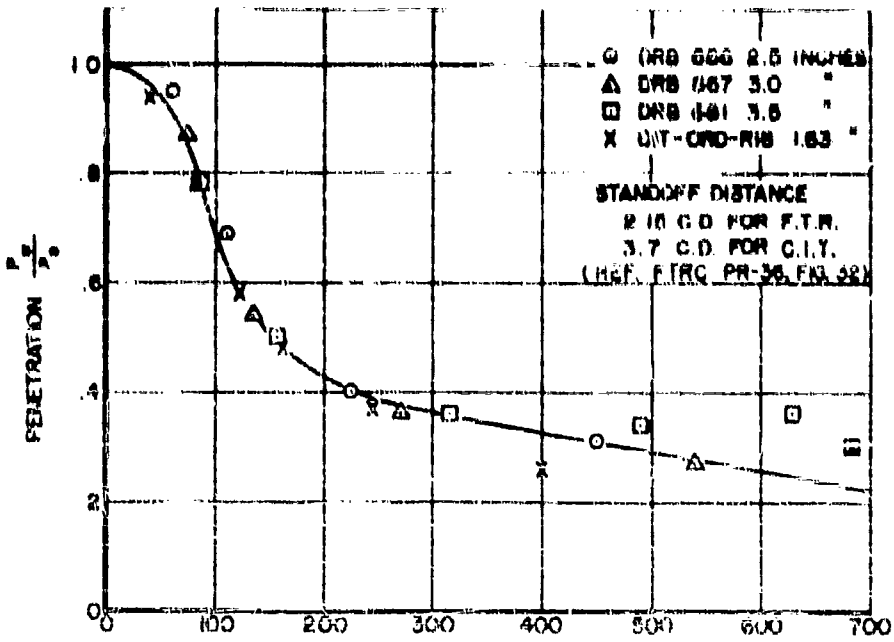

(REV/SEC X INCHES)

It is apparent that one should not expect scaling under rotation to follow if the unrotated penetrations do not scale. Hence in order for the scaling relationship to be applicable at all standoffs it is necessary for the unrotated dimensionless standoff penetration curves, p/d vs S/d to be identical for all calibers to be compared. It may be considered that failure to meet this criterion is an indication either that the geometrical scaling has been improperly carried out, or that factors such as those previously mentioned (thickness and strain rate effects) are preventing the proper scaling.

Another point of interest is the apparent failure of the simple ω d scaling to adequately correlate the data from liners of widely different sizes at the highest rotational frequencies. The apparent failure of the 57mm and 105mm correlations of p_ω/p_o vs ωd at the high frequency end is apparent in Figure 9. How much of this is due to standoff differences is not presently known.

Scaling data on copper liners have been obtained most recently by Firestone* over the fairly narrow range of cone diameters (2D) from 2.5" to 3.5" and the data when plotted as p_ω/p_o vs vd (where ν = rotational frequency which is $\frac{\omega}{2\pi}$) seem to fit the ωd scaling law quite well except possibly for the very high values of ν, in which region the original penetration data for the 3.5" charge behaves strangely. Their results are shown in Figure 10 . When compared with the results for the 57mm size which are to be found in BRL 837 on p. 340, it is again apparent that the results suggest a possible failure of the ω d scaling law at the very high spin frequencies.

If the apparent deviation from the ω d scaling law at high values of ω d turns out to be real, it is believed that an explanation for this will be found in the observations which have been made on the details of the deterioration process. Experiments aimed at ascertaining the scaling relations in the regions in question are being carried out but have not yet been completed. In addition, experiments involving studies of effects of liner thickness upon jet stability will be of interest in interpreting these results of rotation experiments, since if jet break-up was influenced by the liner thickness independently of size, earlier jet break-up of small liners could be contributing to the anomalous results.

In summary, for the designer, the use of ω d as a scaling variable for predicting the results of rotation upon penetration appears to be the best available basis over the range 0 - 100 rps and 57mm to 105mm calibers. For higher spin frequencies it is still the best guide, but experimental verifications are recommended as a check on predictions. It is expected that experiments currently under way will eliminate the uncertainities that exist for the highest values of ω d.

*The author is grateful to Dr. Hugh Winn of the Firestone Tire and Rubber Co. for making his data available prior to publication.

THE EFFECT OF CONE ANGLE UPON PENETRATION UNDER ROTATION

Theory.

An analysis of the effect of cone angle can be attempted in terms of the parameter ω_o, by trying to determine the effect of cone angle upon ω_o. Thus by differentiating ω_o with respect to θ

$$\omega_o = \frac{\tau v_j \sin^2 \beta/2}{RS}$$

and hence if τ remains constant

$$\frac{d\omega_o}{d\theta} = \frac{\tau RS \left[v_j \sin \beta/2 \cos \beta/2 \frac{d\beta}{d\theta} + \sin^2 \beta/2 \frac{dv_j}{d\theta}\right] - \tau v_j \sin^2 \beta/2 \left[R \frac{dS}{d\theta} + S \frac{dR}{d\theta}\right]}{R^2 S^2}$$

It would be necessary to evaluate $\frac{d\beta}{d\theta}$, $\frac{dv_j}{d\theta}$, $\frac{dS}{d\theta}$ and $\frac{dR}{d\theta}$ for corresponding elements on the jets being compared. It is very difficult to do this quantitatively but the following qualitative analysis can be made.

1. As θ decreases v_j increases.

2. As θ decreases β decreases.

It will therefore be assumed that to a first order approximation the numerator $\tau v_j \sin^2 \beta/2$ remains constant because of the compensatory variation of the last two factors. Furthermore

3. As θ decreases R remains approximately constant.

4. As θ decreases S increases.

Therefore the denominator of ω_o increases with decreasing θ.

The overall effect is then a decrease in ω_o as θ decreases. This would lead one to expect an increased sensitivity of small angle cones to rotational deterioration. This is contrary to the prediction of Tuck (2) on the basis that the miss distance $x' = \frac{\omega r_o^2}{v_o \cos \theta}$, is smaller if θ is smaller.

However, a more careful analysis of Tuck's formula shows that although x' does indeed become smaller for decreasing θ, the smaller cone angle results in a greater effective standoff for the jet element from the point of formation on the axis to final target impact. This allows correspondingly greater deviation radially at any given point along the axis. Therefore because the collision point for jet elements from small angle cones is nearer the apex of the cone, it suffers a smaller Tuck type malformation, but the same jet element after formation must

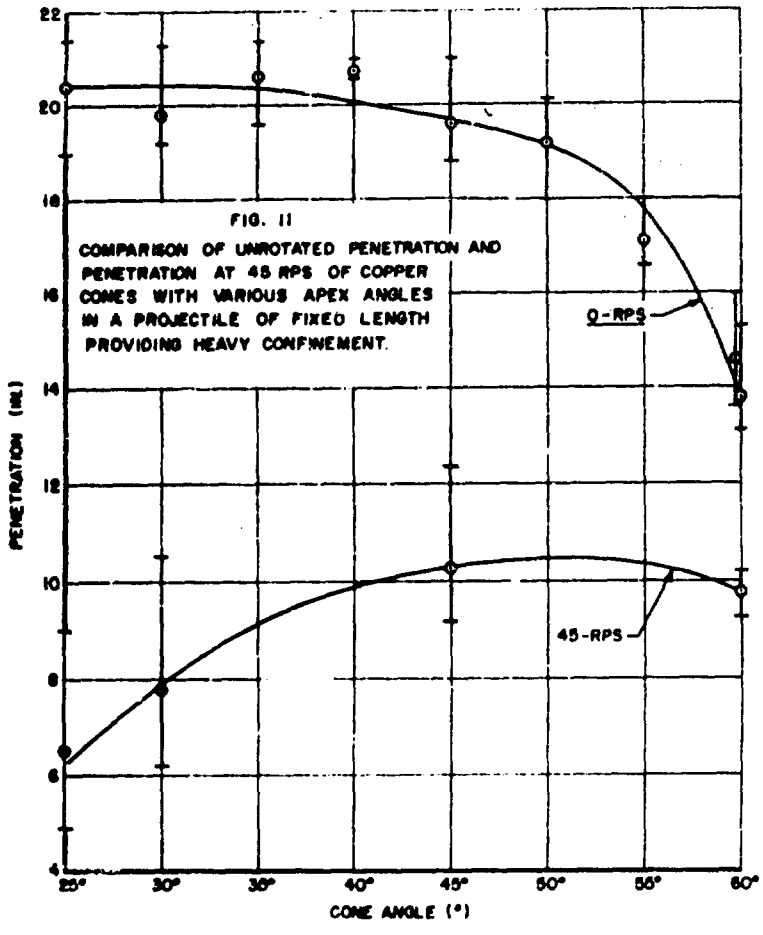

FIG. 11

COMPARISON OF UNROTATED PENETRATION AND PENETRATION AT 45 RPS OF COPPER CONES WITH VARIOUS APEX ANGLES IN A PROJECTILE OF FIXED LENGTH PROVIDING HEAVY CONFINEMENT.

FIG 12

APEX ANGLE OF THE CONE vs. PERCENTAGE LOSS OF PENETRATION AT 45 RPS

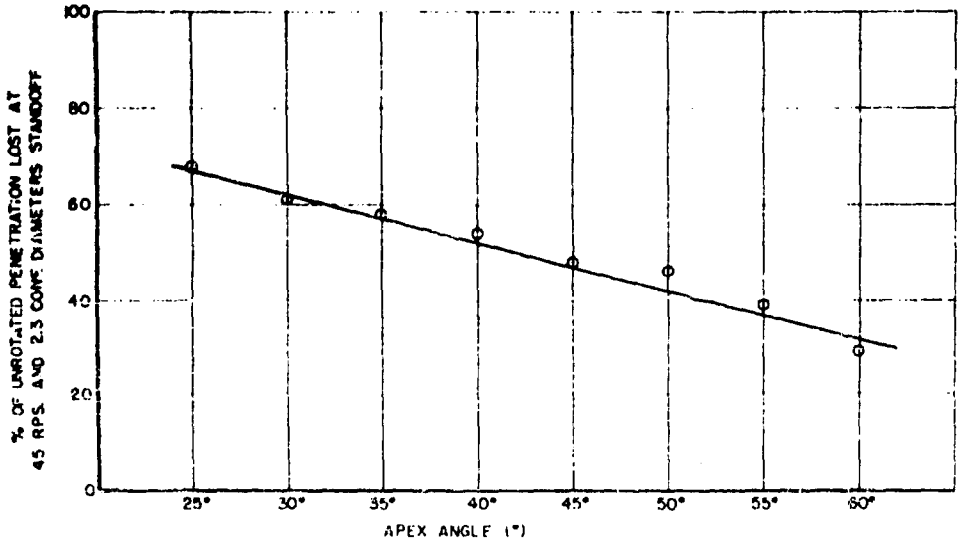

travel a greater distance to target impact for the same reason, and hence suffers greater radial spread after formation. Hence the conclusion drawn from Tuck's equation seems more uncertain than that drawn from considerations of ω_o. At any rate, considerations of the effect of θ on ω_o lead to the expectation that small angle cones will be more sensitive to rotation.

Experimental Results

The experimental data obtained during the war by OSRD (6), on the effects of cone angle are not easy to interpret because of large experimental dispersions. However, the general conclusions drawn by their investigators are essentially as follows:

1. At short standoff the larger angle liners show little deterioration due to rotation. However, since their unrotated penetration is relatively poor this is of little practical value.

2. Because of the increased effective standoff (due to the increased cone height) of a small angle cone, it is more seriously affected at a given external standoff and its penetration is therefore not appreciably better than that of a large angle cone (6).

These conclusions are unfortunately not as specific as would be desired by a designer. Additional experimental data which has been obtained at the Ballistic Research Laboratories using 105mm charges of a given fixed height at a standoff of 7 1/2" which is near the common built-in standoffs for ammunition (~2.3 cone diameters) are shown plotted in Figures 11 and 12. In these curves comparisons are made of the unrotated penetration and the penetration at 45 rps, as a function of cone angle. The results within the range of variables so far explored clearly indicate an increased sensitivity of small angle cones to deterioration by rotation. From the practical viewpoint of the designer, the best cone angle from these experiments at 45 rps appears to be about 45°, even though the smaller cone angles gave better unrotated performance and the larger cone angles showed reduced sensitivity to rotation. These results are consistent with the crude analysis in this section. However, caution must be used in extrapolating to other conditions. The experiments which are being continued will cover a much larger range of the variables ω, and the standoff for various cone angles.

In summary, the designer can expect to find small angle cones more sensitive to rotational deterioration than large angle cones under standoff conditions normally existing for ammunition. There is not sufficient good information on the cone angle effect at large standoffs.

THE EFFECT OF LINER THICKNESS ON PENETRATION UNDER ROTATION

Theory

For a given liner diameter and standoff, the liner thickness enters the expression for ω_o in the numerator, i.e., $\omega_o = \frac{\tau v_j \sin^2 \beta/2}{RS}$. On the other hand, the other factor in the numerator $v_j \sin^2 \beta/2$ would be expected to decrease with increasing thickness since β should decrease with increasing τ, and v_j would normally decrease due to the decreased value of β (which makes the collision point coordinate system move more slowly relative to the ground). Hence the effect of liner thickness upon ω_o would depend upon the extent to which either of these two potentially compensatory factors τ, and $v_j \sin^2 \beta/2$ dominated the numerator.

Thus if the numerator $\tau v_j \sin^2 \beta/2$ increased as τ increased, ω_o would increase with the thickness τ. Increasing ω_o would result in reduced sensitivity to rotational deterioration since a higher rotational frequency ω would be required to give the same fractional reduction in penetration.

Conversely if the numerator decreased with increasing τ the sensitivity to rotational deterioration would be increased as τ increased.

Since it is apparent that the two factors in the numerator vary in opposite directions in such a manner that they tend to compensate, one might expect that the effect of liner thickness upon ω_o might be relatively small, and perhaps of second order. This analysis, of course, does not take into account the other possible independent effect of increased thickness, i.e., increased jet stability with respect to breakup. Such an effect would, of course, tend to make thicker liners less sensitive to rotational deterioration.

Experimental Results

There have been very few rotation experiments reported* involving liner thickness as a variable. Those which have been carried out up to the present time seem to confirm the expectation that over the range of thickness studied the effect of thickness is not of major importance, and that the penetration performance of a uniform conical liner under rotation is, within the precision of the experiments, essentially unaffected by thickness.

*The author is grateful to Messrs. Eichelberger and Litchfield of the Carnegie Institute of Technology for making their experimental data available prior to publication.

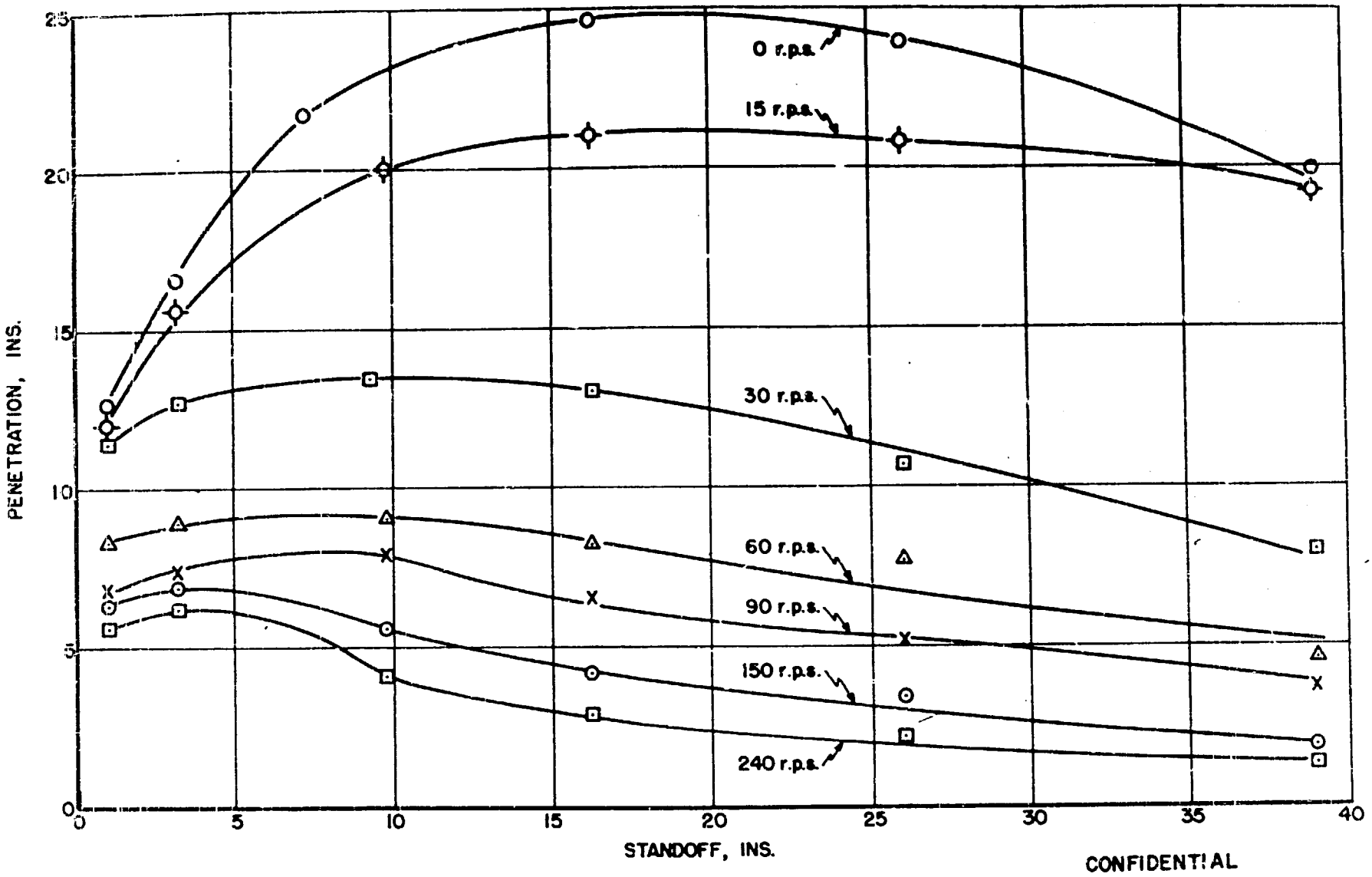

Fig. 13

Effect of Rotation and Standoff Upon the Penetration of 105mm 45° Drawn Copper Cones.

Improved experiments, with extra care taken to reduce dispersion, will be required to establish the existence and magnitude of the thickness effect in rotation. Separate experiments are required to ascertain the contribution, if any, of the liner thickness to changes in jet stability to break-up. Such experiments are under way at the Ballistic Research Laboratories and at Carnegie Institute of Technology but at the time of this review there are no definitive results. The best course for the designer at this time is to treat the thickness variable as if it has no effect upon rotational penetration, and that the best performance under unrotated conditions should determine the thickness.

THE EFFECT OF STANDOFF UPON PENETRATION UNDER ROTATION

There has recently been completed at the Ballistic Research Laboratories a very comprehensive experimental study of the effect of rotation and standoff upon the penetration of heavily confined 105mm drawn copper liners. The most useful way to summarize this study is to present the experimental results in graphical form. These are shown in Figure 13.

These results can be considered typical of good liners since the unrotated performance of the basic liners compares favorably with the best results ever reported.

The conclusions of value to the designer, which may be drawn from these results are as follows:

1. The Penetration at a given standoff decreases monotonically as the rotational frequency increases.

2. The standoff corresponding to peak penetration decreases as the rotational frequency increases until at the highest frequencies used ($\sim$240 rps), the optimum standoff is only a few inches.

3. At low rotational frequencies useful penetrations are obtainable even at the largest standoffs (42") used. The implications of this result are important for the problem of defense by spaced armor.

THE EFFECT OF LINER MATERIAL UPON PENETRATION UNDER ROTATION

There have been penetration experiments comparing various liner materials under rotation carried out by OSRD (21) by Firestone (22),(23) and by Carnegie Institute of Technology (24). In addition, flash radiographic jet studies have been carried out by the Ballistic Research Laboratories. The penetration experiments generally lead to the conclusion that no material studied so far offers any striking advantages over any other material insofar as rotational effects are concerned; the predominant role of the unrotated penetration makes copper still the proper choice for penetration purposes according to the penetration experiments.

FIG. 14

COMPARISON OF PENETRATIONS OBTAINED WITH POINT INITIATED CONICAL LINERS AND PERIPHERALLY INITIATED TRUMPET LINERS

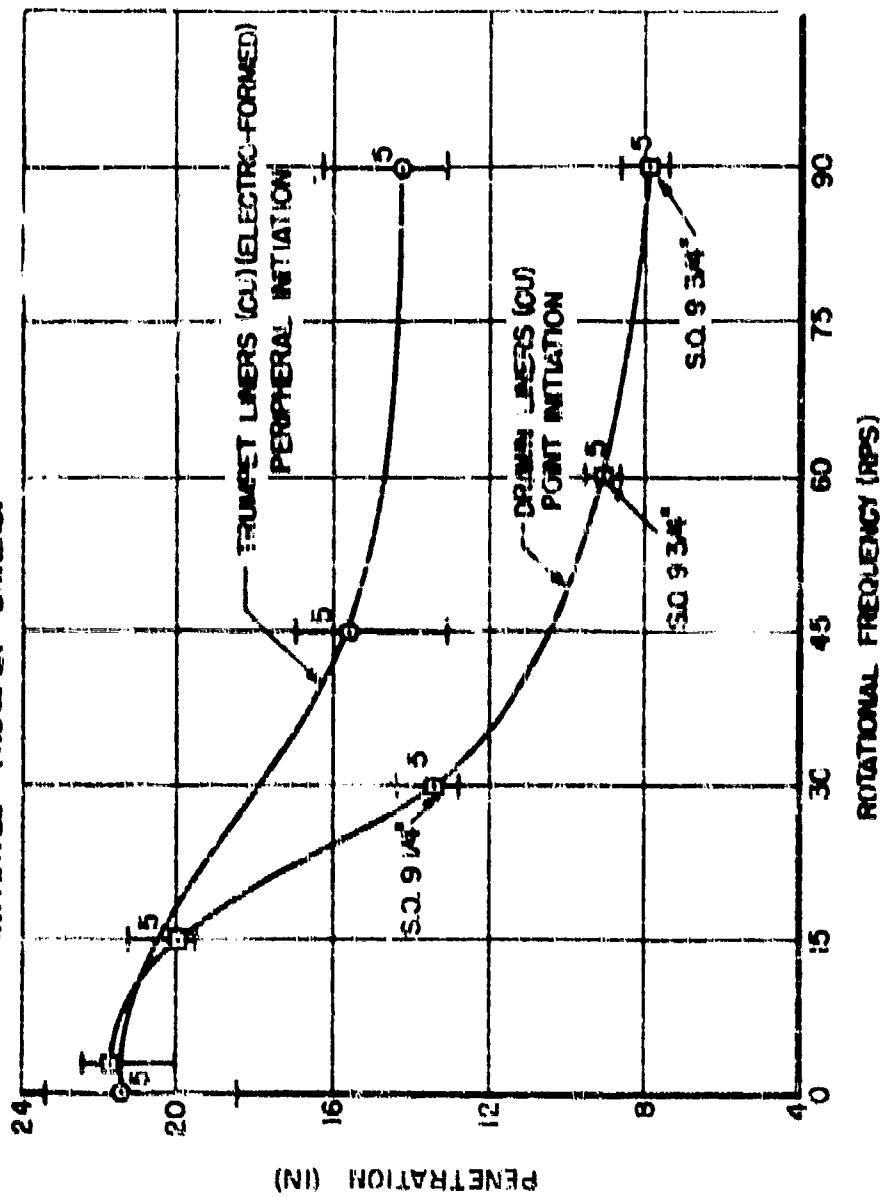

The flash radiographic studies by the Ballistic Research Laboratories have indicated a basis for expecting differences in the behavior of various materials because of the expected dependence of the critical frequency for bifurcation upon the physical properties of the materials. Such differences have actually been observed. These studies have, however, not yet progressed to the point where conclusions of value to a designer may be drawn. It may even turn out that the differences which seem to exist may be too small or may require the use of strategic material for their exploitation.

THE EFFECT OF LINER SHAPE UPON PENETRATION UNDER ROTATION

It has been suggested by various investigators (e.g., Birkhoff BRL 623) that trumpet shaped liners might show increased resistance to deterioration by rotation. This view is based on the notion that since the trumpet liner is on the average nearer to the axis of rotation than the equivalent cone of equal altitude, it ought to be less affected by rotation.

Experiments by the Carnegie Institute of Technology several years ago did not bear out such expectations. However, experiments which have been carried out at the Ballistic Research Laboratories using trumpet liners with peripheral initiation have indicated that one can indeed obtain reductions in the deterioration of the performance under rotation by means of a trumpet shape.

These experiments were for some time plagued by an inability to reproduce the experimental results. This difficulty has recently been traced by Lieberman to an inadvertently overlooked mechanical interference with the late collapse stages which has been eliminated. In addition, asymmetries in the explosive have also been shown by Lieberman to be of importance in hindering reproducibility.

A comparison of the most recent performance of peripherally initiated trumpets with the corresponding cones of 45° apex angle is shown in Figure 14. The performance of electroformed trumpets (peripherally initiated) is compared with the best drawn conical liners available at the Ballistic Research Laboratories in the same caliber. It is quite evident that the peripherally initiated trumpets are resisting deterioration quite effectively. More complete coverage of the pertinent variables is still needed, but the effect is sufficiently clear to warrant consideration of this system in applications involving lower rotational frequencies. This system may be considered competitive with fluted liners in this range, and may have advantages since there is no peaking of the penetration performance at a given rotational frequency but rather a reduced deterioration, the performance improving monotonically as the rotational frequency decreases. The possibility of increased sensitivity to loading asymmetries is a disadvantage that must also be considered. It should, however, be possible to overcome this with careful loading techniques.
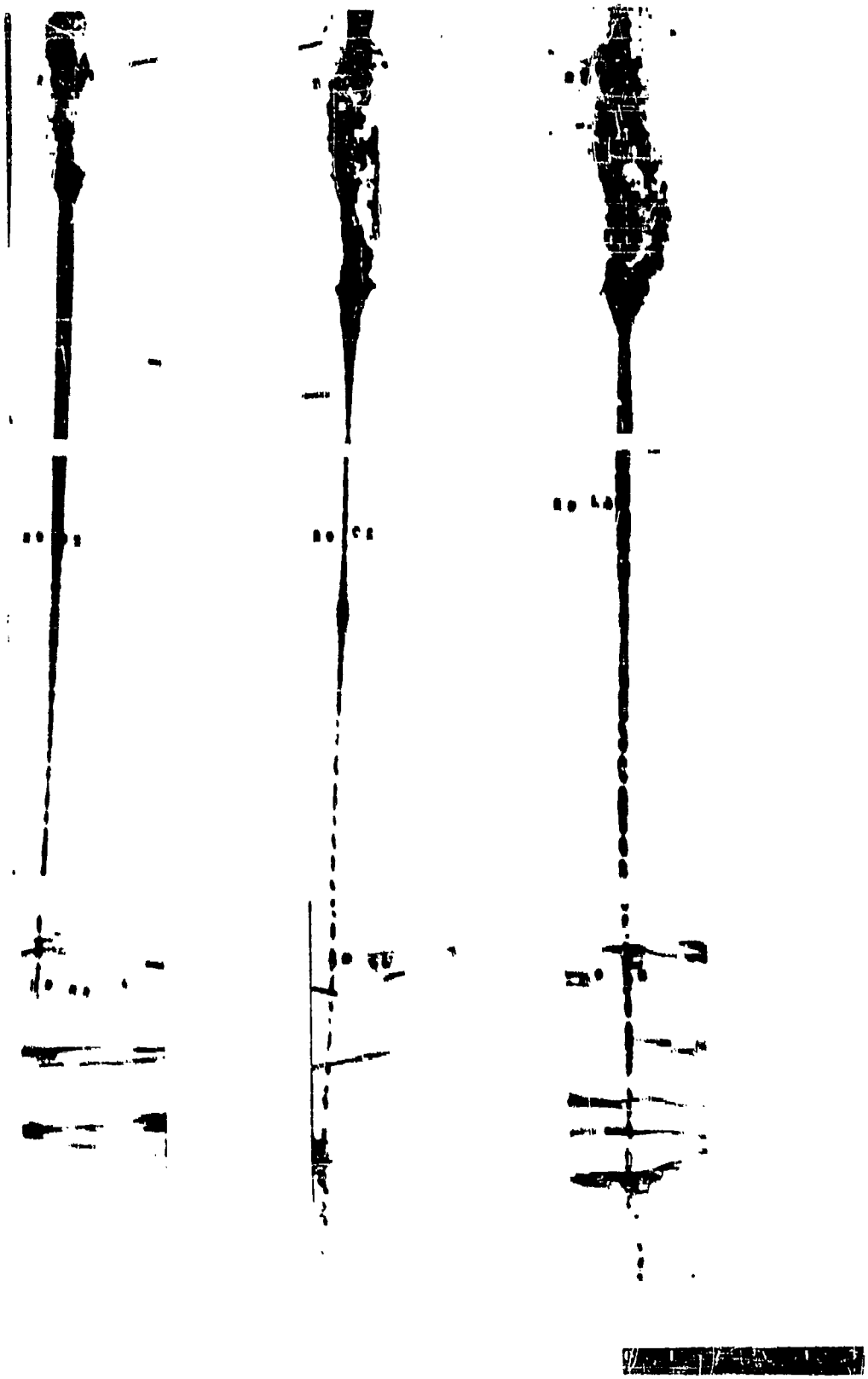
FIG. 15. Jets from peripherally initiated trumpets rotated at 45 rps

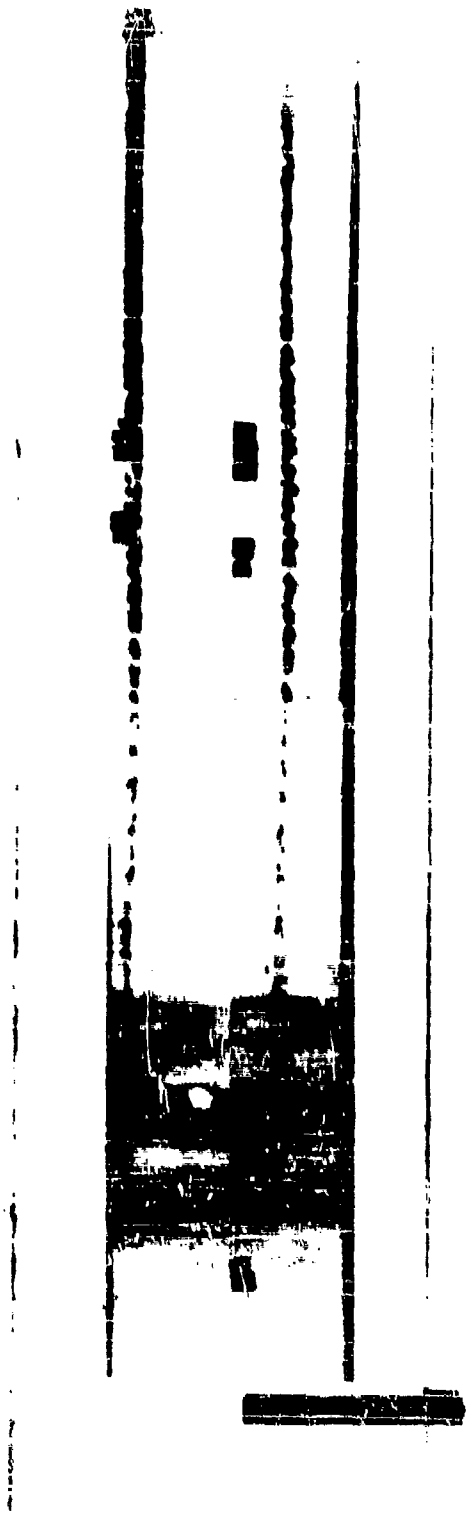

FIG. 16. Jets from peripherally initiated trumpets rotated at 45 rps

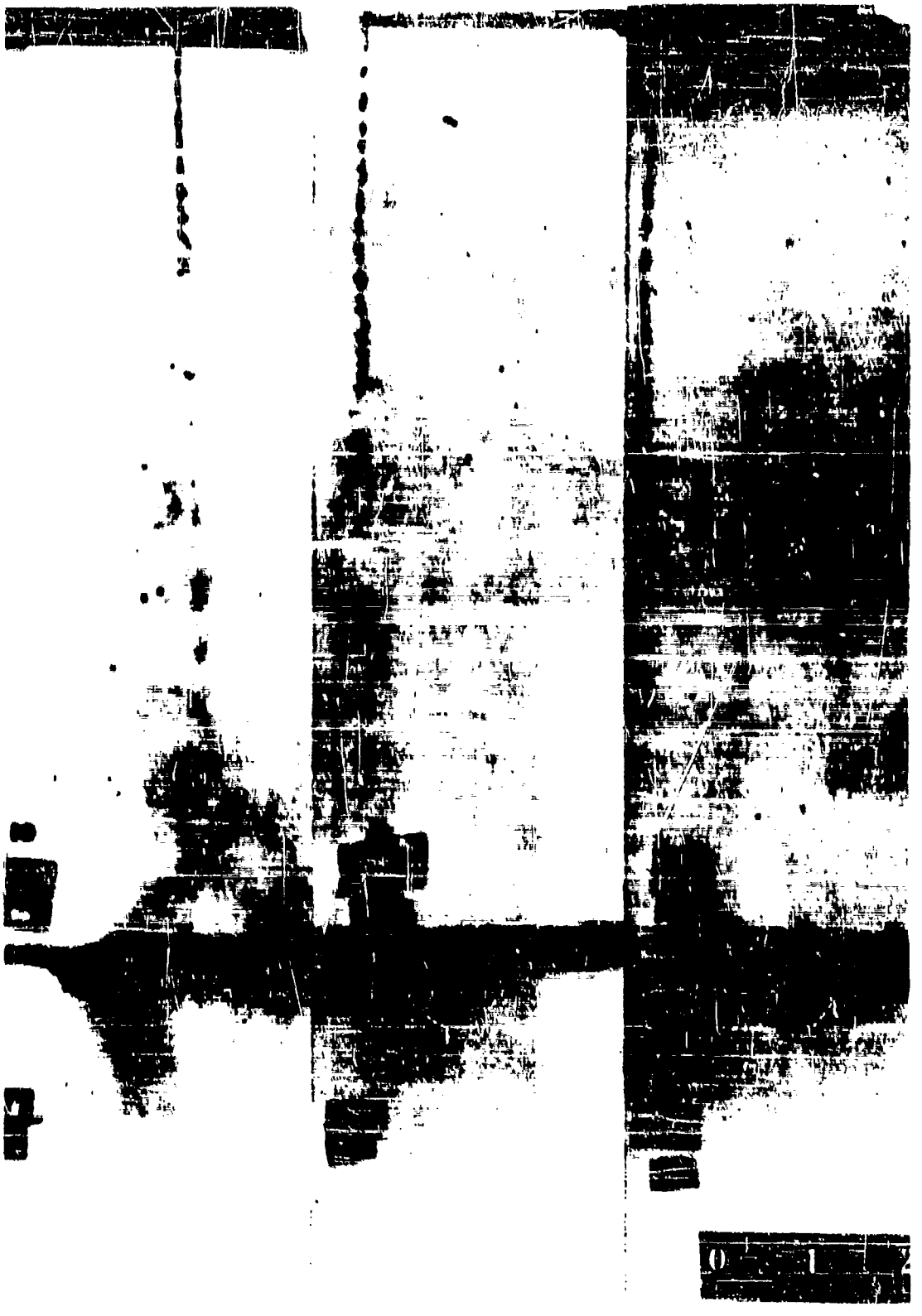

FIG. 17. Jets from a 1" diameter cylindrical liner in a 105mm body

The flash radiographs of the jets shown in Figures 15 and 16 bear out the increased resistance of this system to rotational deterioration.

In order to minimize the effects of rotation it is logical to start the collapse as near the axis as possible, e.g., by the use of a cylindrical liner. The earliest recorded experiments with cylindrical liners are those of the British (25). The group at the Ballistic Research Laboratories, unaware of such experiments started a similar investigation in 1950 (26) and since that time, investigators at Frankford Arsenal have also attacked the problem and have produced the wave shaping system which so far has given the best penetration performance. This performance level, however, and the reproducibility have both been inadequate.

The major problems in the investigation of cylindrical liners are:

1. Devising a system whose unrotated performance will compare favorably with that of a conical liner in the same projectile.

2. Perfecting a wave shaping system which will be sufficiently reproducible to make experimental investigation of other parameters possible.

The advantages of a small diameter cylindrical liner are:

1. The cylinder should exhibit a high ability to resist deterioration by rotation.

2. There is potential value in the possibility of making the penetration depend upon projectile length rather than projectile caliber.

3. The simplicity of the geometry should have advantages from the production viewpoint.

The possible disadvantages of such a liner are:

1. Very high precision will probably be required for the cylinder liner.

2. A wave shaping system is required according to present designs to get enough material into the jet to make a sizeable hole diameter which is essential for lethality purposes.

3. Present designs have up to this time given penetration performance no better than half of that attainable with a cone in the same projectile.

Figure 17 shows the appearance of the jet from a 4" long cylindrical liner whose interior diameter is 1" and whose exterior diameter is 1.1" in a heavily confined 105mm body.

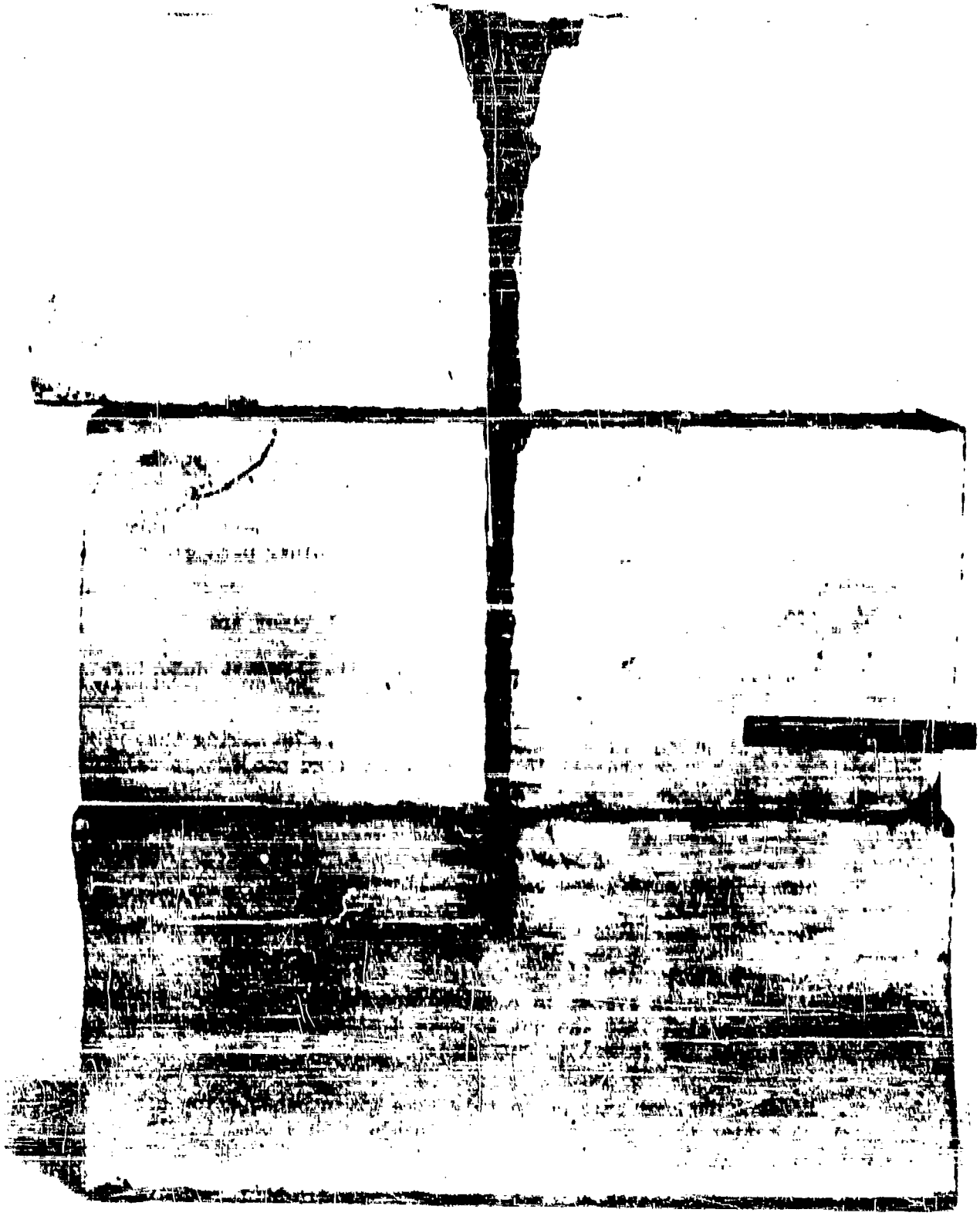

FIG. 18. Hole in mild steel made by the type of jet shown in Figure 17
(Note the small diameter)

Figure 18 shows the hole in mild steel by such a jet.

In summary, the designer should be aware of two developments involving liner shapes aimed at reducing sensitivity to rotational deterioration. Of the two, the system involving trumpets with and without peripheral initiation is much nearer realisation and application than the system involving a cylindrical liner with a wave shaping device. Both of these systems should be distinguished from the fluted liners and other methods which are discussed in Chapter VIII. The latter are more properly considered methods for actively overcoming the effects of rotation, while the systems discussed in this chapter are passive systems.

REFERENCES

1. A. Schofield, "Survey of Published Information on the Effect of Rotation on Target Penetration by Hollow Charges," Survey No. 1/49, Armament Research Establishment, Fort Halstead, Kent, March 1951.

2. James L. Tuck, "A Note on the Theory of the Monroe Effect," - AC3596, Phys/RX393, SC3, Explosives Research Committee, Shaped Charge Sub-Committee - Feb. 27, 1943.

3. Walter Trinks, "Mathematical Study of Lined Hollow Charges," Report 43/6, Translated as OTIB No. 1484, April 30, 1943.

4. "Hollow Charge Rotated Projectiles," by MDl-AC3987, SC27, Advisory Council on Scientific Research & Technical Development, Shaped Charges Sub-Committee, May 7, 1943.

5. H. Schardin, "Recent Studies in the Field of Hollow Charges (Translated from the German Original), SR7/46/115, Fort Halstead, Kent, June 1943.

6. "Target Penetration by the Jet from a Rotating Cone Charge," OSRD 1680, Explosives Research Laboratory, Bruceton, Penna. Aug. 5, 1942

7. "Target Penetration by the Jet from a Rotating Cone Charge," OSRD3874, Explosives Research Laboratory, Bruceton, Penna. July 10, 1944.

8. "Target Penetration by Rotating Cavity Charges, OSRD 5598, Explosives Research Laboratory, Bruceton, Penna. September 20, 1945.

9. Leslie E. Simon, Col., Ord Dept., "Report on German Scientific Establishments" Chief of Ord, Washington, D. C., Sept. 1945, p. 97.

10. "Hollow Charge Rotated Projectiles" by M.D.1. AC3987-SC27, Advisory Council on Scientific Research & Technical Development, Shaped Charges Sub-Committee, May 7, 1943, page 1, Figures 5a, b.

11. J. C. Clark and R. O. Fleming, Jr. "Effect of Rotation upon the Explosive Collapse of Thin Metal Surfaces of Revolution," BRL Report No. 671, Ballistic Research Laboratory, Aberdeen Proving Ground, Md., July 1948.

12. S. Kronman and L. Zernow, "A Wire Driven Projectile Rotating Device for Hollow Charge Investigations," BRL Report No. 798, Ballistic Research Laboratories Aberdeen Proving Ground, Md., March 1952.

13. L. Zernow, S. Kronman, F. Rayfield, J. Passek, B. Taylor, "Flash Radiographic Study of Jets from Rotated 105mm Shaped Charges," BRL Report No. 856, Ballistic Research Laboratories, Aberdeen Proving Ground, Md., April 1953.

14. S. Kronman, J. Simon, F. Rayfield, L. Zernow, "A Triple Flash Field Radiography System for Studying Jets from Large Shaped Charges," BRL Memorandum No. 659, Ballistic Research Laboratories, Aberdeen Proving Ground, Md., March 1953.

15. L. Zernow, J. Ryan, J. Simmon, I. Lieberman, "Study of the Effect of Rotation Upon the Penetration of Jets from 105mm Shaped Charges" BRL Report No. 837, Ballistic Research Laboratories, Aberdeen Proving Ground, Md., Nov. 1951, page 319.

16. G. Birkhoff, "Hollow Charge Anti-Tank Projectiles," BRL Report No. 623, Ballistic Research Laboratories, Aberdeen Proving Ground, Md., 10 Feb. 1947.

17. E. L. Litchfield, F. P. Beitel, R. J. Eichelberger, "Rotated Charges" CIT-GALCIT-R26, Carnegie Institute of Technology, Pittsburgh, Penna, 31 Oct. 1952. Page 16-21.

18. Ibid page 22.

19. H. Winn, "Minimizing the Effect of Rotation upon the Performance of Lined Cavity Charges," BRL Report No. 837, Ballistic Research Laboratories, Aberdeen Proving Ground, Md., Nov. 1951, p. 339-40.

20. FTRC Progress Report No. 36, The Firestone Tire & Rubber Co, Defense Research Division, Akron, Ohio, July 1953, p. 27-28.

21. N. D. R. C/Div 8, SC-10, "Shaped Charges, National Defense Research Committee, May, June 1944, Page 3, 9., N. D. R C/Div 8, SC-11 "Shaped Charges," June, July 1944, National Defense Research Committee, page 7,8.

22. FTRC Progress Report No. 26 (Supplement) The Firestone Tire & Rubber Co., Defense Research Division, Akron, Ohio, September 1952, page 2.

23. FTRC Progress Report No. 27, The Firestone Tire and Rubber Co., Defense Research Division, Akron, Ohio, October, 1952., p. 9, 17.

24. Personal communication from Litchfield.

25. M. R. Jefferis, "Cylindrical Shaped Charges," AC8518, SC159, Phys. EX676, Advisory Council on Scientific Research and Technical Development, Shaped Charges Sub-Committee, 26 September 1945.

26. L. Zernow, S. Kronman, F. Rayfield, J. Pennak, B. Taylor, "Flash Radiographic Study of Jets from Rotated 105mm Shaped Charges" BRL Report 856, Ballistic Research Laboratories, Aberdeen Proving Ground, Maryland, April 1953.

APPENDIX I

DERIVATION OF THE EXPRESSION FOR ω_o IN TERMS OF CHAROF PARAMETERS

by

F. P. Deitel

Carnegie Institute of Technology

We wish to find an expression for the effect of rotation upon penetration of a conical liner. Since a non-steady collapse theory seems to be required, only elemental rings on the cone will be considered. In addition, the cone wall will be assumed to be thin wherever this assumption seems to be desirable.

Let ω = angular velocity of uncollapsed cone

R = radius of uncollapsed ring

r_j = radius of the ring after collapse

ω_j = angular velocity of collapsed ring

d = wall thickness of cone

β = collapse angle of the cone

S = standoff for the ring element

V_j = jet velocity of jet element arising from ring under consideration

m = mass of ring element

m_j = mass of jet element formed

P = element of penetration due to the ring element spun at angular velocity ω

P_o = penetration for $\omega = 0$

A = cross-sectional area of jet

If we assume that the angular momentum of the mass m_j is conserved we can write at once

$$I\omega = I_j \omega_j \qquad (1)$$

Taking the initial configuration to be a hollow cylinder and the final one (at the axis) to be a solid cylinder we have

$$I = \frac{1}{2} m_j \left[R_o^2 + R_i^2 \right] \simeq m_j R^2 \tag{2}$$

$$I_j = \frac{1}{2} m_j r_j^2 \tag{3}$$

Substitution of these quantities yields the relation

$$R^2 \omega = \frac{1}{2} r_j^2 \omega_j \tag{4}$$

Now to find the radius of the jet at the target we can assume that the mass m_j is subjected to a centrifugal force due to the rotation of the jet.

$$F = m_j F_j = m_j r_j \omega_j^2 \tag{5}$$

or

$$F_j = r_j \omega_j^2$$

But from (4) we can find $\omega_j = \omega_j (r_j)$ to obtain

$$F_j = \frac{4 R^4 \omega^2}{r_j^3} \tag{6}$$

To solve this we let $v = \dot{r}_j$. Then

$$F_j = \frac{d}{dt} \dot{r}_j = \frac{d}{dt} v = \frac{dv}{dr_j} \frac{dr_j}{dt} = v \frac{dv}{dr_j}$$

and $v\, dv = 4 R^4 \omega^2 \dfrac{dr_j}{r_j^3}$

whence $v^2 = b - 4 R^4 \omega^2 \dfrac{1}{r_j^2}$, b = arbitrary constant

$$v = \frac{dr_j}{dt} = \sqrt{b - \frac{4 R^4 \omega^2}{r_j^2}} \tag{7}$$

This is easily integrated to yield

$$t = \frac{1}{b} \sqrt{b r_j^2 - 4 R^4 \omega^2} + c \tag{8}$$

To evaluate the constants b and c, we take the initial conditions

$r_j = r_o$, $\frac{dr_j}{dt} = 0$ at $t = 0$.

We find $b = \frac{4 R^4 \omega^2}{r_o^2}$, $c = 0$

Substituting in (8) and solving for r_j we get

$$r_j^2 = r_o^2 \left\{ 1 + \frac{4 R^4 \omega^2}{r_o^4} t^2 \right\} \tag{9}$$

Now to find r_o we can go to the initial configuration and require the conservation of mass. From the non-steady collapse theory we have

$$\frac{m_j}{m} = \sin^2 \beta/2 \tag{10}$$

Assuming that the density and length of the element do not change as it moves from the original position to the axis we can write

$$m_j = \rho \pi r_o^2 \ell \tag{11}$$

Also, since we have assumed the liner to be very thin,

$$m = \rho (2\pi R) \ell d \tag{12}$$

Hence, combining (10), (11), and (12) we get

$$\rho \pi r_o^2 \ell = \rho(2\pi R) \ell d \sin^2 \beta/2$$

or
$$r_o^2 = 2 R d \sin^2 \beta/2 \tag{13}$$

Also, the time the element requires to reach the target is approximately

$$t = \frac{S}{V_j} \tag{14}$$

If we take the penetration element as inversely proportional to the jet cross-section we get (i.e., for the expanding jet)

$$\frac{P}{P_o} = \sqrt{\frac{A_o}{A}} = \sqrt{\frac{\pi r_o^2}{\pi r_f^2}} = \frac{r_o}{r_f} \tag{15}$$

where r_f is the radius of the jet at the target. Hence

$$\frac{p}{p_o} = \left[\frac{r_o^2}{r_o^2 \left\{ 1 + \frac{4 R^4 \omega^2}{r_o^4} t_f^2 \right\}} \right]^{1/2} \quad \text{from (9),}$$

$$\text{or} \qquad \frac{p}{p_o} = \frac{1}{\sqrt{1 + \omega^2/\omega_o^2}}$$

where $\omega_o = \dfrac{V_j \, a \sin^2 \beta/2}{R \, s}$ follows from substitution of r_o^2 and t_f from (13) and (14).

CHAPTER VIII

SPIN COMPENSATION

R. J. Eichelberger

Carnegie Institute of Technology
Pittsburgh, Pennsylvania

Introduction

The title of this chapter will be interpreted literally. The chief content will be a discussion of fluted liners, the most extensively investigated means of compensating for initial spin of a shaped charge and its liner. Other methods of eliminating the detrimental effects of spin will be treated only briefly. Means of avoiding, rather than eliminating, the effects of spin are not terminal ballistic problems*, and will be mentioned only for purposes of evaluating and comparing the present and potential practicality of all means of dealing with the problem of spin degradation.

Present requirements for spin-compensated liners are largely determined by the spin rates of the spin-stabilized H.E.A.T. rounds now in field use. These vary only slightly for rounds of different sizes; e.g., the 57mm H.E.A.T. has a spin of about 210 r.p.s., the 75mm and 105mm round have spin rates of about 180 r.p.s. to 200 r.p.s. There is presently a trend toward higher muzzle velocities that would increase all spin rates by as much as a factor of two, and some new rounds currently under consideration have proposed spin rates as high as 1200 r.p.s. Even fin-stabilized rounds sometimes have slight spin usually of the order of 25 r.p.s. which is of considerable importance in large calibre rounds (see Chapter VII).

Historical Background of Fluted Liners

So far as is known, the development of fluted liners for purposes of spin compensation has been carried out exclusively in the United States. The original suggestion is credited in the literature (1) to Linus Pauling but has been made independently by many other persons interested in shaped charges. It is interesting to note that the basis of the suggestion has been similar in all cases and is not significantly related to the actual mechanism of compensation.

---

* They include:

(a) Means of stopping the spin of the shell near the target (e.g. by means of vanes or peripheral jet engines).

(b) Means of preventing spin of the charge and liner while allowing the shell body to spin for stability (e.g. by mounting the charge in bearings).

(c) Elimination of spin by use of fin stabilization.

All of these methods are discussed briefly near the end of this chapter.

The earliest experimental work was carried out during World War II by the Explosives Research Laboratory. The results obtained (1), (2) indicated that a spin compensation tendency existed in fluted liners but was opposite in direction to the anticipated effect. Basic development since the war has been carried out largely at Carnegie Institute of Technology (since 1948). The early work at C.I.T. proved the existence of spin-compensation and revealed its true complexity. Most of the effort has been directed toward an identification of the physical phenomena responsible for compensation and attempts to reduce them to a tractable form for detailed investigation.

In 1950, the Firestone Tire and Rubber Company became interested in spin-compensation in connection with a program for developing the 105mm B.A.T. weapon[P]. For practical reasons, their work has often followed different lines from that at C.I.T. and has provided a greater variety of experimental observation.

While all of the experimental work on fluted liners has been carried out with shells spun in stationary apparatus, several field tests have by now been carried out, also. The first, a premature attempt to apply very early C.I.T. laboratory observations, was carried out by the British in 1949 or 1950 (unreported) with very unsuccessful results. The second was carried out by Picatinny Arsenal in 1951 (also unreported), using some C.I.T. experimental liners mounted in standard 57mm shells. In spite of the facts that considerable adaptation was necessary in mounting the liners in the shell and the compensation frequency was about 30 r.p.s. less than the spin frequency of the shells (180 r.p.s. as compared with 210 r.p.s.) the results were very satisfying. Three shots out of three perforated 4 in. (2.3 charge diameters) of armor plate, and ten shots out of sixteen perforated 5 1/2 in. (3.3 charge diameters) of armor. These results are to be compared with 70% perforations through 3 in. of armor by the standard 57mm H.E.A.T. shell. Just prior to the time of writing, Picatinny has completed tests with a modification of the C.I.T. experimental liner designed specifically for the standard shell. In this case, ten shots out of twenty-four perforated 6 in. of armor plate. The liners tested represented a variety of manufacturing conditions. There is evidence in the data that most of them over-compensated and that even better performance could be expected from an appropriately chosen procedure of manufacture.

Firestone has also carried out field tests with fluted liners designed for slow spin (about 50 r.p.s.) 105mm rounds. These tests indicated that the fluted liner was compensating almost completely for the spin, although difficulties with ogive shape caused some reduction in penetration (entirely incidental as far as spin compensation is concerned).

P Battalion Anti-Tank: A light, recoilless rifle designed for use on the battalion level by infantry, with H.E.A.T. shells.

The net result of the field tests thus far shows that the performance of a fluted liner in a shell is no different from that obtained in the laboratory, provided the shell design does not interfere with proper jet formation.

From the viewpoint of application, the best results that have been obtained to date with fluted liners are:

57mm liners (charge diameter 1 5/8 in.)	4.0 charge diameters penetration at 360 r.p.s. 5.0 charge diameters penetration at 180 r.p.s. 4.7 charge diameters penetration at 250 r.p.s.
105mm liners (charge diameter 3 1/4 in.)	6.2 charge diameters penetration at 50 r.p.s. 4.5 charge diameters penetration at 85 r.p.s.

The potential performance of the 57mm cones (as represented by smooth liners fired statically) is about 5.3 diameters penetration and that of the 105mm liners about 6.7 diameters, under appropriate conditions for comparison with the above. By interpolation from laboratory results, a penetration of 4.8 charge diameters should be readily obtainable from a 57mm H.E.A.T. round at its standard spin frequency of 210 r.p.s. No liner has yet been tested that would provide very good spin compensation in standard 105mm H.E.A.T. rounds (spin frequency about 200 r.p.s.).

Mechanism of Spin Compensation by Fluted Liners

It is now generally accepted that the detrimental effects of rotation are due to the requirements of conservation of angular momentum and the consequent tremendous rotational frequencies of the jet (see Chapter VII). In order to counteract this effect, it is obviously necessary that a tangential component of velocity be imparted to each element of the liner, by some means, which is equal in magnitude but opposite in direction to that set up by the initial spin of the liner. The simplest means of accomplishing this is to find a way of using the energy of the explosive to produce a counter-torque on the liner.

The basis of all the original suggestions for use of fluted liners has been the idea of simply altering the direction of liner collapse, by canting the surface in segments, so as to compensate for the tangential velocity vector due to initial spin (1). This idea is still implicitly included in the theory of compensation, but plays only a minor role in most cases. The very first E.R.L. tests in which an indication of spin compensation was observed showed that this mechanism was not predominant in that they indicated compensation in the direction opposite to that anticipated (1), (2). The E.R.L. group then developed a theory based on unequality of torques produced by pressure of the explosive products on the canted and the offset surfaces of a liner segment (2). This concept was later modified by C.I.T. (11) to take into account non-steady state conditions in liner collapse, but the theory has since been proven incorrect.

The present concept of spin compensation is based on two phenomena that have been studied at C.I.T. under far simpler circumstances than those existing in collapse of a fluted liner. One, sometimes called the "thick-thin" effect, is the observed dependence upon the thickness of the liner of the impulse delivered to a liner element by the product gases of detonation. The second, named the "transport" effect, is the dependence of the impulse delivered to the liner upon the angle at which the detonation products impinge on the liner. Both of these effects are strictly dynamic phenomena; that is, they are to be observed only in a rapidly flowing fluid and they represent departures from Archimedes' principle.

The thick-thin effect is represented graphically in Fig. 1. The curve shown was derived from the theory of shock waves (24) and has been verified by experiment (26). A very similar result has also been obtained on the basis of gas kinetics (3). Application of the thick-thin effect to a fluted liner is also illustrated in Fig. 1. The impulse per unit area is always greater on the offset surface, since the thickness normal to that surface is greater. Furthermore, the impulse is directed along the surface normal. When the impulses delivered at all surface elements are resolved into radial and tangential components and summed, the total tangential component does not vanish, as in the case of a static fluid, but has a net resultant which produces a torque, in the direction shown, which can be used for spin compensation.

The transport effect can be represented simply by the equation

$$I_\theta = I_n\left(\frac{5 + v\cos^2\theta}{6}\right),$$

where I_θ is the impulse delivered to unit area of a liner whose surface normal forms the angle θ with the direction of propagation of the detonation wave, and I_n is the impulse delivered in normal impact. This equation has also been derived from both shock theory (16) and gas kinetics (21) and has been verified by experiment (12). It is significant in spin compensation because the angle θ at which the detonation wave strikes the canted surface is generally (except in spiral flutes) less than for the offset surface. As a result, a net torque is produced in the direction opposite that from the thick-thin effect.

Mathematical treatments of spin compensation have been carried out by L. H. Thomas (4) and by C.I.T. (16), the latter being an attempt to refine the assumptions used by Thomas. These treatments are based on shock theory and implicitly contain both the effects to which spin compensation has been ascribed. They demonstrate theoretically the feasibility of spin compensation, and Thomas has shown the possibility of reversals in direction of the net torque. Unfortunately, the simplifications required to make the mathematical treatment tractable prevent their application to test conditions except under very special circumstances. At present, the mathematical theory provides only a

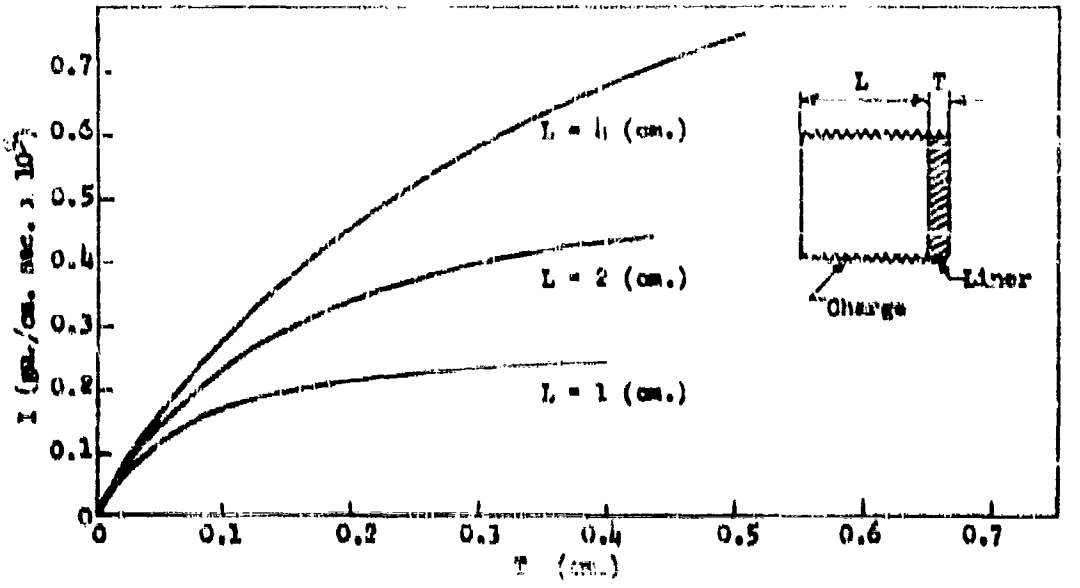

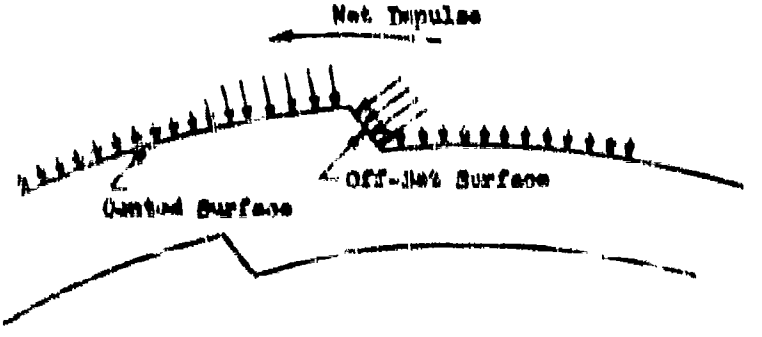

Fig. 1 Illustration of the thick-thin effect and its application to a fluted liner. Due to the variation with liner thickness of impulse per unit area delivered by the explosion products to the liner (see upper figure), the impulse delivered to an element of a fluted liner depends upon the shape of the liner in the neighborhood of the element. The greater the thickness of the liner element (measured normal to the outer surface) the greater the impulse delivered to it. The result is illustrated schematically in the lower figure, where the lengths of the arrows roughly represent the magnitudes of the impulses. Because of the non-uniformity of the impulse, there is in general a net force tending to rotate the configuration in the direction of the curved arrow. The illustration, of course, oversimplifies the application, but conveys the general idea.

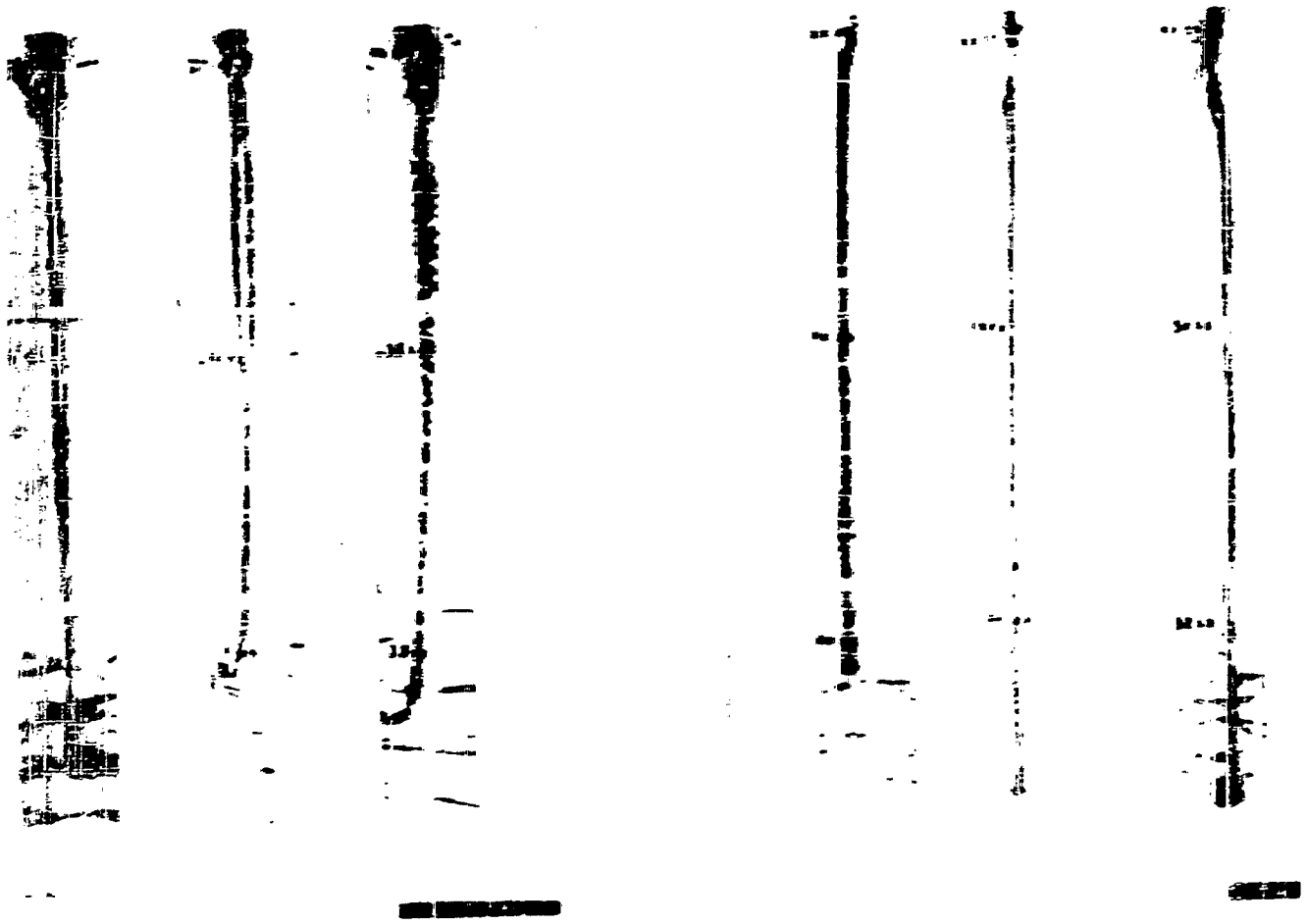

(a) (b)

FIG. 2. Flash Radiographs of jets from 105mm fluted liners fired (a) statically, and (b) at optimum spin rate (45 r. p. s.). Comparison with similar photographs of jets from smooth liners shows clearly that the fluted liner fired at its optimum frequency produces a jet like that from a statically fired smooth cone, while the statically fired fluted liner produces a jet like that from a smooth liner fired at 45 r. p. s. The pictures show each jet at three different times and viewed from three different positions. The relative insensitivity to rotation of the front of the jet is evident in (a); the very rear of the jet is just newly formed and has not had time to spread at the time of the picture. Photographs by courtesy of L. Zernow, S. Kreeman, and J. Simon, Ballistic Research Laboratories, Aberdeen Proving Ground.

qualitative guide for experimental work. Attempts have been made at C.I.T. to apply observations on the thick-thin and transport effects directly to fluted cones in a semi-empirical fashion. This procedure also produces many difficulties, however, and has not to date yielded any very useful results except of a qualitative nature.

Even though a rigorous mathematical treatment of fluted liners seems, at present, very remote indeed, it is possible to rationalize in self-consistent fashion the entire body of experimental observations made thus far with fluted liners. Furthermore, by combining information gleaned from theoretical considerations, basic experiments, and observations with fluted liners, the following conclusions can be reached:

(i) The phenomena responsible for spin compensation (i.e., the thick-thin effect and the transport effect) are second-order in magnitude compared with the overall effect of an explosion on an inert liner.

(ii) The two effects are of approximately the same magnitude, but are opposite in direction under the conditions studied experimentally thus far. They are largely independent of one another and can be separately varied. Consequently, they are competitive, and either can be made dominant by appropriate design, leading to the possibility of reversals in direction of spin compensation*.

General Experimental Results with Fluted Liners

We shall first consider the very general and fundamental aspects of the experimental observations with fluted liners. In the first place, it seems adequately proven now that the essential effect of the fluting is to introduce an angular impulse in the collapsing liner which, under appropriate conditions, can be made to compensate for the angular momentum due to initial spin. Thus, a fluted liner spun at its designed optimum frequency produces a jet exactly like that produced by an equivalent smooth liner fired statically. When fired statically, the fluted liner produces a dispersed jet like that from a rotated smooth liner. Indirect evidence of these facts has been described many times including hole profile observations, jet velocity measurements, penetration velocities, etc. A set of flash radiographs taken at the Ballistic Research Laboratory recently, and shown in Fig. ?, provide the first direct and incontrovertible proof, however.

* The use of tightly spiralled instead of straight flutes would presumably make the two effects mutually reinforcing instead of competitive, thus leading to higher optimum frequencies. See Chapter II, page 54 , and the discussion of experimental results later in this chapter.

**Editorial Note: Additional redesigns maybe found elsewhere: L. Zernow and J. Simon, "Flash Radiographic Study of Spin Compensation with 105mm Fluted Liners," Shaped Charge Journal, Vol. 1, No. 1, July 1954.

Further evidence of the effects of compensation is shown in the plots of Fig. 3 where experimental points and curves are given for the depth of penetration as a function of rotational frequency for smooth and fluted 57mm and 105mm liners. It is evident that the behavior of the fluted liners as the frequency is changed is the same as that of the equivalent smooth liners, except that the maximum penetration is obtained with the fluted liners at some rotational frequency other than zero, the optimum frequency being determined by the design of the flutes, wall thickness, etc. The cases shown are typical. For the 105mm liners, the fluted liners gave a higher average penetration at their optimum frequency than was obtained with the statically fired smooth liners. (The ostensible increase in penetration is due to a reduction in average wall thickness of a cone initially thicker than optimum due to machining of flutes; this is not a typical characteristic, of course.) With the 57mm liners, the penetration at optimum frequency by the fluted liners is somewhat less than obtained with statically fired smooth liners, but it will be noted that the optimum frequency is 250 r.p.s. (well above the rate of spin of a standard 57mm H.E.A.T. shell). The experimental points shown on the plots also illustrate that the variability in performance with a satisfactorily made fluted liner is no greater than the variability of the equivalent smooth liners.

Scaling relations for fluted liners are not yet well established. Theoretical considerations based on modelling laws lead one to expect that, for liners and charges that are geometrically similar in all respects, the optimum frequency (i.e., the frequency at which the highest degree of compensation is obtained) should vary as $1/D$, D being the charge diameter. The only experimental evidence available at present is obtained by comparison of results with liners of different sizes that are not really scaled replicas. Early comparisons of this sort seemed to indicate that v_o was more nearly proportional to $1/D^2$, but this has since been contradicted by work at both Firestone and Curtiss. At present, it appears that $v_o \propto \frac{1}{D^n}$ with n slightly larger than unity. The uncertainty of the experimental comparisons is such that the departure from the theoretical expectations is not certain. Consequently, through the remainder of this chapter, the theoretical scaling relation $v_o \propto \frac{1}{D}$ will be adopted. Definitive scaling tests are being carried out at the time of writing, but have not been completed.

It must be noted that even the most favorable scaling law that can be anticipated raises a great deal of difficulty in obtaining compensation at standard spin rates with large liners. In order to obtain compensation in a 105mm shell, the ratio of flute depth to charge diameter or to liner wall thickness must be about twice as great as that required to obtain compensation at the same spin rate in a 57mm shell. With flute designs that have been tested to date, it has not been possible to achieve a useful depth of penetration

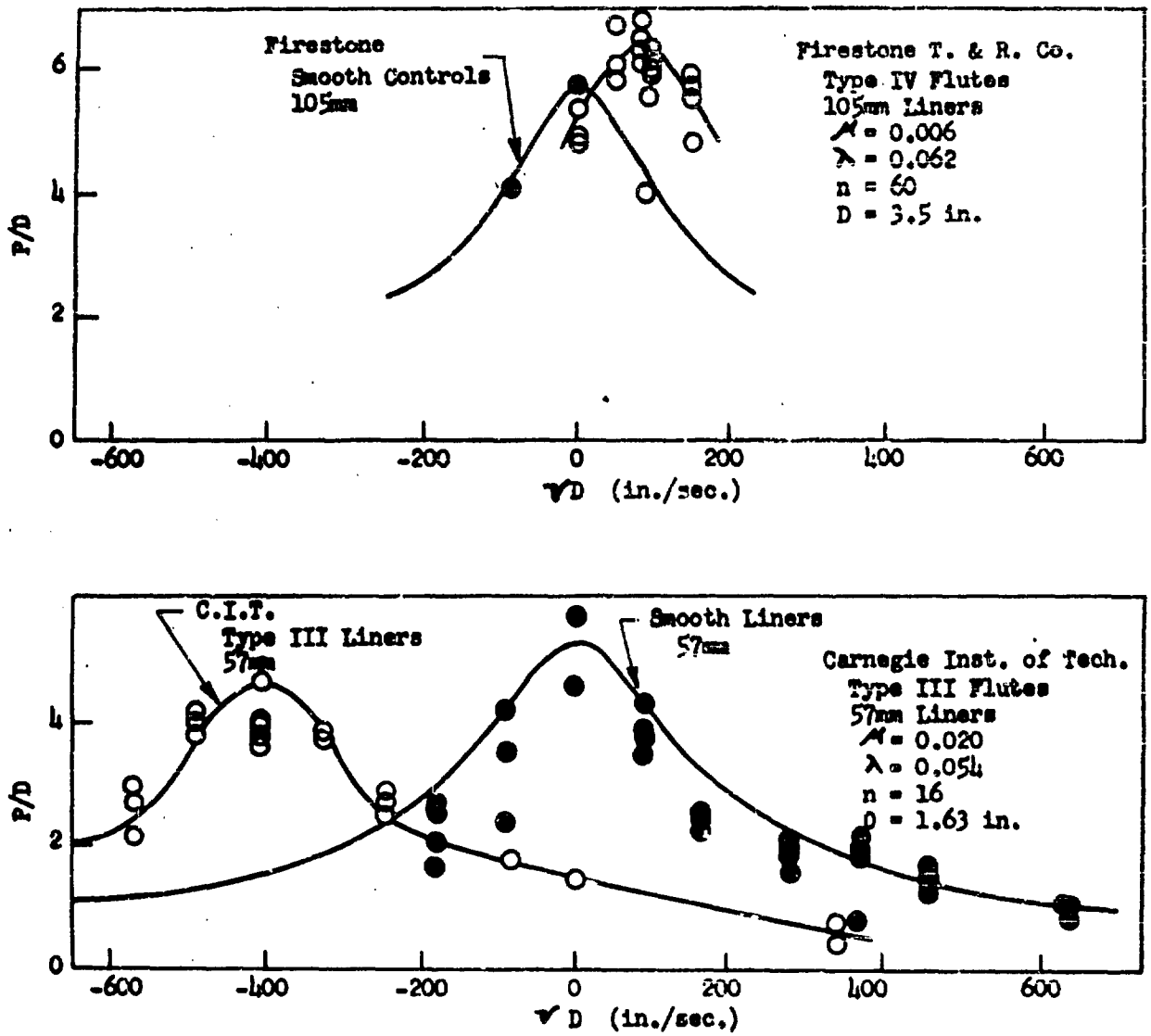

Fig. 3 Plots of typical data from 105mm and 57mm fluted liners, compared with observations for equivalent smooth liners. Both abscissae and ordinates are normalised in accordance with accepted scaling relations for purpose of comparison (D is the base diameter of the liner in each case, P is the depth of penetration and ν the spin frequency at which the observation was made). There are too few 105mm data to conclude much, except that the fluted liners perform at least as well at their optimum frequency as the statically fired smooth liners. For the 57mm liners, the peak penetration by the fluted liners is somewhat less than that by the smooth liners but the optimum frequency is high (about 250 r.p.s.). The variability is no worse than with smooth liners, however. Relative degradation in performance as a function of departure from optimum frequency is the same for fluted and for smooth liners. [Note: description of method of curve-fitting may be found in CIT-ORD-R23, R25 and R26.]

with the larger liners at standard spin rates for this reason.

With regard to the possibility of achieving compensation at very high spin rates, it can only be stated now that there has appeared no essential limit to the attainable optimum frequencies. It is certain, however, that the difficulties will increase rapidly as the optimum frequency sought increases. Certainly, the simple designs of flute and the relatively liberal tolerances used to date must be altered. A practical limit to the attainable compensation frequency exists, certainly, but its magnitude cannot be estimated from present information. It seems entirely possible that compensation can be achieved at values of $v_o D$ as high as 1000 in/sec. without requiring impractical designs.

Specific Experimental Results with Fluted Liners

Five distinct types of flutes have been tested to date. They are illustrated in Fig. 4 and given designations that will be used throughout the following discussion. Class I and Class II flutes are formed between one fluted metal die (male for Class I, female for Class II) and a rubber padded smooth mate. The undulating flute formed by the padded tool characterizes both types. Class III flutes are formed between matching fluted metal dies and Classes IV and V between one fluted die (female for Class IV, male for Class V) and a smooth metal mate*. As will be seen presently, quite different results are obtained with the various types of flutes.

All significant flutes tested thus far have been made so that (at least nominally) their depth increased linearly with cone radius, hence the flute depth can, at least nominally, be represented by $a = \mu R$ where μ is a constant for each cone. The designs have been limited so that any one be nominally described by five design parameters illustrated in Fig. 5, and defined as follows:

$\mu = a/R$, a = flute depth, R = pitch radius of liner element

$\lambda = T/R$, T = wall thickness of blank before fluting

n = number of flutes

ψ = angle between flute offset and radius through its root

δ = angle of indexing (when matching fluted tools are used).

Systematic investigations of all the design parameters have not yet been carried out for all classes of flutes. The following table indicates which have been studied for each type (C indicates investigation by C.I.T. with 57mm liners; F, by Firestone with 105mm liners):

*More detailed description of forming techniques is included later in this chapter.

CONFIDENTIAL

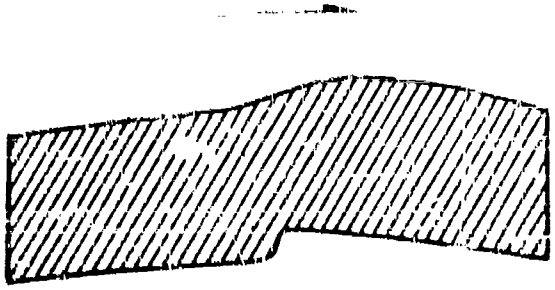

Class I

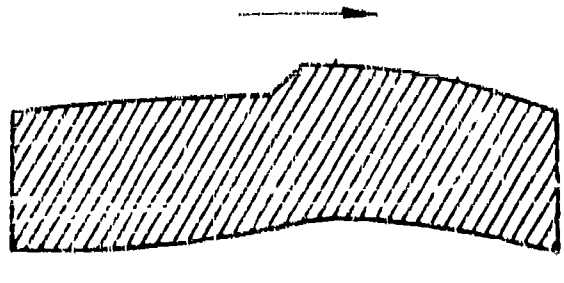

Class II

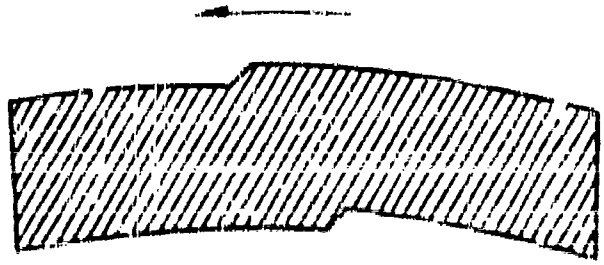

Class III

Class IV

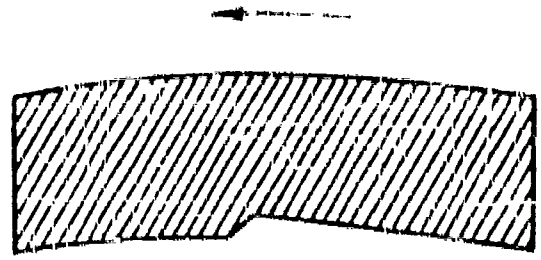

Class V

Fig. 4 Profiles typifying five general classes of flute design. Arrows indicate direction of compensative impulse for small numbers of flutes; for Class III flutes, direction of compensation depends on index angle as well as on number of flutes.

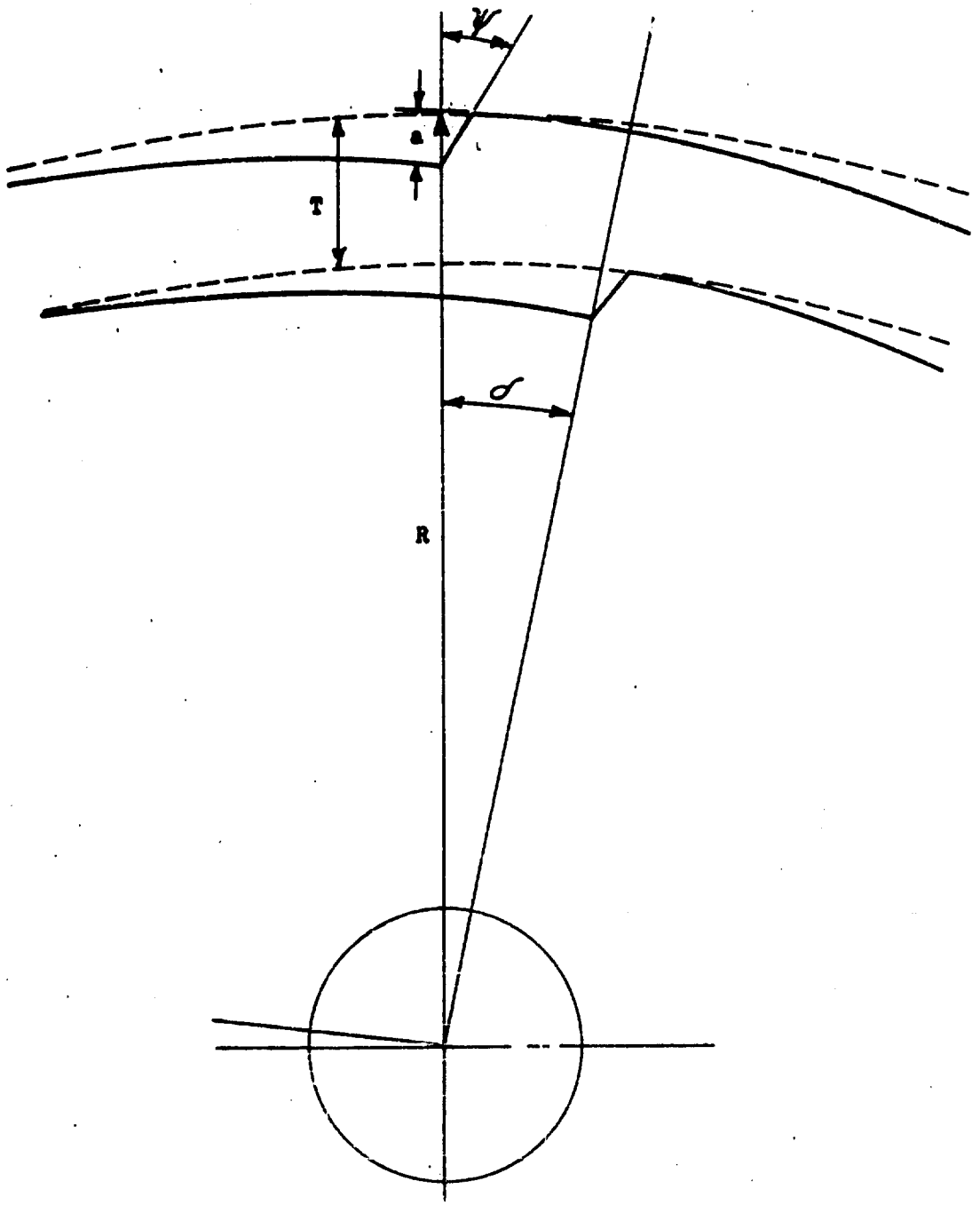

Fig. 5 Definition of design parameters for fluted cones.

Flute Design	Parameter Varied				
	μ	n	λ	ψ	δ
I	C*	C	C	-	-
II	C*	C*	C	C	-
III	C*	-	C*	-	C*, F
IV	F	F	C, F	-	-
V	F	F	-	-	-

*Note: Cases indicated by asterisks have been systematically investigated by strings of experiments in which only one parameter was varied insofar as control was attainable. In other cases, not so marked, two or more sets of tests are used as a basis for correlation. The C.I.T. liners are only nominally 57mm; actually they are about 0.2 in. smaller in base diameter than the liners now being used in shells.

This table should be referred to in reading the discussion that follows in order to ascertain the combinations to which any statement is known from experiment to apply, and those to which it can be applied only by inference.

The following statements briefly summarize the present state of knowledge of the dependence of fluted liner performance on the primary design parameters for flute types I, II, IV, and V. These may be considered "simple" flute designs, and follow relatively simple empirical laws. Type III flutes follow more complex laws because of the additional variable, index angle δ, which is peculiar to this particular design. All the known aspects of behavior of Type III flutes are discussed separately**.

For types I, II, IV, and V, then, the following relations have been found:

(1) Flute depth: For Types I, II and IV the optimum frequency of spin is approximately a linear function of flute depth, the magnitude of v_o increasing (regardless of direction) with increasing flute depth (20), (23). Departures from linearity are found at both very small and large flute depths, but these are of little practical importance because of the low-compensation frequencies attached to the former and the low penetrations obtained with the latter. Tests with Type V flutes have, as yet, revealed no systematic variation of v_o with flute depth (9).

**In the experimental data presented in the following, the experimental conditions are as follows:

C.I.T. (57mm liners) - Targets, mild steel
Standoff, 6 in. (3.7 chg. diam.)
Charge confinement, 1/4 in. aluminum

F.T. & R (105mm liners) - Target, mild steel
Standoff, 7 1/2 in. (2.1 chg. diam.)
Charge confinement, 3/8 in. steel

The experimental conditions will affect to some slight extent the evaluation of optimum frequencies and to a much larger extent the level of performance achieved and the variability.

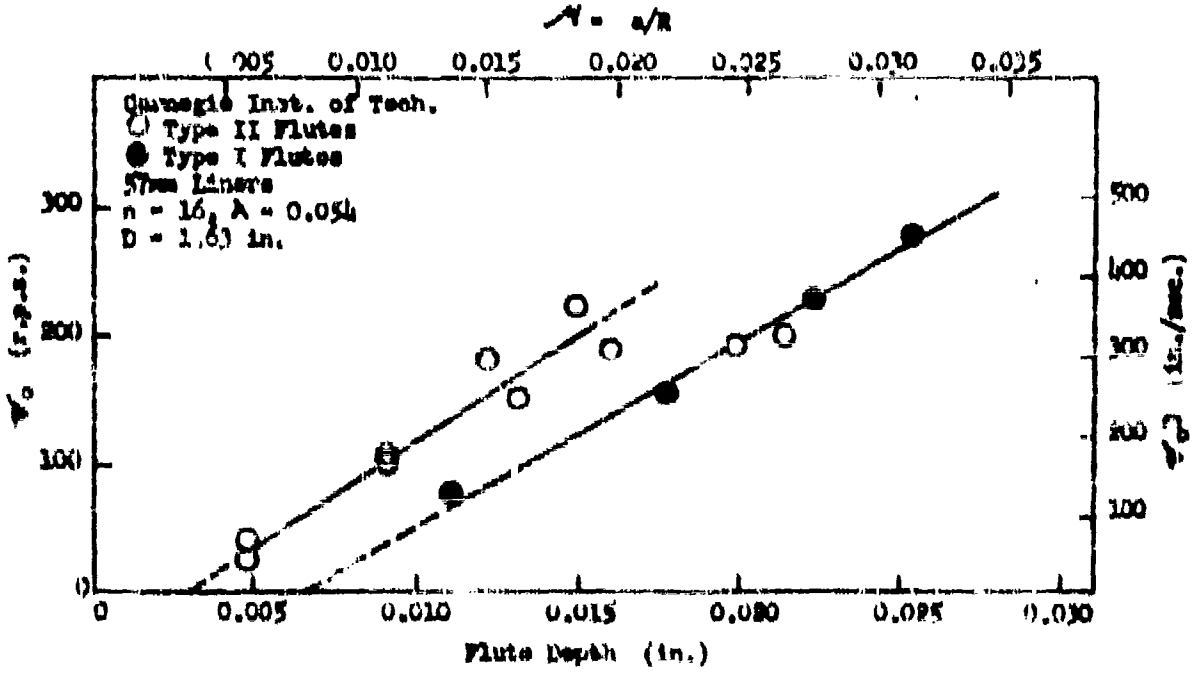

Fig. 6 Dependence of optimum frequency on flute depth for Type I and Type II flutes. The results are interpreted as being indicative of a fundamentally linear relationship, although it is generally masked for these types of flutes. For the Type II flutes, both the shape of the outer surface of the liner and the penetration obtained are consistent only over the middle of the range of flute depths covered, and a good linear correlation is obtained over that range. For the Type I flutes, the interior flute shapes become progressively sharper as flute depth increases over the entire range.

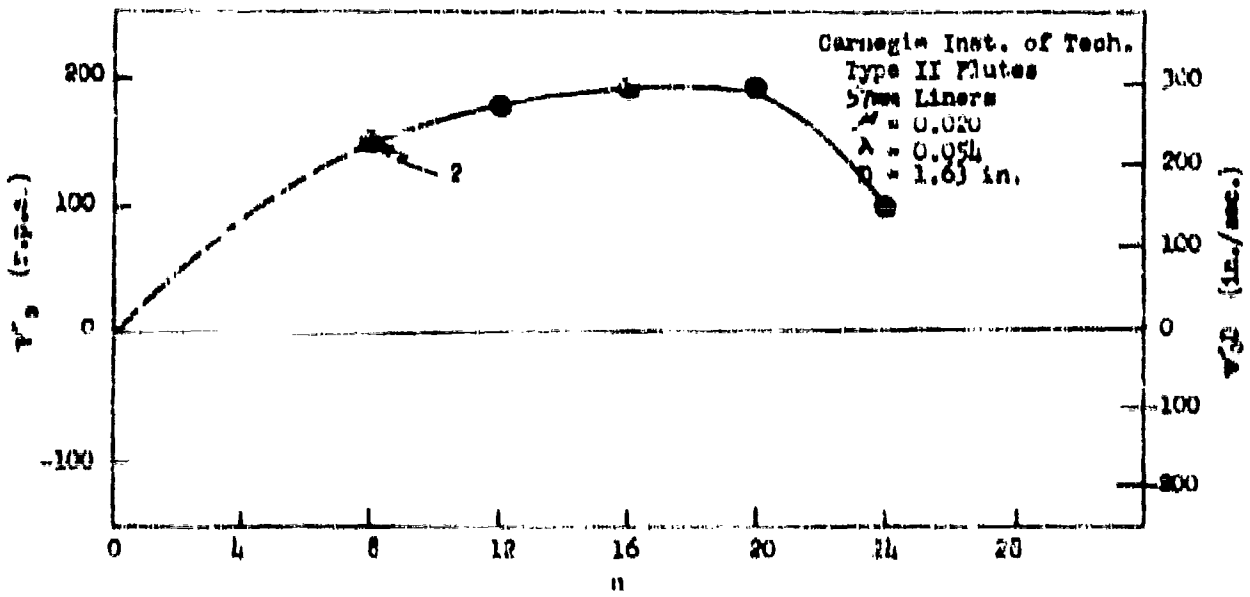

Fig. 7 Dependence of optimum frequency on number of flutes for a series of 57mm liners having Type II flutes of constant depth 0.016 inch.

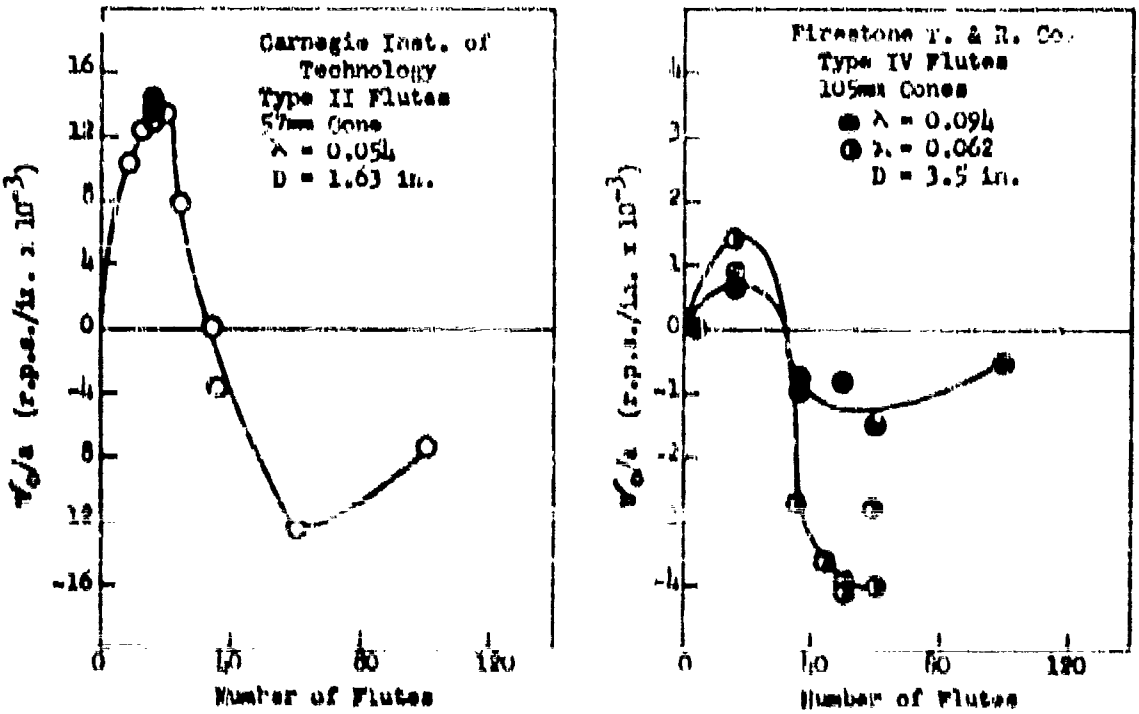

Fig. 8 Dependence of Ψ_0/a on number of flutes for Type II and Type IV flutes. The optimum frequency has been divided by flute depth in order to permit use of more data. The similarity of the curves for small and large liners, especially when λ is nearly constant, is particularly noteworthy. From the Firestone data, it appears that wall thickness considerably affects the relative magnitudes of the maximum Ψ_0/a for small and for large numbers of flutes. The number of flutes at which reversal in direction of compensation takes place is not a function of wall thickness, however. In Fig. 9 the thickness of the wall is taken into account and a single curve obtained for all liners of a given flute type.

Plots of typical data are shown in Fig. 6; further evidence is presented later in discussing a general correlation formula.

(ii) Flute number: The dependence of optimum frequency on the number of flutes is too complex to be briefly expressed. The experimental evidence shows that for Types I, II, and IV, flutes the optimum frequency first increases with increasing number of flutes to a maximum at about n = 16 (17), (22). Further increase in n produces a decrease in ν_o until, at about n = 32, no net compensation is obtained. Still further increase in n produces a reversal in the direction of compensation; the magnitude of the optimum frequency increases with increasing n, but approaches a saturation value for n > 60 (13).

For Type V flutes, no significant variation of ν_o with n has been found (9).

A plot of experimental results for $8 \leq n \leq 24$ for Type II flutes is shown in Fig. 7; in the tests represented, only the flute number was varied nominally. In Fig. 8 is a plot showing compiled results of a larger number of tests with Type II flutes (57mm) and Type IV flutes (105mm); the coordinate axes have been normalized so as to permit combination of results involving variations in flute depth.

(iii) Wall thickness: The best present estimate of the effect of wall thickness on compensation is that the optimum frequency decreases with increasing wall thickness as $1/\lambda^2$. A rapid decrease is to be expected on theoretical grounds, but more data are needed to verify the form of the relation. Wall thickness has a very drastic influence on the potential penetrating power of a fluted liner, aside from its effect on optimum frequency, which is discussed later in this chapter.

(iv) Offset angle: The accumulated evidence from variations in ψ indicates that, for values between 0 and 30°, variations of reasonable magnitude have little effect on the compensation (22), (23). For angles greater than 30°, variations become increasingly important, in agreement with theoretical considerations.

While the Firestone tests have not included sufficiently long strings of homologous designs to lead to the above conclusions separately, Winn has set up an empirical formula including all of the major design parameters except ψ (which has not been varied in general) and δ (applicable only for Class III flutes). The formula to which he fits his data is (6), (9).

$$f(n) = \nu_o T'^2 \quad \frac{R}{a}$$

where T' is defined as the minimum thickness of the fluted cone. For the Type IV and V liners used most by Firestone $T' = T - a = (\lambda - \mu)R$. It is desirable here to use a wall thickness that corresponds more nearly to the wall thickness of the blanks used for Type I, II, and III flutes, so that we can compare correlations. For this reason we shall here use an average thickness $\frac{T' + T}{2}$ for the Type IV flutes.

We shall take another liberty with Winn's correlation in order to bring it into closer agreement with the remarks made above concerning scaling. If the Firestone formula is rewritten in terms of the dimensionless parameters defined earlier, it yields

$$f(n) = v_o \frac{\lambda^2}{\mu} R^2 ,$$

implying that, for scaled liners, v_o varies as $1/R^2$. Actually, the Firestone data that are correlated involve such small variations in R that one can equally well justify using

$$f(n) = v_o \frac{\lambda^2}{\mu} R ,$$

which would agree with the remarks made above. Closer agreement between C.I.T. correlations with 57mm liners and Firestone's with 105mm liners is obtained in this way.

Fig. 9 shows correlations for 57mm liners with Type II flutes and for 105mm liners with Type IV flutes. The general similarity between the two is evident. It is also interesting to note the differences, which are presumably due to the difference in the type of flute used. The Type II flutes tend to give the highest values of f(n) for 16 flutes, whereas the highest values for Type IV flutes are obtained with about 50 flutes.

The most interesting feature of the type of correlation shown in Fig. 9 is that it does permit a reasonably good correlation of tests that are not simply related (i.e. are not parts of strings of tests). This fact lends considerable support to the remarks above concerning the dependence of v_o on various design parameters.

The behavior of Type III flutes is best described by considering series of tests in which only index angle has been varied. The results of a series of tests with 1 5/8 in. charges containing liners with 16 flutes of maximum depth 0.015 in. are illustrated in Fig. 10 (19). The relation between optimum frequency and index angle is, of course, cyclic, repeating itself at intervals of 360/n degrees - that is, at 22 1/2 degree intervals for the case illustrated.

It is evident from the plot that variations in indexing alone, and the attendant changes in relative magnitude of the competing mechanisms of compensation, cause drastic variations in optimum frequency. The range covered in the experiment illustrated is from +275 r.p.s. to -250 r.p.s. - i.e., a range of 525 r.p.s. Of especial academic interest are the index angles 1 1/2 and 11 1/2 degrees, at which the competing mechanisms exactly balance and produce zero optimum frequency. Of more practical interest are the indexings -1/2 (or +22) and 6 degrees, where the largest (absolute values) optimum frequencies were obtained. It is evident that there is a definite preference, on the basis of penetrating ability, for the 6 degree index angle.

The results illustrated in Fig. 10 have now been substantiated by tests with 105mm liners (10) that are approximate scaled models of the 57mm liners used in the original tests. The results of the larger scale tests are compared in Fig. 11 with the original; the close agreement between the two sets of observations is evident.

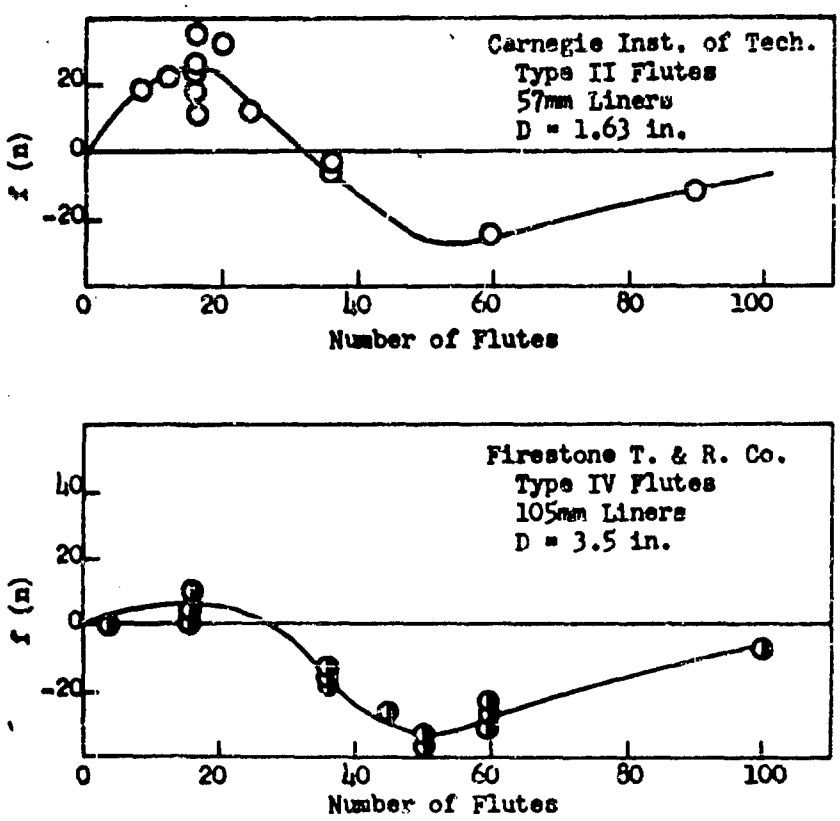

Fig. 9 Correlation of $f(n) = \nu_0 \lambda^2 R$ with number of flutes for both C.I.T. and Firestone data. This is a modification of the correlation function $\nu_0 \lambda^2 R^2$ used by Winn. The interesting feature is that a considerable variety of flute depths, numbers of flutes, and wall thicknesses are covered by the correlation. This indicates that the function does really depend, to a reasonably good approximation, only on the number of flutes. The similarities of the two curves are evident, especially as regards location of maximum and minimum values, and the null value of the function. The dissimilarities are also of interest since they are presumably characteristic of the different flute designs. The existence of such a correlation supports the conclusions drawn from individual experiments concerning dependence of optimum frequency on the various individual parameters of design.

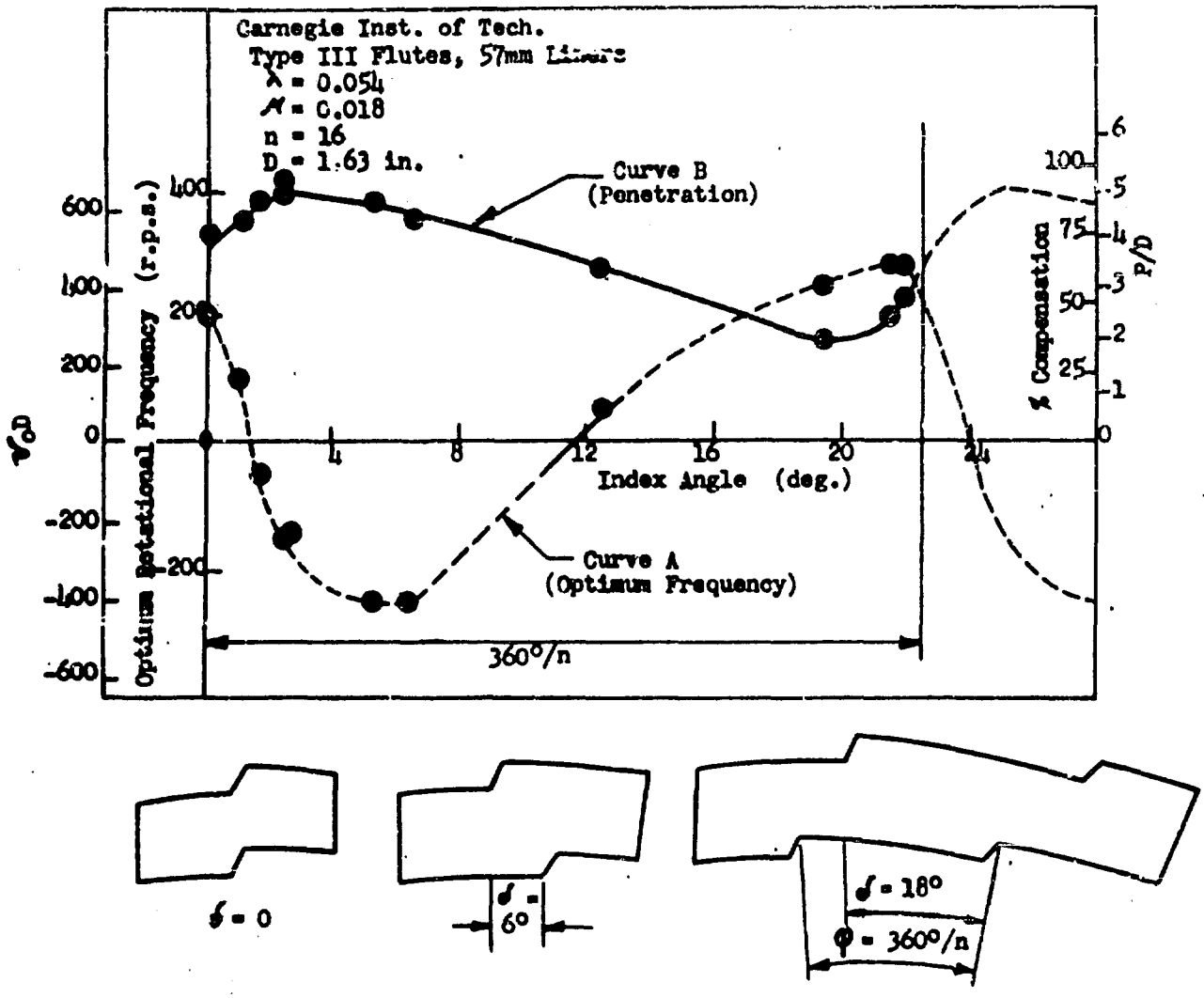

Fig. 10 Variation of optimum frequency (Curve A) and of penetration at optimum frequency for a specific group of liners with Type III flutes. Sketches illustrate appearance of liner profiles for several index angles. Variations in penetration are due to varied degrees of necking of the flute profile. Sketches illustrate change in flute contour with varying index angle.

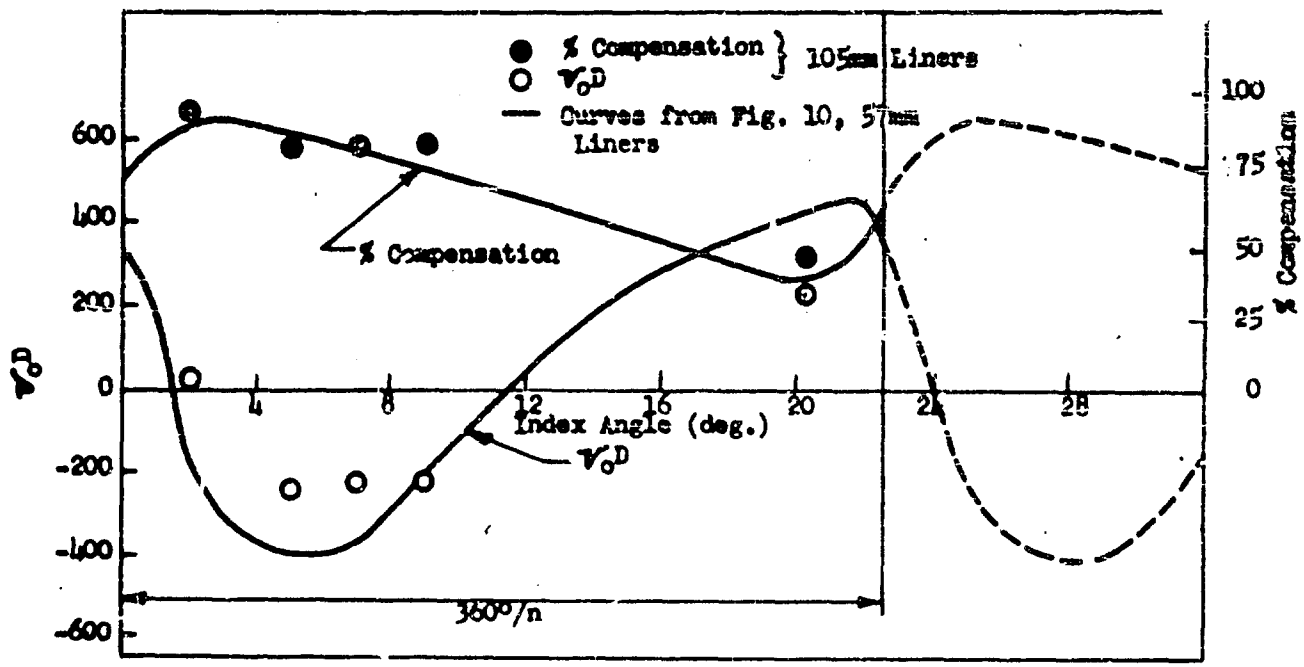

Fig. 11 Comparison of Firestone tests with 105mm liners having Class III flutes with results on 57mm liners. Coordinate axes are normalised to permit combination of data. Since the two sets of liners and charges were not accurate scaled models, exact quantitative agreement is not to be expected. The close qualitative similarity substantiates the original C.I.T. observations.

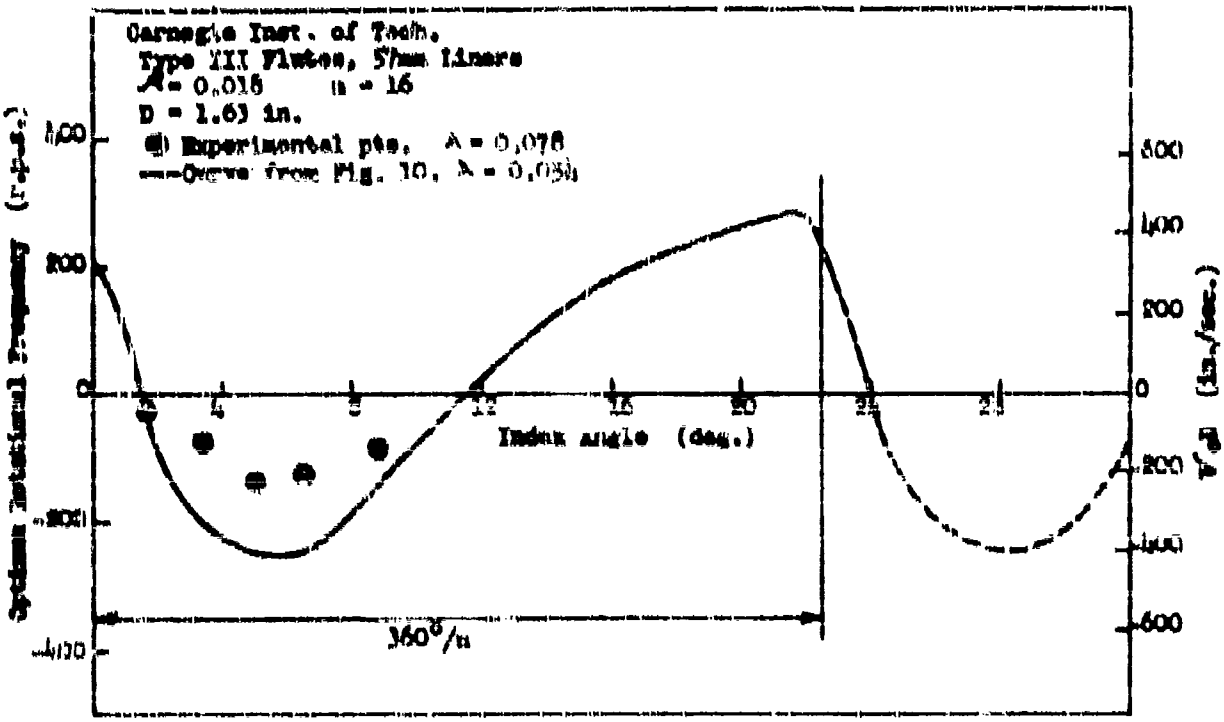

Fig. 12 Comparison of optimum frequencies at various index angles obtained with liners of 0.063 in. wall thickness and with 0.045 in. wall thickness. The experimental points representing the thicker liners are tentative and subject to slight changes pending completion of gauging analysis.

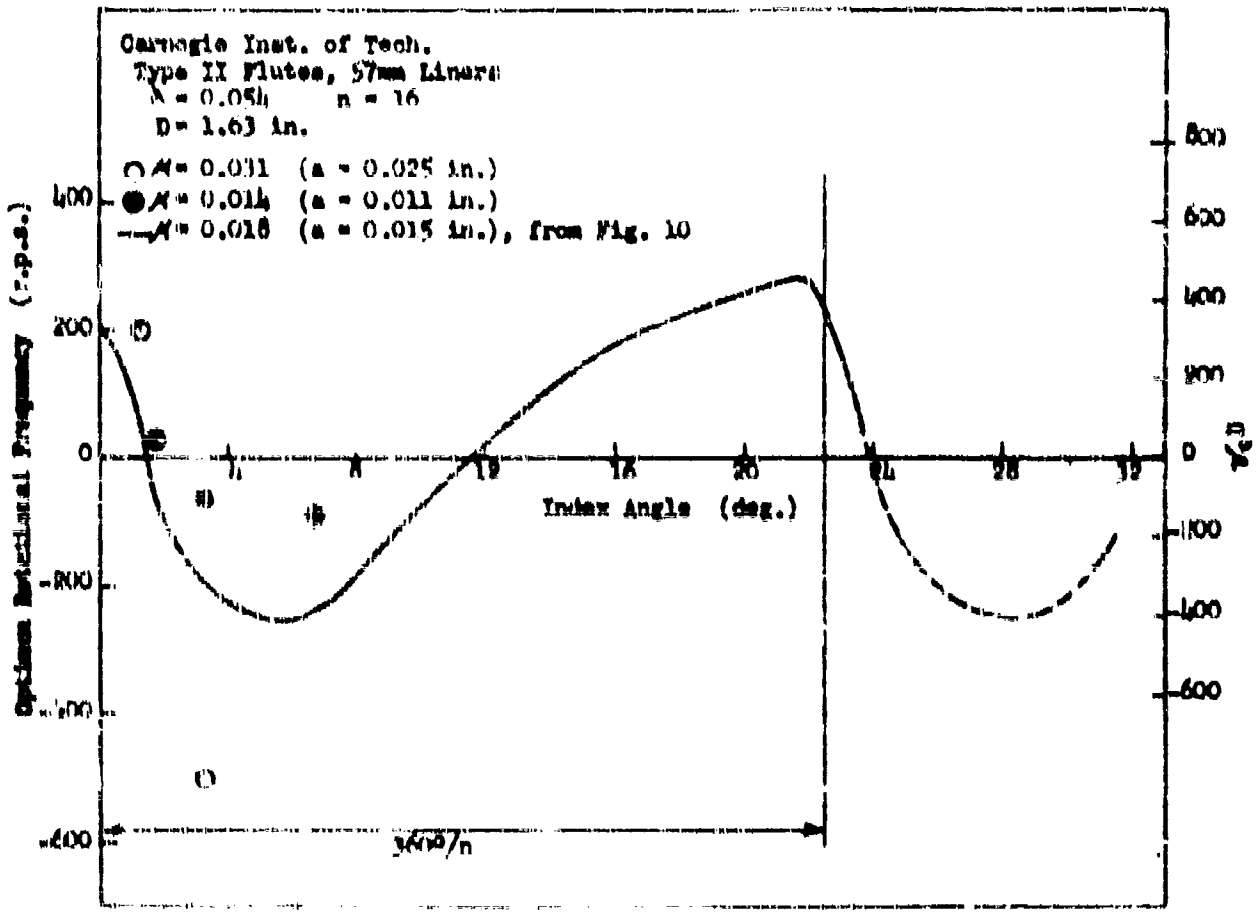

Fig. 11 Comparison of optimum frequencies at various index angles for three flute depths. The experimental points are tentative and subject to slight changes pending completion of gauging analysis.

A brief series of tests has also been completed with liners formed with the same dies used in the experiment illustrated in Fig. 10, but with liners of approximately 50% greater wall thickness (0.063 in. instead of 0.045 in.)* The results are compared in Fig. 12 with those of the original tests. While the general features of the two sets of observations are very similar, there is some evidence that the ratio of the optimum frequencies obtained with the two different wall thicknesses varies with the index angle and that the indexing at which zero compensation is observed may also depend upon wall thickness. If these indications are substantiated by further tests, it will mean that the behavior of Type III flutes cannot be reduced to simple empirical relations like those described above for the simpler designs.

Still a third set of experiments** are illustrated in Fig. 13. In these tests, the wall thickness of the liners was the same as that used in the original tests (i.e., 0.045 in.) but two different flute depths were used, one shallower and one deeper than in the original series. Both sets of observations exhibit general features similar to those of the first tests, although there is some unsubstantiated evidence of variations in the indexing that produces zero compensation and of a non-linear relation between optimum frequency and flute depth for a given index angle.

The fact that the behavior of Type III flutes is even more complicated than that of the four types formed with single dies should not be surprising. Variations in the additional variable, δ, produce complex changes in the geometry of the liner, and, consequently, in the shock interactions that affect spin compensation. The very considerable technical advantages of the Type IV flute, which are discussed more fully later, more than recompense for their more complex behavior.

The fluting of a liner can also affect its potential penetrating power quite drastically. Even though the impulses involved in compensation at spin rates attained thus far are too small to appreciably affect the basic character of the cone collapse or of the jet formed (i.e., specifically, one does not expect an appreciable change in the distribution of energy in the jet), it is quite evident from both Firestone and C.I.T. experiments that mechanical strength effects govern to a very large degree the depth of penetration obtained at optimum frequency. This is to be expected of liners having linear flutes (i.e., $\mu = \frac{a}{R}$ constant along the flute), since all theoretical and experimental evidence indicates that the ideal flute is far from linear. When a linear or any other non-ideal flute, the various

*A portion of the data used will be found in reference 21. The remainder have not been reported at the time of writing.
**Not yet reported at time of writing.

elements of the liner tend to compensate at different frequencies rather than at a common frequency of rotation. So long as the natural frequencies of adjoining elements are not too different, or so long as the liner wall is sufficiently strong to resist the tendency for relative rotation of the elements, this causes no serious difficulty. But if the liner is badly necked in the fluting, the strains set up by such a situation cause the liner to rupture instead of collapsing coherently and forming a jet. Theory, however, cannot be made to yield a usable design. The task of determining the ideal form of a/R as a function of position on the liner must for the present be an empirical one and has been undertaken, but no reportable results are available as yet.

The experimental evidence of deterioration in penetration due to mechanical strength effects is best illustrated by means of correlations between the depth of penetration at optimum frequency and the minimum thickness of the wall of the fluted liner. (Usually the minimum thickness is found near the base of the flute, where necking occurs). Fig. 14 shows plots for both C.I.T. and Firestone data (6) of correlations between the maximum penetration observed and the minimum wall thickness. It is evident that there is a critical value of the minimum wall thickness. When the thickness falls below this value, the penetration falls off very rapidly with decreasing thickness. There is, of course, a secondary correlation between flute depth and maximum penetration for any homologous series of cones, because increasing flute depth inevitably produces more pronounced necking of the liner wall and decreases the minimum wall thickness. Analysis shows that the primary correlation is that with minimum wall thickness, however.

One of the most interesting observations of this sort has been made in connection with the indexing tests described earlier. If the two curves, P_{v_o} versus δ and v_o versus δ, shown in Fig. 10 are used to eliminate δ, the plot of P_{v_o} versus v_o shown in Fig. 15 is obtained. Such a correlation is of practical interest although, as pointed out above, it does not represent any fundamental relationship (these same liners are included in the general correlation between P_{v_o} and minimum wall thickness shown in Fig. 14). Fig. 15 shows that for Type III flutes, within the limits of optimum frequency fixed by the values of μ, λ, n, etc. used, one can obtain a given magnitude of optimum frequency by four different indexings. But, because the different indexings result in different degrees of necking in the liner wall, different penetrations are obtained, so that there is a clearly optimum choice of indexing for overall performance*.

*Caution must be used in generalizing from Fig. 15. It applies only to a specific group of liners and does not in any way represent limitations on either the optimum frequency or the depth of penetration that can be obtained with other designs.

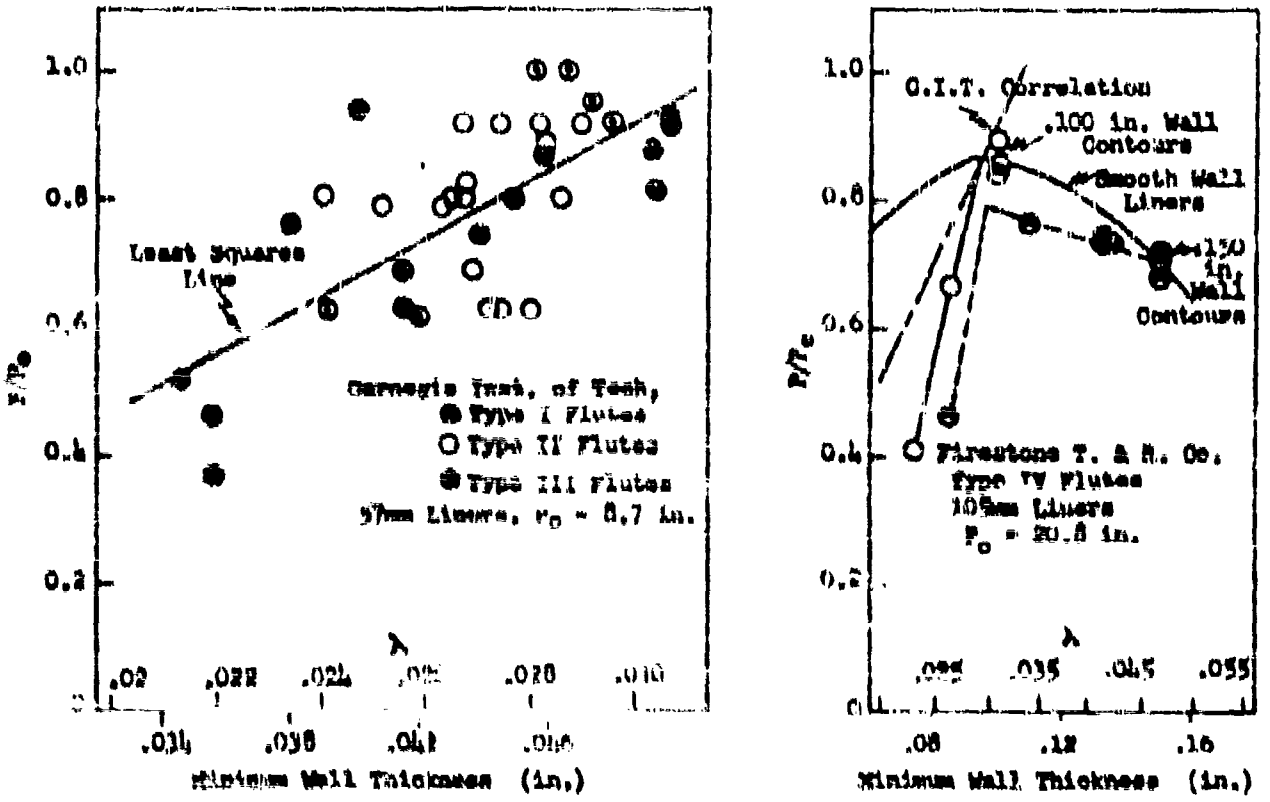

Fig. 14 Correlation between penetration obtained at optimum frequency of rotation and the minimum wall thickness across a flute profile. The observed penetrations have been divided by the penetration obtained from optimum smooth liners fired statically. The large scale plot of C.I.T. data on the left shows a great deal of scatter but a correlation is evident. It has been assumed that all three types of flutes included can reasonably be treated as a single statistical population in this treatment. On the right, the C.I.T. correlation line is shown with the correlation of Firestone data. The agreement is as good as can be expected in view of the scatter of the C.I.T. data and the relative sparsity of Firestone data. It is tempting to conclude that all four types of flutes follow the same correlation, and that linear scaling laws hold. (P_o indicates the average penetration by the best available smooth liners of each size.)

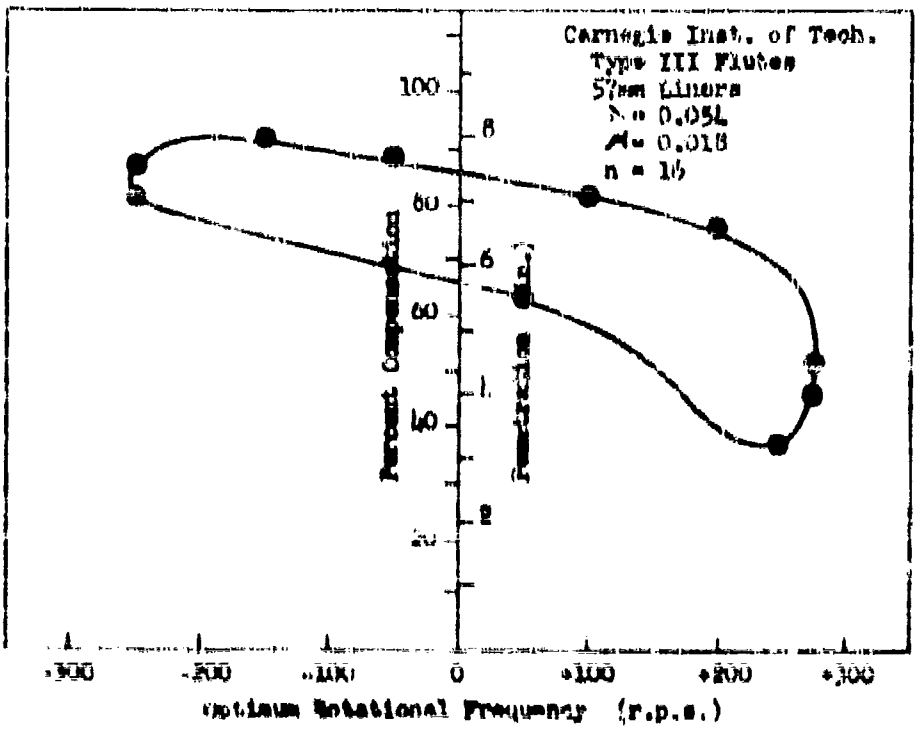

Fig. 15 Correlation between penetration at optimum frequency and the optimum frequency of rotation for a particular group of liners having Type III flutes, the index angle being varied. For any (absolute magnitude) frequency up to 250 r.p.s., any one of four index angles can be used. Only the one having the greatest minimum wall thickness is of practical interest, however, because it yields better penetration than the others. Consequently, only those liners corresponding to the upper left branch of the above plot ($1\frac{1}{2}° \leq \beta \leq 6$ degrees) are of interest. Since liners of this series follow the correlation of Fig. 10, it is possible to predict, within limits, the range of index angles that are of interest in a series of this sort. The range will, of course, depend on the specific values of h, Δ, etc. used.

While compromises between wall thickness and flute depth can temporarily provide suitable combinations of optimum frequency and maximum penetration, the ultimate solution is to eliminate the influence of mechanical strength effects by use of appropriate non-linear flutes.

Miscellaneous Observations Pertinent to Fluted Liners

(i) Fluted steel liners (18) and fluted aluminum liners (8) have been tested by C.I.T. and Firestone, respectively. Neither showed any spin-compensation benefit to offset the intrinsically poorer penetration by steel and aluminum jets.

(ii) Fluted trumpets have been tested briefly by E.R.L. (2) and C.I.T. (11), but showed no advantage over fluted cones as far as the tests were carried. They are considerably more difficult to manufacture, so that no further tests are planned unless experiments with smooth trumpets give evidence of some presently unknown advantage.

(iii) Spiral flutes were first tested by E.R.L. (2) and more recently by Firestone (7). No detectable advantage over straight flutes has been observed. It is entirely possible, however, that spiral flutes of smaller pitch than have been used might afford considerable benefits (See Chapter II). Theoretically, it is possible to reverse the direction of the transport effect by using a tight enough flute spiral, and make it reinforce rather than compete with the thick-thin effect. Accurate spiral flutes are more difficult to manufacture, but not exorbitantly so; the benefits derived may well be worth the extra effort involved.

(iv) Symmetrical flutes have been tested by C.I.T. with no significant results except to substantiate the dependence of penetration on minimum wall thickness for fluted cones.

(v) Special liners to which Thomas' theory (4) can be applied have been obtained by C.I.T., but are not of sufficiently high quality to justify testing. They have sine-wave flutes with wall thickness varying in an unsymmetric manner (16), and are extremely difficult to manufacture to close tolerances. They are of purely academic interest at present.

Variability in Performance of Fluted Liners and Tolerances Required

Exhaustive gauging data have been obtained by both Firestone and C.I.T. on all fluted liners tested except the earliest lots. C.I.T. has developed and built a special transducer gauge (15) for the purpose, which gives very precise measurements and permanent records of all measurements. No statistical tests have been made as

yet with any kind of fluted liner, however, since only small numbers are obtained, in general, and all are needed to determine relations between penetration and spin frequency. Conclusions concerning tolerances and their effect on performance must be drawn from a qualitative survey of observations on many lots of liners.

The accumulated data indicate that, for the types of liners tested to date by C.I.T. and Firestone, variations of the magnitude given below yield performance that is not appreciably more erratic than that of equivalent smooth liners:

Parameter	Permissible Tolerances (Nominal) 57mm	105mm
a	± 0.001 in.	± 0.002 in.
T	± 0.002 in.	± 0.004 in.
360°/n*	± 15 minutes	± 15 minutes
ψ	± 2 degrees	± 2 degrees
δ	± 15 minutes	± 15 minutes

*Note: The angle subtended at the axis by each flute.

The tolerances quoted are somewhat conservative. Quite respectable performance could be expected with somewhat more liberal figures. In the case of the 57mm cones, especially in the early tests, the variations in test pieces have been much larger than the tolerances given. There seems no reason, however, why reasonably careful techniques should not be capable of providing pieces well within the specifications".

The shapes of the flutes must also be consistent, of course, although it is difficult to give quantitative tolerance for shape. Other parameters should be kept to the same tolerances that have been established for smooth liners.

Methods of Manufacturing Fluted Liners

One of the chief obstacles in early research on spin-compensation was the procurement of suitable test pieces. The difficulties now have been very largely overcome, although manufacturers undertaking the task of producing fluted liners for the first time still sometimes experience recurrence of the old troubles.

"For detailed description of variability of several specific lots of 57mm liners, see "Related Charges", CIT-OSRD-R22 and CIT-OSRD-R23. Firestone reports have included detailed flute depth measurements on nearly all liners tested.

The only significant method of manufacture used to date is pressing. Firestone has made extensive use of machined liners of Type IV design, which are entirely satisfactory for laboratory purposes, for that one design only. The method is entirely unsuited to quantity production. Die casting has been considered many times, but thus far appears unlikely to yield pieces of adequate homogeneity or dimensional stability. It is improbable that die casting could compete with pressing on an economical basis, in any event. Electrodeposition of liners with flutes has also been considered, but never been attempted. There is little chance that such a procedure would be competitive either economically or in quality of product.

The first step in any of the manufacturing processes is the machining of a fluted punch (male die). This has been done, in cases where flat canted surfaces were tolerable, by simply machining the flutes directly into the punch with a milling machine. The more common procedure, which is necessary in producing the more desirable canted surfaces in the form of arcs, is to form a scaled-up replica of a single flute by milling, and then duplicating that profile on a smaller scale, any desired number of times (depending on the number of flutes specified) on a blank punch by means of a pantograph milling machine. For flutes whose depth is a linear function of liner radius, a simple two-dimensional template serves as an adequate template. For non-linear flutes, a three-dimensional replica is necessary. The National Bureau of Standards has developed a beautiful automatic guide arrangement for a pantograph machine, in which a two-dimensional template can be made to serve for either linear or non-linear flutes.

Most of the commercial suppliers of fluted liners have used matching fluted dies, the female being hobbed from a fluted punch. The chief requirement for producing good pieces in this manner is an intimate knowledge of techniques for making accurate dies, heat-treating to obtain maximum die strength, accurately controlled hobbing, and good technique in forming liners under conditions that produce unusually large stresses in the dies. In using matched male and female dies to form Type III flutes, provision must also be made for accurate control of the indexing of the dies. Type IV flutes are formed between a fluted female die and a smooth metal punch, Type V between a smooth female and a fluted punch. It has been found highly desirable to use loads of the order of 400 tons in forming 57mm liners and of the order of 900 tons for 105mm liners by this method. A relatively slow pressure application and a brief "dwell" at peak pressure (of the order of 40 to 60 seconds total) has also been found desirable in order to reduce elastic recovery of the liner metal and assure accurate reproduction of the flutes. This technique requires use of a hydraulic press, but the process can be economically accomplished by using mechanical presses and engineering the dies to allow for a certain amount of elastic recovery. Annealing of the blanks prior to forming would be desirable under these circumstances.

Firms and agencies that have used this method of manufacture include:

Frankford Arsenal
Bridesburg Station
Philadelphia, Penna.

Westinghouse Electric Corporation
East Pittsburgh,
Pennsylvania

The Pally Die & Mold Company
2900 Bradwell Avenue
Cleveland 9, Ohio

Mason, Shaver & Rhoades
Fifth Avenue & Congress Street
East McKeesport, Penna.

Eastern Tool & Manufacturing Company
1 Montgomery Street
Belleville, New Jersey

The cost of a complete set of dies to form Type III flutes has usually been of the order of $1000 for 57mm liners and $1200 for 105mm liners. The cost is less, of course, for Type IV and considerably less for Type V flutes.

The Type I and Type II flutes are made by a method developed at the National Bureau of Standards. Instead of using two metal dies, in this process one (smooth) die is fitted with a conical rubber pad. The blank liner is then pressed between a fluted tool and its rubber padded mate. Because the Bureau of Standards did not have a heavy press at the time this work was being done, all flutes of this type were formed at loads of only 75 to 100 tons. As a result, even the side of the liner formed by the metal die did not conform exactly to the die; the side toward the rubber pad was always formed with very much rounded flutes, of course. Although this process was ultimately developed to the point where satisfactory reproducibility could be obtained on a laboratory scale of production, it seems definitely unsuited to mass production. The Sanin Laboratory of Brooklyn is the only commercial supplier to use this method.

The Bureau of Standards also developed a procedure for making fluted female dies without hobbing that may be of considerable potential importance. The technique consisted of electrodepositing a cobalt-phosphorous alloy on a fluted punch; very accurate replicas were obtained in this manner. The cobalt-phosphorous die was then set in a tool-steel block for use in forming liners. The Sanin

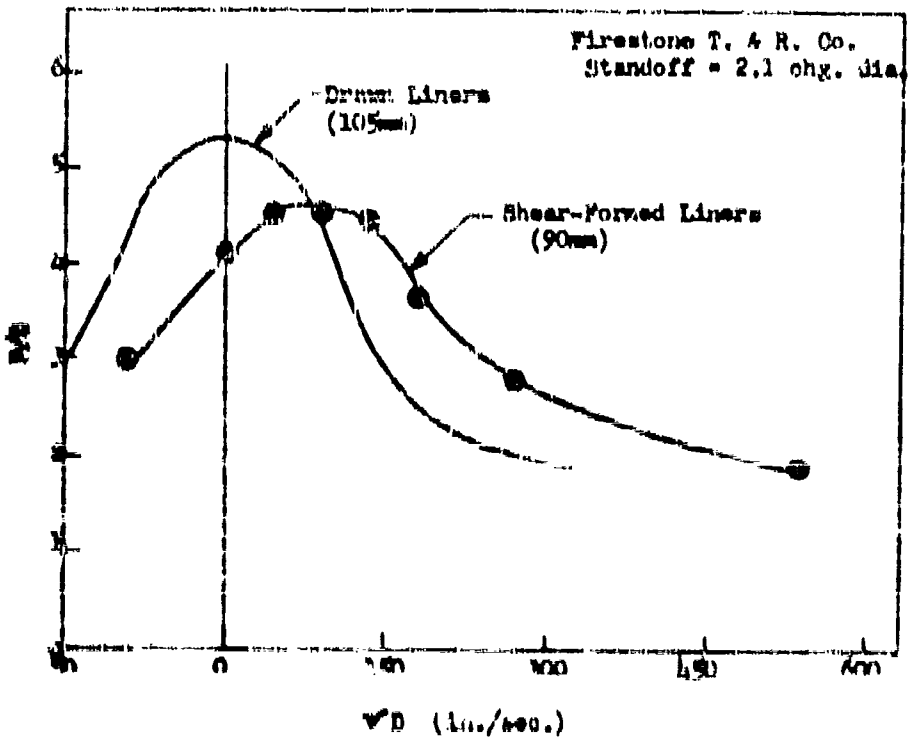

Fig. 1f Experimental observations by Firestone showing spin compensation by smooth liners made by shear-forming process.

Laboratory used this same procedure and applied loads of 360 tons to the dies without damage. The technique is more expensive than hobbing, and could be used by fewer suppliers, but might be useful in cases where extreme die precision is required.

Means of Spin-Compensation other than Fluted Liners

(i) The use of spiral detonation guides (variously called "lawnmowers" and "spiral staircases") to guide the detonation wave in sections along separate spiral paths have been tested by Firestone (5) and C.I.T. The technique introduces a component of impulse in the appropriate direction for spin-compensation. Experiments indicate that the principle operates as expected but that the optimum frequencies attainable without excessive loss of penetrating power are relatively low.

(ii) A technique of fluting the explosive adjacent to a smooth liner has been tested by C.I.T. (14) The flutings were similar to those ordinarily used on the liner. Spin-compensation was observed, as expected, but the procedure seems unlikely to afford as great benefits as fluted liners.

(iii) Very recently, Firestone has carried out a series of tests with smooth liners made by a "shear-forming" process*. The liners were very well made insofar as dimensional characteristics are concerned, and the charges were of standard design. The shear forming process, however, tends to produce spiral deformations of the liner, even though they may be invisible to superficial inspection. The deformations may be manifested in the final product by asymmetric variations in density, metallurgical properties, or dimensions. Liners made by this process had previously been tested statically at B.R.L.** and found to perform poorly; these results had prompted an analysis by Pugh (25) that may have some bearing on the Firestone results.

Firestone fired shear-formed liners of 90mm size at several different spin rates, obtaining the penetration depth versus frequency plot shown in Fig. 16. The liners showed a definite and, for liners of the size, fairly large optimum frequency. The tendency of these liners to compensate for spin is presumably due to the asymmetries caused by the method of manufacture. Much more experimental work must be done before the practical significance of this observation can be evaluated.

* Forty (41st) Progress Report of the Firestone Tire and Rubber Co., on BAT Project, Contract Nos. DA-33-019-ORD-33 and DA-33-019-ORD 1202, December 1953, pp. 43-46.

** Unreported. Editorial Note: These investigations have been reported and discussed in references (27), (28), and (29).

Conclusions, Future Prospects in Spin Compensation

The only important development to date in the field of spin-compensation is the fluted liner. The other techniques described above have been only cursorily investigated by experiment, but theoretical considerations give no hope that they would provide less complicated or more practical solutions to the problem. For the present, it seems best to concentrate on the fluted liner and continue its development.

So far as fluted liners are concerned, there is as yet no evidence of any benefit to be gained by using materials other than copper or shapes other than conical. Tests with a great variety of smooth liners (including cylinders and trumpets) and with various types of detonation wave shaping are being carried out in connection with fundamental studies at nearly all of the interested laboratories and the results inspected for any possible advantages in spin compensation. Until some evidence of a potential benefit is found, there is little profit to be gained by extensive experiments with varied types of fluted liners.

Of the various types of flute tested, the Type III, formed between matching metal dies, affords the greatest promise for practical application. Types I and II have exhibited no real advantages in the form of higher optimum frequency or better penetration and have a very grave disadvantage for application in that the shape of the liner surface adjacent to the padded die is not controllable. This makes it very difficult to design liners for a specific optimum frequency and at the same time tends to increase variability of performance.

Type IV flutes do not involve the lack of control in manufacture and have been used to very good advantage by Firestone in developing a highly satisfactory liner for slow-spin 105mm rounds. They lack the versatility and potential benefits of Type III, however. The possibility of indexing Type III flutes makes available greater flute depths without excessive necking of the liner (and consequent decrease in penetration) and without using heavier blanks (with the attendant drop in optimum frequency). The Type III flute has a very considerable advantage that is peculiar to it alone in that the optimum frequency of liners produced with a <u>given pair of dies</u> can be adjusted over a wide range by merely altering the indexing. Thus, the designer and the manufacturer are relieved of the necessity of designing and making dies that will yield <u>exactly</u> the desired optimum spin rate. Type V liners appear to have only academic interest, but are important in that respect for the opportunity they afford of better understanding of the spin-compensation process.

The determination of the proper variation of flute depth with position to have all elements of the liner compensate at the same spin rate is the most important problem at present. The linear flute used thus far is adequate for 57mm HEAT at present standard spin rates

(about 210 r.p.s.) and for 105mm HEAT slow spin shells (to at least 50 r.p.s.). The optimum frequency attainable with linear flutes may be pushed considerably above the present limits, but there seems no hope of achieving the high spin rates contemplated in proposed small calibre rounds (up to 1200 r.p.s.) or even the present standard spin for large calibre rounds without using non-linear flutes. The theory of spin compensation in its present state is of only nominal help in this problem. The means of obtaining an empirical determination are at hand, however, and the task has been started at C.I.T. There is no evidence as yet of any essential upper limit to the frequency at which spin-compensation can be achieved, but there are obvious difficulties ahead.

Spin-Compensation (by use of fluted liners) Compared with other Methods of Eliminating Spin Degradation

For standard small calibre weapons (57mm and probably 75mm) there is little room for argument concerning the best method of eliminating spin-degradation. Designs are already available and tested for fluted liners that will provide performance at the standard spin-rate of the 57mm H.E.A.T. round essentially equal to that obtained with smooth liners fired statically. The development of a comparable liner for 75mm rounds should be relatively simple. There is no comparison so far as simplicity and low-cost of application are concerned between fluted liners and the other methods available.

For larger weapons (90mm, 105mm, and larger), the situation is quite different. In the special case of the 105mm B.A.T. weapon, Firestone has found the slow-spin T-138 round with a fluted liner to be the best solution. Static, smooth cone performance is obtained at spin rates up to about 60 r.p.s. with available fluted liner designs, and shells have been designed that afford sufficient accuracy at spin rates below 60 r.p.s. The design is not a satisfactory solution to the general problem, however, because it requires a special rifle. It is necessary to find a shell design that can be fired from guns currently in the field or in production.

There are three alternative, exterior ballistic solutions to the problem under consideration. The concept of using peripheral jet engines on the shell to stop its spin before the target is reached has not yet been adequately tested. Firestone, in conjunction with Picatinny Arsenal, has some tests planned, but computations of the torque needed offer little hope that this method will prove practical

The use of bearing-mounted charges that permit part of the shell to spin, for stability, while the charge itself spins only slowly, if at all, has been proven practical by Firestone and Frankford Arsenal and by Midwest Research. Two designs have been used - one, a tandem arrangement, in which the front part spins; the other, a concentric arrangement in which the outer shell casing spins about a relatively

slow-spinning core containing the charge. Either design seems capable of providing charge spin rates of the order of 50 r.p.s. or less when fired from currently standard rifles. Clearly, a fluted liner is needed to compensate for even those low spin rates in large shells, and it immediately becomes critical to know whether the spin frequency of the charge is consistent.

A number of laboratories, both industrial and military have been working on fin-stabilised rounds. Both long-boom and folding-fin models have been designed that can be fired from standard weapons with apparently satisfactory accuracy. Even these have a small amount of spin imparted to them (ordinarily less than 20 r.p.s.) to improve interior ballistics, so a fluted cone might be desirable for large calibre shells.

A comparison of the bearing-mounted charge with the fin-stabilized shells is very difficult at present, because of the limited experience with bearing-mounted projectiles. It seems certain that they must weigh more than a standard spin stabilised projectile of similar calibre and that the concentric design demands the use of a smaller-than-normal liner. It is not at all certain, however, that they will weigh more or be more costly than finned rounds. The fin-stabilized shells involve some complications in design and firing, but would appear to offer the better solution of the two for larger calibre rounds.

It seems clear, however, that any technique for reducing the rate of spin of the charge must provide only an interim solution. Once a fluted liner can be designed to compensate for the frequency of spin of a standard round of any given calibre, it immediately provides the most convenient and economical solution to spin-degradation for that calibre.

REFERENCES

1. D. P. MacDougall, M. A. Paul, E. J. Bureik, "Target Penetration by the Jet from a Rotating Cone Charge," OSRD 5874, July 1943

2. D. P. MacDougall, M. A. Paul, E. J. Bureik, E. G. Broge, M. A. Strecker, "Target Penetration by the Jet from a Rotating Cone Charge," OSRD 5598, July 1944

3. T. E. Sterne, "A Note on the Initial Velocities of Fragments from Warheads," Ballistic Research Laboratories Report No. 648, September 2, 1947

4. L. H. Thomas, "A Zero Order Theory of the Initial Motion of Fluted Hollow Charge Liners," Ballistic Research Laboratories Report No. 765, December 1951

5. Secret Supplement to the Fourteenth Progress Report of the Firestone Tire & Rubber Company, "105MM Battalion Anti-Tank Project," September 1951

6. Secret Supplement to the Sixteenth Progress Report of the Firestone Tire & Rubber Company, "105MM Battalion Anti-Tank Project," November 1951

7. Secret Supplement to the Twentieth Progress Report of the Firestone Tire & Rubber Company, "105MM Battalion Anti-Tank Project," March 1952

8. Secret Supplement to the Twenty-Sixth Progress Report of the Firestone Tire & Rubber Company, "105MM Battalion Anti-Tank Project," September 1952

9. Secret Supplement to the Twenty-Ninth Progress Report of the Firestone Tire & Rubber Company, "105MM Battalion Anti-Tank Project," December 1952

10. Secret Supplement to the Thirty-Fourth Progress Report of the Firestone Tire & Rubber Company, "Battalion Anti-Tank Project," May 1953

11. E. M. Pugh, R. J. Eichelberger, N. Rontoker, First Bimonthly Report (CIT-ORD-R1), "Rotated Charges," August 31, 1948, Contract No. W-36-061-ORD-2879

12. E. M. Pugh, R. J. Eichelberger, E. L. Litchfield, Eleventh Bimonthly Report (CIT-ORD-R11), "Rotated Charges," April 30, 1950, Contract No. W-36-061-ORD-2910

13. E. M. Pugh, R. J. Eichelberger, E. L. Litchfield, Third Bimonthly Report (CIT-ORD-R15), "Rotated Charges," December 31, 1950, Contract No. DA-36-061-ORD-7

14. E. M. Pugh, R. J. Eichelberger, A. L. Litchfield, Fourth Bimonthly Report (CIT-ORD-R20), "Rotated Charges," October 31, 1951, Contract No. DA-36-061-ORD-28

15. R. J. Eichelberger, A. L. Litchfield, F. P. Baital, Second Bimonthly Report (CIT-ORD-R22), "Rotated Charges," February 29, 1952, Contract No. DA-36-061-ORD-122

16. N. Rostoker, R. J. Eichelberger, Fourth Bimonthly Report (CIT-ORD-R24), "Rotated Charges," June 30, 1952, Contract No. DA-36-061-ORD-122

17. R. J. Eichelberger, E. L. Litchfield, F. P. Baital, Fourth Bimonthly Report (CIT-ORD-R25), "Rotated Charges," August 31, 1952, Contract No. DA-36-061-ORD-122

18. E. L. Litchfield, F. P. Baital, R. J. Eichelberger, Sixth Bimonthly Report (CIT-ORD-R26), "Rotated Charges," October 31, 1952 Contract No. DA-36-061-ORD-122

19. F. P. Baital, R. J. Eichelberger, E. L. Litchfield, First Bimonthly Report (CIT-ORD-R27), "Rotated Charges," December 31, 1952, Contract No. DA-36-061-ORD-291

20. R. J. Eichelberger, E. L. Litchfield, F. P. Baital, Second Bimonthly Report (CIT-ORD-R28), "Rotated Charges," February 28, 1953, Contract No. DA-36-061-ORD-291

21. E. L. Litchfield, F. P. Baital, R. J. Eichelberger, Third Bimonthly Report (CIT-ORD-R29), "Rotated Charges," April 30, 1953, Contract No. DA-36-061-ORD-291

22. R. J. Eichelberger, E. L. Litchfield, F. P. Baital, Fifth Bimonthly Report (CIT-ORD-R31), "Rotated Charges," August 31, 1953, Contract No. DA-36-061 ORD-291

23. E. L. Litchfield, K. R. Becker, R. J. Eichelberger, F. P. Baital, Sixth Bimonthly Report (CIT-ORD-R32), "Rotated Charges," October 31, 1953, Contract No. DA-36-061-ORD-291

24. N. Rostoker, T. P. Murray, Second Bimonthly Report (CIT-ORD-37), "Fundamentals of Shaped Charges," February 29, 1952, Contract No. DA-36-061-ORD-122

25. E. M. Pugh, First Bimonthly Report (CIT-ORD-42), "Fundamentals of Shaped Charges," December 31, 1952, Contract No. DA-36-061-ORD-291

26. E. M. Pugh, R. J. Eichelberger, T. E. Morrisson, Fourth Bimonthly Report (CIT-ORD-M4), "Misnay-Schardin Effect," October 31, 1948, Contract No. W-36-061-ORD-2079

E. M. Pugh, R. J. Eichelberger, Twelfth Bimonthly Report (CIT-ORD-M12), "Minsnay-Schardin Effect," February 28, 1950, Contract No. W-36-ORD-2910

E. M. Pugh, R. J. Eichelberger, Fourteenth Bimonthly Report (CIT-ORD-M14), "Minsnay-Schardin Effect," June 30, 1950, Contract No. W-36-061-ORD-2910

27. L. Zernow and J. Simon, "Plastic Behavior of Polycrystalline Metals at Very High Strain Rates ($\sim 10^4$/sec.)", paper presented at Physical Society, Durham, N. C., March 26-28, 1953, Physical Review 91 233 A (1953).

28. L. Zernow and J. Simon, "Flash Radiographic Study of Grain Compensation in Shear Formed Liners (ITE)," Shaped Charge Journal Vol., 1, No. 1, July 1954.

29. J. Simon and L. Zernow, "Grain Compensation in Smooth Electroformed Liners," Shaped Charge Journal, Vol. 1, No. 1, July 1954.

CHAPTER IX

DEFEAT OF SHAPED CHARGE WEAPONS

R. v. Heine-Ge. ern

Carnegie Institute of Technology
Pittsburgh, Pennsylvania

Abstract

Of all possible means of defeating shaped charges, the most promising found to date consists of a combination of glass and steel armor. The glass may be in the form of plates, blocks, or large balls, possibly in conjunction with a suitable shock absorbing material. This means of protection has the advantage of low density and hence low over-all weight, in addition to utilizing the abnormal stopping power of glass, which has not been approached by any other method of passive defense. Titanium displays abnormal stopping power to a much smaller extent. Recent results suggest that explosive pellets or linear shaped charges can provide a very high degree of protection under certain circumstances, but these last two methods have not been developed to the point where they can be considered practical.

Introduction

The problem of protecting military vehicles and other targets against attack by shaped charges has been the subject of two recent papers (1), (2). It is assumed that the reader has access to these two papers; the current report requires some familiarity with their contents. Instead of starting from first principles, as is done in references 1 and 2, the present chapter will give a brief summary of the situation, and will discuss in detail the few methods of protection which appear most practical at the present time. In addition, an attempt will be made to clarify certain principles of protection which are frequently misunderstood.

The scope of this chapter is further restricted to the problem of preventing perforation of targets that are hit by shaped charges, neglecting the problems of increasing maneuverability to reduce the probability of a hit, of camouflaging the target, or of designing its interior so that a perforation will cause minimum destruction.

Weapons other than shaped charges will also be neglected, but it is very likely that adequate protection against shaped charges will defeat kinetic energy projectiles as well as squash-heads of comparable calibers.

Survey of Possible Protections

It has long been customary to distinguish between "active" and "passive" protection (3). The first type induces malfunction of the charge or of the ensuing jet. The second simply absorbs the kinetic energy of the jet.

Recent efforts on active protection have been centered around spikes (4), explosive pellets (5), and linear shaped charges (6) mounted on the outside of the tank.

In the case of spikes, it was found that they are ineffective against shaped charge projectiles with fast-acting fuzes, although they had been quite effective against the World War II weapons with slow fuzes. Explosive pellets and linear shaped charges are capable of spectacular performance against attacking weapons. The drawback at the moment lies in the fact that no sensing device has been developed which will allow them to function only when required, without setting them off as a result of small arms fire.

The design of passive protection is very simple in principle, since remarkably accurate predictions regarding the stopping power of any given combination of materials can be made on the basis of residual penetration theory (see below). Before considering this type of protection in detail, it is desirable to examine some of the pertinent implications of this theory and to clarify certain prevalent misconceptions regarding its applicability.

Comments on Residual Penetration Theory

The hydrodynamic nature of the penetration process was apparently first recognized by the E.R.L. group in 1943 (7) and was subsequently refined and expressed mathematically by Hill, Mott, and Pack (8) in England and independently by Pugh (9) in this country. From the point of view of protection, one of the most important consequences of this theory is given by the "density law"

$$dP_x/dP_y = \sqrt{\rho_y/\rho_x} \qquad (1)$$

where dP_x is the penetration in material x and dP_y that in material y, each caused by a given jet element of length dl, and where ρ_x and ρ_y are the densities of materials x and y.

Since this law is correct for the fast front elements of the jet and definitely incorrect for the slow rear elements, complete predictions regarding the performance of various target materials (singly or in combinations) could not be made until the residual penetration theory was developed by Pugh and Fireman (10), (11). This theory, recently summarized in reference 1, is very important for the whole problem of passive protection. A few of its aspects which are particularly important are discussed here in some detail.

a. Residual penetration theory compares the stopping powers of two materials by using equal thicknesses of both, the thickness to be such that only the faster parts of the jet will be absorbed in the materials under examination. The stopping powers of the materials are expressed in terms of residual penetrations into a standard material, usually mild steel or armor plate. This method is adopted in order to compensate for an over-simplification inherent in the basic theories of references 8 and 9. These theories assume that the entire penetration process is of hydrodynamic character, i.e., the pressure exerted by the jet on the target is so great that the strength of the target material is negligible compared to it. While this is nearly true for the fast moving front portion of the jet, it is not true for the much slower moving rear portion.

In the procedure described above, the two materials under test are used to absorb only the fast portion of the jet, while the slow portion is absorbed in a single standard material so that deviations from the hydrodynamic density law will tend to cancel out.

b. Residual penetration theory makes no assumptions regarding the shape of the penetration-standoff curve (Fig. 1) for the charge under consideration, but uses the experimentally determined curve to predict the stopping powers of various materials. The simple density law expressed in equation 1 is frequently visualized in the integrated form $P_x/P_y = \sqrt{\rho_y/\rho_x}$. This simple integration is justified only if all the jet elements have the same high velocity, high enough so that the strengths of all target materials may be neglected. Even then the integration would be exact only for perfectly aligned jets. Since these two conditions are never satisfied in practice, the few experiments in which P_x/P_y was observed to be equal to $\sqrt{\rho_y/\rho_x}$ must be considered accidental.

To illustrate these considerations by just one example, consider the comparison between a soft aluminum alloy (such as 2S) and a hard one (such as 24ST). In the light of the preceding remarks one would expect different total penetrations into the two materials, the strong 24ST alloy exhibiting the higher stopping power. When the comparison between the two materials is made by the method outlined above, the two materials exhibit nearly equal residual penetrations and therefore equal stopping powers against the fast portion of the jet.

c. The conical liners used in service weapons and in most laboratory charges have apex angles in the neighborhood of 45°. The comments made under (a) concerning deviations from hydrodynamic theory, and hence from the density law, become even more pertinent for liners of larger apex angles such as the DuPont "Jet Tappers" with their 80° cones. In general, the wider the cone angle the slower the jet and the more readily target strength will become apparent. When looking for exceptions from the density law among a number of materials, a wide-angle cone will identify the exceptions more readily than a

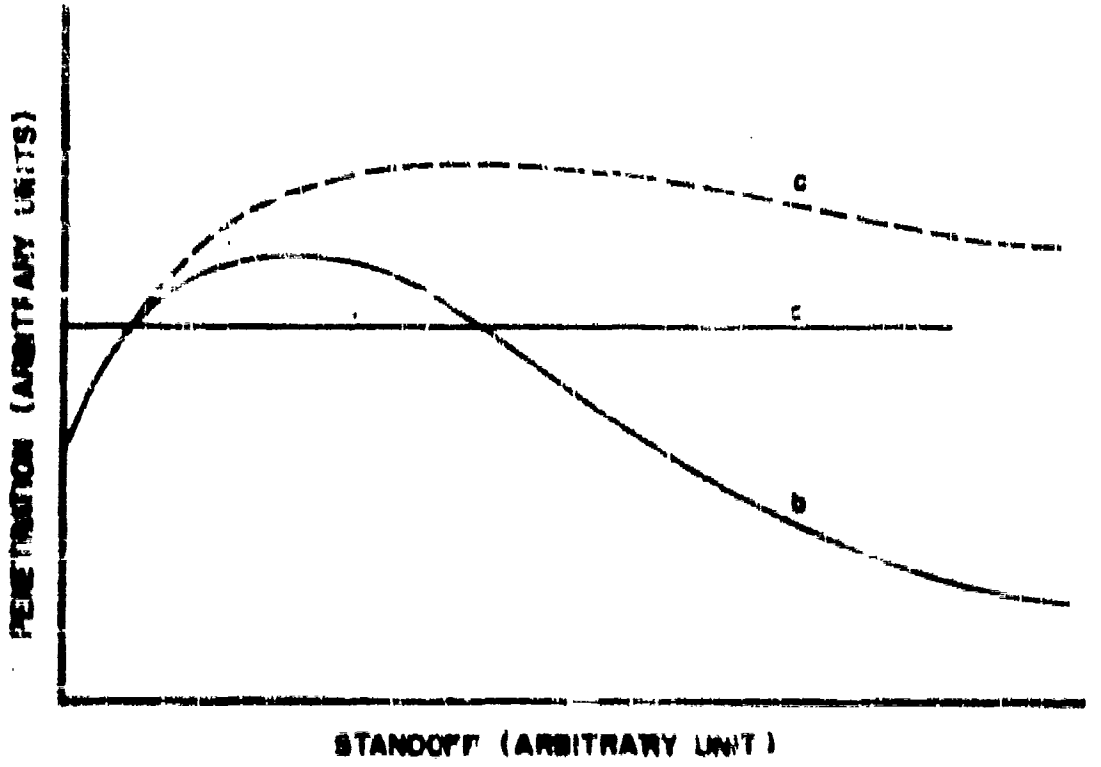

Fig. 1 - Penetration standoff curves for three hypothetical charges.

Curve a : Idealized (but not ideal) charge, without velocity gradient and without tendency of the jet to "waver" or disperse.

Curve b : Typical poor charge with small optimum standoff and rapid fall-off at larger standoffs.

Curve c : Typical good charge with large optimum standoff and gradual fall-off at larger standoffs.

narrow-angle cone, but it must be remembered that a material which shows considerable "abnormal" stopping power (see below) against slow jets from wide-angle cones may display very little of it against fast jets from small-angle cones.

d. Residual penetration theory answers the frequently raised question regarding the effectiveness of spaced armor or skirting plates as follows. The question is meaningless unless the exact position of the skirting plate is super-imposed on the penetration-standoff curve of the attacking projectile. If the projectile detonates at less than optimum standoff, then the air space between skirting plate and basic armor may actually increase the resultant penetration by increasing the standoff more nearly to optimum value. For charges fired near optimum standoff, skirting plates will be effective only against relatively poor charges such as those represented by curve b in Fig. 1, but will be quite ineffective against the good charges whose penetration-standoff curves have the appearance of curve c.

e. According to residual penetration theory, alternate layers of high and low density material will provide less protection than the same thickness of a single material having the same average density as the laminated target. An actual case is illustrated in Fig. 3 of Ref. 1, where solid aluminum is shown to be more effective than a target of the same thickness and areal weight, but composed of thin steel plates separated by air-spaces.

Thus, while spaced armor or skirting plates were useful against the relatively poor projectiles of World War II, they will be worse than useless against projectiles capable of defeating armor at long standoffs by virtue of proper design and construction.

Design of Passive Protection

Equal degrees of protection can obviously be obtained from a large thickness of low density material and from a small thickness of high density material. To illustrate this by an extreme example, assume that a given charge gives a penetration of 10 in. of armor plate at optimum standoff and of 1 in. armor plate at a standoff of 20 ft. For this particular case it might be said that 9 in. of armor plate provides the same protection as 20 ft. of air. Since the latter has obviously less areal density than the former, it might be considered superior to the armor plate on a weight basis. For practical purposes the density of materials which might be considered will vary from about 2 (magnesium or Dow metal) to about 11 (lead) or more probably from 2.7 (aluminum) to 7.8 (steel or homogeneous armor).

As pointed out in some detail in reference 1, penetration theory indicates that even over this limited range of densities, the less dense material is always superior to the denser material on a weight basis, but inferior on a thickness basis. Specifically, the following approximate relations hold for most materials: For any desired amount of

protection, the required areal density varies as $1/\sqrt{\rho}$, while the required thickness varies as $\sqrt{\rho}$. To illustrate this, consider a 5 in. thickness of armor plate which is to be protected against a shaped charge capable of perforating 10 in. of armor. The necessary protection could be provided either by an additional 5 in. of armor (about 200 lbs/ft^2) or by an additional 8.5 in. of aluminum (about 120 lbs/ft^2). Except for economical considerations, it is primarily a matter of weighing the thickness advantage of armor plate (3.5 in) against the weight advantage of aluminum (80 lbs/ft^2).

Glass

The abnormal* stopping power of glass, first reported by the author in 1945 (12), (3), has only recently been verified by two other research laboratories (13), (14).

Briefly summarized, the following observations have been made on glass:

A. Its stopping power is nearly independent of its chemical composition or heat treatment (15).

B. A glass target consisting of a few thick plates is more effective than an equally thick target consisting of many thin plates (16), (17).

C. Starting from small areal dimensions, the effectiveness of glass increases as its areal dimension is increased, until the linear dimension of the glass plate is about 3 charge diameters (16), (17).

D. Targets made of smooth glass plates perform better than targets made of glass having rough surfaces. Good mechanical contact between all glass-to-glass and glass-to-steel interfaces improves the performance of the target. However, the detrimental effect of rough surfaces can be reduced by separating the individual plates with shock absorbing materials such as thick plates of gasket rubber (2).

E. Glass is most effective against the fastest moving front portion of the jet and loses most of its abnormal performance when used to absorb the slow rear portion of the jet. As a corollary, the first few plates in the stack of glass plates are more effective than the plates near the bottom of the stack (18).

F. Glass is more effective against copper jets than against steel jets (19). It is very probable, but has not yet been verified experimentally, that glass is more effective against jets from ductile materials than against jets from more brittle materials.

---

*The term "abnormal" refers to the fact that it does not behave like a material of density 2.5 gm/cc, but rather like a material having many times this density. Although hundreds of materials have been tested, glass and glass-like materials are the only ones which have significantly abnormal stopping powers when tested against high speed jets using the Pugh-Fireman procedure.

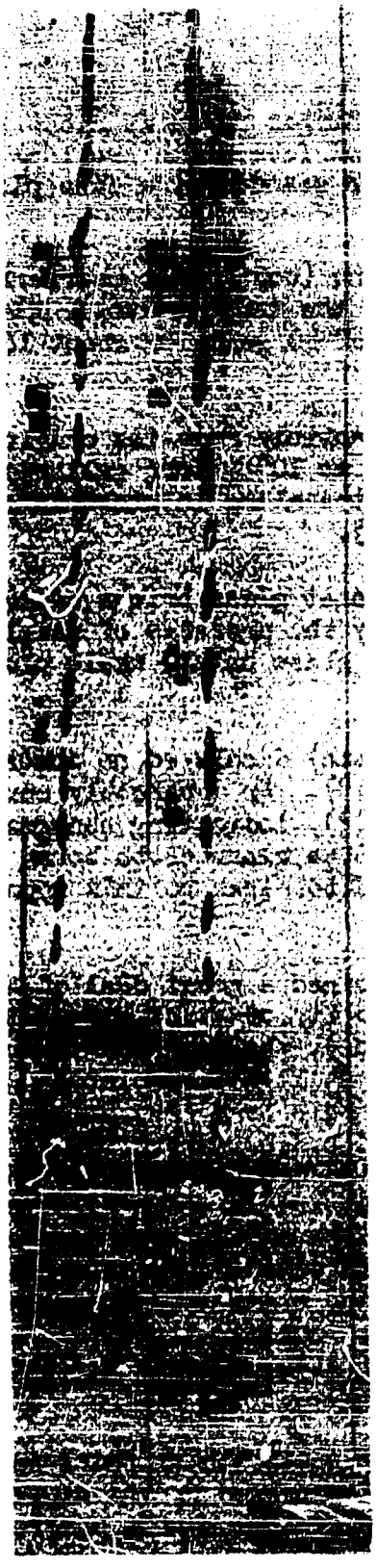

FIG. 1a. Radiograph of jet from 105mm copper liner after passing through six inches of 1020 mild steel

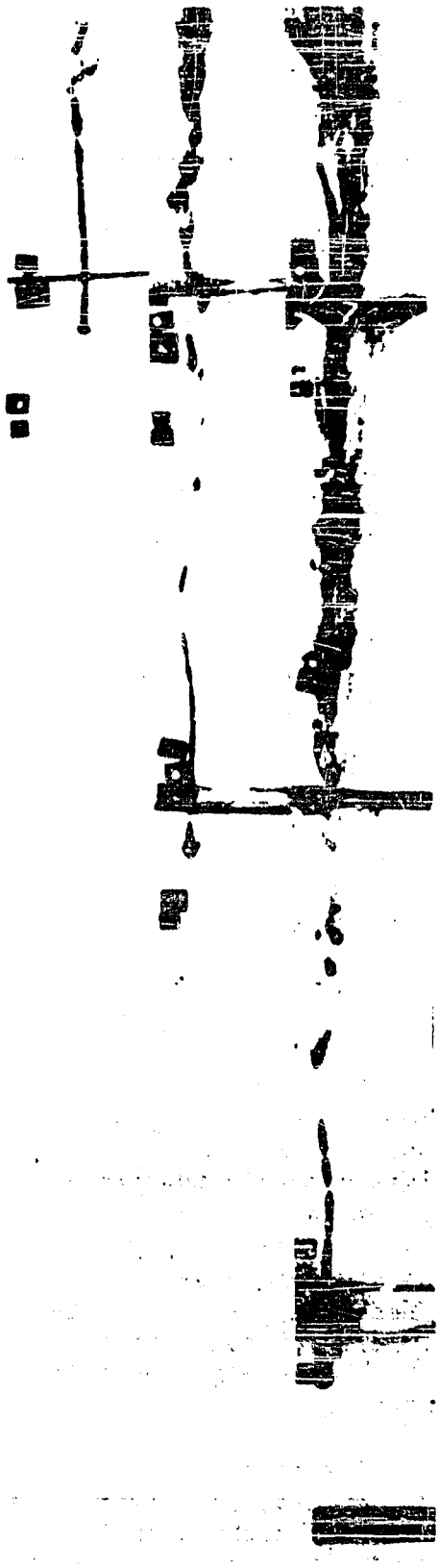

FIG. 1b. Radiograph of jet from 105mm copper liner after passing through five inches of glass protected by 1/2" steel and 1/4" rubber

"Photographs by courtesy of L. Zernow and J. Simon, Ballistic Research Laboratories."

G. Glass is most effective against charges fired at close to optimum standoff (19). In that case a steel face plate provides only little additional benefit (20). At smaller standoffs, a face plate seems to be desirable (20).

H. Under the most favorable conditions (copper jet charge fired at optimum standoff, glass near the top of the target, etc.), glass frequently behaves as if it had a density of 40 gm/cc or about 16 times its actual density.

I. Glass does not deflect a jet perceptibly from its original direction for angles of incidence as small as 10°. Kerr cell pictures taken under those conditions show the jet traveling in glass in exactly the same direction as the incident jet (21).

J. Plate glass performs better than cast glass bricks of equal thickness (20). This is probably caused by the presence of small imperfections, especially air-bubbles in the glass brick, while plate glass is quite free of such imperfections.

K. Doron (glass fibers bound to plastic) displayed no abnormal properties when tested by Carnegie Tech. (18). An apparently contradictory result was obtained by Flintkote (22), indicating abnormal stopping power on the part of Formica FF-55, a glass cloth bound to plastic. Additional experiments are needed to clear up this apparent contradiction in results.

While the Carnegie Tech group has obtained a great deal of additional information on glass (e.g., the velocity of shock propagation, the velocity of crack propagation (23), etc.), the mechanism responsible for the unusual stopping power of glass is still not completely understood. Kerr cell pictures obtained by Carnegie Tech (24) and more recent radiographs obtained by Zernow and Simon of B.R.L., prove beyond doubt that glass disrupts the jet during the penetration process in the manner suggested by this author (24). The B.R.L. radiographs are shown in Figures 1a and 1b. It seems very probable, but remains to be proven experimentally, that the stopping power of glass is caused by the same mechanism as the "rebound" effect (24), (25). Whatever the explanation, glass possesses the unusual property of being most effective against the charge with the highest possible penetrating ability, a remarkable asset for any protective material.

The remarkable manner in which glass adjusts its stopping power to the penetrating ability of the charge is illustrated by the experimental results presented in Fig. 2. Starting from zero standoff, the residual penetrations expected on the basis of hydrodynamic theory increase steadily until they double at optimum standoff, while the observed residual penetrations remain constant.

A recent BRL report (14) shows the results of a very complete series of tests on the performance of glass against statically fired 3.5 in. bazookas. Under the conditions of these tests the most effective thickness of glass did not exceed appreciably the stopping power of an equal

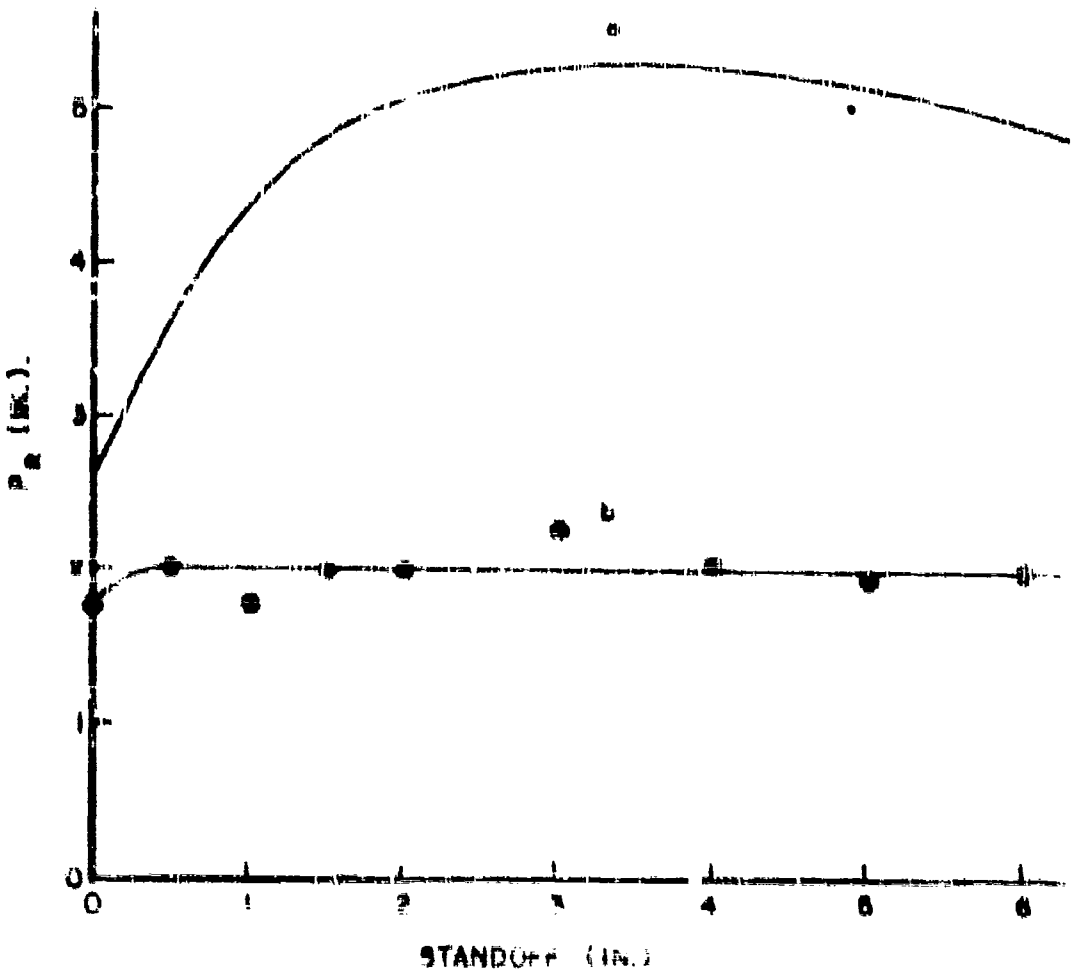

Fig. 2 - Residual penetration (P_R) versus standoff.

Target: 1/4 in. mild steel face plate
6 plates 1/2 in. homogeneous glass

Charge: Copper cone

Curve a: Theoretical Penetrations

Curve b: Experimental Penetrations
(averages of 10 shots)

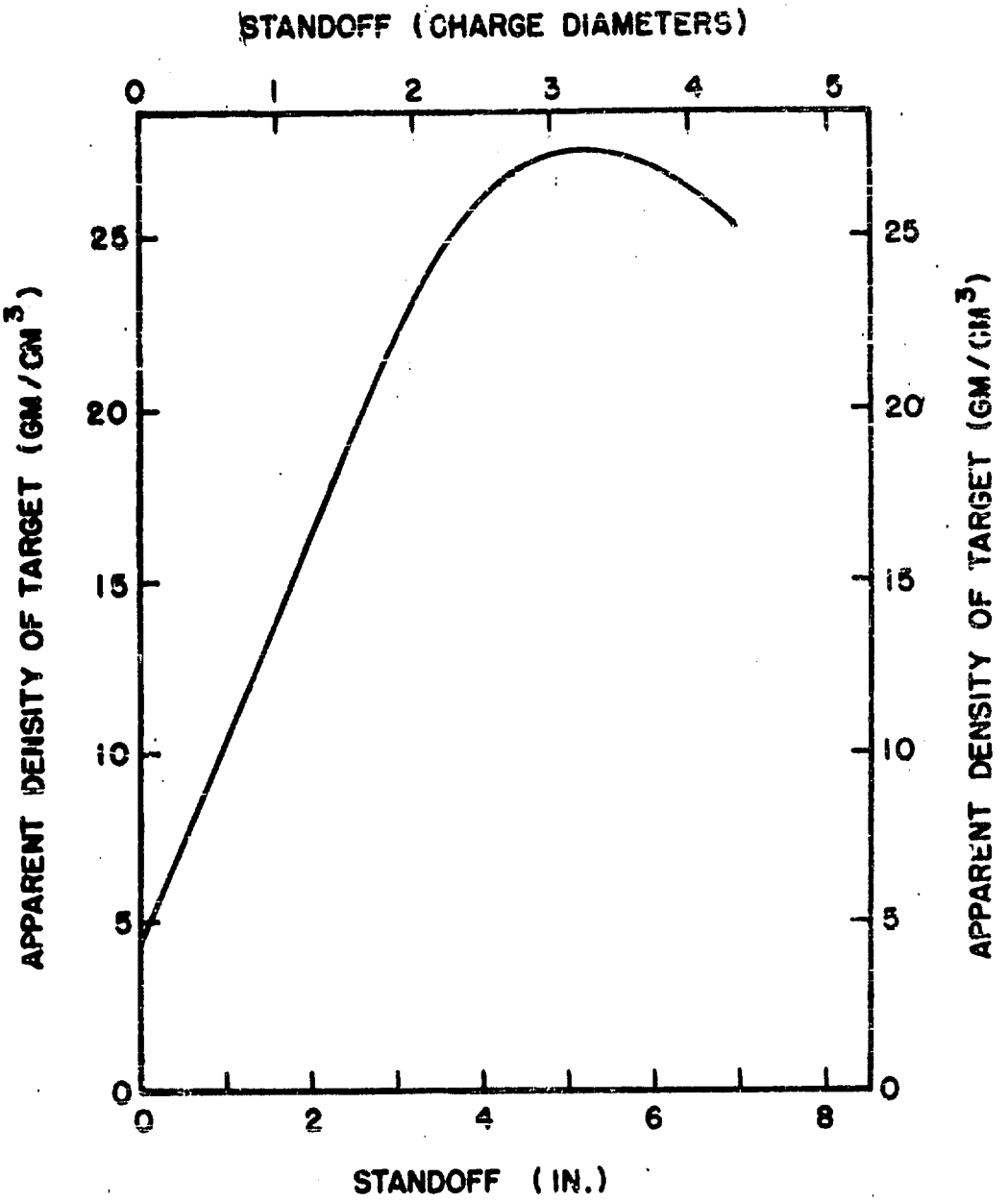

Fig. 8 - Apparent density of a glass target versus standoff.

Target: Stack of 6 plates of 1/2 x 3 x 3 in. hammered glass, with 1/4 in. mild steel face plate

Charge: C.I.L. standard, [illegible] copper cone

thickness of mild steel, which would be considered rather poor performance by this group. This poor performance can probably be ascribed to the fact that the BRL experiments were carried out without steel face plates, and that the bazooka has a built-in standoff, provided by the ballistic cap, of only 4.2 in. or 1.2 charge diameters. (Fig. 3 shows how the performance of glass varies as a function of standoff for the CIT standard charge, similar in most essentials to the 3.5 in. bazooka.) There is little doubt that increasing the standoff of the bazooka and providing face plates for the glass targets would provide complete agreement between the results obtained by BRL and those obtained by Carnegie Tech.

The relevant observation (or prediction) to be made here is the following: Suppose that two tanks were protected against the 3.5 in. bazooka, one using aluminum and the other using glass protection. Both of these designs could be carried out in principle on the basis of recent BRL results. Suppose further that after the tank had been protected as specified, the performance of the attacking weapon were suddenly improved considerably by providing it with a greater standoff. This would mean that the aluminum protection on the first tank would become inadequate against the improved weapon; glass, on the other hand, is somehow able to compensate for this improvement in the attacking weapon (Fig. 2), and the second tank would still be adequately protected. In other words, glass is probably a much better protective material than would be suggested by the BRL observation that at best it about equals mild steel on a thickness basis.

It remains to consider very briefly the manner in which glass must be used in order to provide maximum protection for tanks. (Details of fastening any proposed protection to tanks will not be considered here.)

The most effective protection would probably employ a total thickness of glass equal to one to two charge diameters. The required thickness would be made up of individual plates, each of maximum available thickness, or of glass bricks. In either case, each piece would be separated from its neighbors by a shock-absorbing material such as sponge rubber, gasket rubber, magnesia, etc., to minimize shattering and cracking. (By virtue of the presence of such absorbing materials, this type of protection would probably be quite effective against attack by squash-heads.) A number of such stacks of glass plates or bricks will be enclosed in a steel panel of such size as dictated by the geometry of the tank surfaces and considerations of ease of handling.

The outside surface of each panel should consist of 1/2" to 1" armor plate to protect the panels against small arms fire, and the inside surface resting against the tank's basic armor should be strong enough to prevent appreciable buckling of that surface after a hit.

There is also the possibility of using glass in the form of very large balls, each 3 inches or more in diameter, densely packed in a

steel panel with all voids filled with a mastic binder such as the one used by Flintkote. While this method would be less effective than the ones just discussed, it would have the advantage of smaller costs and easier manufacture.

It should be remembered that the basic armor of the tank to which these panels are attached is a very necessary part of the protective device. Tests on such panels should never be made without this armor plate backing. The panels will effectively stop the fast front end of the jet, but hard armor plate remains the most effective material against the slower rear portion.

Recently, a major advance has been made on the subject of protection by the personnel at Detroit Arsenal, who found that armor could be cast around a solid core of fused silica without resorting to any unusual casting procedures. Preliminary tests of such protective panels against conventional armor-piercing ammunition as well as shaped charges appear quite encouraging. This subject is now under extensive investigation.

REFERENCES

1. R. J. Eichelberger, "Defenses Against Hollow Charges" paper given at the Shaped Charge Symposium at B.R.L. in November, 1951; reprinted in B.R.L. Report No. 837, pp. 373-383.

2. E. M. Pugh, "Survey of Devices for Protecting Armored Vehicles Against Shaped Charges," special report on Contract No. W-36-061-ORD-2879 (June, 1949).

3. Carnegie Institute of Technology Final Report, "Protection Against Shaped Charges" OSRD No. 6384 (November, 1945).

4. J. P. Shanley and R. L. Kirkpatrick, "An Analysis of Results of Some Dynamic Firings of Shaped Charges Against Plated Armor," B.R.L. Memorandum Report No. 694 (June, 1953).

5. J. P. Shanley, "Status of Explosive Armor Studies," B.R.L. Memorandum Report No. 648 (February, 1953).

6. While other reports on this subject are probably in existence, the only reference available to this author is contained in the Minutes of Meeting of Shaped Charge Committee of Picatinny Arsenal, 17 June 1953.

7. Kistiakowski, MacDougall, and Manneriy, "The Mechanism of Action of Cavity Charges," OSRD No. 1338 (April, 1943).

8. Hill, Mott, and Pack, "Penetration by Munroe Jets," ORD No. 2/44; #072; OSRD Liaison Office MA-1620-8 (February, 1944).

9. E. M. Pugh, "A Theory of Target Penetration by Jets," Armor and Ordnance Report No. A-274, NDRC Div. 2 (June, 1944).

10. Pugh and Firman, "Fundamentals of Jet Penetration: Theory of Jet Penetration," Monthly Report OTB-4f, OSRD 4357f (November, 1944).

11. Pugh and Firman, "Fundamentals of Jet Penetration," Monthly Report OTB-11a, OSRD 5462a (April, 1945).

12. R. Heins-Gelder, "Glass Targets," Monthly Report OTB-13, OSRD-5462a (August, 1945).

13. Consult the complete set of Flintkote reports on Contract No. DA-30-069-ORD-245.

14. J. P. Shanley, "Analysis of Some Experimental Data on Glass as a Tank Armor to Defeat Shaped Charges," B.R.L. Memorandum Report No. 643 (February, 1953).

15. R. Heine-Geldern, "Fundamentals of Shaped Charges," CIT-ORD-2 (April, 1945).

16. R. Heine-Geldern, "Fundamentals of Shaped Charges", Final Report (June 30, 1946).

17. R. Heine-Geldern, "Fundamentals of Shaped Charges," CIT-ORD-7 (February, 1947).

18. R. Heine-Geldern, "Fundamentals of Shaped Charges," CIT-ORD-9 (June, 1947)

19. R. Heine-Geldern, "Fundamentals of Shaped Charges," CIT-ORD-5 (October, 1946).

20. R. Heine-Geldern, "Fundamentals of Shaped Charges," CIT-ORD-45 (June, 1953).

21. Heine-Geldern, Foner, Mutschler, "Fundamentals of Shaped Charges," CIT-ORD-31, Part III (February, 1951).

22. F. R. Smith, Flintkote Progress Report of January 26, 1953, Contract No. DA-30-069-ORD-245.

23. Pugh, Heine-Geldern, Foner, Mutschler, "Fundamentals of Shaped Charges", CIT-ORD-38, (April 1951).

24. Heine-Geldern, Holmes, Mutschler, "Fundamentals of Shaped Charges," CIT-ORD-41 (October 1952).

25. Foner, Heine-Geldern, Mutschler, "Fundamentals of Shaped Charges," CIT-ORD-74 (December 1949).

CHAPTER X

TERMINAL BALLISTIC EFFECTIVENESS OF SHAPED CHARGES AGAINST TANKS

F. I. Hill

Ballistic Research Laboratories
Aberdeen Proving Ground, Maryland

Introduction

The shaped charge is one of the more effective weapons for the defeat of tanks. The principal design objective in the past has been simply to perforate the armored envelope of tanks. In general, the armor of a tank has been assumed to be equivalent to a flat piece of armor plate and design of shaped charges has progressed toward the most efficient perforation of this target. Such an objective is a logical initial one since the Infantry has had no weapons of reasonable weight that could perforate modern armor by means of kinetic energy rounds.

However, the criterion of shaped charge effectiveness must in the final evaluation be its ability to defeat an armored vehicle—not just perforate its armor. The first element to be considered in the criterion is that of perforation; the second element is damage after a perforation. Perforation of a tank's armor is not the same as perforation of an idealized target. Much of the target presented by a tank is irregular and non-homogeneous in composition so that predictions of the effect of perforation cannot be done from flat plate data. Damage does not occur to a tank just because a perforation of the armored envelope occurs. The perforation must cause further destruction inside. This damage depends upon where the perforation occurs and the residual damaging effect of the jet after the perforation. Other factors such as stand-off, liner material, etc., also are involved.

It is desirable to consider just what a "tank kill" is. Tanks cannot be shot down like airplanes or sunk like ships. Medium tanks cannot be reduced to a twisted hulk by any but the most intense of blasts. Usually, a tank is destroyed by releasing the forces that it carries within it. Thus, tank destruction depends to a great extent on ignition of the ammunition or fuel. However, other types of damage reduce tank effectiveness equally well depending upon the circumstances of combat. For instance, if a tank is immobilized during a retreat it is lost just as a surely as though it had been burned. In the case of an attacking force, if the fire power of the tank is destroyed the tank is no longer of use in the particular action.

Three categories of damage to a tank have been defined.

K Damage is that damage that will cause the tank to be destroyed.

F Damage is damage causing complete or partial loss of the ability of the tank to fire its main armament and machine guns.

M Damage is damage causing immobilization of the tank.

Sources of Terminal Ballistic Data

There are three sources of data for terminal ballistic damage of shaped charges to tanks: historical data, terminal ballistic firings at tanks and box tests. Each of these three methods has its importance.

Historical Data

The principal historical data compiled on the damage effectiveness of shaped charges was obtained by the MORU in Great Britain (ref. 1 and 2). The data available are entirely for German infantry hand-fired weapons, such as the Panzerfaust and the Raketenpanzerbuchse (German 3.5 in. Bazooka), vs U. S. and British Tanks. This information is valuable in that it gives some idea of the points of impact, the ranges of engagement, and the crew casualties experiences in World War II. Table I, prepared from Ref. 1, shows the proportion of Sherman and Stuart Tanks that burned completely and the proportion that were repairable, as a result of shaped charge attack.

TABLE I

Total No. Considered	No. Burned	% Burned	% Casualties Repairable
64	27	42	54%

This table suggests that most of the tanks that were not burnt were repairable. Table II, taken from Ref. 2, suggests that the rule of thumb that one man killed and one wounded for a perforating round is a good one for shaped charge rounds.

TABLE II

No. of men Exposed	% Killed	% Wounded	% Burned
235	20	24	6

These are short range weapons. Kills rarely occurred at ranges greater than 120 yards. The mean range of 227 allied casualties (all the collected data available on shaped charges from World War II) is 43.5 yards. The angular distribution of casualty producing attack data available for these short range weapons is shown in Table III.

TABLE III

No. of Perforations	No. on Front	No. on Side	No. on Rear
100	30	63	7

All of the above data were taken from references 1 and 2.

Terminal Ballistic Firings

The second and the most definitive source of damage information is the proving ground firing at a tank. Such firings have been carried out by the British, the BRL and other organizations from time to time. References to the detailed data on these firings are given in reference numbers 3 to 21.

The largest and most systematic program has been at the Ballistic Research Laboratories. The method of obtaining these data has been as follows. A fully equipped tank (usually a T26E4 or T26E5) is loaded with wooden crew members in each crew position and stored with inert ammunition. A small amount of fuel is placed in the fuel tanks to operate the engine so that it can be running when the tank is fired on. A round is then fired on a selected surface of the tank. The angles of fire usually considered are normal to front and side and 45° azimuth to front and side. Another angle of attack is at 45° elevation angle. The range of firing varies depending upon the round to be tested. For instance, the 90mm T108 round was fired at 500 yards and the 3.5 in. rocket was fired at 100 yards. For the first firings the attempt is made to cover the tank in a fairly uniform manner with hits. However, after the nature of the damage of a particular round is generally understood, the rounds are fired at the surfaces of a tank where there is the greatest doubt about the damage.

As soon as a hit is obtained on the tank, two combat experienced assessors go to the tank and examine the damage. As long as the tank is operable, operable components are checked (such as, turret traverse, gun elevation, radio intercommunication, etc.). The damage is then assessed with a description of every item of damage to the tank. These descriptive assessments are then translated into numerical assessments, which have been determined by the assessors to be standard. A list of standard assessments of components is given in Table IV. M, F, and K damage are defined in the "Introduction."

TABLE IV

LIST OF STANDARD ASSESSMENTS

Ammunition	Probability of Overall Damage to Tank when Destroyed M	F	K
Cases - Main Gun			100
H. E. Projectile			100
Small Arms stowed in turret bustle		.15	
" " " in driving comp't	.20	.10	
" " " near loader		.15	
Grenade Box	.30	.15	
Personnel			
Commander	.30	.30	
Gunner		.20	
Loader		.15	
Driver	.10	.10	
Bow Gunner	.10		
Gun			
Main gun and breech		.80	
Equilibrator		.80	
Elevating and traversing mechanism		.80	
Recoil mechanism		.80	
Coaxial machine gun		.10	
Bow machine gun		.10	
Engine Compartment			
Engine, transmission	1.00		
Oil and Coolant coolers	1.00		
Fuel tanks			1.00
Battery	.10	.10	
Fighting Compartment			
Radio and Intercommunication	.50	.10	
Fire Control - Dependent on system			
Driving Controls	1.00		
Heater (using liquid eng. coolant)	1.00		

TABLE IV (Cont'd)

	Probability of Overall Damage to Tank When Destroyed		
	M	F	K
Exterior Components			
Front Idler Hub	.50		
Track	1.00		
Driving sprocket	1.00		
Final drive	1.00		
Track guides	.10		

The above table is representative and is not inclusive of all the damage that could happen to such components as the electrical circuit, etc.

The determination of a personnel kill is made from examination of the wooden dummies. While wound criteria as determined from wooden dummies are admittedly inaccurate, cases that are marginal are usually rare. Assessment of the possible damage that could have occurred from fuel or ammunition fires is made by observing where the hits occurred and correlating this with actual experiments carried out against these components separately. Fuel and ammunition are removed from the tank prior to firing for practical reasons. When a tank is perforated with live ammunition in it, it is highly unsafe to investigate it even though no immediate fire occurs for several hours. In the case of a fire which consumes ammunition or fuel there is nothing left of the tank to access.

After the perforation has been assessed the tank is cleaned, previous damage carefully marked, new wooden dummies installed and minor damage repaired. As successive shots hit the tank the quality of the data obtained decreases since the assessor's estimates of the actual damage that would have occurred in the absence of previous damage become more difficult. The tank is fired on until no more data can be obtained. (In the case of the 3.5 inch rocket over 70 hits and 35 perforations were obtained on a single tank.)

The descriptive and numerical assessments are the basic data for the analysis of tank vulnerability. The information is contained in this form in the firing records (ref. 3 through 16). British data are presented in a somewhat different form in that only the descriptive part of the damage is given. British data available are given in (ref. 17 through 21).

Box Tests

The so-called "box tests" are thoroughly described in Ref. 22. A box is placed behind the armor plate. In this box are instruments to measure pressure and temperature and usually witness plates to give an indication of scatter. The box appears to be an admirable way to obtain developmental data on shaped charge design. Its value will probably increase as correlation can be established between box measurements and tank damage.

A BRIEF SUMMARY OF TERMINAL BALLISTIC FIRINGS

Data Obtained at Aberdeen Proving Ground

Using the methods of gathering data outlined in the previous section, several firings of shaped charge ammunition against tanks have been conducted. A detailed description of these firings is given in the APG Firing Records (refs. 3 through 10). Table V summarizes the number of each type of round that has been fired and the amount of data from perforations that are available. Most of the attacks were against the T26E4 tank which in armor and most other respects is similar to the M26 (Pershing) tank. The armor is the same as the M46 and similar to the M47. A few firings were against the T26E5 tank, which is a considerably up-armored version of the M26 tank. Table V is presented to show what basic data is available at the time of writing. No conclusions should be drawn from this table concerning perforation probabilities. The range of firing was established for the sake of convenience and safety. "Static firings" or firings from shaped charges set in place were used when it was not feasible to launch the rockets.

TABLE V

SUMMARY OF SHAPED CHARGE FIRINGS ON T26E4 and T26E5* TANKS

Type Round	Ref.	Type of Attack	Range	Total No. of shots	Crew Comp. Perf.	Eng. Comp. Perf.	Non Perf. Hits
3.5" HEAT Rocket M28	6	Ground	100 yds.	70	33	6	31
90mm HEAT T108*	4	Ground	500 yds.	24	11	1	12
5" copper cone	9	Ground	Static	2	2	-	-
5" copper cone*	9	Ground	Static	9	9	-	-
5" aluminum cone*	9	Ground	Static	8	6	1	1
75mm HEAT M310A1	3	Ground	100 yds.	25	8	3	14
105mm HEAT M67	8	Ground	100 yds.	20	6	1	13
2.75" FFAR	5	30° air	500 yds.	31	11	5	15
8cm Oerlikon	5	30° air	500 yds.	39	14	2	23
3.5" HEAT Rocket M28	7	45° air	13 yds.	15	10	5	-
6.5" ATAR (Steel Cone)	10	45° air	Static	6	5	-	1

*Rounds marked by asterisk were fired against T26E5 tank.

Of all the firings listed in Table V only that of the 3.5 inch Rocket is likely to give any valid data in an unreduced form for the expected number of kills on the T26E4 tank. Table VI separates the damage to the T26E4 tank into damage from armor fragments and damage from the shaped charge jet itself. It is significant that no K damage was caused by fragments. Figure 1 shows the results of the 3.5 inch (ground) firings as a cumulative distribution. The use of a cumulative distribution of numerically assessed damage is of considerable aid in the comparison of two rounds.

TABLE VI

3.5" HEAT, M28 vs M26 Tank

(Avg. Results of 70 Rds.)

	Avg. Prob. of a hit being a kill due to					
	Jet Only			Frags. Only		
	M	F	K	M	F	K
Avg. of all hits	.13	.12	.07	.14	.10	0
Avg. of hits that did damage	.59	.55	.31	.46	.34	0

	Frags & Jet		
	M	F	K
Avg. of all hits	.26	.21	.07
Avg. of hits that did damage	.78	.70	.31

56% of hits caused no damage

44% of hits caused damage. Of these:

45% caused frag. damage only

29% caused jet damage only

26% caused jet and frag. damage

The reduction of the data shown in Table V is of little importance for the T26E4 tank because this tank is obsolete. The data are primarily used as a basis for estimates of damage to other tanks. Such estimates are given for many of these rounds in subsequent sections of this chapter.

In addition to firings on tanks a number of tests have been made firing on gasoline and Diesel fuel.

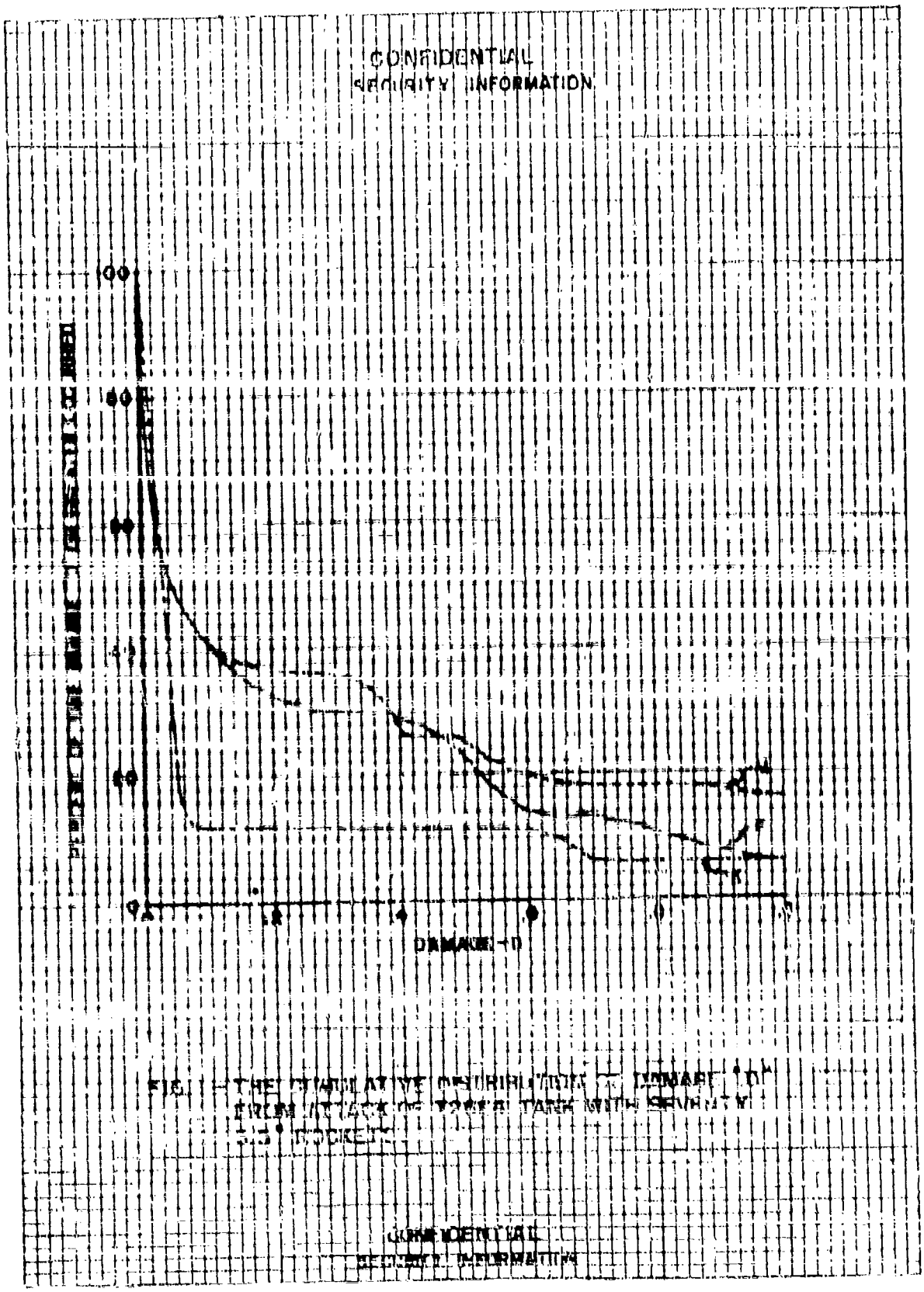
CONFIDENTIAL
SECURITY INFORMATION
DAMAGE-D
CONFIDENTIAL
SECURITY INFORMATION

Summaries of the firings against gasoline and diesel fuels are given in Table VII and VIII respectively. Conclusions derived from the table are given at the bottom of each table.

TABLE VII

SUMMARY OF SHAPED CHARGE FIRINGS AGAINST EIGHTY OCTANE GASOLINE

Round	t	Armor Obl.	Cap. of Container (gal.)	Where* Hit	No. of rds. fired	No. of fires	% fires
2.36" HEAT	3"	0°	5	BFL	10	9	90
	1"	0°	5	BFL	10	10	100
	3"	0°	16	AFL	10	9	90
	1"	0°	16	AFL	10	9	90
	3"	0°	16	BFL	6	6	100
			TOTAL (2.36" HEAT)	AFL	20	18	90
				BFL	26	25	96
3.5" HEAT	3"	45°	5	AFL	6	6	100
	3"	45°	5	BFL	3	3	100
	5 1/4"	45°	5	BFL	5	5	100
	2-3/4"	0°	55	BFL	1	1	100
	3"	0°	T26E4	AFL	12	10	83
	3"	0°	T26E4	BFL	3	3	100
			TOTAL (3.5" HEAT)	AFL	18	16	89
				BFL	12	12	100
			TOTALS (all rds.)	AFL	38	34	90
				BFL	38	37	97

*AFL - Above Fuel Level
BFL - Below Fuel Level

Derivative Facts

1. 2.36" gave slightly lower no. of fires than 3.5" on rds. fired below fuel level.
2. No difference in the two rds. fired above fuel level.
3. No difference apparent between rds. fired at various container sizes.
4. Rds. fired below fuel level gave slightly greater no. of fires than those fired above fuel level.
5. No difference because of armor thickness.

TABLE VIII

SUMMARY OF SHAPED CHARGE FIRINGS AGAINST DIESEL FUEL

Round	Armor t	Armor Obl.	Container Capacity (gal.)	Where* HIT	No. of Rounds	No. of Fires	% Fires
2.36" M6A6 HEAT	3"	0°	16	AFL	10	2	20
"	1"	0°	16	AFL	10	2	20
"	3"	0°	16	BFL	16	2	12
90mm T108E15	3"	0°	16	AFL	4	4	100
"	3"	0°	16	BFL	3	3	100
3.5" HEAT	5-1/4"	45°	55	AFL	11	5	45
"	2-3/4"	0°	55	AFL	9	2	22
"	5-1/4"	45°	55	BFL	13	5	38
"	2-3/4"	0°	55	BFL	15	6	40
					91	31	29

*AFL - Above Fuel Level
BFL - Below Fuel Level

Derivative Facts

1. 27% of hits above fuel level caused fires.
2. 31% of hits below fuel level caused fires.
3. 30% of rounds detonated against 16 gal. containers caused fires.
4. 37% of rounds detonated against 55 gal. containers caused fires.

Conclusions

1. There is not sufficient reason, on the basis of these firings, to reject the hypothesis that probability of causing a fire is independent of position of hit with respect to fuel level.
2. Considering variations in types of armor plate and detonated round, no significant difference in vulnerability of 16 gal. containers and 55 gal. containers is evident.
3. On the basis of these firings, it is not possible to establish the probability of a fire as function of detonated round or armor plate thickness.

There have been relatively few firings of shaped charges against ammunition because of the difficulty of doing the test safely. Table IX outlines data obtained by firing at three rounds placed approximately one inch apart.

TABLE IX

90mm T108E1 vs. Ammo.

No. rds. Fired	TARGET	Armor t	Obl.	No. of Expl.	No. of times 1,2, or 3 rds exploded		
					1 rd.	2 rds.	3 rds.
7	3 rds. of 90mm AP,T33	3"	0°	7	2	4	1
7	2 cartridge cases of Russian 85mm and 1 rd. of inert 90mm AP, T33	3"	0°	7	3	4	-

It is notable that the ammunition, both U.S. and Soviet, were ignited when the propellant cases were hit.

Data Obtained by the British

The British have conducted several firings of shaped charge ammunition against tanks, ammunition, and fuel. The detailed description of these firings is given in ref. 17 through 21. In addition to these firings they have done a large number of witness plate firings, which are firings through armor with measurement of back damage made by setting up thin plates at various distances behind the armor.

One of the most extensive firing programs has been carried out in firings ordered in British Ordnance Board proceeding 6 6867 which gave some considerable data on the performance of the Energa rifle grenade, the 3.5 inch rocket, and the 95mm HEAT round against fuel, ammunition, and witness plates. Table X summarizes these firings for the Energa Grenade against plate.

Conclusions that may be drawn from this table are that the cone of damage is independent of plate obliquity and that the cone of damage is very narrow for the near critical thicknesses of armor fired on. The cone of damage is defined as the cone including all the lethal spray of fragments striking and perforating a 1/16 inch mild steel plate 36 inches behind the main armor.

Table XI shows the results of the Energa Grenade firing through armor of approximately 245mm thickness at a group of nine rounds of 17 pdr. APCBC ammunition placed approximately 41 inches behind the armor.

TABLE X

Performance of Energa Grenade

Static Witness Plate Firings of the Energa Rifle Grenade										Witness Damage 1/16 MS@ 36"
	Armor									
No. Grenades Detonated	Thickness (mm)	Obliquity Angle (Deg)	Equivalent Thickness (mm)	Front Hole Avg. Dia. (in)	No. Perforations	Back Hole Avg. Dia. (in)	No. Rounds	Avg. Frags/ Rd.	Cone of Damage
11	200	27	224	1.4	11	.6	2	21.5	13°
6	200	32	236	1.3	4	.5	4	18.8	10°
1	200	35	244	1.4	1	.5			
8	200	37	250	1.5	3	.4	1	1.2	13°
1	200	40	261	1.5	10	.4	4	5.8	13°
7	200	42	269	1.7	3	.4	2	4	4°
11	150	54	221	1.7	11	.6	2	11	4°
15	130	56	232	2.2	11	.5	4	10.5	10°
12	130	58	245	2.4	7	.5	5	7.2	12°
7	130	60	260	2.4	6	.6			
Average			244.8		67/104	.52	24	10.9	10°

CONFIDENTIAL

CONFIDENTIAL

TABLE XI

ENERGA GRENADE vs. 17 pdr. APCBC AMMUNITION

Total No. of Shots	12
No. of Occasions Rounds Damaged	10
No. of Occasions Fire Occurred	3
Average No. of Rounds Damaged when Damage Occurred	5.5
No. of Fires Per Round Damaged	6/11

TABLE XII

WITNESS PLATE FIRINGS OF STATICALLY FIRED 3.5" HEAT ROCKETS

No. Rounds	Armor			Front Hole	No.	Back Hole	Witness Damage(1/16"M.S@36")		
	Thickness mm	Obliquity deg	Equiv. thickness (mm)	Avg.dia. (in)	Perf.	Avg.Dia. (in)	No. Rds.	Avg.No. Frag/Rd	Avg. Cone Angle/Rd
10	200	32	236	2.1	9	1.0	4	28	31°
3	200	37	250	2.1	3	1.2	2	21	26°
25	130	56	232	3.1	18	1.0	4	28	37°
6	130	58	245	3.1	3	.8	1	14	--
5	130	60	260	2.6	4	1.4	1	15	--

Table XI indicates that with low residual penetration there is a low probability of igniting ammunition fires with the Energa grenade.

Table XII summarizes the British witness plate firings with the 3.5" rocket showing a mean cone angle of damage of the order of 33° at three feet behind the armor.

In firing the 3.5" rocket four times against 17 pdr APCBC ammunition in a test arrangement approximately the same as that of the Energa described in Table XI four fires were obtained for four shots. Two fires were also obtained for two shots into caliber .30 ammunition.

Table XIII shows witness plate data on the 95mm HEAT projectile. The data indicate approximately the same mean cone of damage for this round as the 3.5" rocket, which is a substantially greater one than that for the Energa. In firing on ammunition with approximately the same test set-up as that of Table XI five fires were obtained with

five 95mm HEAT shots against 17 pdr. APCBC ammunition. Static firings of this round into diesel fuel filled tanks caused one small fire in five attempts. The one shot into a gasoline filled tank caused a fire.

TABLE XIII

STATIC WITNESS PLATE FIRINGS OF QF95 MM HEAT SHELL

No. Fired	Armor Thickness mm	Obliquity deg	Equiv. Thickness mm	Witness Plate Data: Mean Front Hole Dia. in.	No. Rds. (Perf. 1/16" M.S. 3 ft. range)	Avg. Frags/rd.	Cone of damage at 3 ft. deg.
12*	200	15	208	1.8	7	31.5	27
11**	130	51	206	2.5	3	18	30

* 10 Perforations; 0.6" mean back hole dia.
** 9 " 1.0" " " " "

For the firings against the plate at 51° obliquity in Table XIII witness plates were set up at six inches and one foot as well as three feet. The cone of damage varied as follows:

Cone of damage degrees	Distance to Witness Plate ft.
75	.5
59	1.0
30	3.0

These data are closely fitted empirically by the relation:

$$\text{Distance to witness plate(ft.)} = 9.6\ e^{-.039 \times \text{cone angle in degrees}}$$

Although limited in nature such data suggests that the higher velocity fragments are near the jet after it passes through the armor. The results so far on witness plate firings show promise as an aid to the analysis of tank vulnerability. However, much more firings will be needed to supplement the existing fragmentary information.

A Qualitative Description of Shaped Charge Damage

For reasons of conciseness, data have been given in the form of numerical assessments. However, the analyst of tank damage must rely heavily on descriptive assessments. For this reason, a brief qualitative

description of the damage to be expected from shaped charges is given. Reference to Table V shows that the rounds fired can be divided into several easily defined groups.

The first group is fin stabilized shaped charge rounds with copper liners such as the 3.5" Rocket, 90mm T108, 2.75" FFAR and 8 cm AR. These rounds will usually do damage (providing "sufficient residual penetration" is available) in a narrow cone along the path of the jet. Fragments can be expected to do damage to soft targets such as personnel and communications equipment. The fragments are not likely to ignite ammunition. The jet will ignite the projectile propellant. The jet also will ignite gasoline by a perforation into the fuel tanks either above or below the fuel level.

Diesel fuel is not nearly so easily ignitable as can be seen in Tables VII and VIII. There appears to be some dependence upon ignitability of the diesel fuel and the size of the charge. Rounds with a large residual penetration have an appreciably better chance of igniting this type of fuel. Another effect in the diesel fuel firings has been one of container size. In the firings of the 3.5 inch rockets, small containers containing five gallons of Diesel fuel were not ignited in 13 attempts. (See ref. 26)

Exactly what constitutes "sufficient residual penetration" cannot yet be specified. The amount of damaging power left in a shaped charge jet after a target perforation that is necessary to do damage will vary depending on the point of entry into the tank. If "residual penetration" is acceptable as an index, the range of values that can be selected is probably greater than one inch and less than three inches to do the type of damage that is confined to a narrow path behind the perforation. A figure frequently used is 2.5 inches residual penetration. (See ref. 27)

The damage from shaped charges using other liner materials is somewhat different. Detailed reports of this have been made in refs. 22 and 23. Materials such as steel or aluminum tend to cause more fragments to fly off the rear face of the armor and thus fragment damage is more widespread than from copper cones. However, neither steel nor aluminum lined cones have as great a penetration as copper cones of the same diameter. Both steel and aluminum cone shaped charges produce considerable pressure effects inside a tank upon perforation. The pressure from aluminum cones is apparently somewhat greater than from steel. Tests (ref. 16) on animals placed in a tank fired on by a 5 inch shaped charge showed them to be unharmed unless hit by fragments. The approximate pressure measured by paper blast gages was of the order of 50 psi. This pressure did, however, tear off hatch doors and bend bulkheads within the tank.

Although shaped charges do not in general wreck a tank by their own energies, they are nearly equally as efficient as the kinetic energy rounds in igniting fuel and ammunition in the tank. Shaped charges are equally as good as kinetic energy rounds at knocking out the engine or transmission.

They do not, however, assure a kill when a perforation of the tank's armor occurs any more than do kinetic energy rounds of the same caliber.

Target Characteristics

Tables XIV, XV, and XVI contain information regarding the armor of various tanks and the effectiveness of several HEAT projectiles in penetrating this armor.

Table XIV gives the probability of encountering an obliquity of θ or less for various tanks averaged over the expected angles of attack if the attacking projectile strikes the presented surface of the tank in a random manner. In averaging, the distribution of angles of attack was considered to be either circular or in the form of a cardioid, as noted in the table. The circular distribution is approximately what would be expected in the case of attack by hand held AT weapons and the cardioid distribution is what would be expected from mounted AT guns. Ref. 25. contains a discussion and derivation of the latter distribution.

TABLE XIV

DISTRIBUTION OF ANGLES OF OBLIQUITY (GROUND ATTACK)

Probability of Encountering Obliquity θ or less

θ (Deg.)	M-48 (Circular)*	M-48 (Cardioid)+	T-43 (Circular)*	T-43 (Cardioid)+	JSU152 (Cardioid)+	SU100 (Cardioid)+	T34/85 (Cardioid)+	JS III (Cardioid)+
0	.03	.03	.05	.05				
10	.05	.05	.06	.06	.09	.08	.06	
20	.06	.06	.07	.07	.31	.11	.13	.08
30	.17	.16	.16	.16	.39	.31	.23	.27
40	.24	.24	.27	.24	.53	.43	.38	.32
50	.43	.40	.46	.43	.69	.56	.49	.41
60	.59	.58	.64	.56	.89	.79	.71	.68
70	.77	.77	.84	.82	.95	.96	.86	.88
80	.95	.95	.95	.95	.99	.99	.95	.98
90	1.00	1.00	1.00	1.00	1.00	1.00	1.00	1.00

* - Circular (Uniform) Distribution of Angles of Attack Considered.

+ - Cardioid Distribution of Angles of Attack Considered $f(\gamma) = \frac{1}{2\pi} (1 + \cos \gamma)$.

Table XV shows the probability of HEAT projectiles encountering an equivalent armor thickness t_e or less averaged over the expected angles of attack for various tanks assuming that the projectiles strike the presented area of the tank in a random manner. An equivalent armor thickness is a thickness at 0° obliquity which gives the same protection as some other combination of thickness and obliquity. The distributions of attack angles are the same as used in Table XIV. Shielding by external components was not considered in the preparation of Tables XIV and XV. However, the net effect of external components is to lower the values in Table XV by about 10%.

TABLE XV

DISTRIBUTION OF EQUIVALENT ARMOR THICKNESS WITH RESPECT TO HEAT ROUNDS (Ground Attack)

t_e (in)	Probability of Encountering t_e* or less					
	M48 (Circular)**	M48 Cardioid)+	T-43 (Circular)**	T-43 (Cardioid)+	T34/85 (Cardioid)+	JS III (Cardioid)+
0	-	-	-	-	-	-
2	.18	.07	.06	.04	.22	-
4	.48	.37	.41	.31	.62	.16
6	.63	.57	.59	.48	.72	.23
8	.72	.68	.68	.62	.76	.46
10	.74	.72	.72	.66	.78	.67
12	.76	.76	.74	.71	.78	.72
14	.77	.77	.75	.72	.78	.74
16	.77	.77	.75	.73	.78	.74
18	.77	.77	.76	.73	.78	.74

* t_e = equivalent thickness at 0° for HEAT rounds (= thickness of armor x secant of the angle of obliquity) of armor measured from the normal plane

** Circular Distribution of Attack Angle.

\+ Cardioid " " " " .

Table XVI gives the portion of the presented area of the armored parts of various tanks which can be penetrated from various angles of attack. Shielding by external components was not considered in the preparation of this table.

TABLE XVI

Portion of Presented Area of Hull & Turret That is Penetrable* (Ground Attack)

Angle of Attack (deg)	2.36" HEAT M6A6			
	M48	T43	T34/85	JS III
0	.06	.22	.72	.08
30	.29	.16	.70	.00
60	.59	.66	.69	.00
90	.74	.73	.75	.61
120	.65	.70	.77	.62
150	.58	.53	.64	.0
180	.74	.76	-	-
	3.5" HEAT, M28A1			
	M48	T43	T34/85	JS III
0	.60	.63	.75	.73
30	.67	.55	.79	.70
60	.72	.75	.77	.70
90	.86	.84	.76	.73
120	.71	.79	.79	.74
150	.74	.76	.79	.73
180	.75	.78	-	-

*Remember that a penetration does not insure a kill.

TABLE XVI (Continued)

Angle of Attack (deg.)	6.5" ATAR			
	M48	T43	T34/85	JS III
0	.72	.77	.79	.760
30	.74	.63	.79	.760
60	.75	.77	.79	.760
90	.87	.85	.76	.768
120	.72	.80	.79	.768
150	.74	.76	.79	.760
180	.75	.78	-	-

	90mm HEAT, T108			
	M48	T43	T34/85	JS III
0	.60	.53	.75	.702
30	.67	.52	.79	.637
60	.72	.74	.76	.623
90	.86	.84	.76	.713
120	.71	.79	.79	.737
150	.74	.74	.75	.629
180	.75	.78	-	-

TABLE XVI (Continued)

Angle of Attack (deg)	75mm HEAT, M66			
	M48	T43	T34/85	JS III
0	.02	.05	.53	0
30	.07	.06	.53	0
60	.29	.37	.61	0
90	.44	.56	.74	.504
120	.34	.50	.60	.171
150	.35	.33	.13	0
180	.64	.67	-	-
	105mm HEAT, M67			
	M48	T43	T34/85	JS III
0	.05	.10	.60	.063
30	.20	.15	.62	0
60	.55	.53	.61	.099
90	.65	.63	.75	.596
120	.63	.62	.63	.576
150	.53	.51	.53	0
180	.72	.74	-	-

METHODS OF DATA ANALYSIS

The reduction techniques of damage data for tanks have not yet provided simple indices for the measure of the probability of a given round killing a tank. Such firings assemble basic data from firing on obsolete vehicles to provide an accurate estimate of vulnerability of new or proposed tanks that have not been fired on. The problem here is to use a small number of actual firings to give reliable overall damage probability estimates.

The technique of data reduction is influenced by what the data are to be used for. One use is the comparison of the effectiveness of specific weapons. A second is estimation of the number of weapons needed to counter an enemy force. Assembly of data on relative kill probability on the particular target tanks used in experiments provides a reservoir

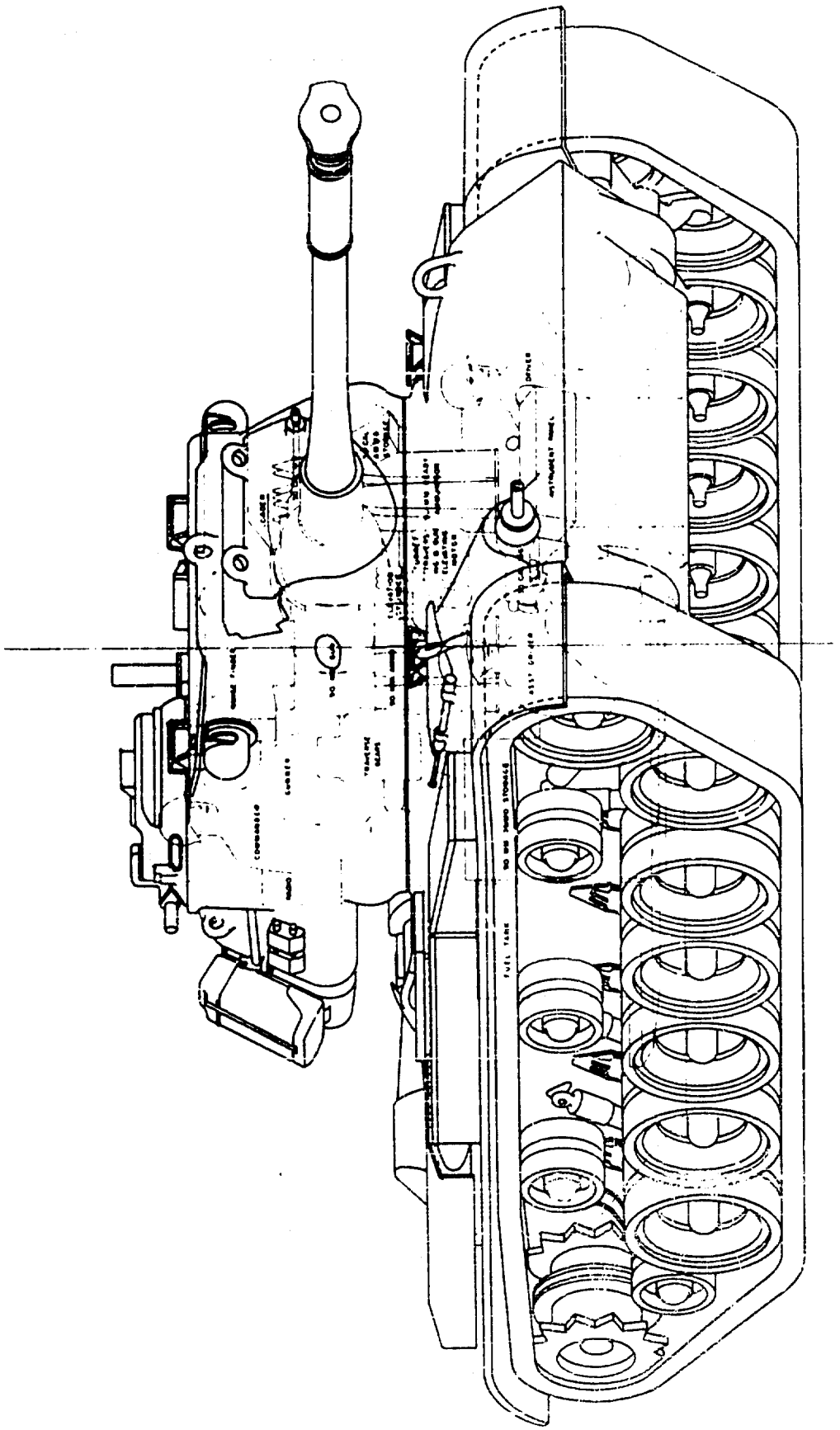

FIG. 2. Tank, M47 - 30° right

of knowledge the analyst must assimilate prior to making an estimate of a weapon's effectiveness or computing a kill probability against any target type.

Two principal methods are used for data reduction. These are called the vulnerable area method and the distributed area method. The "vulnerable area method" is used when the target is small compared to the dispersion of hits on the target. The "distributed area" method is used when the dispersion of the hits is small compared to the size of the target. These methods and some approximations that have been made are discussed below.

The Distributed Area Method

The distributed area method will be described first since the vulnerable area method is essentially a simplification of it. Consider the case when the probability of a hit being a kill by a projectile of high velocity and low dispersion is desired (such as the 90mm T108 round against the JSIII). Terminal ballistic damage data of this round on the T26E4 tank are first assembled. These data include both the numerical and descriptive assessments. Examination is made of the damage resulting from hits on components where damage is obtained only a part of the time, such as the suspension, the turret ring, hull in front of driver's controls, etc. For many other areas kill probability will depend only upon probability of perforating. Numerical assessments of damage for various types of rounds are compared to see if terminal ballistic damage after perforation is comparable (as are the 90mm T108 Rd and the 3.5 inch rocket). Examination of the perforating and non-perforating hits is made to determine reliability of fuze action of chemical energy rounds.

Vulnerability drawings of the target tank are prepared which show the arrangement of the interior components to the line of fire (see Fig. 2) Using an overlay grid the probability of a hit, the chance of perforating and probability of a perforation being a kill are entered into each square for a given point of aim.

The probability of a perforation being a kill is determined by estimating the fragment pattern and the expected damage of the jet. Reference to the qualitative description of damage from each round is used here. Numerical damage is computed by combining the damage from components lying in the path of the jet and fragments by the formula

$$P_M = 1-(1-P_a)\ (1-P_b)\ (1-P_c)\ \ldots\ (1-P_k)$$

where P_M is the probability of M damage occurring.

P_a is the percent of M damage resulting from a hit on component, "a", etc.

This calculation is carried out for M, F and K damage for several views about the tank and hit probability figures are varied for each range. By summation, the probability of an aimed round killing as a function of range r and azimuth θ is obtained. These data can be combined with the expected angular and range frequency of attack to give an overall figure of the vulnerability of one tank to an antitank gun firing a certain round. Such values have been computed in the following table taken partly from Ref. 24.

TABLE XVII

PROBABILITY OF KILLING JSIII TANK

Projectile	Kill Category		
	M	F	K
90mm HEAT T108	.50	.47	.44
5" Cu Liner H.C. (assumed same dispersion as 90T108)	.66	.66	.60

All shots are aimed fire without range finder at center of largest concentration of target vulnerable area. Answer averaged using range and angular distribution functions of BRL M590 ref. 25.

Another calculation made for the front of the JSIII compares the 90mm T108 HEAT round and the 105mm BAT HEAT round fired at the JSIII Tank. The T108 round is fired under the conditions of Table XVII above and the BAT guns were fired in a salvo of two using a spotting rifle for aim. No mis-match in the spotting rifle and the 105mm rifles was assumed, (at the present the mis-match is such that the values for the BAT rounds beyond 1400 yards will not be appreciably higher than that for the T108 round).

TABLE XVIII

COMPARISON OF EFFECT OF TWO 105mm BAT ROUNDS WITH EFFECT OF 90mm T108 ROUND

Range - Yds	Probability of F Damage on Front of JSIII	
	90mm T108	105mm BAT
500	.33	.33
1000	.10	.25
1500	.04	.16
2000	.02	.10

The Vulnerable Area Method

The vulnerable area, which is the product of the hit probability on the presented area and the probability of a random hit on this area being a kill, is computed from the overlay of figure 2 by merely assuming a uniform hit probability in each square. It is assumed that the point of aim may be anywhere on the tank. There is no range effect to be considered for shaped charge ammunition. Many of the present day shaped charge rounds have sufficient dispersion for hits to be considered in this manner. Several calculations have been carried out on tank vulnerability using this method and are included in the following table. Probabilities are given in terms of either vulnerable area or the probability of a random hit being a kill, the vulnerable area being the latter probability multiplied by the presented area of the tank.

TABLE XIX

VULNERABLE AREAS OF JSIII TANK TO GROUND ATTACK
BY SHAPED CHARGE ROUNDS - FT^2

Angle of Attack Round	6.5" ATAR			5" Cu Liner			90mm T108		
	M	F	K	M	F	K	M	F	K
Front	39	34	21	32	23	14	5	6	3
60°	77	51	31	68	37	23	30	20	6
Side	75	54	33	76	47	27	35	28	11
120°	74	51	30	73	42	24	41	24	14

To convert from vulnerable area to probability of a kill, the total presented areas are needed.

TABLE XX

PRESENTED AREA OF JSIII TANK* - FT^{2*}

Angle of Attack	Ultimate Penetrable Area	Total Area Including Suspension
Front	34	62
60°	82	142
Side	84	137
120°	86	146

* From ref. 24.

The probability of a random hit causing a kill averaged over the expected angles of attack, $f(\gamma) = \frac{1}{2\pi}(1 + \cos\gamma)$ is given in the following table and may be compared with Table XVII which gives the same figure for aimed fire averaged over the expected ranges of engagement.

Best Available Copy

TABLE XXI

PROBABILITY OF RANDOM HIT FALLING ON TOTAL PRESENTED AREA OF JSIII CAUSING KILL

Projectile	Kill Category		
	M	F	K
90mm T108	.18	.12	.05
5" HC (Cu lined)	.49	.30	.17
6.5" ATAR (Steel Lined)	.55	.41	.26

Comparison of Tables XVII and XXI shows the requirement for larger shaped charge rounds when inaccurate fire is to be used.

The following table gives a summary of vulnerable areas on the T34/85 Russian Tank to the 2.36 in and 3.5 in Rockets.

TABLE XXII

VULNERABLE AREA OF T34/85 - FT^2

Angle of Attack	Presented Area Ft^2	2.36 HEAT M6			3.5" HEAT M28		
		M	F	K	M	F	K
Ground Attack							
Front	45	7	5	4	9	6	5
45°	95	18	11	8	20	13	9
Side	97	36	17	15	37	21	16
135°	95	35	14	11	40	17	14
Rear	45	23	5	5	25	6	6
30° Air Attack							
Front	87	19	17	15	21	19	16
45°	135	30	16	14	35	21	17
Side	140	38	18	16	45	23	19
135°	135	45	17	14	51	20	17
Rear	87	41	7	6	46	9	7

Table XXIII gives the vulnerable area of the M26 to the 3.5 inch rocket.

TABLE XXIII

VULNERABLE AREA OF M26 TO 3.5" ROCKET Ft^2

Angle of Attack	Kill Category		
	M	F	K
Front	7	7	2
30°	18	11	6
60°	29	16	11
Side	36	23	17
120°	33	16	11
150°	27	8	5
180°	22	2	1

Some calculations using an approximation of the vulnerable area technique have been made using the product of the probability of a perforation averaged over the expected angles of attack and the probability of a kill in the unarmored components of the tank averaged over the expected angles of attack. Calculations were made for the average of the front and sides of the tanks only. These calculations approximate the probability of a random hit being a kill on the ultimate penetrable area, which is the penetrable area a tank presents to a round of infinite penetration.

TABLE XXIV

APPROXIMATE PROBABILITY OF A RANDOM HIT ON ULTIMATE PENETRABLE AREA OF SEVERAL SOVIET ARMORED VEHICLES GIVING A KILL

Tank/Round	76mm HEAT			90mm HEAT			105mm HEAT		
	M	F	K	M	F	K	M	F	K
JSIII	.20	.16	.08	.37	.31	.18	.50	.41	.24
T34/85	.46	.38	.22	.47	.39	.23	.53	.42	.26
JSU 152	.44	.34	.19	.49	.40	.24	.53	.42	.26
SU 100	.44	.34	.19	.45	.40	.23	.54	.44	.27

Tank/Round	Energa Rifle Grenade		
	M	F	K
JSIII	.09	.08	.04
T34/85	.38	.31	.17

A rough check of the consistency of these approximations can be made by comparing Tables XX and XXI. This check shows that the values shown for the 90mm T106 vs. the JSIII shown in Table XXI should be approximately half of those shown in Table XXIV, which is approximately so.

Evaluation of Present Methods of Analysis

The present methods of analysis are not completely satisfactory. Fairly reliable estimates of the probability of a hit causing a kill can be made but the method is tedious. Additional data is needed to reduce the subjective elements of damage assessment. Further reduction of existing damage data should help.

The computation of vulnerability by considering the chance of a kill after perforation on each small area is cumbersome. However, it is reasonably reliable and until a body of this reliable information is assembled approximations must be viewed with suspicion.

The method of analysis does not yet accurately account for the transition point between the inaccurate fire where vulnerable areas can be used and accurate fire where the distributed area technique can be used. Where the gunner starts aiming at spots on a tank rather than the whole tank as a target is not known and probably will depend to some extent on the training of the gunner.

Future analysis will be helped by witness plate data such as the British have been obtaining for many years. However, there appears little likelihood that the vulnerability of a tank can be computed from syntheses of many tests made only with simulations of tanks. The analyst of vulnerability must never be misguided into the assumption that an exact measurement made of an assumed condition (such as the box tests represent) can be used to the exclusion of the inexact measurement of the real condition (vulnerability firings at vehicles).

BIBLIOGRAPHY

1. "A Survey of Tank Casualties," British Report No. 19 (Study No. 82), Military Operational Research Report, Department of the Scientific Advisor to the Army Council. March 1947 (Secret).

2. "Operational Research in North West Europe," The Work of No. 2 Operational Research Section with 21 Army Groups. June 1944 - July 1945 (Secret).

ABERDEEN PROVING GROUND FIRING RECORDS

3. 75mm M310A1 vs T26E4 Tank (100 yds) AR-17727

4. 90mm T108E4 vs T26E5 Tank (500 yds) AR-17728 (Confidential)

5. 2.75 in FFAR and 8cm Oerlikon Rocket vs T26E4 Tank (air to ground 600 yds) AD1166 (Confidential)

6. 3.5 in. M28 Rocket vs T26E4 Tank (100 yds) AR-17193

7. 3.5 in. M28A1 Rocket vs T26E4 Tank (40 ft) AR-17340

8. 105mm M67 vs T26E4 (500 yds) AR-17726

9. 5 in. (Al cone and Cu cone vs T26E4 & T26E5 (static) AD-1151

10. 6.5 in. ATAR M101A T26E4 (static) AR-17336

11. 6.5 in. ATAR MK2 vs T26E4 (air to ground) R2560

12. 90mm T108E15 vs Tank stowed 90mm APT33 and 85mm (Soviet) (100 and 50 yds) AR-17707 (Confidential)

13. 2.36 in M6A6 Rocket vs Diesel fuel and gasoline (static) AR-18761

14. 90mm T108E15 vs Tank Stowed Diesel Fuel (50 yds) AR-18617 (Confidential)

15. 3.5 in. M28A1 vs Gasoline filled Fuel Tanks (static) AR-17341

15a. 3.5" M28A2 vs Diesel fuel filled containers (static) AR-17650

16. 5 in. (Al cone) vs Stowed Ammunition and Diesel Fuel (static) AR-18614 (Confidential)

BRITISH VULNERABILITY DATA

17. BOB Proc Q6887 - To Estimate the Degree of Overmatching necessary to obtain Lethality against Tanks by Use of Hollow Charge Projectiles.

18. BOB Proc Q7615 - Performance of British Projectiles Against Foreign A.F.V.'s

19. FVDE AT320 Energa Grenade vs German Panther Tank

20. FVDE AT320/? Effect of Energa Grenades Against Live Ammunition, Petrol and Diesel Fuel.

21. FVDE AT320/8 Ammunition Fires in A.F.V.'s

22. "Investigations of the Effects of Shaped Charges Beyond Defeatable Armor," NOTS TM NO. 462 (Problem G of Phase 1, Task Assignment NOTS RE 20-46-1-s1B) U.S. Naval Ordnance Test Station, Inyokern China Lake, California. 27 June 1952 (Confidential).

23. "Method for Increasing the Destructiveness and Lethality of Lined Cavity Charges," BRL Report No. 848 (Project TB3-0134), Aberdeen Proving Ground. March 1953.

24. BRLTN 592 - A Partial Evaluation of the Comparative Effects of the 90mm T108 HEAT Round Against The Russian JSIII Tank

25. BRLM 590 - Range and Angular Distribution of AP Hits on Tanks

26. BRLTN 735 - Vulnerability Firing Against Tank Fuel Containers

27. BRLM 612 - Distribution of Soviet Armor

28. Summary of Firings of 3.5 in Rocket, 90mm T108E15 and 90mm MC150E1 vs spaced armor. AR-18504

APPENDIX I

AMERICAN HEAT AMMUNITION

Cartridge, HEAT, T108, 90mm Gun 300
Grenade, Rifle, HEAT, M31 (T37E4) 301
Rocket, HEAT, 3.5" T230 301
Grenade, Rifle, HEAT, M28 (Energa) T41 302
Shell, HEAT, M307A1 for 57mm Rifle 303
Shell, HEAT, M310A1 for 75mm Rifle 303
Rocket, HEAT, M28 (T80E2) 304
Rocket, HEAT, T205, 3.5" 305
Rocket, FFAR, 2.75" T2016 306
Shell, HEAT, M67, 105mm Howitzer 307
Shell, HEAT, M324 (T43) for 105mm Rifle 308
Shell, HEAT, M344 (T119E11) for 106mm Rifle 309
Shell, HEAT, M66 for 75mm Howitzer 310

NOTE: Specific penetration performance for the ammunition described in this appendix is not given here. A list of some of the most useful references where penetration data may be found is given. Penetrations are not given here for one or more of the following reasons:

a. Much of the data expresses penetration performance in terms of complete or incomplete perforation of a given target thickness instead of absolute penetration.

b. Target materials used to obtain penetration data are sometimes insufficiently described to permit use of data reported.

c. Penetrations given are frequently achieved with experimental modifications of the round which do not permit it to be considered as typical.

d. Much of the penetration data which can be found was obtained by probing the hole in the target. The error possible in such a determination of penetration, because of variations in slug length, and of the amount of jet material deposited in the bottom of the hole suggests caution in citing this data for penetration.

All references cited are available at the Technical Information Branch Aberdeen Proving Ground, Maryland. Abbreviations used in designating references are as follows:

AFF - Army Field Forces
ARG-FR - Aberdeen Proving Ground Firing Record
NAVORD - Navy Ordnance Reports
NPG - Naval Proving Ground
OCM - Ordnance Committee Minutes
OCO - Office, Chief of Ordnance
OIO - Ordnance Intelligence Office
TM - Technical Manual
WDA - Weapons for Defeat of Armor

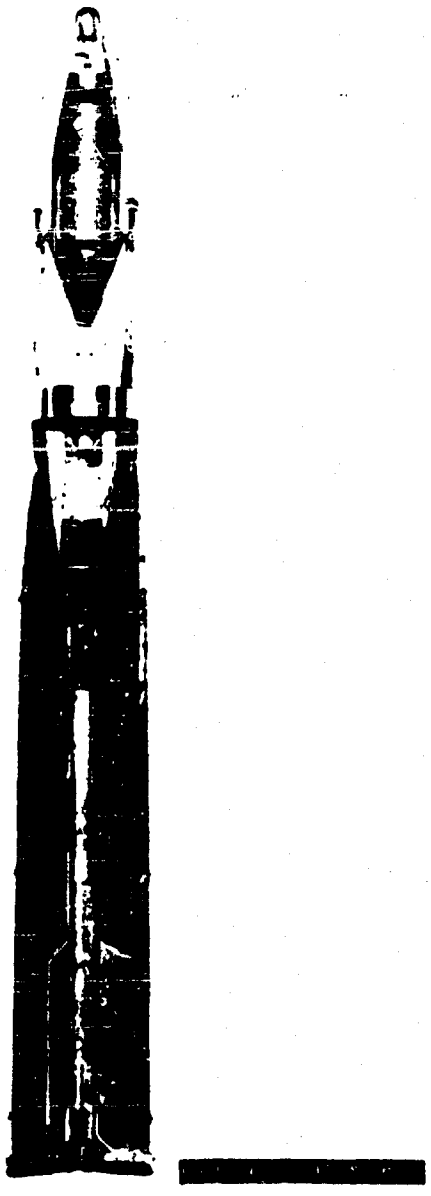

CARTRIDGE, HEAT, T108, 90MM GUN W/FUZE PIBD T208E7

Reference: WDA, OCO, Vol 1, Apr. 1953

Muzzle Velocity: 2800 f/s
Explosive Charge: Composition B

Reference: OCM 33165, 16 Feb. 1950

Penetration Requirements: Through 5" of Homogeneous Armor at 60° Obliquity

Penetration References:

APG FR 49200, Sept. 1951
APG FR 51386, Apr. 1952
APG FR 52898, Aug. 1952
APG FR 55338, Oct. 1952
APG FR 55812, Mar. 1953
APG FR P-59892 (Not yet published)
WDA OCO, Vol. 1, Apr. 1953

GRENADE, RIFLE, HEAT, M31 (T37E4) W/FUZE, GRENADE RIFLE, PIBD M211

Reference: AFF Board No. 3 Report P2543, Mar. 1953

Fin Stabilized
Cone Characteristics:

Material:	Copper
Apex Angle:	45°
Cone Diameter:	2" (Approx.)

Explosives: 0.78 lb. Composition B
Total Weight: 1.6 lb.

Reference: WDA, OCC, Vol. 2, Nov. 1953

This round is to replace Grenade, Rifle, M28

Penetration References:

APG Report, Project TA3-5911/1, June 1952
APG Report, Project TA3-5911/2, July 1952
APG Report, Project TA3-5911/3, Nov. 1952
WDA, OCO, Vol. 2, Nov. 1953

ROCKET, HEAT, 3.5", T230

Reference: WDA, OCO, Vol. 2, Nov. 1953

Similar in most respects to the T205 except that the round will have a maximum velocity of 700 fps. Total weight of round is to be 4.5 lb.

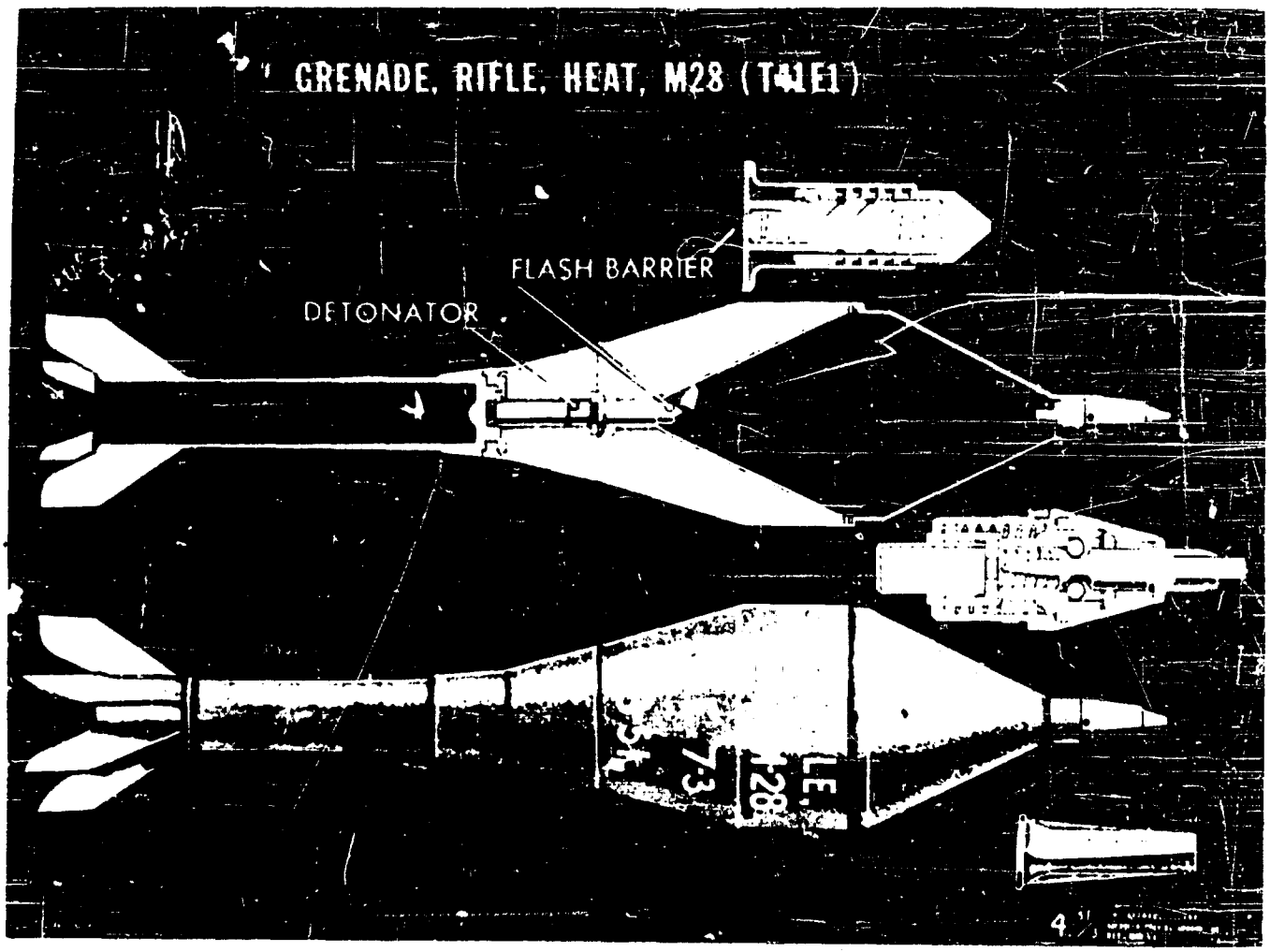

GRENADE, RIFLE, HEAT, M28 (ENERGA) T41

Reference: WDA, OCO, Vol. 2, Nov. 1953

This round is the American version of the Belgian Energa and is to be replaced by Grenade, Rifle, HEAT, M31

Reference: AFF Board No. 3 Report P2543, Mar. 1954

Muzzle Velocity: 174 f/s

Reference: OIO 325, Sept. 1947

Explosives: 0.75 lb. Composition B
Total Weight: 1.45 lb.

Penetration References: APG Report, Project TA3-5911/1, Jun. 1952

SHELL, HEAT M307A1 FOR 57MM RECOILLESS RIFLE

Reference: Ord. Dwg. 75-2-354, 28 Apr. 1953

Liner Characteristics:

Hemispherical type with Spitback Tube	
Material:	Copper
Wall Thickness:	.048"
Liner Diameter:	1.6" (Approx.)
Radius of Curvature:	0.84"

Reference: Firing Table FT57-E-1

Muzzle Velocity:	1200 f/s
Rifling:	1 Twist/30 Caliber
Spin Rate of Shell:	213 Revolutions/sec.

Penetration References: APG FR PL9028, 21-28 Apr. 1951

SHELL, HEAT, M310A1 FOR 75MM RECOILLESS RIFLE

Reference: APG FR 50546, 6 Nov. 1951

Striking Velocity: 1000 f/s

Reference: Ord. Dwg. 75-2-315, 17 Mar. 1953

Cone Characteristics:

Material:	Copper
Wall Thickness:	.073"
Cone Diameter	2.4" (Approx.)
Apex Angle:	42°

NOTE: The same liner as is used in the 75mm Howitzer HEAT round M66 is used in this round.

Reference: Firing Table FT-75-BB-2

Muzzle Velocity:	1000 f/s
Rifling:	1 Twist/22 Caliber
Spin Rate of Shell:	135 Revolutions/sec.

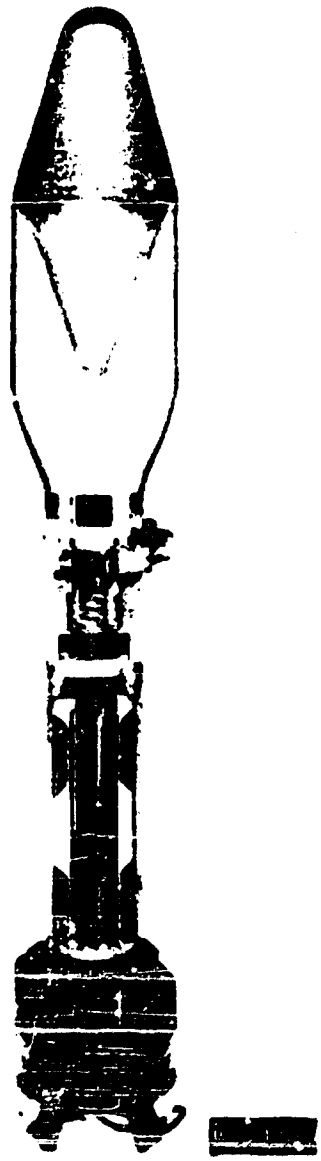

ROCKET, HEAT, M28, (T80E2)

Reference: OCM 32304, Aug. 1948

Modified to M28A2 by replacing the base fuze P. D. T200GE2
Fin Stabilized
Muzzle Velocity: 325 f/s
Explosive: 1.93 lb. Composition B

Reference: Ord. Dwg. 82-5-131, 28 Mar. 1952

Cone Characteristics:

Material:	Copper
Wall Thickness:	.093"
Cone Diameter (Approx.):	3.08"
Apex Angle:	42°

Penetration Requirements:
Defeat 12" of armor 60% of the time
Defeat 11" of armor 100% of the time

Penetration References:
AFF Board No. 3, P-2579 APG FR R2889, Jul. 1952
APG FR R2888, Jul. 1952 APG FR R2890, Jul. 1952

ROCKET, HEAT, T205, 3.5" W/FUZE PIBD T2030

Reference: APG Report, Project TU-2-1015 A/1, Jul. 1953

Cone Characteristics:

Material:	Copper
Wall Thickness:	.075"
Cone Diameter:	3.09"
Apex Angle:	45°

Muzzle Velocity:	440 f/s
Explosive:	1.5 lb. Composition B

Reference: OCM 32753, Feb. 1949

Penetration Requirements:

Defeat 12" of Armor at 0° Obliquity)
Defeat 7.9" of Armor at 45° Obliquity) 90% of the time
Defeat 4.7" of Armor at 60° Obliquity)

Accuracy Specifications:

75% probability of hitting a target 7' wide x 8' high at 500 yards with first round.

Penetration References:

APG FR 3036, Jun. 1953

APG Report, Project TU2-1015 A/1, Jul. 1953

CONFIDENTIAL

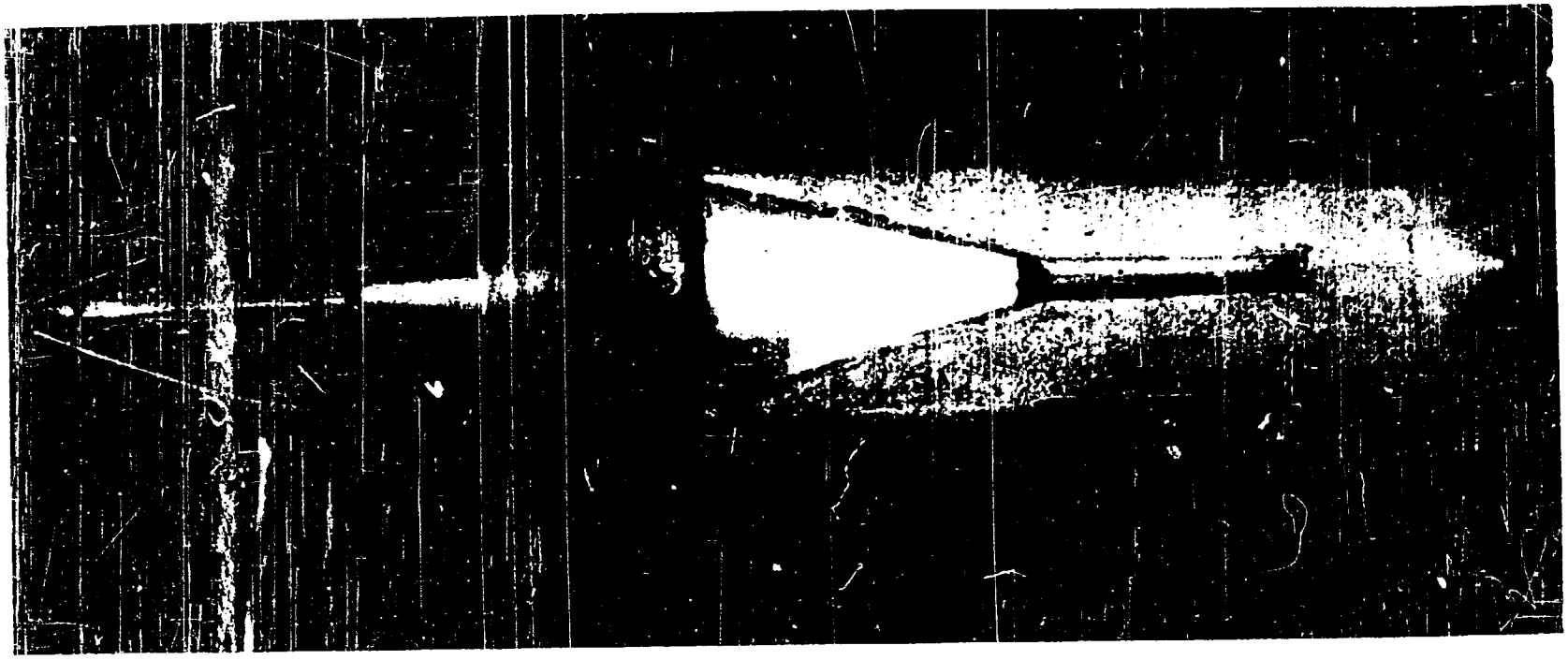

ROCKET, FFAR, 2.75" T2016 W/F PI T2023 (ROCKET HEAD T208)

Reference: US NPG Report 779, May 1951

Striking Velocity:	2100 f/s
Explosive:	.9 lb Composition B
Cone Characteristics:	
Material:	Copper
Wall Thickness:	.096"
Cone Diameter:	2.33" (Approx.)
Apex Angle:	42°
Spitback Tube	

Penetration References:

Report No. 779, May 1951, U.S.N.P.G. APG FR R2923, Oct. 1952

CONFIDENTIAL

SHELL, HEAT, M67, 105MM HOWITZER

Reference: Ord. Dwg. 75-4-107, 29 Aug. 1950

Cone Characteristics:

Material:	Steel
Wall Thickness:	.103"
Cone Diameter:	3.23" (Approx.)
Apex Angle:	42°

Reference: Complete Round Chart, Apr. 1954

Explosive: 2.93 lb. Composition B

Reference: Firing Table, FT 105-H-4

Muzzle Velocity:	1020 f/s
Rifling:	1 Twist/20 Caliber
Spin Rate of Shell:	148 Revolutions/second

Penetration References:

APG FR 33438, Sept. 1944
APG FR 34445, Nov. 1944
APG FR 36802, Apr. 1945

SHELL, HEAT, M324 (T43) FOR 105MM RECOILLESS RIFLE

Reference: Ord. Dwg. 75-4-107, 29 Aug. 1950

Cone Characteristics:
- Material: Copper
- Cone Diameter: 3.23" (Approx.)
- Wall Thickness: .103"
- Apex Angle: 42°
- The cone dimensions are identical with the cone prescribed for the 105mm M67 shell.

Explosive: 3.00 lb. Composition B
Spin Stabilized (Pre-engraved Band)
Muzzle Velocity: 1250 f/s

Penetration References:

APG FR 48650, 18 Jul. 1951 APG FR 52363, 23 Jul. 1952

Reference: Firing Table FT 105-AH-2

Muzzle Velocity: 1250 f/s
Rifling: 1 Twist/20 Caliber
Spin Rate of Shell: 181 Revolutions/sec.

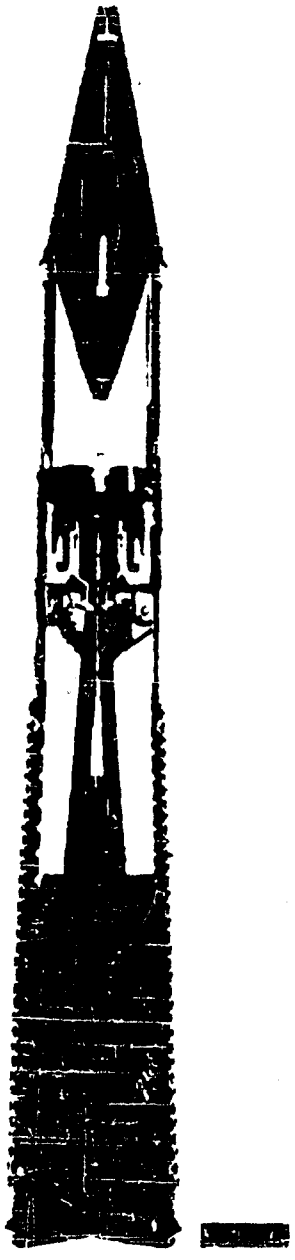

SHELL, HEAT, M344, (T119E11) W/F PIBD
T208E7 (ELECTRIC) FOR 106MM RIFLE

Reference: OCM 34899, 1 Jul. 1953

Folding Fin
Explosive: 2.79 lb. Composition B
Muzzle Velocity: 1650 f/s

Reference: Ord. Dwg. 75-2-510, 31 Mar. 1954

Cone Characteristics:
Material: Copper
Wall Thickness: .100"
Cone Diameter: 3.56"
Apex Angle: 42°

Penetration References: 1st Memorandum report on the "Lethality Tests of 106mm Shell, HEAT, T119E11 (M344) "Project TA1-1540 Jul. 1954, from APG to OCO.

SHELL, HEAT, M66 FOR 75MM HOWITZER

Reference: Ord. Dwg. 75-2-315, Rev. 17 Mar. 1953

Cone Characteristics:

Material:	Copper
Wall Thickness:	.073"
Cone Diameter:	2 1/8" (Approx.)
Apex Angle:	42°

Explosives: 1 lb. Composition B

Reference: Firing Table FT-75-1-3

Muzzle Velocity:	1000 f/s
Rifling:	1 Twist/20 Caliber
Spin Rate of Shell:	200 Revolutions/sec.

Penetration References: APG FR P33263, Sept. 1944
APG FR 48424, Mar. 1951

APPENDIX II

FOREIGN TYPES OF AMMUNITION (SOVIET)

Soviet HEAT Projectile for
12mm Mow., Mod - 38 312

Soviet HEAT Projectile for
76.2mm Regt. Gun Mod - 27 313

Hollow Charge Shell 7.5cm GR 38 314

Soviet Grenade, Hand, HEAT, Model RPG-6 . 315

Soviet Grenade, Hand, AT, Model 1943 . . . 316
RPG 43

Intelligence Reports on Miscellaneous . . 317
Soviet HEAT Ammunition

NOTES: All references cited are available at the Technical Information Branch, Aberdeen Proving Ground, Maryland. Abbreviations used in designating references are as follows:

DA-PAM	- Department of the Army - Pamphlet
OIN	- Ordnance Intelligence Number Ordnance Technical Intelligence Office
OTIO	- Ordnance Technical Intelligence Office
OTIS	- Ordnance Technical Intelligence Section
ST-F	- Special Text - Foreign
TM	- Technical Manual

As will become apparent from a perusal of the following pages, there is a severe lack of information regarding Soviet Ammunition.

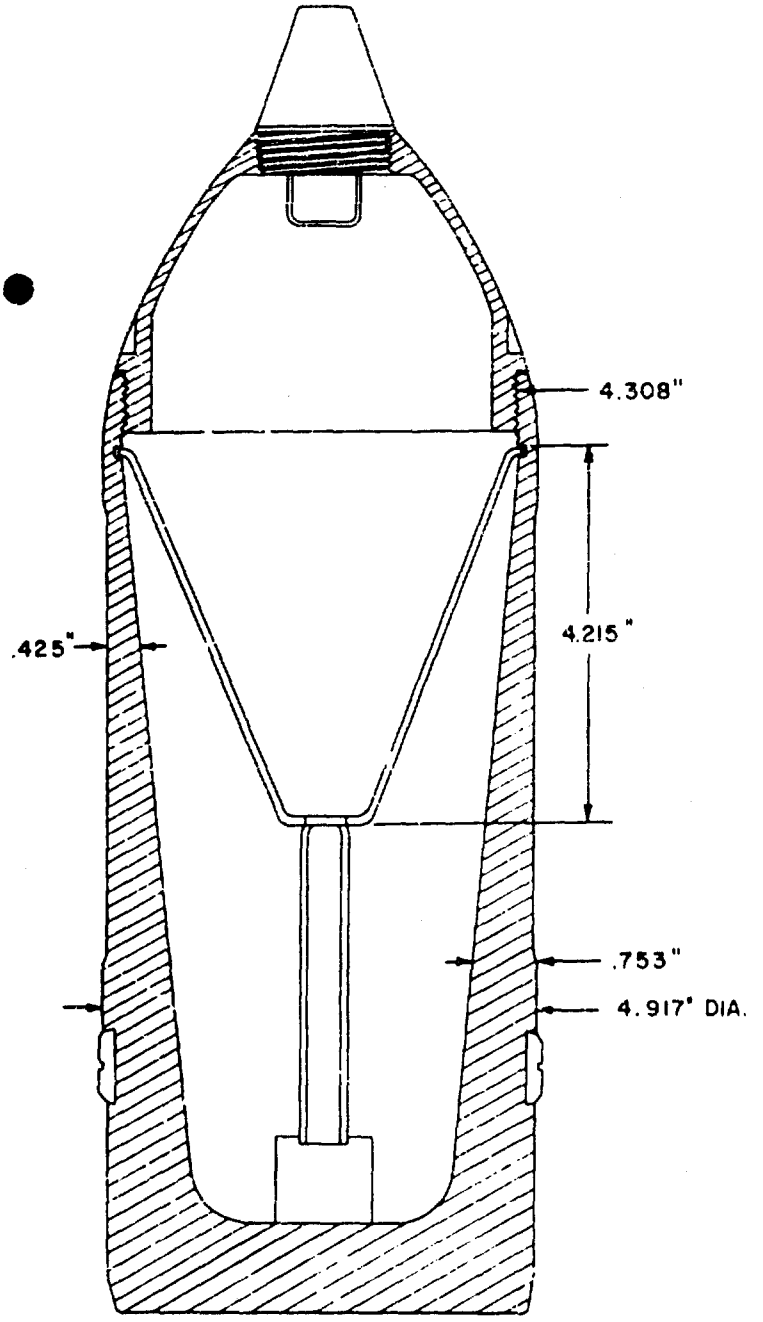

SOVIET HEAT PROJECTILE FOR 122MM HOWITZER - MODEL 38

References:

ST-F-87 p. 261	OIN 3317	ST-F-66
TM [illegible] p. 72	OIN 4204	ST-F-74
OIN 5451	OIN 5050	OTIO Dwg. No. 40
OIN 4920	OIN 2009	APG TMI-5002/3

Cone Characteristics:

Material: Ferrous, Cast
Wall Thickness: .106"
Apex Angle: 40°

Explosive: 3.13 lb. Cyclotol

Penetration against homogeneous armor plate, statically fired: Max. penetration 5.5"

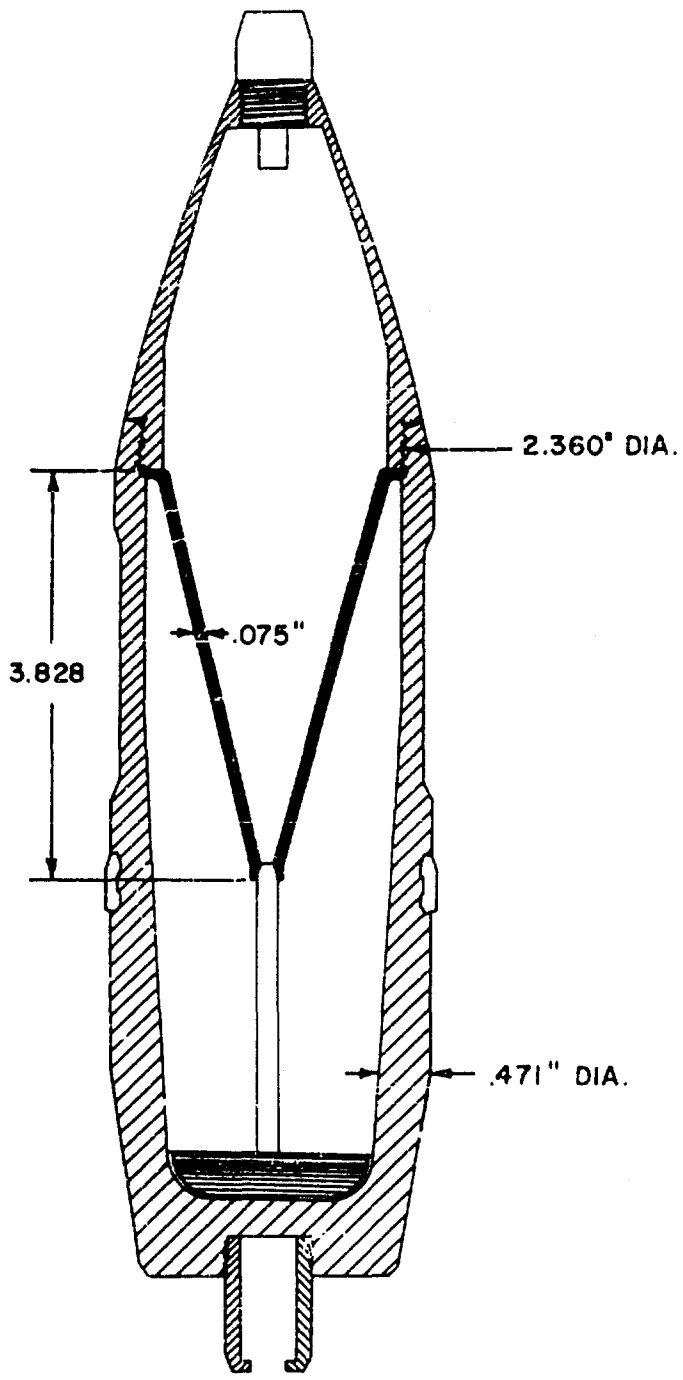

SOVIET HEAT PROJECTILE FOR 76.2MM REGIMENTAL GUN, MODEL 27

References:

ST-F-87 p. 190-193	ID 588910 p. 109	OIN 4617
ST-F-66	TM 30-240 p. 54	OIN 3197
ST-F-74	OIN 3352	OIN 4178
		OTIO Dwg. No. 22

Weight of Projectile: 6.7 lb.
Explosive: 1.14 lb. Cast Cyclotol

NOTE: Tracer element in base of shell

HOLLOW CHARGE SHELL, 7.5CM GR 38

References:

ST-F-87 p. 190-193	OIN 3352
ST-F-66	OIN 4617
ST-F-74	OIN 3197
ID586910, p. 109	OIN 4178
TM 30-240, p. 54	OTIO Dwg. No. 22

Static Fired Penetration: 1.8" at 30° Obliquity
2.17" at 0° Obliquity

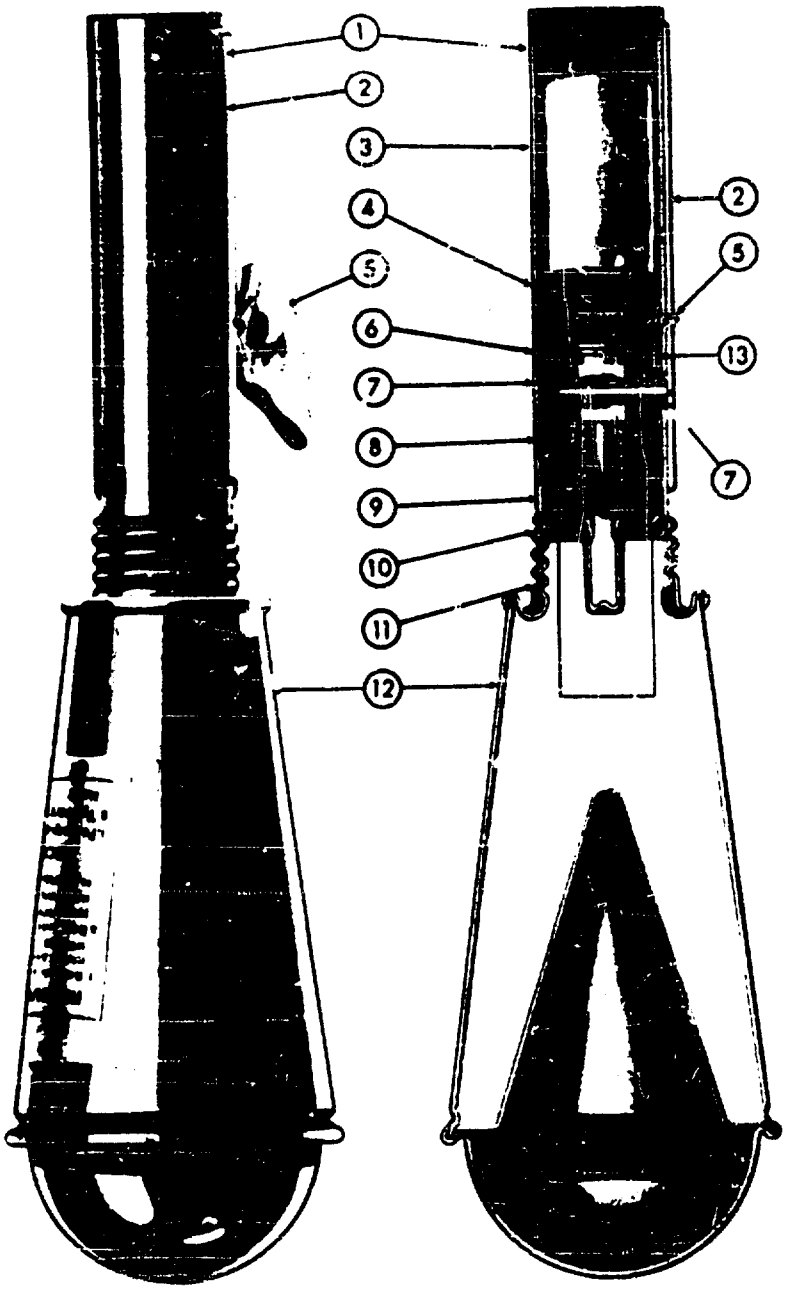

① HANDLE ASSEMBLY ④ SAFETY CAP (CH

①Handle Assembly
②Safety Lever
③Stabilising Ribbon
④Safety Cap (Check Ball Retainer Cap)
⑤Pull Pin and Tab
⑥Striker
⑦Striker Retaining Pin and Spring
⑧Anti-Creep Spring
⑨Striker Body
⑩Striker Lock
⑪Detonator Booster Assembly
⑫Grenade Body
⑬Check Ball

SOVIET GRENADE, HAND, HEAT, MODEL RPG-6

Reference: DA PAM 30-2, p. 13

Penetration: Up to 3.94" armor

Reference: DA PAM 30-50-1, p. 102

Effective against concrete pillboxes

Reference: ONI 5050, p. 4

Explosive Filler:	TNT
Average Range:	17-25 yds.
Radius of Fragmentation:	26 yds.

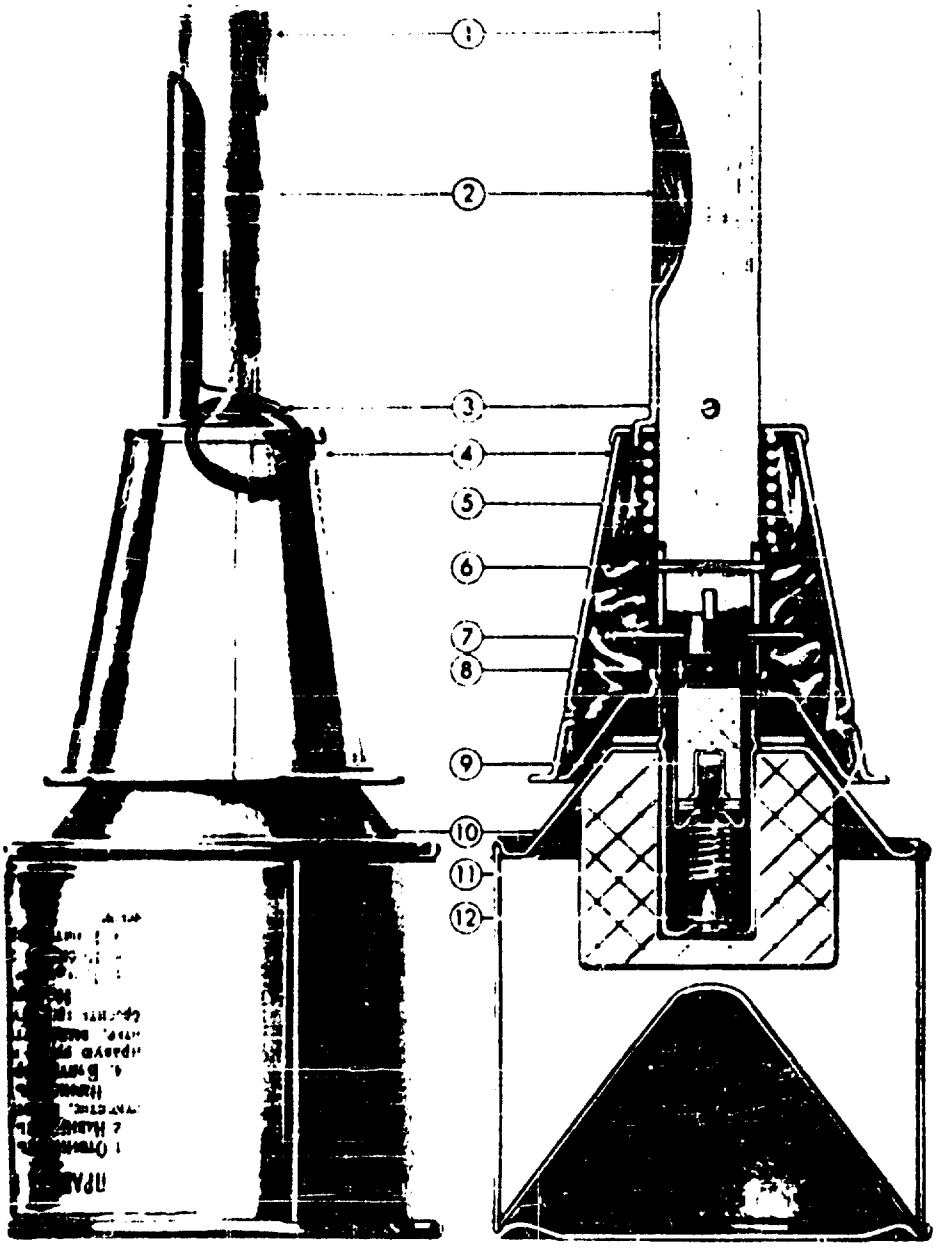

(1) Handle Assembly
(2) Safety Lever
(3) Pull Pin and Ring
(4) Stabilizing Cap
(5) Stabilizing Cap Spring
(6) Fabric
(7) Safety Pin
(8) Safety Screw
(9) Detonator Booster Assembly
(10) Grenade Body
(11) Safety Spring
(12) Firing Pin
(13) Closing Cap Disc
(14) Closing Cap

SOVIET GRENADE, HAND, AT, MODEL 1943 RPG 43

Reference: APG-OS-501-C

Weight of Grenade: 1,200 gms.
Penetration in Armor: Up to 75mm
Not recommended for use against the track of suspension system of a tank.

INTELLIGENCE REPORTS ON SOVIET HEAT AMMUNITION

Panzerfaust: A copy of the German Panzerfaust 150 which had a range of 165 yards and the ability to penetrate 8" into armor, Ref: DA-PAM-30-2

Rifle Grenade Model VPT-6-41: Armor penetration given as 1.8" Ref: DA-PAM-30-2

Hand Grenade, Model RG-43: Effective against armor up to 2.95" thick. Ref: DA-PAM-30-2
Average range: 17-22 yds. DA-PAM-30-50-1
Explosive Filler: 1.35 lbs cyclotol OIN 5050

Anti-Tank Rifle Grenade, VPG

Ref: OTIS File
Range: 50-75 meters
Explosive Charge: 334gms. of Compressed TNT
Penetration: Armor at 60° Obliquity: 30mm

APPENDIX III

FOREIGN (MISCELLANEOUS)

Heller 320

8cm Oerlikon 321

Panzerschreck 322

Panzerfaust 323

NOTE: All references are available at the Technical Information Branch, Aberdeen Proving Ground, Maryland. Abbreviations used in designating references are as follows:

CARDE - Canadian Armament Research and Development Establishment
NAVORD - Navy Ordnance Reports
APG-FR - Aberdeen Proving Ground - Firing Record
ID - Intelligence Department
Ordnance Technical Intelligence Office

CONFIDENTIAL

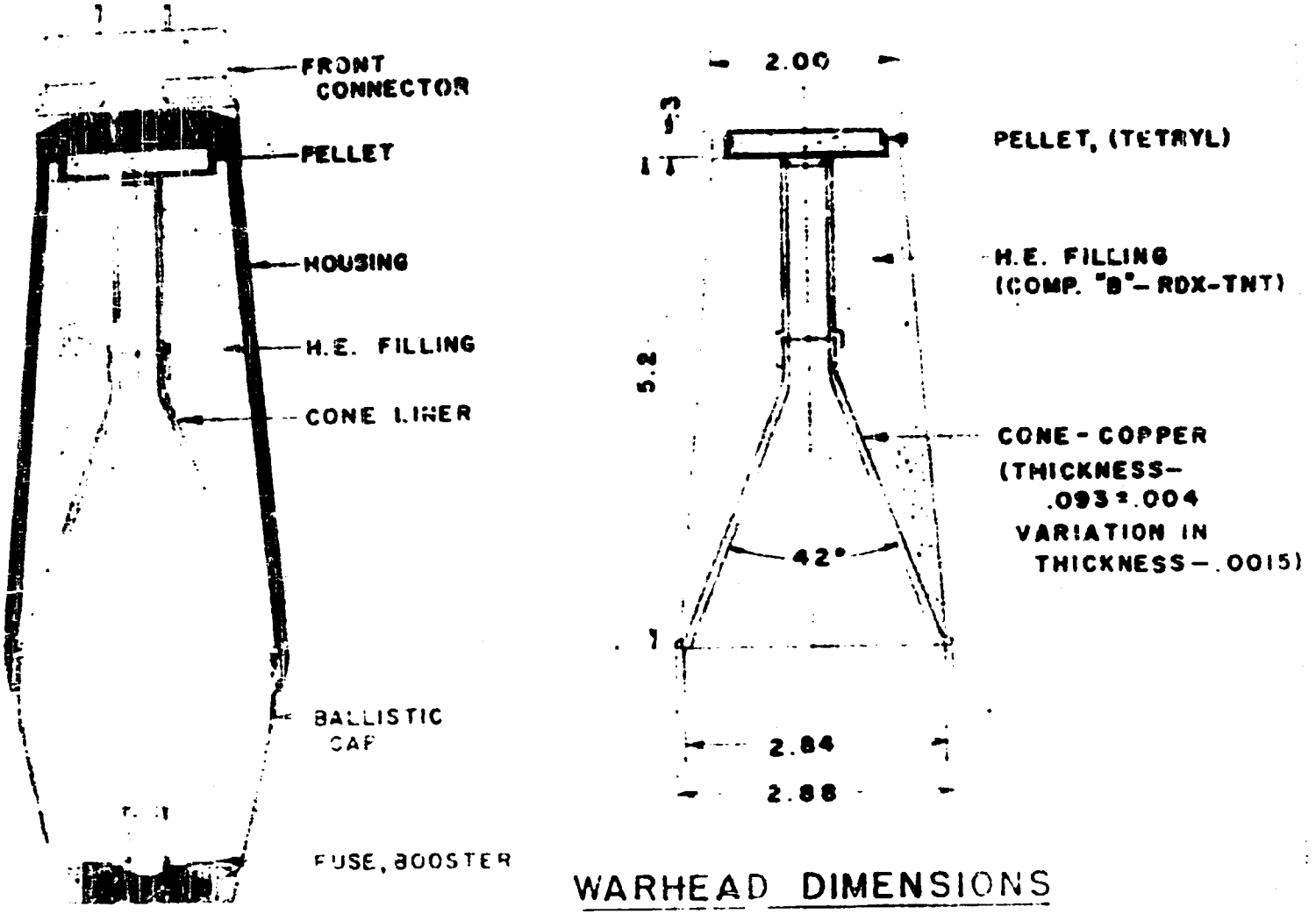

WARHEAD DIMENSIONS

ROCKET, HELLER, 3.2" W/FUZE M52

Reference: Miscellaneous Report 51/53, CARDE, Nov. 1953

Total Weight of Round:	8.5 lb.
Muzzle Velocity:	720 f/s
Dispersion at 500 yds:	1.2 mils
Penetration:	10 to 11" homogeneous armor

CONFIDENTIAL

8CM OERLIKON (SWISS) AIRCRAFT ROCKETS

Reference: Navord Report 1901, 16 Aug. 1951

Weight of Explosive:	1.4 lb.
Maximum Spin Rate Due to 8 Canted Nozzles:	1200 rpm
Penetration into Plate: At 0° Obliquity:	7.09"

Reference: APG Firing Record R-2617, 26-28 Feb. 1951

Explosive Loading: Pentolite

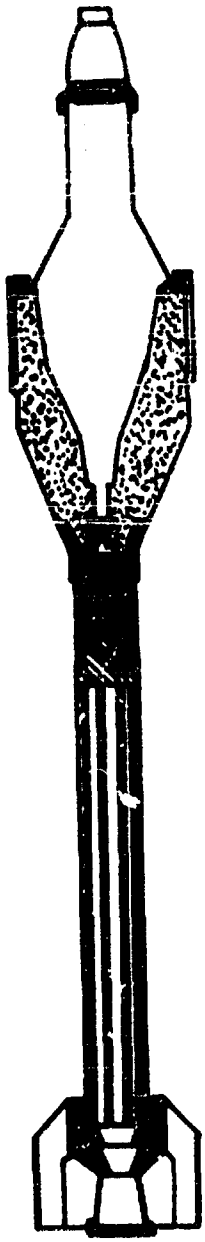

PANZERSCHRECK

Reference: ID 945677/13, dated 1949

Maximum Range: 150 meters
Penetration: 7.9" Armor

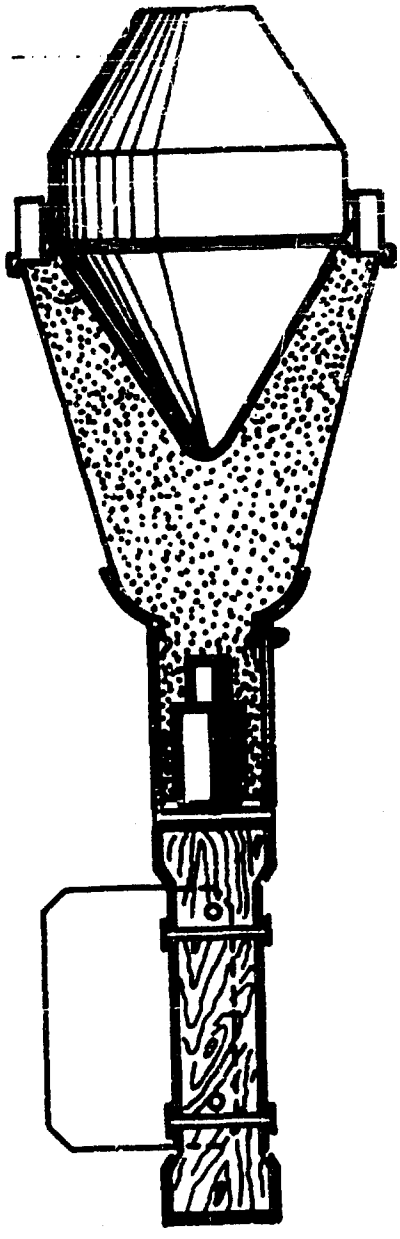

PANZERFAUST

References: ID 945677/13 dated 1949 DA - PAM 30-2, p. 22

Explosive: 3.5 lb. 55/45 Cyclotol
Penetration: 7.9" Armor

ARMY---OO---ABERDEEN PROVING GROUND, MD

APPENDIX IV

SOVIET ARMOR

Tank, Soviet, JS III 326

Tank Soviet T34/85 327

Self-Propelled Gun, Soviet, SU-100 . 328

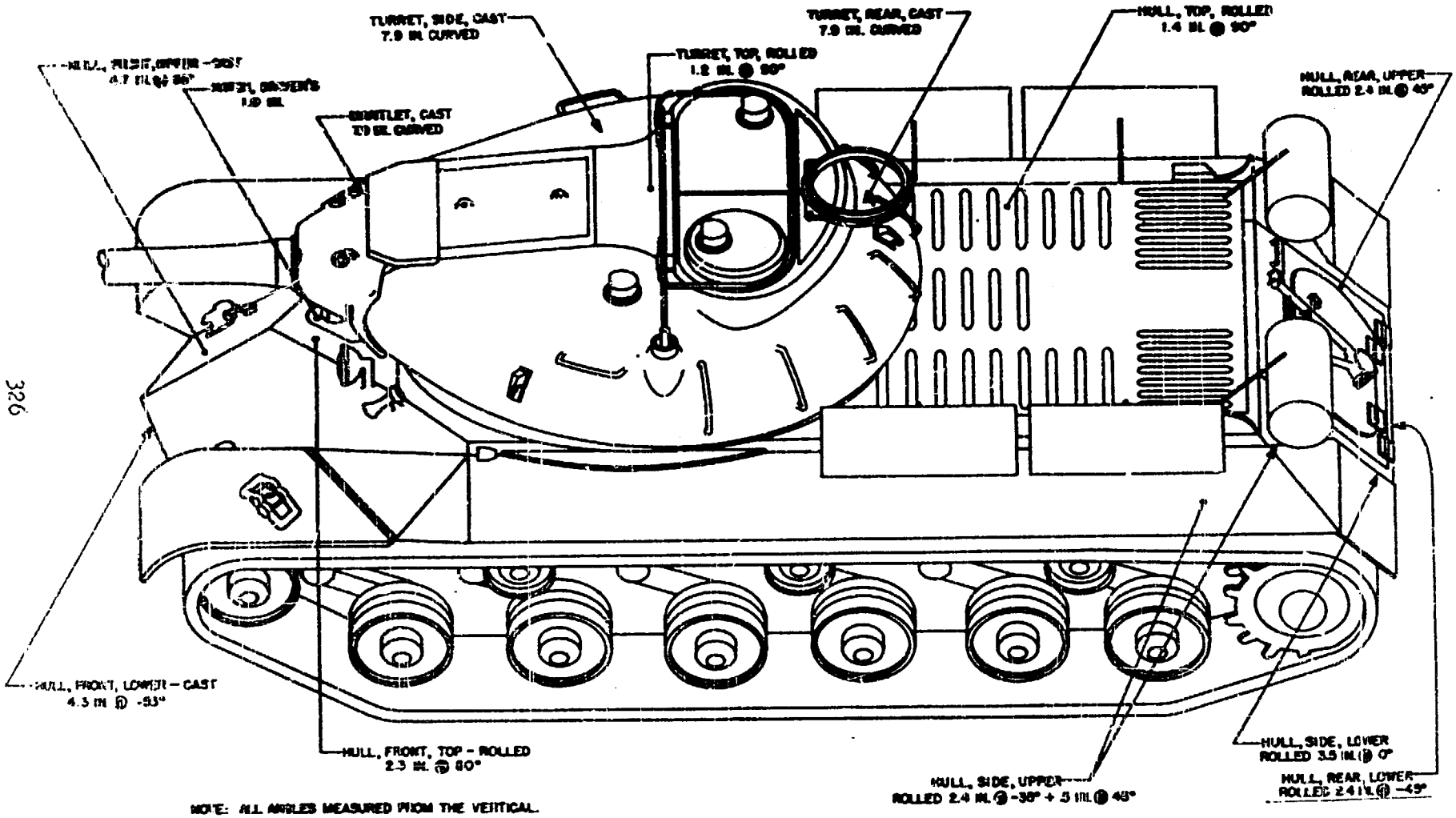

NOTE: ALL ANGLES MEASURED FROM THE VERTICAL.
BELLY ARMOR THICKNESS:
CREW COMPARTMENT = 2.4 IN.
ENGINE " = 0.8 IN.

TANK, SOVIET, JS III

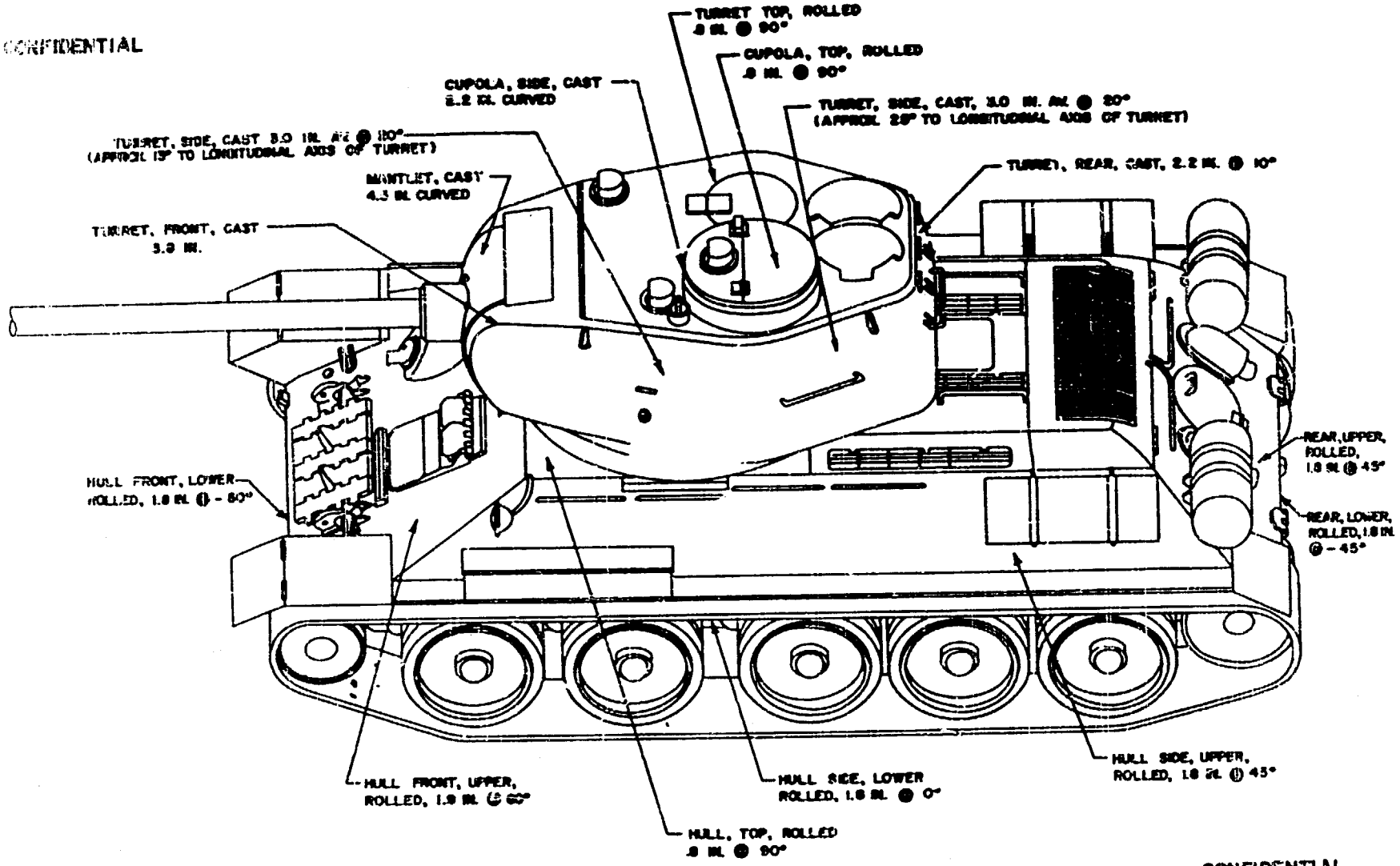

CONFIDENTIAL

NOTE:

ALL ANGLES MEASURED FROM THE VERTICAL.

BELLY ARMOR THICKNESS = 1 IN.

TANK, SOVIET, T34-85

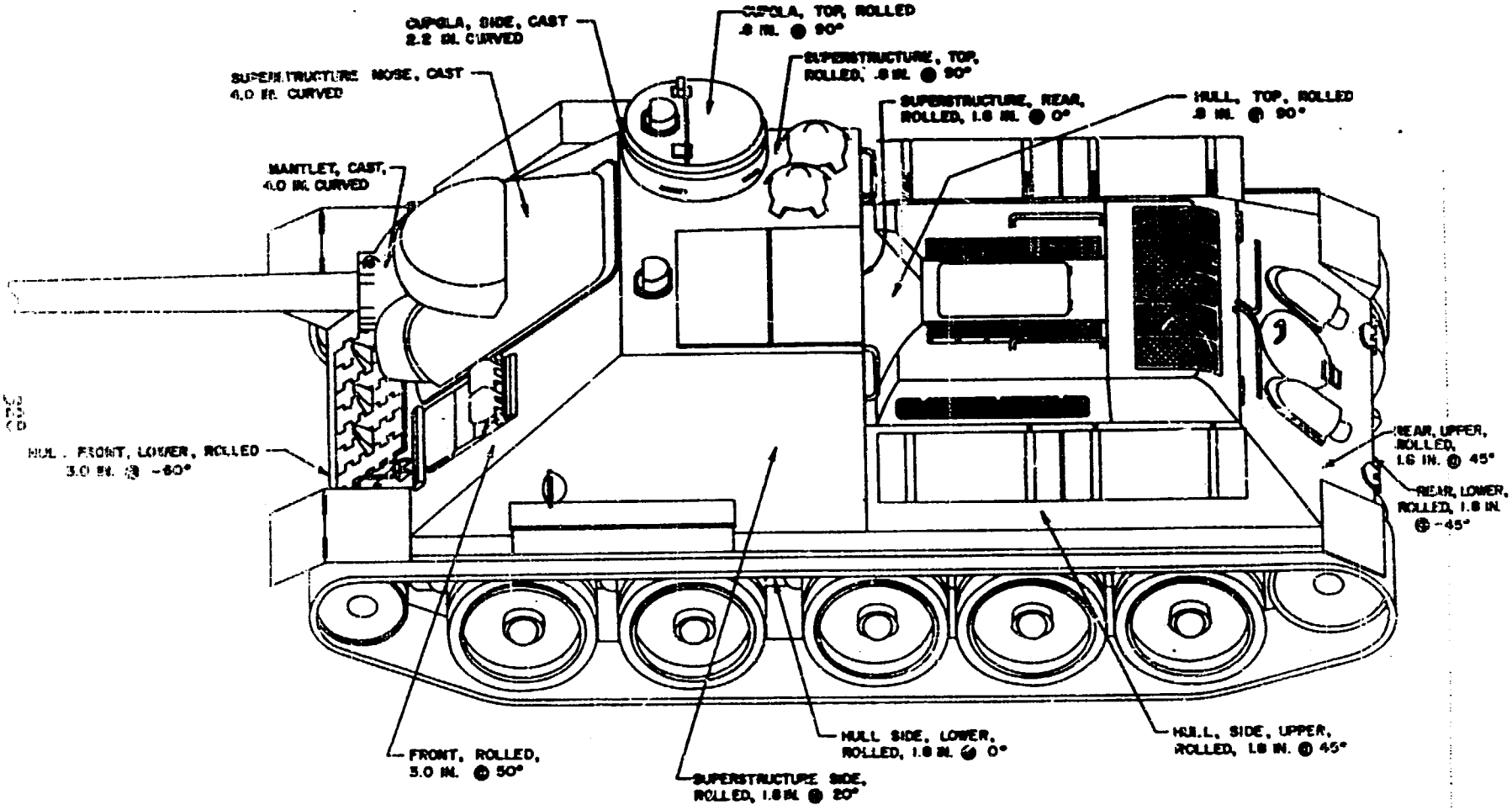

NOTE:
ALL ANGLES MEASURED
FROM THE VERTICAL.
BELLY ARMOR THICKNESS = 1.6 IN.

CONFIDENTIAL

SELF-PROPELLED GUN, SOVIET, SU-100

DISTRIBUTION LIST

No. of Copies	Organization
6	Chief of Ordnance Department of the Army Washington 25, D. C. Attn: ORDTB - Bal Sec - 1 cy ORDTA - 1 cy ORDTS - 1 cy ORDTT - 1 cy ORDTU - 1 cy ORDTX-AR - 1 cy
10	British - ORDGU-SE, Foreign Relations Section for distribution 2 cys - British Joint Services Mission Attn: Miss Mary G. Scott 3 cys - A.R.E., Of interest to: W. E. Soper A. Highfield J. Lyall
7	Canadian Joint Staff - ORDGU-SE, Foreign Relations Section for distribution Of interest to: C.A.R.D.E., Valcartier R. F. Wilkinson Edward Greenwood W. B. McKay Maj. J. M. Saldon Mr. R. W. Foster Dr. A. L. Wright
5	Chief, Bureau of Ordnance Department of the Navy Washington 25, D. C. Attn: Re3 Re2c - Mr. J. S. McCorkle
2	Commander Naval Proving Ground Dahlgren, Virginia
3	Commander Naval Ordnance Laboratory White Oak Silver Spring 19, Maryland Of interest to: Dr. S. J. Jacobs Dr. C. K. Hartman Mr. D. T. O'Connor
1	Commanding Officer Naval Ordnance Laboratory Corona, California Attn: Documents Librarian
5	Commander Naval Ordnance Test Station Inyokern P. O. China Lake, California Attn: Technical Library
1	Director Naval Research Laboratory Washington 25, D. C. Attn: Tech. Information Div.
1	Commander Naval Air Development Center Johnsville, Pennsylvania Attn: Aviation Armament Lab.

DISTRIBUTION LIST

No. of Copies	Organization
2	Commandant U. S. Marine Corps Washington 25, D. C. Attn: Div. of Aviation Plans and Policies Div.
2	Chief of Staff U. S. Air Force Washington 25, D. C. Attn: AFDRD - AR
2	Commander Wright Air Development Center Wright-Patterson Air Force Base, Ohio Attn: WCLG
5	Director Armed Services Technical Information Agency Documents Service Center Knott Building Dayton 2, Ohio Attn: DSC - SA
4	ASTIA Reference Center Technical Information Div. Library of Congress Washington 25, D. C.
2	Atomic Energy Commission 1901 Constitution Avenue Washington 25, D. C. Attn: Division of Military Applications
1	Los Alamos Scientific Lab. P. O. Box 1663 Los Alamos, New Mexico Attn: D. P. MacDougall
2	Bureau of Mines 4800 Forbes Street Pittsburgh 13, Pennsylvania Attn: Chief, Explosive & Physical Sciences Div.
1	National Advisory Committee for Aeronautics Ames Aeronautical Laboratory Moffett Field, California Attn: Dr. A. C. Charters
2	Commanding Officer Diamond Ordnance Fuze Laboratories Connecticut Avenue at Van Ness St., N.W. Washington 25, D. C. Attn: Ordnance Development Lab.
2	Commanding Officer Detroit Arsenal Center Line, Michigan Attn: Mr. C. B. Salter
3	Commanding Officer Frankford Arsenal Philadelphia 37, Pennsylvania Attn: Mr. H. S. Lipinski
1	Commanding Officer Holston Ordnance Works Kingsport, Tennessee
3	Commanding General Picatinny Arsenal Dover, New Jersey Attn: Technical Div.
2	Commanding General Redstone Arsenal Huntsville, Alabama Attn: Technical Library

DISTRIBUTION LIST

No. of Copies	Organization
1	Commanding Officer Watertown Arsenal Watertown, Massachusetts
3	Commanding Officer Office of Ordnance Research Box CM Duke Station Durham, North Carolina
1	Professor of Ordnance U. S. Military Academy West Point, New York
1	Commanding Officer Chemical Corps Chemical & Radiological Laboratories Army Chemical Center, Maryland
1	Commanding Officer Engineer Research & Development Lab. Fort Belvoir, Virginia Attn: Technical Intelligence Branch
2	Chief of Engineers Department of the Army Washington 25, D. C. Attn: ENGNE Structure Dev. Branch
1	Commanding Officer Rock Island Arsenal Rock Island, Illinois Attn: Mr. Donald L. Meyers
1	American Machine & Foundry Co. 188 W. Randolph Street Chicago 1, Illinois Attn: Mr. K. H. Jacobs Mechanics Research Dept. THRU: District Chief Chicago Ordnance District 209 West Jackson Boulevard Chicago 6, Illinois
1	Director Applied Physics Laboratory 8621 Georgia Avenue Silver Spring, Maryland Attn: Mr. H. S. Morton THRU: Naval Inspector of Ordnance Applied Physics Laboratory 8621 Georgia Avenue Silver Spring, Maryland
1	Armour Research Foundation 35 W. 33rd Street Chicago 16, Illinois THRU: District Chief Chicago Ordnance District 209 W. Jackson Boulevard Chicago 6, Illinois
1	Arthur D. Little, Inc. 30 Memorial Drive Cambridge 42, Massachusetts Attn: Dr. W. C. Lothrop THRU: District Chief Boston Ordnance District Boston Army Base Boston 10, Mass.
1	Budd Manufacturing Co. Red Lion Plant Philadelphia, Pennsylvania THRU: District Chief Philadelphia Ord. Dist. 1500 Chestnut Street Philadelphia 2, Penna.
5	Carnegie Institute of Technology Pittsburgh, Pennsylvania Attn: Dr. E. M. Pugh THRU: District Chief Pittsburgh Ordnance District 200 Fourth Avenue Pittsburgh 22, Pennsylvania

DISTRIBUTION LIST

No. of Copies	Organization
1	Cornell Aeronautical Laboratory, Inc. 4455 Genesee Street Buffalo 21, New York Attn: Mr. Richard A. Eldridge Special Projects Dept. THRU: District Chief Rochester Ord. Dist. Sibley Tower Bldg. Rochester 4, New York
1	E. I. du Pont de Nemours & Co., Inc. Eastern Laboratories Gibbstown, New Jersey Attn: Dr. C. O. Davis THRU: District Chief Philadelphia Ord. Dist. 1500 Chestnut Street Philadelphia 2, Penna.
2	Firestone Tire and Rubber Co. Akron 17, Ohio Attn: E. W. Ford H. Winn THRU: District Chief Cleveland Ord. Dist. 1367 East Sixth Street Cleveland 14, Ohio
1	Professor J. W. Beams Chairman, Department of Physics University of Virginia Charlottesville, Virginia
1	Institute for Air Weapons Research University of Chicago Museum of Science and Industry Chicago 37, Illinois Attn: Mr. Paul F. Shanahan THRU: Commanding Officer Mid Central Air Procurement District 165 North Canal Street Chicago 15, Illinois
1	Stanford Research Institute Stanford, California Attn: Dr. T. C. Poulter THRU: District Chief San Francisco Ord. Dist. P. O. 1829 Oakland 14, Calif.
1	Hesse-Eastern Corp. 22 Palmer Street Harvard Square Cambridge 38, Mass. Attn: Mr. F. C. Hutchinson THRU: District Chief Boston Ord. Dist. Boston Army Base Boston 10, Mass.
1	University of Utah Department of Physics, Bldg. 206 Salt Lake City, Utah Attn: Professor Melvin Cook THRU: Chief of Naval Research Department of the Navy Washington 25, D. C. Attn: Code 425

DISTRIBUTION LIST

No. of Copies	Organization
1	Professor Walker Bleakney Palmer Physical Laboratory Princeton University Princeton, New Jersey
1	Professor George F. Carrier Division of Applied Science Harvard University Cambridge 38, Massachusetts
1	Professor Francis H. Clauser Chairman, Department of Aeronautics The Johns Hopkins University Baltimore 18, Maryland
2	Professor Richard Courant Institute for Mathematical Sciences New York University New York 3, New York
1	Dr. Harold E. Edgerton Massachusetts Institute of Technology Cambridge 39, Massachusetts
1	Professor Howard W. Emmons Harvard University Cambridge 38, Massachusetts
1	Dr. A. W. Hull Research Laboratory General Electric Company Schenectady, New York
1	Professor John G. Kirkwood Department of Chemistry Yale University New Haven, Connecticut
1	Professor G. B. Kistiakowsky Department of Chemistry Harvard University Cambridge 38, Massachusetts
1	Professor Walter S. Koski Department of Chemistry The Johns Hopkins University Baltimore 18, Maryland
1	Professor Joseph E. Mayer Institute for Nuclear Studies University of Chicago Chicago 37, Illinois
2	Dr. W. H. Prager Chairman, Physical Sciences Council Brown University Providence 12, Rhode Island
1	Professor N. F. Ramsey, Jr. Department of Physics Harvard University Cambridge 38, Massachusetts
1	Dr. L. H. Thomas Watson Scientific Computing Laboratory 612 West 116th Street New York 27, New York
1	Professor John von Neumann The Institute of Advanced Study Princeton, New Jersey

INDEX

The references are to pages

Abel's equation of state, 122
Ammunition (See "Rounds")
Annealing of liners, 87, 89

Barium titanate generators, 142, 150, 151, 167
Birkhoff, G., 5, 13, 19, 185, 186, 187, 189, 191, 201
Blackington, G. W., 4
Blast damage from HEAT ammunition, 107, 108
Boostering (See "Explosive Charge")
Breidenbach, H. I., 15, 24

Calhoun, J. J., 4
Chapman-Jouguet, 19, 121
Church, J. H., 4
Clark, J. C., 5, 13, 24
Clark and Fleming, 177
Clark and Seeley, 14
Conant, J. B., 5
Corning Glass Co., 5
Cranz, Law of 29, (See also "Scaling of Shaped Charges")

Damage beyond target
  Liner material for, 108
Davis, C. O., 5
Defense against shaped charges, 7 (See also "Targets")
  Active vs passive, 256
  Armor for, 10, 31
    Doron, 262
    Explosive, 255, 256
    Formica FR-56, 262
    Glass, 11, 256, 260, 265
      Installation of, 265, 266
    HCR of, 11
    Spaced, 107, 199, 258, 259
    Spikes as, 256
    Thickness requirements of, 11
    Titanium as, 255
    Weight of, 11
  Cutting charges for, 256
Del Campo, A., 1
Demolition charges
  M2A3, 5
  M3, 5
Density laws, 10
Detonation (See "Explosive Charge")
Detonators
  Electric, 144
  Research in, 169, 170

Effectiveness of shaped charge, 269
"Anti-ammunition" evaluation, 279, 281, 282
"Box" test for evaluation of, 274
Damage defined
"F" damage, 270
"K" damage, 270
"M" damage, 270
Historical data on, 270
Ignition of fuel and ammunition, 269, 277, 278
Liner material related to, 283
List of standard assessments for evaluation, 272
"Personnel kill" evaluation for, 273
Proving Ground firings for evaluation of, 271, 274
"Residual" penetration for, 269, 281, 283
"Tank Kill" defined, 269, 270
Witness plate firings for evaluation of, 279, 281, 282, 296
Eichelberger, R., 10, 11, 15, 20, 23
Energa rifle grenade, (See grenades)
Eshbach, Wilhelm, 4
Evans, W. M., 5
Explosive
"belt", 113, 114, 127, 128
Chapman-Jouguet condition in, 19, 121
Charge
Charge to mass ratio, 22
Chemical energies in, 19
Explosive charge
Asymmetries within, 119, 129, 132, 133, 134, 201
Characteristics of, Table 135
Correlation between, 124, 125
Densities of explosives, 124, 134
Detonation velocities of explosives, 124, 134
Sensitivities of explosives, 124
Confinement of, 20, 63, 86, 107, 109, 110, 113
Confined vs unconfined charges, 86, 107, 113, 114, 127
Detonation of
Chapman-Jouquet condition in, 121
Conservation, equations of, 121
Parameters of detonation vs performance, 134
Pressures in the detonation process, 19, 122, 123, 124, 127, 129, 133
Process of, 19, 119, 121
Rankine-Hugoniot relation in the, 120, 121
Reaction zone in the, 19, 119
State, Equations of
Abel, 122
Jones, 122
Leonard - Jones - Devonshire, 122
Wilson - Kistiakowsky, 122
Temperatures in, 19
Theory of the, 119

Explosive Charge (Continued)
Detonation of (Continued)
Tilt of detonation front, 133
Velocity of 122, 123, 124, 134
Pin technique for obtaining, 22
Explosive "Compensated" charges, 99
Geometry of
Cylindrical vs tapered charges, 107
Diameter of charge/diameter of liner ratio, 85, 86, 113, 127, 128
Length of charge, 107, 113, 126, 127, 128, 129
Length of charge/diameter of charge ratio, 127, 129
Length of charge related to hole volume, 107
Tapered charge, 106, 107
Initiation of
Boostering height, effect of, 112
Eccentric, 113
Types of initiation
Peripheral, 19, 128, 129
Plane, 128, 129
Point, 113, 128, 129, 134
Materials for, 123, 124
Aluminized explosives, 127
Ammonium perchlorate compounds, 127
BTNEN/WAX 90/10, 124
BTNEU/WAX 90/10, 124
Composition A, 124, 135
Composition B, 134, 135
Composition C, 124, 126
Cyclotol, 60/40 124, 126
Cyclotol 70/30, 124, 135
Cyclotol 75/25, 124, 135
Ednatol 50/50, 124, 126
HBX-1, 124, 135
HMX, 130
Nitroglycerine, 132
Nitromethane, 132
Octol, 134
Octol 75/25, 124, 135
Octol 77/23, 124, 135
Pentolite 50/50, 124, 126, 128, 135
Pentolite 25/75, 124, 126
PTX-2, 124, 135
RDX, 130, 134
Tetratol 65/35, 124, 126
Tetratol 70/30, 124, 135
TNT, 124, 126, 135
Torpex 50/36.5/13.5, 124, 126
Multiple shock reflections in, 20
Parameter of explosive charge related to hole volume, 125, 126, 127, 129
Preparation of, 107, 129
Casting, 129, 130, 132

Explosive Charge (Continued)
Preparation of (Continued)
Centrifuging casting, 131
Fundamental procedure in, 130
Machining from larger casting, 131
vacuum melting, 131, 132
Vibration of casting, 131
Goals in
Axial Symmetry, 129, 130
Maximum density, 129, 130, 132
Uniformity of explosives, 129, 132, 134
Liquid, 132
Pressing, 129, 130, 132, 134
"Release Wave" concept in, 20, 24
Shape of, 107
Unlined cavity explosive charge, 2, 3
Penetration vs standoff for, 2
Wave shaping, 19, 119

Fireman, E. L., 10, 31
Flintkote, 11
Flash radiography of
Collapsing liners, 13
Glass effects on jets, 11, 261
Jet pictures from:
Cylindrical liners, 204
Fluted liners, 220, 221
Rotated liners, 177, 178, 179, 180, 181
Trumpet shaped liners, 202, 203
Three tube system for 177
Fragmentation damage from HEAT, 107, 108
French 73mm HEAT ammunition, 107, 108
Fuchs, K., 27
Fuzes
Arming systems for, 142, 144
Acceleration devices in, 143, 144
Electrical systems for, 141, 142
"Graze" action in, 144, 150, 153, 155, 156, 157
Hermetic sealing of, 144
High velocity projectiles, 139, 141, 142
Long standoff type, 169
Low velocity projectile, 139, 142
"Lucky", 142, 145, 150
Mechanical, 141, 157
Proximity, 139
Safety elements in, 139, 144, 145, 170, 171, 175
Spitback type, 113, 141
Time requirements for functioning of, 139, 141
Types of
"One piece", 168
Model L9MK1, 171, 173
Model L9MK2, 171, 174

Fuzes (Continued)
Types of (Continued)
M404, 157
T208, 141, 145, 146, 147, 148, 150, 152
T208E7, 145, 148
T224, 142, 161, 162, 163, 164
T1014, 142, 161, 166
T2028, 142
T2030, 142, 158, 159, 160, 165

Gray, J. C., 4
Grenades
Energa rifle, 171, 172, 280, 281
Fuzing for, 171, 173, 174, 175
Hand and rifle, 169
T37, 168
Gulf Research Laboratories, 6

HCR, 11
HEAT, 1
Heine-Geldern R, 11
Helie's Law, 34
Hill, F. I., 269
Hill - Mott - Pack
Penetration equation, 30
Theory of jet penetration, 9, 11, 256
Hole volume
In target, 34, 45, 104, 113, 114, 129
Related to charge parameters, 125, 126, 127, 129
Vs charge length, 107

Jets
Area cross-section of, 7, 79, 185
Bifurcation of, 34 (See also "Rotation")
Break-up of 27, 29, 37, 49, 99, 190, 193 (See also "Rotation")
Density of 7, 8, 31, 32, 34, 49, 50, 108, 185
Diameter of, 5
Ductile drawing of, 9, 27, 29, 32, 108
Glass Effects on Jets, 11
Length of, 8, 21, 96, 97, 99, 100, 108, 185, 195
Mass distribution of, 23, 27
Mass ratio slug/jet, 20, 22, 26
Momentums of, 8, 34
Obstructions in jet axis, 85
Penetration vs. jet length, 30, 49, 100, 185
Rotation effects upon jets (See Rotation)
Slug to jet mass ratio, 20, 22, 26
Stability of jet vs. liner thickness, 193
Stresses and strains within, 99, 190
Theories of
"First order" theory of formation, 22, 23
Hydrodynamical theory, 13, 20, 25, 26
"Zero Order" theory of formation, 20

Jets (Continued)

Ultra fast jets, 27
Velocity gradient within, 5, 8, 23, 27, 31, 32, 49, 94, 95, 96, 97, 98, 99, 100, 190
Velocity of jets from cylindrical liners, 14
Velocity of jet vs liner apex angle, 89, 91, 93, 257
Velocity of jet vs. liner thickness, 89, 90, 92
Velocity of jet tail, 99
Velocity of jet under peripheral initiation, 32
Velocity of jet vs velocity of penetration, 7, 8
Velocity of penetration of, 7, 30
Velocity ratio slug/jet, 20, 22

Jones' equation of state, 122
Jones, H., 122
Jones, W. N., 5

Kanders, Erich, 4
Kerr cell photography, 177
Kessenrich, G. J., 4
Kistiakowsky, G. B., 5, 6

Lawson, W. E., 12
Leonard - Jones - Devonshire equations of state, 122
Liners
Alignment of liner in charge, 112
Apex
Angle
Apex angle vs penetration, 60, 62, 257 (See also "rotation")
Apex angle in projectiles, 109
Initial jet velocity vs apex angle, 89, 91, 93
Configuration of, 46
Sharp apex vs spitback, 111
Assembly: Liner to body
Cementing, 111, 112
Crimping, 111
Locking groove, 111, 112
Ring, 111, 112
Axial symmetry of, 58
Collapse
Angle of, 14, 15, 20
Process of, 20, 119
Profile of, 23
Velocity, 20, 22
Configuration
Conical, 20, 46, 108
Cylindrical, 14, 83, 204, 205, 206
Double Angle, 46, 83, 108, 109
Fluted, 20, 34, 177 (See also "Spin Compensation")
Hemispherical, 45, 46, 82, 83, 109, 177
Non-conical, 34

Liners (Continued)
Configuration (Continued)

Spherical capped, 45, 82
"Spiral" fluted liners, 35
Trumpet, 45, 46, 109, 177 (See also "Rotation" and "Spin Compensation")
"Wavy" fluted liners, 35
Design parameters for, 62, 104, 107, 109, 110 (See also "Spin Compensation")
Diameter of
Defined, 46
Penetrations requiring specific diameter, 104
langes in, 85, 86, 113
Fluted (See "Spin Compensation")
Geometrical accuracies in, 49
Manufacturing methods
Casting, 47
Drawing, 47
Electroforming, 47, 63, 78
Machining, 47
Shear-forming, 247
Spinning, 46, 47
Materials, 9, 29, 108, 199, 201
Aluminum, 9, 50, 63, 66, 67, 70, 71, 72, 73, 92, 93, 95, 108, 242, 283
Beryllium copper, 89
Bimetallic, 79, 108
Brass, 3
Copper, 9, 27, 50, 63, 64, 65, 70, 71, 72, 73, 74, 84, 87, 89, 92, 93, 95, 108, 199, 200
Copper clad, 79, 108
Glass, 49, 50
Iron, 29
Lead, 50, 63, 69, 95
Paraffined paper, 3
Steel, 3, 9, 27, 29, 50, 62, 63, 70, 71, 72, 73, 84, 85, 86, 87, 89 93, 93, 108, 128, 129, 242, 283
Zamac-5, 47, 63
Zinc, 3, 50, 63, 68
Metallurgy of, 49, 87, 89, 200, 247
Annealing, 47, 87, 89
Crystalline structure of liner material, 29, 49
Ductility of liner material, 108
Melting point of liner material, 108
Non-Alignment of liner in charge, 112, 113
Tilted liner, 112
Offset liner, 112
Obstructions within cavities of, 85
Performance
Measures of performance, 45, 104, 107, 108
Penetration, 2
Spitback tubes in, 87
Attaching spitback to liner, 111
Dimensions for, 111
Sharp apex vs spitback, 111

Liners (Continued)

Tapered walls of, 83, 84, 85, 109
Thickness (See also "Spin Compensation")
Apex angle as related to thickness, 61, 62, 109
Confinement as related to thickness, 109, 110
Geometrical non-uniformities, 51
Initial jet velocity as related to thickness, 89, 90, 92
Jet stability as related to thickness, 193
"Optimum" wall thickness, 109
Penetration under rotation, as related to thickness, 197, 199
Variations in thickness, 3, 57, 109
Waviness in liner wall, 49, 57
Tolerances in dimensions for, 58, 62, 109
Walls (See also "Configuration" under "Liners")
Grooves in, 51, 57
Non-uniform, 51
Tapered, 83, 84, 85, 109
Thickness of (See "Thickness" under "Liners")
Warping of, 51
Waviness in, 49, 57
Wedge-type, 27
Critical angle for jetless impact, 27

Lucky Fuze (See "fuzes")
Hemispherical lucky, 160

McDougall, D. P. 5, 6, 7, 8, 10, 11
Misznay-Schardin effect, 4
Mohaupt, Berthold, 4
Mohaupt, Henry, 4
Munroe, C. E., 3
Murray, 20
Muskat, Morris, 6

Obstructions within liner cavity (See "Liners")
Ogive (See also "standoff")
Geometry of, 114, 115
Thickness of, 168
Overmatching the target, 108

Patents on shaped charges, 3, 4
Pauling, Linus, 215
Penetrations (See also "Targets")
Armor penetrations, 45
Caliber of Round vs Penetration, 105
Cylindrical liners, 205
Estimates of, 104
Explosive parameter related to penetration, 123
Charge Asymmetries related to penetration, 132, 133
Charge height related to penetration, 107, 113, 126, 127, 128, 129
Density of explosive related to penetration, 133
Detonation pressure related to penetration, 123
Dupont Laboratories, 123, 124, 125

Penetrations (Continued)
Explosive Parameters Related to Penetration (Cont)

Naval Ordnance Laboratory, 125
Peripheral initiation related to penetration, 32
Various explosives as related to penetration, 123, 124
Wave shaping related to penetration, 119, 129
Flange effects on penetration, 85, 86, 87, 113, 114, 128
Fluted liner penetrations 227, 228, 229 (See also "Spin Compensation")
Liner design as related to penetration
Apex angle, 60, 62, 63, 76, 81, 95, 109, 111, 194, 196
Apex angle vs standoff
Aluminum liners, 63, 70, 71, 72, 73
Copper liners, 63, 70, 71, 72, 73, 74, 84
Steel liners, 63, 70, 71, 72, 73, 84
Optimum apex angle for penetration, 111, 196
Optimum standoff for various apex angles, 62
Sharp apex vs spitback, 111
Spitback tube, 87
Thickness of wall as effected by apex angle, 61, 62, 109
Asymmetries as effecting penetration, 51, 57
Diameter of liner, effects on, 104, 105
Flange effects, 85, 86, 87, 113, 114, 128
Material 50, 62, 108
Aluminum, 9, 63, 70, 71, 72, 73
Hemispherical, 82
Bimetallic liners, 79
Brass hemispherical, 82
Cadmium hemispherical, 82
Copper liners
Drawn, 9, 63, 70, 71, 72, 73, 74, 84
Electroformed, 63, 78
Hemispherical, 82
Spherical capped, 82
Copper clad, 79
Steel, 62, 63, 70, 71, 72, 73, 84
Hemispherical, 82
Spherical capped, 82
Wall thickness, 63, 75, 78, 79, 80, 109, 197, 199
Tapered wall liners, 84, 85, 109
Thickness as a function of apex angle, 61, 62, 109
Variations in wall thickness, 57
Process of, 256, 257
Rate of penetration, 30, 31
Rotation vs Penetration
Effects upon penetration, 186, 190, 191 (See also "Rotation")
57mm and 105mm penetration compared, 191, 192, 193
Liner material, effects on penetration under rotation (See "Rotation")
Round - Penetration Performance
57mm, 216, 217, 223, 232, 233, 234, 235
73mm, 83

Penetrations (Continued)
Rounds - Penetration Performance (Continued)
75mm, 105
90mm, 105
105mm, 105, 216, 217, 223, 232, 233, 234, 235
120mm, 105
Scaling penetrations for different calibers, 193
Standoff as effecting penetration
Optimum standoff vs apex angle, 62
Penetration vs standoff, 8, 32, 34, 62, 63, 64, 65
Target Density related to Pene., 7, 10,
Theory
"First Order" Theory of penetration, 31
Hill - Mott - Pack, Equation for penetration, 30
"Residual" penetration, 10, 32, 104, 256, 257
Theory of jet penetration, 9, 49, 186
"Zero" order theory of penetration, 30
Trumpets, 177, 200, 201
Peripheral initiation, 19, 201
Piezo-electric effect, 142
Projectile (See "Warhead" and "Rounds")
Pugh, E. M., 1, 22, 23, 27, 31, 256

Radiographs (See "Flash Radiography")
Rankine-Hugoniot, 120, 121
Rayleigh, 36
Release wave theory, 20, 24
Applied to flange effects, 86, 87
Applied to liner collapse, 119
Applied for qualitative predictions, 129
Residual penetration theory, 32, 104, 256, 257
Roberts, C. H. M. 5, 6, 14
Rostoker, N., 15, 20, 23
Rotation
Effects upon:
Jet, 34, 177, 183, 217 (See also "Spin Compensation")
Bifurcation of Jet, 183
Deterioration of jet, 177, 178, 179, 180, 181
Penetration
Liner apex angle effects on penetration, 109, 194, 196
Larger apex angles, 196
Smaller apex angles, 196
Theory of, 194
Liner material effects on penetration, 199
Liner thickness effects on penetration, 197, 199
Penetrations compared 57mm, 3.5", 105mm, 191, 192, 193
Standoff effects on penetration, 34, 107, 198, 199
Historical notes on rotation, 177
Reducing effects of rotation (See also "spin compensation")
Built-in spin compensation in liner, 247, 248
Cylindrical liners, 204, 205, 206

Rotation (Continued)
Reducing Effects of Rotation (Continued)
Double-body projectiles, 215, 249, 250
Fin stabilization, 215, 250
Fluted explosives, 247
Fluted liners, 177
Hemispherical liners, 177
Lawn mowers, 247
Peripheral jet engines, 215, 249
Spiral detonation guides, 247
Spiral staircase, 247
Trumpet liners, 177, 200, 201, 202, 203
Rotation with wire driven rotator, 177
Scaling relationships under rotation, 29, 187, 188, 189, 191, 192, 193
Theory of effects of rotation, 182, 183, 184, 185
Rounds
57mm (See also "Rotation")
Liner, dimensional tolerances, 58
Penetrations w/fluted liners, 216, 217, 223, 249
75mm
Penetrations w/fluted liners, 247
90mm, T108, 57
Fuzing for, 145, 150, 152, 161
Liner dimensional tolerances, 58
105mm (See also "rotation")
Fuzing for T184, 161
Liner dimensional tolerances, 58
Penetration with fluted liners, 216, 217, 223, 249
Round performance in tank vulnerability
Grenade energy, 280
Panzerfaust, 270
2.36" HEAT round, 277, 278
75mm HEAT M310A1, 274, 287
75mm HEAT M66, 284
8 cm AR, 283
2.75" FFAR 274, 283
3.5" Rocket, M28, 27, 274, 275, 277, 278, 281, 283, 287, 295
90mm AP T33, 279
90mm T108, 271, 274, 278, 283, 288, 292, 294
95mm QF, HEAT, 282
105mm M67, 274, 289
105mm BAT, 292
6.5" ATAR, 274, 288, 294

SAGEB Society, 4
Scaling laws for shaped charges, 5
Law of Cranz, 29
Linear relation of, 46
Rotational effects upon, 187, 188, 189, 191, 192, 193, 196, 222
Schultze, M. A., 3
Seeger, 12
Seitz, Frederick, 6

Shofield, A., 185, 186
Simon, J., 11
Skinner, L. A., 4
Slack & Ehrke, 5
Slug
  Formation of, 20
  Length of, 22
  Slug to jet mass ratio, 20, 22, 26
  Slug to jet velocity ratio, 20, 22
Smith, Turner L., 6, 8
Spin Compensation 34 (See also "Rotation")
  Achievement of
    "Built-in" spin compensation, 49, 247, 248
    Fluted explosives, 247
    Fluted liners, 34, 207, 216, 247
      Linear flutes, 238
      Spiral flutes, 35, 221, 242
      "Wavy" flutes, 35
    Non-conical liners, 34
    "Offsets", 34
    Spiral detonation guides, 247
      ("Lawnmowers")
      ("Spiral staircases")
  Caliber vs spin compensation, 222, 224
  Fluted liners, 34, 207, 216, 247
    Design parameters for, 224, 225, 226, 227, 230, 231, 232, 237, 238, 239
      Flute depths, 237, 238, 239, 242
      Flute types, 224, 225
      Indexing of flutes, 232, 239, 241
      Number of flutes, 231
      Tolerance requirements in liner dimensions, 242, 243
      Wall thickness requirements, 231, 236, 238, 239, 240, 242
    Future prospects for, 248, 250
    Manufacturing methods for, 243, 244, 245, 246
    Materials used in
      Aluminum, 242
      Steel, 242
    Mechanism of, 217, 218, 221
      "Thick-thin" effect, 218, 219, 221, 242
      "Transport" effect, 218, 221, 242
    Penetrations obtainable with, 227, 228, 229, 233, 234, 235
    Scaling relations with, 222, 232, 233
    Static-fired, 221
    Trumpet shaped, 242
    Types of flutes, 224, 225
  Historical background on, 215, 216
  Spin rates requiring, 215
    Very high spin rates, 224
Spin rates of modern HEAT ammunition, 215
Standoff, 2
  Density of jet vs 34
  Fuzes for long standoff, 169
  Curves as standoff 107 114, 168

Standoff (Continued)

"Optimum" standoff, 49, 107, 199
Penetration vs standoff, 31, 32 (See also "Rotation")
Projectile standoff, 107
Spaced Armor vs 107
Stein, Otto, 6
Stein, P., 27

Tank vulnerability to shaped charge
JS III, 292, 293, 295
JSU 152, 295
M26. 295
SU 100, 295
T34/85, 294, 295
Target
Array of, 45
Laminated, 32, 259
Non-homogeneous, 32
Spaced, 32, 107, 199, 258, 259
Cylindrical liner jet into target, 206, 207
Density, 10, 256, 259
"Density Law," 256, 257
Density vs target strength, 10
Penetration vs target density, 31
Hole volume in, 34, 45, 104, 107. 126, 127, 129
Materials
Aluminum 11, 257, 259, 265
Doron, 262
Formica, FF-55, 262
Glass, 11, 255, 260, 261, 262, 263, 265
Laminated glass, 260
Lead, 10
Mild steel vs armor, 10, 31. 45
Titanium, 255
Strength (See also "target density"),
Liner apex angle vs target strength, 247
Thickness and weight of, 11, 259, 260
Taylor-Birkhoff Theory, 14
Taylor, Geoffrey, 14, 36
Thibedeau, W. E., 4
"Thick-thin" effect, 218, 219, 221, 242
Thomas, L. H., 218
Thor, G. C., 47
"Transport" effect, 218, 221, 242
Turk, 183, 194

Ubbelohde, A. R., 5
Uhl, E. G., 4

Von Neumann, J., 12